



UNIVERSITAT_{DE}
BARCELONA

**Gene Silencing of *WEE1*, *CHK1*
and *Thymidylate Synthase* using PPRHS.
Non-Viral and Viral Delivery of PPRHs.**

Eva Aubets Gil



Aquesta tesi doctoral està subjecta a la llicència **Reconeixement- NoComercial – Compartir Igual 4.0. Espanya de Creative Commons**.

Esta tesis doctoral está sujeta a la licencia **Reconocimiento - NoComercial – Compartir Igual 4.0. España de Creative Commons**.

This doctoral thesis is licensed under the **Creative Commons Attribution-NonCommercial-ShareAlike 4.0. Spain License**.



UNIVERSITAT DE BARCELONA

FACULTAT DE FARMÀCIA I CIÈNCIES DE L'ALIMENTACIÓ

DEPARTAMENT DE BIOQUÍMICA I FISIOLOGIA
SECCIÓ DE BIOQUÍMICA I BIOLOGIA MOLECULAR

Programa de Doctorat en Biomedicina

**GENE SILENCING OF *WEE1*, *CHK1* AND *THYMIDYLATE SYNTHASE*
USING PPRHS.
NON-VIRAL AND VIRAL DELIVERY OF PPRHs.**

Eva Aubets Gil
Barcelona, 2021



UNIVERSITAT DE BARCELONA

FACULTAT DE FARMÀCIA I CIÈNCIES DE L'ALIMENTACIÓ

DEPARTAMENT DE BIOQUÍMICA I FISIOLOGIA
SECCIÓ DE BIOQUÍMICA I BIOLOGIA MOLECULAR

Programa de Doctorat en Biomedicina

**GENE SILENCING OF *WEE1*, *CHK1* AND *THYIMIDYLATE SYNTHASE*
USING PPRHS.
NON-VIRAL AND VIRAL DELIVERY OF PPRHs.**

Memòria presentada per Eva Aubets Gil per optar al títol de Doctora per a la
Universitat de Barcelona

Dra. Verónica Noé Mata
Directora

Dr. Carlos J. Ciudad Gómez
Director

Eva Aubets Gil
Barcelona, 2021

ABBREVIATIONS

ABBREVIATIONS

5-FU	5-Fluouracil
A	Adenine
AAV	Adeno-associated virus
AdV	Adenovirus
aprt	Adenine phosphoribosyltransferase
ASGR1	Asialoglycoprotein receptor 1
ASO	antisense oligonucleotide
ATM	Ataxia Telangiectasia Mutated
ATR	Ataxia-telangiectasia and Rad3-related
ATRIP	ATR-interacting protein
BCL-2	B-cell lymphoma 2
BIRC5	apoptosis repeat-containing 5
BRCA1	Breast cancer 1
BRCA2	Breast cancer 2
C	Cytosine
CD7	Cluster differentiation 7
CDC25	Cell division cycle 25
CDK1	cyclin-dependent kinase 1
CHK1	Checkpoint protein 1
CHK2	Checkpoint Kinase 2
CHO	Chinese Hamster Ovary
COVID-19	Coronavirus disease 2019
DC-Chol	3- β -[N-(N,N'-dimethylaminoethane) carbamoyl] cholesterol
DDR	DNA damage response
DHFR	Dihydrofolate reductase
DLS	Dynamic light scattering
DNA-PK	DNA-dependent Protein Kinase
DNA-PPRH	PPRH made out of a non-modified deoxyribonucleotide
DOPE	phospholipid dioleoylphosphatidylethanolamine
DOPY	1,3-bis[(4-oley-1-pyridinio)methyl]benzene dibromide
DOTAP	N-[1-(2,3-Dioleoyloxy)propyl]-N,N,N-trimethylammonium methylsulfate
DOTMA	N-[1-(2,3-dioleoyloxy)propyl]-N,N,N-trimethylammonium chloride
DSB	Double strand breaks
dsDNA	Double-stranded DNA
dTMP	2'-deoxythymidine-5'-monophosphate
dTTP	2'-deoxythymidine-5'-triphosphate

Abbreviations

dUMP	2'-deoxyuridine 5'-monophosphate
dUTP	deoxyuridine triphosphate
EGFP	Enhanced Green Fluorescence Protein
EIPA	5-(N-ethyl-N-isopropyl) amiloride
EMA	European Medicines Agency
EMSA	Electrophoretic Mobility Shift Assay
FAM	6-Carboxyfluorescein
FDA	Food and Drug administration
FdUMP	Fluorodeoxyuridine monophosphate
FdUTP	Fluorodeoxyuridine triphosphate
FUTP	Fluorouridine triphosphate
G	Guanine
G4	G-quadruplexes
G4FS	G4-forming sequence
G4-TYMS	G4FS in the 5'-UTR of TYMS
GalNAc	N-acetylgalactosamine
GFP	Green Fluorescence Protein
H ₂ O DEPC	diethylpyrocarbonate-treated water
HER2	factor receptor 2
HRSV	Human respiratory syncytial virus
HSV-1	herpes simplex-1 viruses
hTERT	Telomerase reverse transcriptase
IAP	Inhibitor-of-apoptosis proteins
IARC	Agency for Research on Cancer
IP	Propidium Iodide
jetPEI	Jet-Polyethylenimine
lncRNA	long non-coding RNA
MOI	Multiplicity of infection
MRN	MRE11-RAD50-NBS1 complex
mTHF	5,10-methylenetetrahydrofolate
MTX	Methotrexate
NFκB	Nuclear factor κB
nt	Nucleotides
PD-1	Programmed cell death 1
PDGF	Platelet-derived growth factor
PEG	Polyethylene glycol

PPRHs	Polypurine Reverse Hoogsteen hairpins
PS	Phosphorothioate
PSMA	Prostate Specific Membrane Antigen
QGRS	Quadruplex forming G-Rich Sequences
RISC	RNA-induced silencing complex
RNAi	RNA interference pathway
RNA-PPRH	PPRH made out of non-modified ribonucleotide
RNA-PPRH	PPRH made out of a non-modified ribonucleotides
RPA	Replication protein A
RSR	Replication stress response
SARS-CoV-2	Acute respiratory syndrome coronavirus 2
SELEX	Systematic evolution of ligands by exponential enrichment
siRNA	Small interfering RNA
ssDNA	Single-stranded DNA
T	Thymine
T5	pentathymidine loop
TFO	Triplex Forming Oligonucleotide
THF	Tetrahydrofolate
TP53	Tumor suppressor p53
TYMS	thymidylate synthase
UPV	Viral vector Production Unit
VEGF	Vascular endothelial growth factor
vWF	von Willebrand Factor
WC-PPRH	PPRH bound by intramolecular Watson-Crick bonds
WT	Wilde type

TABLE OF CONTENTS

TABLE OF CONTENTS

PRESENTATION	1
1. INTRODUCTION	5
1.1. Nucleic acids therapeutics	7
1.1.1. TFOs	7
1.1.2. Antisense Oligonucleotides (ASOs)	8
1.1.3. siRNAs	10
1.1.4. Aptamers	11
1.1.5. Ribozymes	12
1.1.6. Decoys	13
1.2. PPRHs	14
1.2.1. Triple helix formation	16
1.2.2. Other biomedical applications of PPRHs	17
1.3. Relevant targets on cancer	18
1.3.1. Targeting Replication Stress Response	19
1.3.2. The <i>Thymidylate Synthase</i> gene	22
1.3.3. The <i>Survivin</i> gene	25
1.4. Delivery of nucleic acids	26
1.4.1. Viral delivery systems	28
1.4.1.1. Adenoviruses	28
1.4.1.2. Adeno-associated viruses	30
1.4.2. Non-viral chemical delivery systems	31
1.4.3. Non-viral physical delivery systems	35
2. OBJECTIVES	37
3. MATERIAL AND METHODS	41
3.1. PPRHs design	43
3.2. DNA-PPRH binding analyses	47
3.3. RNA-PPRH binding analysis	47
3.4. Plasmid vectors	48
3.5. Viral vector production	51

3.6. Transfection of PPRHs	52
3.7. Transfection of vectors	52
3.8. Transduction of human cells	53
3.9. Cell viability	53
3.10. Annexin V Apoptosis Detection kit FITC	53
3.11. RNA extraction	54
3.12. Reverse transcription	54
3.13. Real-time PCR for <i>survivin</i> detection	54
3.14. Western blot analyses for survivin detection	54
3.15. Transduction efficiency	55
4. RESULTS	57
Informe dels directors	59
4.1. Article I	61
Targeting replication stress response using PolyPurine Reverse Hoogsteen hairpins directed against <i>WEE1</i> and <i>CHK1</i> genes in human cancer cells	61
4.1.1. Additional results to Article I	75
4.2. Article II	77
Detection of a G-quadruplex as a regulatory element in Thymidylate synthase for gene silencing using Polypurine Reverse Hoogsteen Hairpins	77
4.2.1. Additional results to Article II	105
4.2.2. DNA-PPRH binding analysis	105
4.2.3. Effect on cell viability upon transfection with modified PPRHs	109
4.3. Delivery of PPRHs using viral vectors	111
4.3.1. RNA-PPRH binding analysis	113
4.3.2. Effect of an RNA-PPRH targeting <i>survivin</i> on PC-3 cell viability and apoptosis	115
4.3.3. Effect on the levels of <i>survivin</i> mRNA and protein upon RNA-PPRH transfection	117
4.3.4. Effect of an RNA-PPRH targeting <i>survivin</i> on HeLa cell viability and apoptosis	119
4.3.5. Effect of a PPRH delivered into cells using viral vectors	120
4.3.5.1. Results with AAV vectors	120
4.3.5.2. Results with AdV vectors	126

4.4. Article III	129
Synthesis and validation of DOPY: a new gemini dioleilybipyridinium based amphiphile for nucleic acid transfection	129
4.4.1. Additional results to Article III	149
5. DISCUSSION	151
5.1. PPRHs as gene silencing tool	153
5.1.1. Targeting Replication Stress Response gene <i>WEE1</i> and <i>CHK1</i>	154
5.1.2. Targeting the regulatory element G-quadruplex in <i>Thymidylate Synthase</i> gene	156
5.1.3. Improving the structure of PPRHs	159
5.2. Delivery	162
5.2.1. PPRHs delivery using viral vectors	162
5.2.2. PPRHs delivery using non-viral vectors: Synthesis and validation of DOPY	164
5.3. Concluding remarks	167
6. CONCLUSIONS	169
7. BIBLIOGRAPHY	173
8. APPENDIX	198
8.1. Article IV	200
Nucleic Acids therapeutics using PolyPurine Reverse Hoogsteen hairpins	200

PRESENTATION

This work is focused on the study of Polypurine Reverse Hoogsteen (PPRHs) hairpins as gene silencing tool, and the search of alternative methods for their delivery, including viral and non-viral vectors.

PPRHs are gene silencing oligonucleotides developed in our laboratory during the last decade. The ability of PPRHs to downregulate a wide range of genes involved in cancer progression has been demonstrated both *in vitro* and *in vivo* (Noé *et al.* 2020). Furthermore, our group has also validated the use of PPRHs as a gene editing tool (Félix *et al.* 2020b; Noé & Ciudad 2021).

To expand the usage of PPRHs as a gene silencing tool, we attempted to inhibit the expression of *WEE1* and *CHK1*, two genes involved in cell cycle regulation in response to replication stress, and thus, widely studied as targets for cancer therapy. Moreover, we wanted to explore if PPRHs could produce a synergic effect when combined with DNA damaging agents, such as methotrexate or 5-Fluorouracil (5-FU), two chemotherapies very much used in clinical practice.

Also, taking the target gene of 5-FU, *Thymidylate synthase (TYMS)*, we wondered if this gene could have a regulatory structure that could be inhibited, directly or indirectly, by PPRHs. In this direction, it was known the ability of G4 to regulate gene expression at the transcriptional and translational levels. Interestingly, in the 5'-UTR of *TYMS*, we found a sequence that could both form G4 and be targeted, through the complementary strand, by PPRHs. Accordingly, we proceeded to design PPRHs against this region and discovered a new powerful way of decreasing gene expression because of the combination of inhibition of transcription directly produced by the template-PPRH and by that produced by the stabilization of the G4 structure that is formed upon displacement of the forward strand of the DNA. In addition, these effects can be harmonized with the chemotherapeutic action of 5-FU to produce synergism.

Similarly, to other nucleic acids therapeutics, the development of safe, efficient, and tissue-specific delivery systems is the major translational limitation of PPRHs. Therefore, in the second part of this thesis we aimed to study other alternatives for PPRHs delivery.

Presentation

Regarding viral vectors, we set up to study the possible use of viral vectors as a delivery system of PPRH *in vitro*. However, before attempting that approach, we had to determine whether PPRHs could also work as RNA species. Once that accomplished, we studied if an adenoviral vector encoding the PPRH against *survivin* would be able to downregulate survivin mRNA and protein levels and caused a reduction in cell viability.

Finally, we also wanted to develop a new non-viral vehicle to deliver PPRHs in the cells. To do so, in collaboration with other departments of our School of Pharmacy, we synthesized a new gemini cationic liposome-based formulation (DOPY) and characterized the DOPY/PPRHs lipoplexes studying the internalization pathways and the applicability of this transfection agent.

1. INTRODUCTION

1.1. NUCLEIC ACIDS THERAPEUTICS

In recent years, the use of nucleic acids has emerged as a promising therapy tool for the treatment of a wide range of diseases due to their capacity to modulate specifically any gene of interest (Hazan-Halevy *et al.* 2016; Landmesser *et al.* 2020; Nielsen & Nielsen 2013; Parsel *et al.* 2016). Multiple advances in molecular biology have contributed to the development of these technologies, including the discovery of the DNA double-helix structure and the understanding of DNA as a carrier of the genetic information (Avery *et al.* 1944; Watson & Crick 1953), the identification of triple-stranded nucleic acids (Felsenfeld *et al.* 1957; Hoogsteen 1959), the development of techniques to isolate, manipulate and synthesize nucleic acids (Alberts *et al.* 2002; Tüzmen *et al.* 2018), or the launch of the Human Genome Project (Craig Venter *et al.* 2001; Lander *et al.* 2001).

Therapeutic oligonucleotides can modulate gene expression through different processes, such as gene silencing, gene repair, splicing alteration, or transcriptional gene activation (Aartsma-Rus *et al.* 2009; Rice *et al.* 2001; Roberts *et al.* 2020; Yoon & Rossi 2018). To date, multiple nucleic acids with the aim of inhibiting gene expression have been developed including Triplex Forming Oligonucleotides (TFOs), antisense oligonucleotides (ASOs), small interfering RNAs (siRNAs), aptamers, ribozymes or decoys, and some of them have eventually been approved by the Food and Drug Administration (FDA) or European Medicines Agency (EMA). In this introduction, we first introduce different nucleic acids employed to downregulate gene expression, focusing on PolyPurine Reverse Hoogsteen hairpins (PPRHs), a new silencing molecule developed in our laboratory during the last decade. We also describe some relevant targets in cancer that are potential candidates to be silenced using PPRHs. Finally, we expose the difficulties and advances in nucleic acids delivery, mentioning the most commonly used oligonucleotides delivery strategies.

1.1.1. TFOs

TFOs are single-stranded DNA (ssDNA) molecules around 10-30 nucleotides (nt) that bind to the major groove of the duplex DNA. TFOs can hybridize with polypurine sequences through Hoogsteen base-pairing forming a

triplex structure. Relative to the purine strand of the duplex, TFOs can bind either in parallel orientation by Hoogsteen bonds, or in an anti-parallel manner establishing reverse Hoogsteen bonds (Figure 1) (Duca *et al.* 2008). A more detailed description of triplets involved in triplex helix formation can be found in section 1.2.1. Triple helix formation.

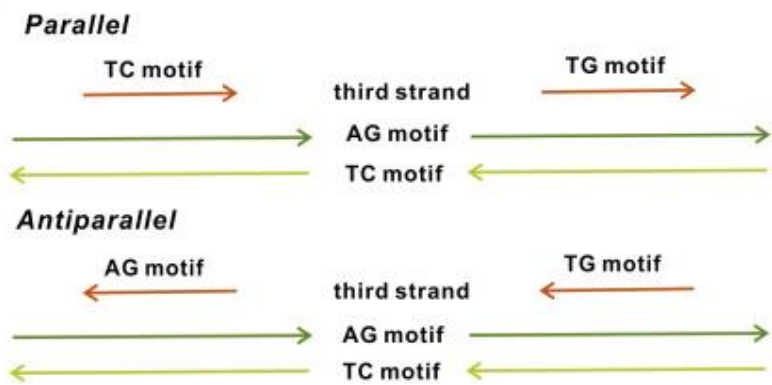


Figure 1. Parallel and antiparallel triplex helix motifs. The arrows indicate 5' to 3' direction. Obtained from (Li *et al.* 2016).

TFOs can alter gene expression by interfering with the binding of transcription factors or the formation of the initiation complex. Alternatively, TFOs can bind to a transcribed sequence and block transcription elongation (Vasquez & Wilson 1998). Furthermore, TFOs have also been studied to produce site-specific mutagenesis and site-specific recombination, thus creating permanent heritable changes in the genome (Knauert & Glazer 2001). Triplex directed mutagenesis can be achieved by TFOs linked to mutagen agents, such as psoralen (Havre *et al.* 1993). On the other hand, triplex-induced recombination can be conducted by coupling a TFO to a donor fragment homologous to the target site, except for the nucleotide to be corrected (Chan *et al.* 1999).

1.1.2. Antisense Oligonucleotides (ASOs)

ASOs are ssDNA molecules of 18-30 nt that are designed to bind to a target mRNA sequence by Watson-Crick (WC) bonds. According to their mechanism of action, ASOs can be divided into two subgroups: RNase H competent or steric block (Figure 2) (Roberts *et al.* 2020). In the former mechanism, ribonuclease H (RNase H) recognize and cleaves the RNA-DNA

heteroduplex, thus inducing gene silencing through mRNA transcript degradation (Wu *et al.* 2004). In contrast, steric block ASOs bind to the mRNA transcript preventing RNA-RNA and/or RNA-protein interactions. Thus, steric block ASOs physically inhibit the progression of the translational machinery or interfere with the alternative splicing by targeting splice sites, exons, or introns. This mechanism has been widely studied to modulate alternative splicing to selectively exclude or retain a specific exons (Aartsma-Rus *et al.* 2009).

To date, three RNase H-competent ASOs (Fomivirsen, mipomersen and inotersen) (Hair *et al.* 2013; Hutcherson & Lanz 2002; Keam 2018), and three splice-switching ASOs (Eteplirsen, nusinersen and golodirsen) (Heo 2020; Hoy 2017; Stein 2016) have been approved by FDA or EMA.

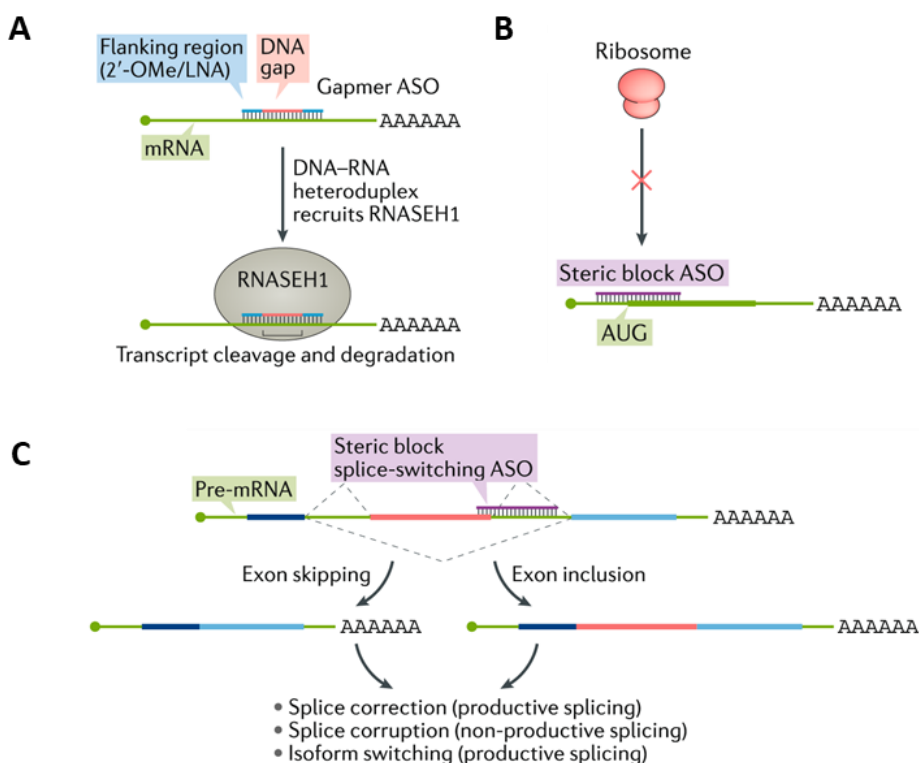


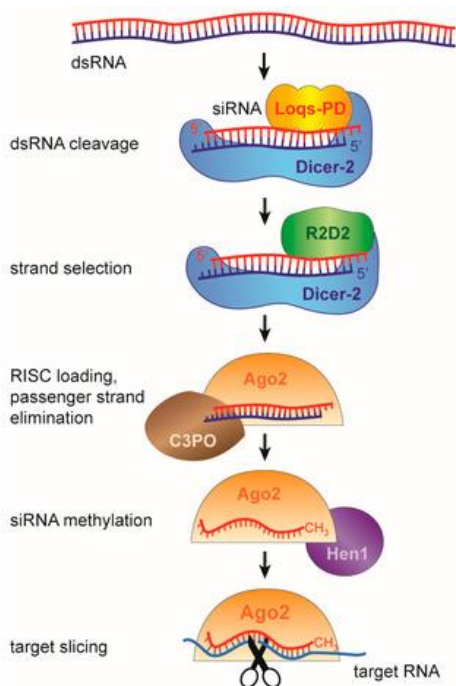
Figure 2: Mechanism of action of ASOs: (A) RNase H-competent ASO. (B) Steric block ASO targeting the AUG start codon. (C) Steric block splice switching ASO targeting signals that modulate alternative splicing (exon skipping or exon inclusion) in the pre-mRNA. Adapted from (Roberts *et al.* 2020).

1.1.3. siRNAs

siRNAs are double-stranded RNA oligonucleotides of 21-22 nt in length with two overhanging nucleotides at the 3'-end of each strand. One of the strands is designated as guide or antisense strand, while the other strand is the passenger or sense strand. Once inside the cell, siRNA enters the RNA interference pathway (RNAi) and is loaded onto the Argonate 2 protein (AGO2), as a part of the RNA-induced silencing complex (RISC). Within the RISC complex, the siRNA is unwound, and the sense strand discarded. Then, the antisense strand guides the RISC complex to its target mRNA and AGO2 cleaves the mRNA (Dana *et al.* 2017). Until date, four siRNAs have received FDA or EMA approval: patisiran (Adams *et al.* 2018), givosiran (Scott 2020), lumasiran (FDA News Release 2020), and inclisiran (EMA 2020).

RNAi process was first discovered in *C. elegans* (Fire *et al.* 1998) and occurs in a wide variety of eukaryotic organisms (Figure 3). The principal function of RNAi is to protect genome integrity against foreign or invasive nucleic acids such as transposons, transgenes, or viruses (Meister & Tuschl 2004).

Figure 3: siRNA interference pathway: Double-stranded RNA precursors of different sources are processed by Dicer-2 into siRNAs. The siRNA is loaded into RISC complex, where the passenger strand is degraded. Then, the guide strand mediates mRNA recognition and AGO2 degrades the target mRNA. Adapted from (Schuster, Miesen, and van Rij 2019).



1.1.4. Aptamers

Aptamers are single-stranded oligonucleotides of either DNA or RNA that fold into defined secondary structures and bind to a specific target. Aptamers are evolved *in vitro* using SELEX (systematic evolution of ligands by exponential enrichment) to bind to the desired target from nanomolar to picomolar affinities (Figure 4) (Gold 2015; Tuerk & Gold 1990). With the advances in the selection processes, several aptamers have been developed against potential targets including von Willebrand Factor (vWF), Platelet-derived growth factor (PDGF), E-selectin, Vascular endothelial growth factor (VEGF), Nuclear factor kB (NFkB), tenascin-C, Nucleolin, Programmed cell death 1 (PD-1) or Prostate Specific Membrane Antigen (PSMA) (Ni *et al.* 2011; Zhang *et al.* 2019). The potential of these aptamers as agonists or antagonists have been tested in pre-clinical and clinical studies (Keefe *et al.* 2010), leading to the approval of the aptamer pegaptanib in 2004, an anti-VEGF for neovascular age-related macular degeneration (Doggrell 2005).

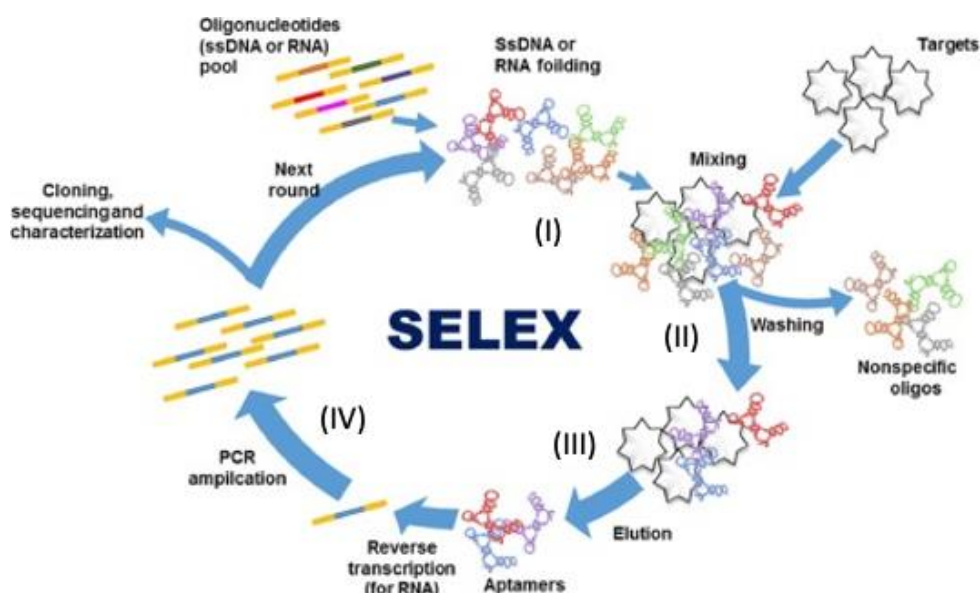


Figure 4: Schematic representation of SELEX: (I) Single stranded DNA or RNA pool is incubated with the target for binding. (II) Targets are washed to remove unbound oligonucleotides, (III) Target-bound aptamers are eluted from the target, (IV) Candidate aptamers are re-amplified and used for next round of selection. Adapted from (Pan *et al.* 2018).

1.1.5. Ribozymes

Ribozymes are single strand RNA molecules with catalytic activity. The first ribozyme was described by Thomas Cech and co-workers in *Tetrahymena thermophila* (Kruger *et al.* 1982). Since then, distinct catalytic RNAs have been identified with diverse biological function in different organisms (Fedor & Williamson 2005; Walter & Engelke 2002). Interestingly, due to their capability of cleaving mRNA molecules in a sequence specific manner, different ribozymes have been artificially designed to down-regulate gene expression. These ribozymes can catalyze reversible cleavage of a specific phosphodiester bond that can be located in an external RNA (trans cleavage) or in a RNA linked to the ribozyme (cis- or self-cleavage) (Müller 2015). The hammerhead ribozyme and hairpin ribozymes are some of the most widely studied due to their small size and cleavage efficiency (Phylactou *et al.* 1998). An example of the structure and the cleavage mechanism of a hairpin ribozyme is depicted in figure 5.

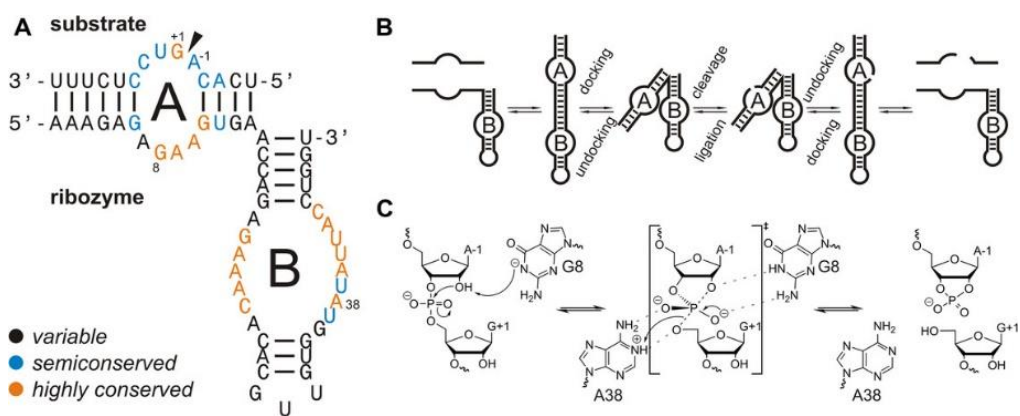


Figure 5. The hairpin ribozyme. (A) Secondary structure of a hairpin ribozyme. Site-specific cleavage is catalyzed at the position marked by an arrow (B) Conformational dynamic generated by binding of the ribozyme to the substrate. (C) Mechanism of hairpin ribozyme: cleavage of a specific phosphodiester bond and ligation. Obtained from (Hieronimus & Müller 2019).

1.1.6. Decoys

Decoys are synthetic double-stranded DNA (dsDNA) that bear the consensus binding sequence recognized by a targeted transcription factor. Decoys can act like a sponge and sequester specific transcription factors, drawing them away from their endogenous binding site, and thus, modulating gene expression (Wang *et al.* 2021). In eukaryotic genomic DNA, transcription factors can bind to other high-affinity binding sites instead of their functional binding sequences, these non-functional sites can act as natural decoys that regulate gene expression (Kempe *et al.* 2016).

Although the most widely studied decoys are dsDNA molecules that contain either one copy or tandem repeat of the target sequence, other strategies have been described, including single-stranded palindromic sequences that self-hybridize to form a duplexes (Ann Liebert & Cho-chung 1998), RNA decoys that interfere with RNA-protein interactions (Makeyev *et al.* 2002), or circular decoys obtained by circularization of the 3' and 5' ends by enzymatic ligation in order to protect the oligonucleotide from nucleases, and thus increasing their stability without modifying the backbone structure (Figure 6) (Ahn *et al.* 2002).

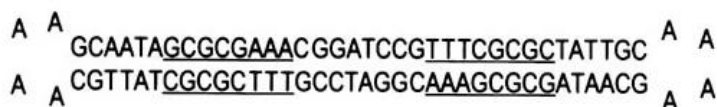


Figure 6: Structure and sequence of a circular decoy against the transcription factor E2F. The two E2F recognition sequences are underlined. Figure adapted from (Ahn *et al.* 2002).

1.2. PPRHs

PPRHs are single stranded non-modified DNA hairpins formed by two antiparallel polypurine mirror repeat strands linked by a pentathymidine loop (5T) and bound intramolecularly by Hoogsteen bonds. PPRHs are designed to hybridize to a specific polypyrimidine sequence in the genomic DNA via Watson-Crick bonds, while maintaining its hairpin structure, and thus producing a triplex DNA. This triplex structure is possible due the capacity of purines to form Watson-Crick bonds with a pyrimidine and, simultaneously, Reverse Hoogsteen bonds with another purine (Figure 7). This triplex conformation leads to the displacement of the fourth strand of the genomic DNA, resulting in the inhibition of gene expression (Figure 7) (Coma *et al.* 2005; de Almagro *et al.* 2009).

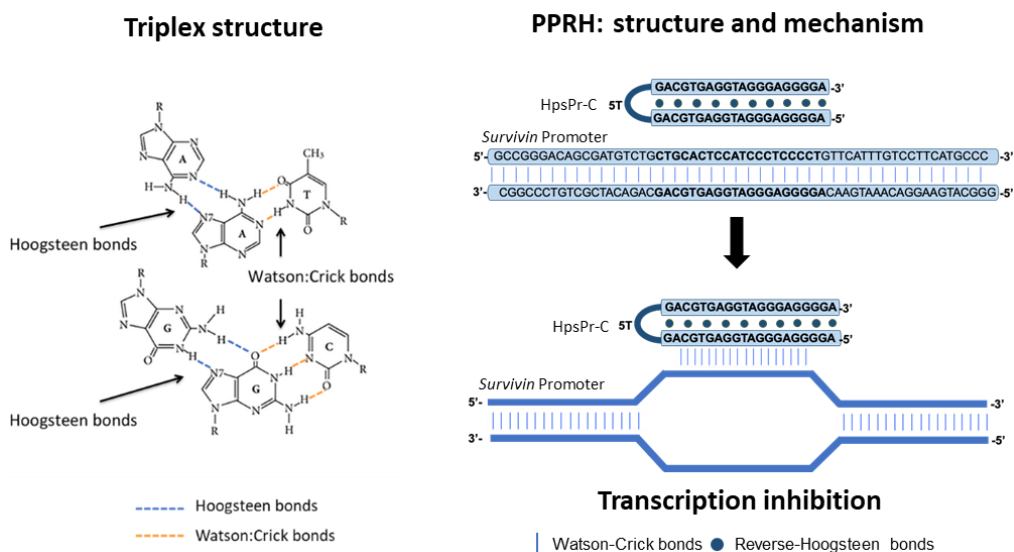


Figure 7. Chemical representation of Hoogsteen and Watson Crick base pairing that participate in triplex formation (left) and representation of a PPRH (HpsPr-C) and its mechanism of action (Right).

PPRHs can be classified depending on the localization of their targeted polypyrimidine domain, which can be placed in either the coding or the template strand of the genomic DNA. PPRHs directed against the template strand of the DNA are termed template-PPRHs, while PPRHs targeting the coding strand are named coding-PPRHs. The latter are also able to bind to the mRNA since the

coding strand of the DNA and the transcribed mRNA have the same sequence and orientation. Polypyrimidine domains are mainly located in promoters and introns, but they can also be found in exons (Goñi *et al.* 2004, 2006). Depending on the location of the target sequence, PPRHs can alter other cellular mechanisms. For instance, previous work in our laboratory showed that a PPRH directed against intron 3 of the coding strand of the *dihydrofolate reductase* (*DHFR*) gene was able to alter the splicing by altering the binding of the splicing factor U2AF65 (Almagro 2011). Furthermore, PPRHs targeting either the coding or the template strand of the promoter of *survivin* demonstrated to interfere with the binding of transcription factors GATA-3 and Sp1, respectively (Rodríguez, 2013).

The ability of PPRHs as a gene silencing tool was first described in *DHFR*, *telomerase* and *survivin* (de Almagro *et al.* 2009). Since then, the capacity of PPRHs to inhibit gene expression has been validated *in vitro* against multiple targets involved in cancer progression, such as *B-cell lymphoma 2* (*BCL-2*), *mechanistic target of rapamycin* (*mTOR*), *DNA topoisomerase 1* (*TOP1*), transcription factors (*C-MYC*), *MDM2* (Villalobos *et al.* 2015), or the immunotherapy tandem targets *SIRP α /CD47* (Bener *et al.* 2016) and *PD-1/PD-L1* (Ciudad *et al.* 2019; Enríquez *et al.* 2018). Furthermore, the gene silencing effect of a coding-PPRH (HpsPr-C) directed against the *survivin* gene has also been demonstrated in two *in vivo* efficacy assays in a prostate xenograft mouse model (Rodríguez *et al.* 2013). This PPRH was able to decrease tumor growth, survivin protein levels and blood vessel formation, thus establishing the proof of principle for the *in vivo* application of PPRHs as gene silencing tool.

To achieve the desired effect on the target gene, PPRHs need a vehicle that enables their internalization into the cytoplasm and their entry into the nucleus. To date, the N-[1-(2,3-Dioleoyloxy)propyl]-N,N,N-trimethylammonium methylsulfate (DOTAP) cationic liposome has routinely been used as a carrier of PPRHs *in vitro* (Rodríguez *et al.* 2013; Villalobos *et al.* 2015). However, this vehicle present low internalization in certain cell lines such as lymphoma B cells (Zhao *et al.* 2012) or neurons (Alabdullah *et al.* 2019). In contrast, in *in vivo* experiments, PPRHs were complexed to the cationic polymer Jet-Polyethylenimine (jetPEI) and administered intratumorally or intravenously into mice (Godbey, Wu, and Mikos 1999). Nevertheless, one limitation of cationic polymers is their possible toxicity (Florea *et al.* 2002; P. Xu *et al.* 2006). Therefore, one of the current goals of our group is to achieve a delivery system safe and efficient for PPRHs.

1.2.1. Triple helix formation

In 1957 it was first described that oligonucleotides were capable of binding to the major groove of the double-stranded DNA generating a triplex-helical structure (Felsenfeld *et al.* 1957). Two years later, Karst Hoogsteen proposed a model that explained the existence of a triple stranded structure (Hoogsteen 1959, 1963). Since nucleic acids can be designed to specifically bind to a target unique sequence, the interest in these structures increased dramatically in the biomedical field.

Two types of triple helix have been characterized according to the orientation of the binding to the DNA major groove: parallel or antiparallel. Parallel triplex occurs when a pyrimidine third strand binds in a parallel orientation to a purine domain of the target duplex forming Hoogsteen hydrogen bonds which typically includes T·AT and C⁺·GC triplets. Antiparallel structures are established when a purine third strand binds in an antiparallel orientation to a purine domain forming reverse-Hoogsteen hydrogen bonds, formed by G·GC, A·AT, T·AT triplets. Parallel triplexes are more stable than antiparallel but require conditions of low pH condition for protonation of cytosines, which might limit their physiological stability. In contrast, antiparallel triplexes occur in a pH-independent manner. The schematic representation of Hoogsteen bonds is depicted in figure 8. The notation X·ZY refers to a triplet in which the third strand X hybridize with the duplex ZY (Goñi *et al.* 2004; Gowers & Fox 1999).

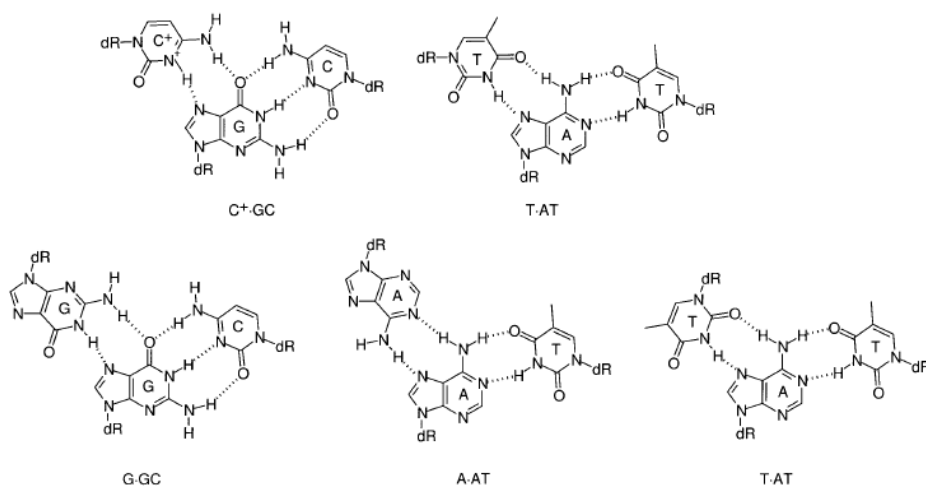


Figure 8: Chemical structures of parallel triplets (Top) and antiparallel triplets (Bottom). Figure from (Gowers & Fox 1999).

In the case of PPRHs, their intramolecular structure is established by reverse Hoogsteen bonds between the two polypurines arms of the hairpin, but hybridization to their targets involves Watson-Crick bonds. Therefore, a polypyrimidine sequence of the target gene is needed to design a PPRH. In general, polypyrimidine sequences are found in all genes with a frequency higher than expected, mostly in gene regulatory areas such as promoters and intronic regions and to a lesser extent in exons (Goñi *et al.* 2004, 2006). Homopyrimidine tracks are not necessary, and the presence of up to three purine interruptions in the DNA target sequence can be allowed (Rodríguez *et al.* 2015). Seeking to overcome this limitation, we studied the possibility to establish other types of triplets, involving inosine nucleosides or G·TA / C·TA triplets:

- **Inosine triplets:** inosine is a modified nucleobase resulted from deamination of adenosine. Inosine substitutions have been explored in triplex formation due to their ability to bind nonspecifically to TA and CG base pairs, and thus act as a “wild-card” in the Hoogsteen position (Mills *et al.* 1996). Furthermore, they have been studied as a “universal base”, capable of binding to any of the four bases in duplexes (Cubero *et al.* 2001).
- **G·TA/T·CG triplets:** G·TA and T·CG are one of the most stable triplets proposed for pyrimidine interruptions using natural bases. However, although the T·CG triplet can be established in both parallel and antiparallel triplexes, G·TA triplet is restricted to parallel structures. For antiparallel structures, the C·TA triplet seems to be the most adequate for recognitions of TA (Gowers & Fox 1999).

1.2.2. Other biomedical applications of PPRHs

The capability of PPRHs to form triplexes has been used in other biomedical applications, including gene repair, gene editing or as biosensors. For gene repair approaches, the sequence homologous to the sequence to be repaired but containing the wild-type nucleotide instead of the mutated one is added to the 5' end of the PPRH core (repair-PPRHs) (Solé *et al.* 2014). These molecules have demonstrated to be capable of correcting point mutations in two collections of Chinese Hamster Ovary (CHO) cell lines bearing different mutations in either *dihydrofolate reductase (dhfr)* (Solé *et al.* 2016) or *adenine phosphoribosyltransferase (aprt)* (Félix *et al.* 2020a) *loci*. More recently, editing-

PPRHs have demonstrated their ability to promote exon skipping at the DNA level in a cell line model bearing an extra copy of DHFR exon 2, restoring the reading frame (Noé & Ciudad 2021). The core of these type of PPRHs bears an extension tail in its 5' end homologous to two separate regions that are apart in parental DNA and that only come together when the skipping of the intervenient sequence takes place. Finally, the triplex structure formed by PPRHs has set the basis for the development of biosensors to analyze DNA methylation status in cancer or for microbiological diseases detection (Calvo-Lozano *et al.* 2020; Huertas *et al.* 2016).

1.3. RELEVANT TARGETS ON CANCER

Cancer is defined as a multistep process that involves mutation and selection of the cells that progressively acquire the capability of surviving, proliferating, and disseminating. In this process, normal cells develop the biological hallmarks of cancer, which include sustaining proliferative signaling, evading growth suppressors, resisting cell death, enabling replicative immortality, inducing angiogenesis, activating invasion and metastasis, reprogramming of energy metabolism, and evading immune destruction. To acquire these properties cells require genomic instability and inflammation (Cooper 2000; Hanahan & Weinberg 2011).

Nowadays, different alternatives for cancer treatment are available, including surgery, radiotherapy chemotherapy, and more recently, biological therapy. However, although great advances in this field have been achieved, the International Agency for Research on Cancer (IARC) estimated 19.3 million new cases of cancer and 10 million deaths in 2020 (IARC 2020). Furthermore, according to the World Health Organization, cancer is still the second leading cause of death worldwide (WHO 2021). These data indicate that standard therapy is unable to control the disease, and thus, more research in this field is required.

The difficulty in cancer treatment relies on its heterogeneity. Cancer includes a large group of diseases that can be originated in almost any organ or tissue. Moreover, a tumor in a specific tissue presents intertumoral heterogeneity between different patients, intratumoural heterogeneity between primary and metastatic sites, and intratumoural spatial heterogeneity. Thus, a deep comprehension of the signaling pathways altered in each cancer is crucial to

develop and implement the proper treatments (Garraway & Lander 2013; Meric-Bernstam & Mills 2012; Sanchez-Vega *et al.* 2018).

In this work we have selected multiple target genes that interfere with essential capabilities of tumor growth and progression, including genes involved in replication stress response (*WEE1*, *CHK1*), nucleotide synthesis (*Thymidylate synthase*) and anti-apoptotic activity (*Survivin*). Many researches have focused on these targets due to their potential in cancer therapy, and thus, we decided to inhibit them using PPRHs.

1.3.1. Targeting Replication Stress Response

Any proliferating cell needs to duplicate accurately its full genome before cell division. Any perturbation that interferes with the correct DNA replication is known as DNA replication stress and includes shortage of histones or deoxyribonucleotide triphosphates, DNA secondary structures such as G-quadruplexes, DNA torsional stress, regions of conflict between replication and transcription or formation of DNA-protein crosslinks (Zeman & Cimprich 2014). Replicative stress results in stalled replication forks that activate the replication stress response (RSR), one of the cell mechanisms to safeguard genome integrity by avoiding the replication of damaged DNA (Dobbelstein & Sørensen 2015; Forment & O'connor 2018).

When replication forks are stalled, DNA helicase moves ahead of DNA polymerase, thereby exposing the ssDNA (Forment & O'connor 2018). Replication protein A (RPA) coats the ssDNA and activates the protein kinase ataxia-telangiectasia and Rad3-related (ATR) through ATR-interacting protein (ATRIP) (Figure 9). Subsequently, ATR phosphorylates and activate CHK1 (CHeckpoint protein 1), which lead to WEE1 protein kinase activation and Cell Division Cycle 25 (CDC25) phosphatase inactivation. WEE1 phosphorylates the cyclin-dependent kinase 1 (CDK1), which prevents the formation of the CDK1-cyclin B complex. Inhibition of CDC25 also prevents the dephosphorylation of CDK1 and thus the formation of the CDK1-cyclin B complex (Rundle *et al.* 2017). As a result, in response to DNA damage, the activation of ATR-CHK1 pathway results in the inhibition of CDK1, which leads to a cell cycle arrest in G2 phase to prevent entry into mitosis until DNA is repaired (Sørensen & Syljuåsen 2012).

The RSR is one of the transduction pathways included in the intricate network of DNA damage response (DDR) (Forment & O’connor 2018). The three most notable protein kinases that initiate the DDR are Ataxia Telangiectasia Mutated (ATM), ATR and DNA-dependent Protein Kinase (DNA-PK) (Figure 9)(Blackford & Jackson 2017). While ATR is activated by ssDNA, ATM and DNA-PK are mainly activated by double strand breaks (DSB). Furthermore, there is a cross-talk between the three pathways (Blackford & Jackson 2017; Zhou *et al.* 2017). DDR can lead to the activation of different checkpoints along the distinct cell cycle stages and initiate mechanisms of DNA repair, senescence, or apoptosis (Patil *et al.* 2014).

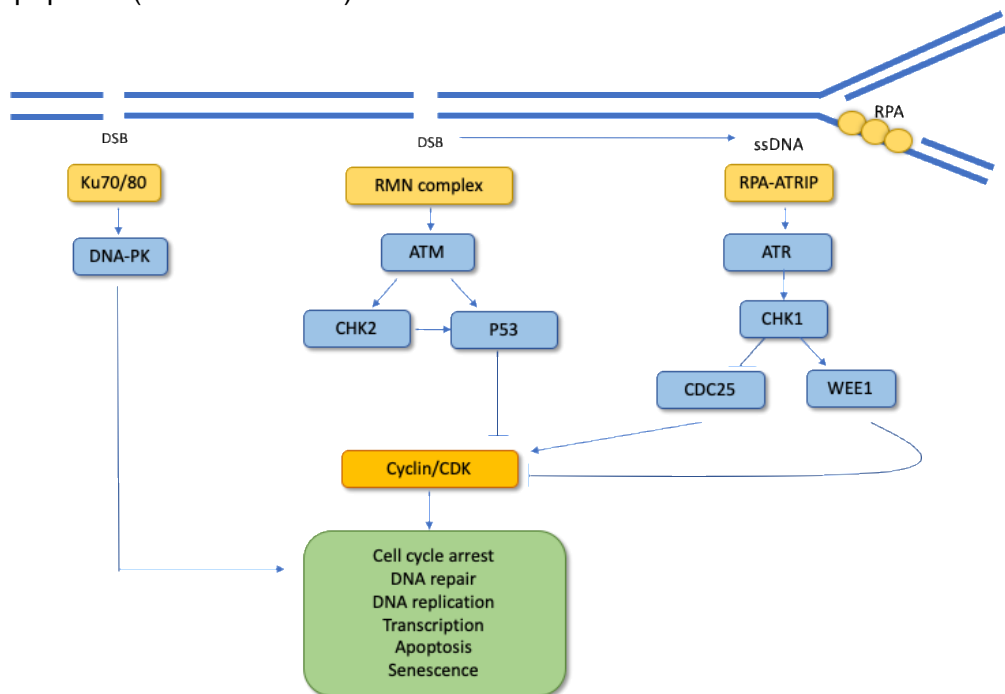


Figure 9. Pathways implicated in DNA damage Response. DNA-PK is recruited and activated by Ku70/80 heterodimer in the presence of DSB. DSBs are also detected by the MRE11-RAD50-NBS1 (MRN) complex, which activates the ATM/Checkpoint Kinase 2 (CHK2) pathway. ssDNA is sensed by RPA leading to activation of ATR/CHK1 through ATRIP. The DDR is transduced to different effectors that activate cell cycle checkpoints, halt cell cycle progression, repair DNA, or that promote cell death (Blackford & Jackson 2017).

In cancer cells, overexpression of oncogenes or reduced expression of tumor suppressor genes promote a premature S phase, which leads to an increase of replication stress by conflicts between replication and transcription, topological stress, or insufficient amounts of nucleotides (Macheret & Halazonetis, 2015). Furthermore, elevated levels of reactive oxygen species in cancer cells also contribute to increase replicative stress by oxidizing nucleotides (van Loon *et al.* 2010). Moreover, the tumor suppressor p53 (*TP53*) gene is the most frequently mutated gene in cancer, which leads to a defective G1/S checkpoint in most tumor cells (Macheret & Halazonetis 2015). Other genes involved in DDR response are frequently mutated such as *ATM*, one of the 20 cancer-driver genes most frequently targeted by single strand substitutions (Macheret & Halazonetis 2015); or the breast cancer 1 (*BRCA1*) and breast cancer 2 (*BRCA2*) genes, which are ascribed to approximately 25% of cases of hereditary breast and ovarian cancer (Nielsen *et al.* 2016). Therefore, the control of cell cycle in cancer cells mainly relies on RSR, and thus, inhibitors of components of ATR-CHK1 pathway have been proposed as an anticancer therapy (Forment & O'connor 2018).

ATR-CHK1 pathway inhibitors are also being investigated in combination with approved drugs that induce RSR (Gralewska *et al.* 2020; Leijen *et al.* 2016; Qiu *et al.* 2018; Seto *et al.* 2013). For instance, drugs targeting nucleotide synthesis such as methotrexate (MTX) or 5-Fluouracil (5-FU) can enhance replicative stress by reducing the available pool of nucleotides (Forment & O'connor 2018). Both drugs block *de novo* synthesis of 2'-deoxythymidine-5'-triphosphate (dTTP), however, while 5-FU inhibits thymidylate synthase (TYMS), enzyme that catalyzes the conversion from 2'-deoxyuridine 5'-monophosphate (dUMP) to 2'-deoxythymidine-5'-monophosphate (dTMP), (Longley *et al.* 2003), MTX inhibits dihydrofolate reductase (DHFR), thus blocking the reduction of dihydrofolate (DHF) to Tetrahydrofolate (THF) required for dTMP and purine synthesis (Hagner & Joerger 2010) (Figure 10).

In this regard, we aimed to design PPRHs as a silencing tool of the replication stress genes *WEE1* and *CHK1* and to test their effectiveness as a single agent and in combination with the inductors of replication stress MTX and 5-FU.

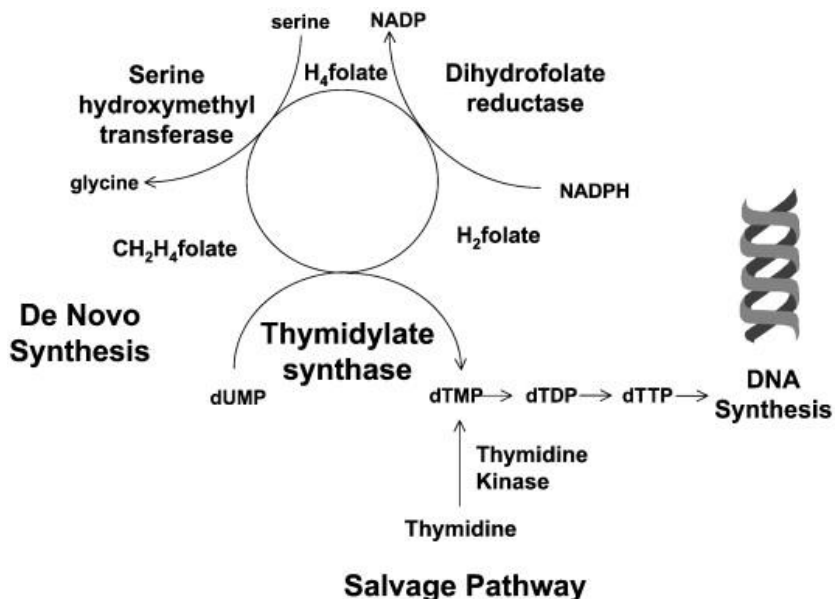


Figure 10. De novo and Salvage pathway of dTTP synthesis. In the novo synthesis of dTTP, TYMS enzyme transfers a methylene group from the methylenetetrahydrofolate (CH₂H₄folate) to dUMP obtaining dTMP and dihydrofolate (H₂folate). dTMP is successively phosphorylated to dTTP. DHF is converted to tetrahydrofolate (H₄folate) in an NADPH-dependent reaction catalyzed by DHFR. Then, THF is converted by a serine hydroxymethyl transferase to CH₂H₄folate. In the salvage pathway, thymidine is phosphorylated by the thymidine kinase to form dTMP (Schmitz *et al.* 2001).

1.3.2. The *Thymidylate Synthase* gene

TYMS catalyzes the reductive methylation of dUMP to dTMP by transferring a methylene group from the cofactor 5,10-methylenetetrahydrofolate (mTHF) (Figure 10) (Carreras & Santi 1995). Then, dTMP is successively phosphorylated to the triphosphate state (dTTP), which is one of the four fundamental nucleosides triphosphates for DNA synthesis (Carreras & Santi 1995; Liu *et al.* 2002). Due its essential role in DNA synthesis, inhibition of TYMS protein leads to repression of DNA replication, and thus, cessation of cell growth and proliferation, affecting in a higher manner highly proliferative cells such as cancer cells (Gmeiner 2012). Furthermore, elevated TYMS protein levels have been found in several tumors, including cervical (Suzuki *et al.* 1999), lung (Shintani *et al.* 2003), bladder (Nomura *et al.* 2002), breast (Pestalozzi *et al.* 1997), kidney (Mizutani *et al.* 2003) or gastrointestinal (Johnston *et al.* 1995; Leichman 2001) cancers and correlated with bad prognosis. Therefore, TYMS

inhibition has been widely studied as an anti-cancer strategy (Chu *et al.* 2003; Rahman *et al.* 2004).

The fluoropyrimidine 5-FU was the first class of TYMS inhibitors (Heidelberger 1981; Heidelberger *et al.* 1957). Since its synthesis in 1957, 5-FU has been widely used in the treatment of a range of cancers, including colorectal, breast, head, neck or gastrointestinal, as a single agent or in combination with other chemotherapeutics (Longley *et al.* 2003; Rose *et al.* 2002). Intracellularly, 5-FU is converted to several active metabolites: fluorodeoxyuridine monophosphate (FdUMP), fluorodeoxyuridine triphosphate (FdUTP) and fluorouridine triphosphate (FUTP). FdUMP acts as an analogue of dUMP and binds to the nucleotide-binding domain of TYMS, forming the ternary complex FdUMP-TYMS-mTHF, instead of the dUMP-TYMS-mTHF complex, leading to TYMS enzyme inhibition. Suppression of dTMP synthesis leads to deoxynucleotide pool imbalance, increased levels of deoxyuridine triphosphate (dUTP) and DNA damage (Longley *et al.* 2003; Zhang *et al.* 2008). Furthermore, dUTP and FdUTP can be misincorporated into DNA, while FUTP can be incorporated into RNA. Thus, 5-FU active metabolites exert the anticancer effects through inhibition of thymidylate synthase and nucleotide misincorporation into RNA and DNA (Longley *et al.* 2003).

Nevertheless, the effectivity in the clinical practice of fluoropyrimidines or other TYMS inhibitors has been limited due to the development of drug resistance (Zhang *et al.* 2008). An autoregulatory mechanism of TYMS protein that induces new synthesis of TYMS protein at the translational level has been proposed as a mechanism of drug resistance (Berger *et al.* 1985; Rooney *et al.* 1998). The ligand-free TYMS protein has been described to bind to its own mRNA and thereby represses its own translation (Figure 11). To date, two mRNA binding sites of TYMS protein have been identified in its mRNA: one located in the 5'UTR containing the translational start site (binding site I), and the other one in the mRNA-coding region (binding site II) (Brunn *et al.* 2014; Chu *et al.* 1991, 1993). When TYMS protein is bound to either its physiologic substrates (dUMP or mTHF) or TYMS inhibitors (fluoropyrimidines or antifolates), TYMS is unable to bind to its own mRNA and TYMS mRNA translation is not inhibited. Therefore, increased levels of TYMS protein levels are detected during 5-FU or other TYMS inhibitors treatments, resulting in tumor resistance (Brunn *et al.* 2014; Chu *et al.* 1991; Lander *et al.* 2001; Schmitz *et al.* 2001).

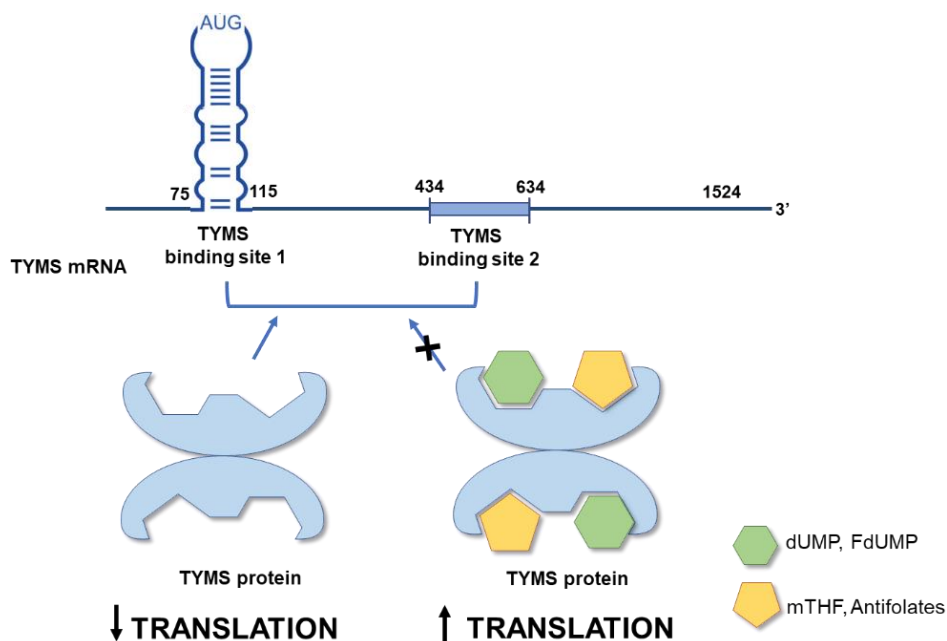


Figure 11. Translational autoregulatory mechanism of TYMS protein. TYMS ligand free is able to bind to its own mRNA, thus repressing TYMS mRNA translation. In contrast, when TYMS protein is bound to its physiologic substrates (dUMP or mTHF) or TYMS inhibitors (FdUMP or antifolates), TYMS is unable to interact with its target mRNA, enabling its own mRNA translation (Schmitz *et al.* 2001).

Seeking strategies to overcome TYMS inhibitors resistance, we intended to find regulatory elements targetable with PPRHs in the *TYMS* gene. We focused on the search of G-quadruplexes (G4s), nucleic acid secondary structures located in guanine-rich DNA or RNA sequences. G4s arise when four guanine bases interact by Hoogsteen hydrogen bonds and form planar G-tetrads that are stabilized by monovalent cations (K^+ , Na^+ , NH_4^+ , Li^+) (Figure 12). These structures are mainly located in regulatory regions such as promoters, 5'UTRs, splicing sites and telomeres, and thus involved in modulation of gene expression (Chambers *et al.* 2015). Furthermore, since a large number of oncogenes have been described to be regulated by a G4 structure, including *C-MYC* (Yang & Hurley 2006), *BCL-2* (Dexheimer *et al.* 2006), *K-RAS* (Cogoi & Xodo 2006) or *c-KIT* (Rankin *et al.* 2005), the interest in developing G4-stabilizing molecules has increased (Kim 2017; Qin & Hurley 2008). Therefore, we decided to design a PPRH to stabilize a G4-structure in the *TYMS* gene, and thus repress its expression (Figure 12).

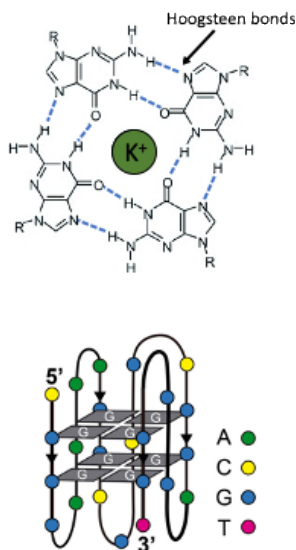
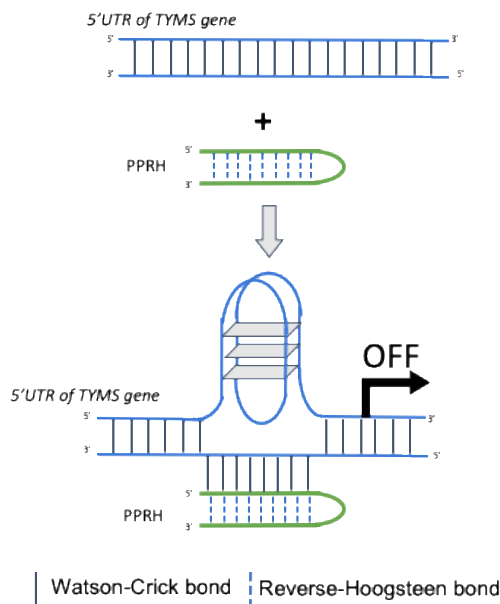
G-quadruplex structure**PPRH stabilizing a G-quadruplex**

Figure 12. Chemical representation of a G-quadruplex structure (left) and hypothesized G4-stabilizing mechanism of a PPRH (right).

1.3.3. The *Survivin* gene

Survivin, also called baculoviral inhibitor of apoptosis repeat-containing 5 (BIRC5), is a member of the inhibitor-of-apoptosis proteins (IAP). Survivin inhibits both extrinsic and intrinsic apoptosis pathways by interacting with proteins involved in the apoptosis pathway, such as caspases (Tamm *et al.* 1998), which induce apoptosis by proteolytic cleavage of several substrates, including cytoskeletal proteins and DNA (Fischer *et al.* 2003).

Survivin is overexpressed in numerous tumors such as lung (Falleni *et al.* 2003), prostate (Ambrosini *et al.* 1997), gastric (Lee *et al.* 2006), colon (Hernandez *et al.* 2011), bladder (Kiu *et al.* 2014), breast cancer (Nasu *et al.* 2002), lymphomas (Gu *et al.* 2005) or neuroblastoma (Azuhata *et al.* 2001). In contrast, its levels are undetectable in most normal tissues in adults, with the exception of thymus (Ambrosini *et al.* 1997), basal colonic epithelium (Gianani *et al.* 2001) and CD34+ cells and normal peripheral blood mononuclear cells (Carter *et al.* 2001). Thus, survivin expression is very differentiated between

normal and tumor cells. Furthermore, its overexpression has been correlated with more aggressive disease and poor prognosis in several cancers (Mittal *et al.* 2015), including non-small cell lung cancer (Ambrosini *et al.* 1997), breast (Li *et al.* 2017), neuroblastoma (Ito *et al.* 2005) or prostate cancer (Zhang *et al.* 2010).

All the characteristics mentioned above, makes survivin an ideal target for cancer therapy. However, although different strategies have been designed against survivin, including (I) Inhibitors targeting survivin expression, (II) inhibitors targeting homodimerization of survivin, or (III) inhibitors targeting survivin interaction with other proteins, there is no current approved drug targeting survivin (Peery *et al.* 2017).

The study of survivin as an anti-tumor target has attracted the interest of our group during the last decades. We demonstrated that inhibition of survivin expression in endothelial cells using either siRNAs or ASOs induces apoptosis, strong growth-inhibitory effect and interruption of tumor angiogenesis and migration (Coma *et al.* 2004). Furthermore, as stated before, we previously validated the antitumor effect of PPRH directed against survivin (HpsPr-C) *in vitro* (de Almagro *et al.* 2009) and in two *in vivo* efficacy assays in a prostate xenograft mouse model (Rodríguez *et al.* 2013). Thus, due to the interest in survivin as a target for anticancer and the consistent data gathered of HpsPr-C, we selected this PPRH for the search of new vehicles to improve PPRHs delivery.

1.4. DELIVERY OF NUCLEIC ACIDS

The development of safe, efficient, and tissue-specific delivery system for nucleic acids therapeutics is the major translational limitation. Oligonucleotides are large hydrophilic polyanions, which complicates crossing the biological membranes (Roberts *et al.* 2020). When nucleic acids are systemically administrated, they must surpass several obstacles to reach the desired target and exert their action. Once in the blood stream, nucleic acids must evade blood nucleases and proteins that may degrade them or trigger immune response (Judge *et al.* 2005), bypass renal clearance or sequestration by certain proteins, traverse the capillary endothelium, cross the cytoplasmatic membrane of the target cell, escape from endosome before lysosomal degradation or endocytic recycling (Sahay *et al.* 2013), and, if required, enter the nucleus (Amantana and Iversen 2005; Dirin and Winkler 2013; Geary *et al.*

2015). If the target tissue is the central nervous system, they must also cross the blood-brain barrier (Roberts *et al.* 2020; Zhu & Mahato 2010).

Currently, different delivery approaches have been developed that are broadly classified into viral vectors (i) or non-viral vectors. Non-viral vectors can be subdivided into (ii) chemical and (iii) physical methods (Nayerossadat *et al.* 2012). The general characteristics of each strategy are described in Table 1.

Method	Principle	Advantages	Disadvantages
Viral	Transfer of DNA or RNA through the natural viral infectious pathway using replication-incompetent viruses.	<ul style="list-style-type: none"> • Relatively high transduction efficiency and persistent gene expression • Highly effective in in vivo and in vitro trials • Can be used with dividing and nondividing cells 	<ul style="list-style-type: none"> • Strong induction of immune response. • Oncogenesis and insertional mutagenesis. • High cost. • Restrictions on the size of transgene.
Chemical	Transfer of DNA or RNA in complex with cationic lipids or polymers through cellular endocytosis pathway.	<ul style="list-style-type: none"> • Much safer and cheaper than viral vectors. • Amenable for chemical modification for targeted delivery • Common and effective in in vitro experiments 	<ul style="list-style-type: none"> • Short duration of gene expression. • Low transfection efficiency in in vivo systems • Low efficiency in nondividing cells. • Hard to target specific cells
Physical	Transfer of DNA or RNA through transient pores in plasma membrane created by mechanical forces.	<ul style="list-style-type: none"> • Can be used effectively in in vitro and in vivo experiments • Specific tissue transfection • Can be used with dividing and nondividing cells. 	<ul style="list-style-type: none"> • Local tissue damage at the site of application • Specialized instrument may be required. • Optimized procedure parameters are required for different types of tissues.

Table 1: General characteristics of biological, chemical, and physical delivery systems. Adapted from (Alsaggar & Liu 2015).

1.4.1. Viral delivery systems

Viral vectors are replication-deficient viruses genetically modified to delete the disease-causing sequences and to contain the nucleic acid sequence of interest on the viral genome. The main advantage of these vectors is the high transduction efficiency on a variety of cells. However, the use of viruses can generate undesired immunogenic response, insertional mutagenesis, and cytotoxicity. Moreover, viruses present a laborious production and a limited transgene size capacity (Thomas *et al.* 2003).

Several types of viruses for gene therapy have been developed with different properties, including adenoviruses (AdVs), adeno-associated viruses (AAVs), retroviruses, lentiviruses, herpes simplex-1 viruses (HSV-1), or baculovirus, whose principal features are described in table 2. AdVs, AAVs and lentiviruses are the key viral vectors strategies currently used in clinical trials (Bulcha *et al.* 2021).

AdVs and AAVs are DNA-based viral vectors, while lentiviruses are RNA-based viral vectors. In general, RNA-based viral vectors can integrate into the host genome, and thus, are capable of long-term transgene expression. In contrast, transgene expression in DNA-based viral vectors normally remains episomal in the nucleus of transduced cells, which can eventually result in the loss of the transgene expression (Kamimura *et al.* 2011). Thus, AAVs and AdVs could be suitable candidates for PPRHs gene silencing application, for which a transient expression might be highly desirable.

1.4.1.1. Adenoviruses

AdVs are non-enveloped viruses with an icosahedral protein capsid that contains a linear dsDNA molecule of 26-45 kb. Several adenoviral serotypes have been identified that have a broad range of hosts. In humans, AdV can cause infections in the respiratory track, but also can affect other organs such as gastrointestinal or urinary tracts. Although, these infections are normally asymptomatic, in immunocompetent individuals can result in severe disease. AdVs are highly prevalent in the general population, thus, most people present immunity against one or more human AdV serotypes. Among the hundreds of human AdV genotypes identified, investigators have focused on serotypes 2 and 5 for gene therapy (Bulcha *et al.* 2021; Kamimura *et al.* 2011).

Viral system	Adenovirus (Ad5)	AAV	Retrovirus	Lentivirus	HSV-1	Baculovirus
Genome material	dsDNA	ssDNA	RNA	RNA	dsDNA	dsDNA
Genome size	36 kb	8.5 kb	7–11 kb	8 kb	150 kb	80–180 kb
Insert size	8–36 kb	5 kb	8 kb	9 kb	30–40 kb	No limit known
Tropism	Broad, low for blood cells	Broad, low for blood cells	Broad	Broad	Neurons	Some mammalian cells
Infectivity	Dividing and non-dividing cells	Dividing and non-dividing cells	Dividing cells	Dividing and non-dividing cells	Dividing and non-dividing cells	Dividing and non-dividing cells
Transgene expression	Transient	Transient or stable	Stable	Stable	Transient	Transient or stable
Vector genome form	Episomal	Episomal (>90%), site-specific integration (<10%)	Integrated	Integrated	Episomal	Episomal or integrated
Inflammatory potential	High (low for HD-AdVs)	Low	Low	Low	High	High
Advantages	High titers; extremely efficient transduction of most cell types and tissues	Safe transgene delivery; non-inflammatory; non-pathogenic	Persistent gene transfer in dividing cells	Persistent gene transfer in most tissues	Large packaging capacity; strong tropism for neuronal cells	Large cargo sizes; high level of gene expression
Drawbacks	Capsid mediates a potent inflammatory response (eliminated in HD-AdVs)	Small packaging capacity; requiring helper AdV for replication and difficult to produce pure viral stocks	Only transduces dividing cells; integration might induce oncogenesis in some applications	Integration might induce oncogenesis in some applications	Inflammatory; no expression during latent infection; transient gene expression in non-neuronal cells	Limited mammalian host range

Table 2. Characteristics of the main groups of viral vectors used for nucleic acids delivery. Adapted from (Lee *et al.* 2017). Abbreviations: HD-AdVs, helper-dependent Adenoviruses; AAV, adeno-associated virus; HSV-1, herpes simplex-1 virus.

Adenovirus vectors present significant advantages: high transduction efficiency with high levels of transgene expression, can be used in dividing and non-dividing cells, broad tropism for different cells, lack of host genome integration, large packaging capacities and availability of scalable production systems. Furthermore, their immunogenic properties have been applied for the development of vaccines and cancer therapies (Bulcha *et al.* 2021; Lee *et al.* 2017). In this direction, Gendicine, the first adenoviral gene therapy for cancer was approved in China in 2003 (Pearson, Jia, and Kandachi 2004; Peng 2005), followed by the approval of Oncorine (Garber 2006), another adenoviral vector for cancer treatment. Later, in 2020, an Ebola vaccine based on a chimpanzee adenovirus vector also received the approval (Johnson & Johnson 2020), and recently, due to the global coronavirus disease 2019 (COVID-19) pandemic, different adenovirus vector vaccines have been urgently approved (Nakagami 2021).

1.4.1.2. Adeno-associated viruses

AAVs are also icosahedra non-enveloped viruses that have a linear ssDNA genome of approximately 4-5 kb. As their name implies, they require the presence of a helper virus, such as an adenovirus, to complete their life cycle (Naso 2017). There are several AAV serotypes identified, of which AAV2 is the most widely studied. To date, although most of the population has been infected for one or more serotypes, AAVs have not been related to any human diseases on their own (Samulski & Muzyczka 2014).

AAV are promising gene delivery systems given their lack of pathogenicity and immunotoxicity. Furthermore, different serotypes are available with different cell tropisms that can efficiently infect both dividing and non-dividing cells (Li & Samulski 2020; Santiago-Ortiz & Schaffer 2017). Furthermore, although AAVs primarily transduce cells as episomes, AAVs can selectively integrate their genome into chromosome 19 and produce the long-term expression of transgenes (Deyle & Russell 2009). However, the main disadvantage of an AAV-based vector is the limited transgene size capacity (Samulski & Muzyczka 2014).

To date, three AAV-based therapies have been approved by FDA or EMA agencies: Glybera™, approved for patients with LPL deficiency in 2012 by EMA, it was the world's first AAV-based drug, although it is currently removed from the market due to economic concerns (Cressey 2012); Luxturna™, approved for

RPE65-associated Leber congenital amaurosis in 2017 (Bainbridge *et al.* 2015); and Zolgensma™, approved in 2019 for the treatment of spinal muscular atrophy (Novartis 2018).

Apart from AdV and AAV, various retroviral and lentiviral vectors have received the approval of FDA or EMA agencies for *ex vivo* gene therapies: Strimvelis™ (Aiuti *et al.* 2017), retrovirus-mediated gene therapy to treat severe combined immune deficiency (2016); Kymriah™ (Maude *et al.* 2018), a lentiviral vector to treat acute lymphoblastic leukemia (2017); and Yescarta™ (FDA 2017), based on a retroviral vector to treat large B cell lymphoma (2017). Other viral gene therapy-based drugs approved in the worldwide are Rexin-G (Kim *et al.* 2017), a tumor-targeted retroviral vector (2007); Imlygic™ (European Medicines Agency 2015; Pol *et al.* 2016), an HSV-1-based drug for melanoma treatment (2015); and Zalmoxis™ (European Medicines Agency 2020b), another HSV-1 vector for certain types of leukemia and lymphomas (2016) (Goswami *et al.* 2019).

1.4.2. Non-viral chemical delivery systems

Chemical based methods for gene delivery are safer than viral vectors, easier to manufacture and susceptible to modifications to enhance targeting specificity. However, chemical methodologies can exhibit lower delivery efficacies and some toxicity (Zhu & Mahato 2010). Extensive research in this field have resulted in the development of multitude of approaches. Some of the most popularly chemical strategies include:

- **Lipid-based vectors:** in this group we find cationic lipids, structures formed by a positively charged head group, a hydrophobic domain and a linker connecting both domains. The cationic head interacts electrostatically with the negatively charged DNA, forming lipoplexes. A great variety of cationic lipids have been reported, such as N-[1-(2,3-dioleoyloxy)propyl]-N,N,N-trimethylammonium chloride (DOTMA), N-[1-(2,3-Dioleoyloxy)propyl]-N,N,N-trimethylammonium methylsulfate (DOTAP), or 3-β-[N-(N,N'-dimethylaminoethane) carbamoyl] cholesterol (DC-Chol) (Zhu & Mahato 2010). Cationic lipids are some the most widely used vehicles for nucleic acid delivery. Indeed, in our laboratory, most of the work *in vitro* has been conducted complexing PPRHs with DOTAP (de Almagro *et al.* 2009, 2011). Additionally, neutral lipids, such as the phospholipid dioleoylphosphatidylethanolamine (DOPE) or cholesterol, have been

included in liposomal formulations as 'helper lipids' to enhance transfection. PEGylated lipids, lipids with polyethylene glycol (PEG) on the surfaces, are other important components added in these vectors to optimize pharmacokinetics and biodistribution (Samaridou *et al.* 2020). Over the years, several formulations for nucleic acids delivery have been developed, leading to the approval in 2018 of patisiran, a lipid-based nanoparticle of siRNA for the treatment of hereditary transthyretin amyloidosis, and, more recently, mRNA vaccines for the COVID-19 emergency (European Medicines Agency 2020a, 2021; Jackson *et al.* 2020; Polack *et al.* 2020).

- **Polymeric vectors:** polymers bearing a positive charged group that interact electrostatically with nucleic acids forming complexes called polyplexes. Diverse cationic polymers with different structures have been studied, including polylysine, chitosan, linear poly(ethyleneimine), branched poly(ethyleneimine), cyclodextrin, spheroidal polymers such as poly(amidoamine) dendrimers or crosslinked polymers such as poly(amino acid)(Pack *et al.* 2005; Zhu & Mahato 2010). Among these polymers, Jet-Polyethylenimine (jetPEI) has been used as vehicle of PPRHs in *in vivo* experiments, in which PPRH/POLYMER complexes were injected intratumorally or intravenously into mice (Rodríguez *et al.* 2013).
- **Inorganic nanoparticles:** a broad range of inorganic nanoparticles approaches have been studied, including gold, silica, magnetic, lanthanide nanoparticles, quantum dots or carbon nanotubes (Luther *et al.* 2020). Nucleic acids can be loaded to the surface of inorganic nanoparticles by different strategies including, covalent binding, electrostatic absorption or encapsulation, depending on the material core (Conde *et al.* 2015).
- **Exosomes:** phospholipid bilayer microvesicles (approximately 100 nm in diameter) that are generated intracellularly as a result of invaginations of the multivesicular body's limiting membrane (Van den Boorn *et al.* 2013). Exosomes can be released into the extracellular space to transfer molecules (e.g. nucleic acids, proteins, and lipids) from one cell to another via membrane vesicle trafficking. Exosomes can cross biological membranes, avoid phagocytosis and are considered non-toxic, thus, there is a rising interest in their use as a nucleic acids carrier (Alvarez-Erviti *et al.* 2011; Liu *et al.* 2015).

- **Bioconjugates:** The delivery of nucleic acids has been studied using different conjugates to promote intracellular uptake (e.g. Cholesterol or Cell penetrating peptides), to improve pharmacokinetic properties (e.g. polyethylene glycol) or to target the oligonucleotide to specific cells/tissues (Juliano 2016; Roberts *et al.* 2020). Among the different targeted conjugates (Figure 13), some notable examples are:
 - **GalNAc conjugates:** nucleic acids are conjugated to *N*-acetylgalactosamine (GalNAc) moieties, which bind to the asialoglycoprotein receptor 1 (ASGR1), predominantly expressed on liver hepatocytes, and thus, ideal for liver-targeted delivery (Springer & Dowdy 2018). In fact, three GalNAc conjugated siRNAs have been approved by FDA or EMA: givosiran (Scott 2020), for the treatment of hepatic porphyria in 2019; lumasiran (FDA News Release 2020), as the first treatment for primary hyperoxaluria type 1 in 2020; and Inclisiran, for the treatment of adults with primary hypercholesterolaemia (heterozygous familial and non-familial) or mixed dyslipidaemia in 2020 (EMA 2020).
 - **Antibodies:** specific interactions between an antibody and a receptor are considered a powerful tool to guide nucleic acids to specific cells. Various receptors have been targeted using either siRNAs or ASOs conjugated to antibodies, such as the human epidermal growth factor receptor 2 (HER2) or the cluster differentiation 7 (CD7) (Arnold *et al.* 2018; Juliano 2016; Roberts *et al.* 2020; Song *et al.* 2005)
 - **Aptamers:** the ability of aptamers to fold into defined three-dimensional structures and specifically bind with a selected protein has also been studied for targeted drug delivery. For instance, by conjugating a siRNA to an aptamer directed to PSMA (Dassie *et al.* 2009), or by fusing a siRNA with the human immunodeficiency virus gp120-specific aptamer (Zhou *et al.* 2008).

Introduction

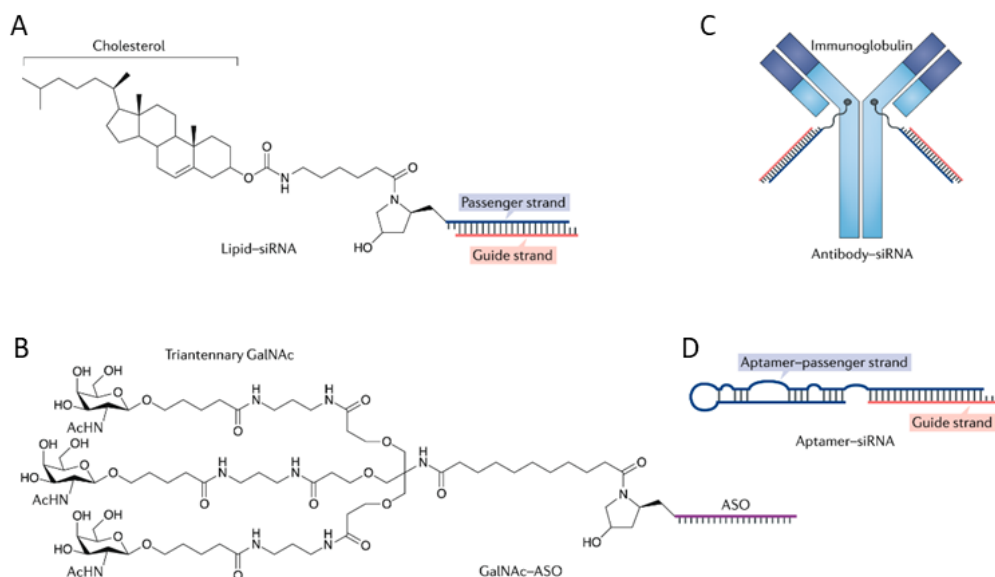


Figure 13: Schematic representation of different bioconjugates: (A) cholesterol-siRNA conjugate, (B) Triantennary N-acetylgalactosamine (GalNAc) moiety conjugated to an ASO, (C) Antibody-siRNA conjugate, (D) Aptamer-siRNA. Figure adapted from (Roberts *et al.* 2020).

Among all the non-viral vectors mentioned above, in lipid-based vectors approaches, we find the new family of cationic gemini surfactants created by Pérez-García and co-workers. The dicationic amphiphiles are formed by two cationic heterocycles, either imidazolium (Sporer *et al.* 2009), pyridinium (Alea-Reyes *et al.* 2017) or bipyridinium rings (Giraldo *et al.* 2020), linked by a 1,3-dimethylenephénylene spacer, and hydrophobic chains incorporated to each cationic ring. The ability of these compounds as anion nanocarriers has been studied over the years, with promising results (Casal-Dujat *et al.* 2012, 2013; Penon *et al.* 2017; Rodrigues *et al.* 2014b; Samperi *et al.* 2019, 2020). Therefore, in this work, we studied a member of the cationic gemini surfactants, the 1,3-bis[(4-oley-1-pyridinio)methyl]benzene dibromide (DOPY), as a non-viral vector for the delivery of PPRHs. This surfactant is formed by two cationic pyridinium heterocycles connected through a 1,3-xylyl spacer and each pyridinium ring bears a hydrophobic oleyl moiety on the position 4 (Figure 14).

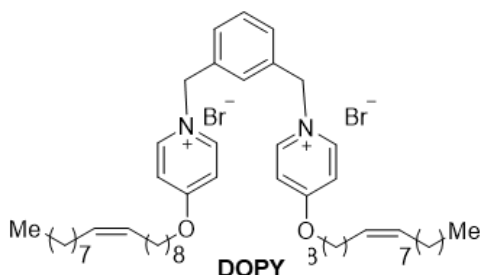


Figure 14. The structure of the cationic gemini surfactant DOPY.

1.4.3. Non-viral physical delivery systems

Physical methods transiently permeate the cell membrane to transfer nucleic acids into the target cells by different physical forces. The most commonly used physical strategies include (Alsaggar & Liu 2015): micro injection, direct injection of nucleic acids into the cell cytoplasm or nucleus using a microneedle (Capecchi 1980); biolistic particle delivery, in which nucleic acid/gold particle conjugates are shot into cells (Klein *et al.* 1987); electroporation, electric pulses generates pores on a cell membrane (Neumann *et al.* 1982); sonoporation, based on ultrasounds that temporarily permeabilize the cell membrane (Kim *et al.* 1996); laser-based methods, a laser pulse is employed to generate transient pores on the cell (Shirahata *et al.* 2001); magnetofection, employs a magnetic field to promote transfection of magnetic nanoparticles complexed to nucleic acids (Scherer *et al.* 2002); or hydroporation, it involves a rapid injection of a large volume of DNA solution via the tail vein in rodents, resulting in a hydrodynamic pressure that enlarge the pores of the liver fenestration, leading to nucleic acid transfer into hepatocytes (Liu *et al.* 1999).

In general, physical methods present lower efficiencies than viral vectors, are difficult to implement at internal organs, can damage the site of application or require specialized instruments. However, physical methods are simpler and safer than other vectors as the nucleic acid is directly delivered into cells without involving any cytotoxic or immunogenic substances. Another significant advantage is that they are not limited to the transgene size (Alsaggar & Liu 2015; Kamimura *et al.* 2011; Kim & Eberwine 2010).

Of note, most of the marketed nucleic acids therapeutics have focused on local delivery (Fomivirsen and pegaptanib, intravitreal injection; or nusinersen, intrathecal administration) and liver delivery (Mipomersen, defibrotide, patisiran inotersen, givosiran, lumasiran and inclisiran). Furthermore, apart from the mentioned delivery strategies, several oligonucleotide therapeutics approved are naked (Fomivirsen, pegaptanib, mipomersen, defibrotide, eteplirsen, nusinersen, inotersen, golodirsen), meaning that nucleic acids are delivered without a carrier, and thus, dependent on chemical modification to improve their pharmacokinetic and pharmacodynamic (eg. Backbone modifications, nucleobase modifications, 2'-ribose substitutions, ribose modifications or bridged nucleic acids) (Roberts *et al.* 2020). Among them, phosphorothioate (PS) oligonucleotides are one of the most remarkable examples of backbone modifications. This modification consists in replacing one of the non-bridging oxygens atoms of the inter-nucleotide phosphate group with a sulfur group. These linkages protect the nucleic acids from nucleases digestion and promotes interaction with plasma protein, thus increasing nucleic acid stability and circulation time (Eckstein 2014). Several marketed nucleotides are based on this modification (Roberts *et al.* 2020). In this direction, we decided to analyze the effect of introducing PS bonds in a PPRH backbone, seeking to improve their stability.

2. OBJECTIVES

This work is divided in two main parts, one centered on expanding the use of PPRHs as a gene silencing tool, and a second part focused on the search of alternative methods for PPRHs delivery. To do so we established the following goals:

1. To expand the use of PPRHs against relevant cancer targets and to improve their properties. This objective is subdivided as follows:
 - To validate the *in vitro* usage of PPRHs as a silencing tool of the replication stress response genes *WEE1* and *CHK1*.
 - To explore the role of G4-quadruplexes in *TYMS* as a regulatory element that could be targeted by PPRHs, as an additional approach to down-regulate *TYMS* expression.
 - To evaluate the effect of different modifications in the PPRH structure on its activity using the antiapoptotic gene *survivin* as a model.
2. To test alternative methods of delivery for PPRHs, including viral and non-viral vectors:
 - To evaluate the efficiency of adenoviruses and adeno-associated viruses as a delivery system for PPRHs and to study the effects of RNA-PPRHs.
 - To evaluate a novel liposome formulation called 1,3-bis[(4-oley-1-pyridinio)methyl]benzene dibromide (DOPY), as a new non-viral vector for PPRHs.

3. MATERIAL AND METHODS

Most of the materials and methods used in this work are described in the articles enclosed in the “Results” section of this doctoral thesis. Nevertheless, a description of the design of the PPRHs and the specific methodologies corresponding to the results that are not published yet (Modifications of PPRHs and viral delivery) are included in this section.

3.1. PPRHs design

To find the polypurine stretches that would hybridize to the polypyrimidine track of the target gene, we used the Triplex-forming Oligonucleotide Target Sequence Search software (<http://utw10685.utweb.utexas.edu/tfo/> MD Anderson cancer center, The University of Texas). BLAST analyses were performed to confirm the specificity of the designed PPRHs.

For inhibition of RSR genes, a total of seven PPRHs were designed. Three directed against *WEE1* (HpWEE1Pr-T, HpWEE1I5-C, HpWEE1E11-C) and four against *CHK1* (HpCHK1I1-C, HpCHK1I1-T, HpCHK1I10-T, HpCHK1I13-C) (Aubets *et al.* 2020b). In the case of *TYMS*, one PPRH targeting the complementary strand of a G4 motif was synthesized (HpTYMS-G4-T) (Aubets *et al.* 2020a).

To evaluate the different delivery systems, we selected a PPRH directed against *survivin* previously validated both *in vitro* and *in vivo* (HpsPr-C-WT) (Rodríguez *et al.* 2013). Since the PPRH would be transcribed in the form of RNA from a viral vector, we tested the effectiveness in silencing *survivin* expression by the HpsPr-C-WT sequence made out of non-modified ribonucleotides (HpsPr-C-RNA, RNA-PPRH).

In addition, to improve the properties of PPRHs, the following modifications were introduced and evaluated in HpsPr-C-WT:

- **PS PPRH:** PS linkages were introduced to the PPRH to increase its stability (HpsPr-C-PS).

- **Substitutions in the sequence:** the pyrimidine interruptions located on the arm of the PPRH that would not bind to the target were replaced by either (I) inosines (HpsPr-C-I) or (II) T>C and C>T to produce C·TA or T·CG triplets (HpsPr-C-Subs), with the aim of overcoming the limitation of 3 interruptions in the PPRH sequence referred to its target.

- **Modifications in the PPRH loop:**
 - Variations of the loop length: PPRHs with the same sequence, but differing from the loop size (3T, 4T or 5T-loop) were analyzed (HpsPr-C-3T, HpsPr-C-4T and HpsPr-C-WT, respectively).
 - Watson–Crick loop: to promote the hairpin formation, we incorporated Watson–Crick bonds in the loop by replacing the 5T-loop by TATTA or TTTAA sequences (HpsPr-C-TATTA and HpsPr-C-TTTAA, respectively).

As negative controls, we used polypurine scrambled hairpins (HpSC4 and HpSC6) or hairpins formed by the same polypurine sequence that binds to genomic DNA but linked to the reverse and complement polypyrimidine sequence bound by intramolecular Watson–Crick bonds. The latter control, named WC-PPRH, can exist either in the antiparallel or parallel orientation.

The PPRH sequences were synthesized as non-modified DNA or RNA oligonucleotides by Merck (Haverhill, United Kingdom). DNA hairpins were resuspended in sterile Tris-EDTA buffer (1 mM EDTA and 10 mM HCl-Trishydroxymethyl-amino-methane, pH 8.0) (Merck, Madrid, Spain) and stored at -20 °C, whereas RNA hairpins were resuspended in DEPC H₂O (diethylpyrocarbonate-treated water) (Merck, Madrid, Spain) and stored at -80 °C until their use. The specific sequences for each of the PPRHs used in this work and the negative controls are shown in the corresponding articles. PPRHs sequences corresponding to modifications in the backbone and substitutions in the sequence of HpsPr-C-WT, modifications in the loop of a PPRH, and the negative controls, are shown in Tables 3, 4 and 5, respectively.

Modifications in the backbone or the sequence of HpsPr-C	
Name	Sequence (5'-3')
HpsPr-C-WT	AGGGGAGGGATGGAGTGCAG T T
	AGGGGAGGGATGGAGTGCAG T T T
HpsPr-C-RNA	AGGGGAGGGGAUGGAGUGCAG U U U
	AGGGGAGGGGAUGGAGUGCAG U U U
HpsPr-C-PS	A*G*G*GGAGGGA*TGGAG*TG*CAG T T T
	A*G*GGGAGGGAT*GGAGT*GC*AG T T T
HpsPr-C-I	AGGGGAGGGATGGAGTGCAG T T T
	AGGGGAGGGAIIGGAGIGIAG T T T
HpsPr-C-S	AGGGGAGGGATGGAGTGCAG T T T
	AGGGGAGGGACGGAGCGTAG T T T

Table 3. Modifications in the backbone or the sequence of HpsPr-C. The abbreviations used in the nomenclature of the PPRHs are: Hp, hairpin; Pr, promoter; s, survivin; -C, Coding-PPRH; RNA, ribonucleotide backbone; PS, phosphorothioate; I, Inosine; S, T>C and C>T Substitution. The PS bonds are indicated with an asterisk, and the modified nucleotides are depicted in red.

Modifications in HpsPr-C loop	
Name	Sequence (5'-3')
HpsPr-C-4T	AGGGGAGGGATGGAGTGCAG T T
	AGGGGAGGGATGGAGTGCAG T T
HpsPr-C-3T	AGGGGAGGGATGGAGTGCAG T T
	AGGGGAGGGATGGAGTGCAG T
HpsPr-C-TATTA	AGGGGAGGGATGGAGTGCAG T A T
	AGGGGAGGGATGGAGTGCAG A T T
HpSPr-C-TTAA	AGGGGAGGGATGGAGTGCAG T T T
	AGGGGAGGGATGGAGTGCAG A A T

Table 4. Modifications in the HpsPr-C loop. The abbreviations used in the nomenclature of the PPRHs are: Hp, hairpin; Pr, promoter; s, survivin; -C, Coding-PPRH; 4T, 4 Thymidines; 3T, 3 Thymidines. The modified nucleotides are depicted in red.

Negative controls	
Name	Sequence (5'-3')
HpsPr-C-WC	TCCCCTCCCTACCTCACGTC T T T
	AGGGGAGGGATGGAGTGCAGT T T
HpSC4	AGAGAAGAGGAAGAGAGGAAAGAGAGGAAGAGGA T T T
	AGAGAAGAGGAAGAGAGGAAAGAGAGGAAGAGGA T T T
HpSC6	AAGGAAGGAAGGAAGGAAGGAAGG T T T
	AAGGAAGGAAGGAAGGAAGGAAGG T T T

Table 5: Name and sequence of the negative controls used. The abbreviations used in the nomenclature of the PPRHs are: Hp, hairpin; WC; Watson-crick bonds; SC, scrambled.

3.2. DNA-PPRH binding analyses

The capacity of the modified PPRHs to bind to their target sequence in the *survivin* promoter was analyzed using electrophoretic mobility shift assays (EMSA). The dsDNA probe corresponding to the target sequence of *survivin* was obtained by mixing equal amounts of each single-stranded oligodeoxynucleotide in a 150 mM NaCl solution (Forward strand, 5'-[FAM]CTGCACTCCATCCCTCCCCT-3'; Reverse strand, 5'-AGGGGAGGGATGGAGTG CAG-3'). The forward strand was labeled with FAM (6-Carboxyfluorescein) at 5'-end. The solution was incubated at 90°C for 5 min and then allowed to cool down slowly to room temperature (about 1h). The duplex was resolved in a nondenaturing 20% polyacrylamide gel, visualized using UV shadowing (254 nm) and gel-purified. DNA concentration was determined by measuring its absorbance at 260 nm using a NanoDrop ND-1000 spectrophotometer (ThermoFisher, Barcelona, Spain).

Binding of PPRHs to their target sequence was analyzed using two approaches: (I) by incubation of the PPRHs with a ssDNA probe, or (II) by incubation of the PPRH with a dsDNA probe. The ssDNA or the dsDNA probes were incubated with the different modified PPRHs in 20 μ L reaction mixtures. In both cases, a buffer containing 10 mM MgCl₂, 100 mM NaCl, 5% glycerol and 50 mM HEPES, pH 7.2 was used (Merck, Madrid, Spain). For ssDNA binding reactions, tRNA was added as unspecific competitor, while for dsDNA binding reactions Poly(dI:dC) was used (1:2 ratio for both cases, ng probe: ng unspecific competitor). ssDNA binding reactions were incubated for 30 min at 37°C, whereas dsDNA binding reactions were incubated for 30 min at 65°C. HpSC6 was used as a negative control in both cases. The products of the binding reactions were resolved by electrophoresis in non-denaturing 8% polyacrylamide gels (PAGE) containing 10 mM MgCl₂, 5% glycerol, and 50 mM HEPES, pH 7.2 (Merck, Madrid, Spain) at a fixed voltage of 220 V and 4°C. The ImageQuant software v5.2 (GE Healthcare, Barcelona, Spain) and GelQuant.NET (Biochemlabsolutions.com) were used to visualize and to quantify the results.

3.3. RNA-PPRH binding analysis

The capacity of the RNA-PPRH to bind to its target sequence in the promoter of *survivin* was analyzed using EMSA assays as described in section 3.2 DNA-PPRH binding analysis but using H₂O DEPC and adding 0.5 μ L of RNase inhibitor in each reaction.

3.4. Plasmid vectors

To proceed to viral-vector delivery, the PPRH sequence had to be cloned in a viral genome. Therefore, we first designed two constructs containing the HpsPr-C-WT sequence under the control of either the U6 or H1 promoters to evaluate their effectiveness.

- **pAAV-HpsPr-C:** This vector contains the HpsPr-C sequence flanked by the restriction enzyme sites NheI (5'-end) and AgeI (3'-end), which allowed its cloning into the AAV genome. The dsDNA sequence was designed to contain a G for the beginning of transcription (5'-end) and a sequence of termination for the end of the transcription (TTTTTGG) (3'-end). The vector is under the control of H1 promoter and contains the Ampicillin resistance gene and the Enhanced Green Fluorescence Protein (EGFP) gene. The synthesis of this vector was ordered to the viral vector production unit (UPV, Autonomous University of Barcelona, UAB, Spain) (Figure 15). Once the vector was produced, it was sent to Macrogen sequencing services to confirm that the insert was correctly cloned (forward primer: 5'-CCCCCTCCCTATGCAAAGC-3').
- **pSilencer™ 2.1-U6 neo-NR/pSilencer-NR:** vector used to generate the construct that would express the HpsPr-C-WT PPRH. The vector is under the control of the human U6 promoter and contains both the Ampicillin resistance and the Neomycin resistance genes. This vector was also used as a negative control in cell viability assays.
- **pSilencer-HpsPr-C:** This construct contains the dsDNA sequence of HpsPr-C into the pSilencer-NR sequence. The dsDNA sequence was designed to contain a G for the beginning of transcription (5'-end) and a sequence of termination for the end of the transcription (3'-end).

In brief, the construct was obtained by amplifying the pSilencer-NR vector with a pair of primers that included a specific sequence hybridizing to pSilencer-NR plus an arbitrary sequence corresponding to one of the strands of HpsPr-C-WT. Thus, ligation of both ends conforms the entire PPRH sequence (Table 6). The reaction was conducted in 50 µL containing 500 ng of pSilencer-NR, 10 µL of buffer 5x, 150 µM dNTPs (Bioline, Barcelona, Spain), 0.5 µg forward primer, 0.5 µg reverse primer, 3.75 U One Taq DNA polymerase (New England Biolabs, Barcelona, Spain) and mQ H2O (SimpliAmp™ Thermal Cycler, SimpliAmp™ Thermal Cycler, Life

Technologies, Thermo Fisher Scientific). A layer of oil on top of the mixture was added before the PCR reaction. PCR cycling conditions were 3 min denaturation at 94 °C; followed by 30 cycles of 30 s at 94 °C, 5 min 68°C; and a final step of 5 min at 68°C. Then, the amplified product was resolved by electrophoresis in a 0.8% agarose gel, electroeluted and ligated at 16 °C overnight.

Transformation of the plasmid DNA into *E. coli* XL1blue was conducted using the heat shock method. Bacteria were plated on LB agar plates containing Ampicillin and incubated 37°C overnight to select colonies containing the plasmid.

To confirm that the insert was correctly cloned, resistant colonies were grown in LB containing ampicillin at 37°C overnight and the pSilencer-HpsPr-C DNA plasmid was obtained using the Monarch plasmid miniprep kit (New England Biolabs, Barcelona, Spain). Then, the insert from the plasmid was PCR-amplified (forward primer: 5'-GGACTATCATATGCTTACCGTAAC-3'; reverse primer: 5'-TGAGTTAGCTCACTCATTAGGC-3'). The reaction was conducted in 50 µL containing 5 µL of buffer 5x, 150 µM dNTPs (Bioline, Barcelona, Spain), 0.5 µg of both primers, 200 ng of template DNA plasmid, 1.25 U One Taq DNA polymerase (New England Biolabs, Barcelona, Spain). PCR (MiniCycler™ MJ Research) conditions were 3 min denaturation at 94 °C; followed by 30 cycles of 30 s at 94 °C, 1 min at 60 °C and 1 min 68°C; and a final step of 5 min at 68°C. The amplified insert was resolved in a nondenaturing 5% polyacrylamide gel, visualized by UV light upon staining with Ethidium bromide and gel-purified. Finally, DNA concentration was determined by measuring its absorbance at 260 nm using a NanoDrop ND-1000 spectrophotometer and sent to MacroGen sequencing services (forward primer: 5'-GGACTATCATATGCTTACCGTAAC-3'). The vector map is shown in figure 16.

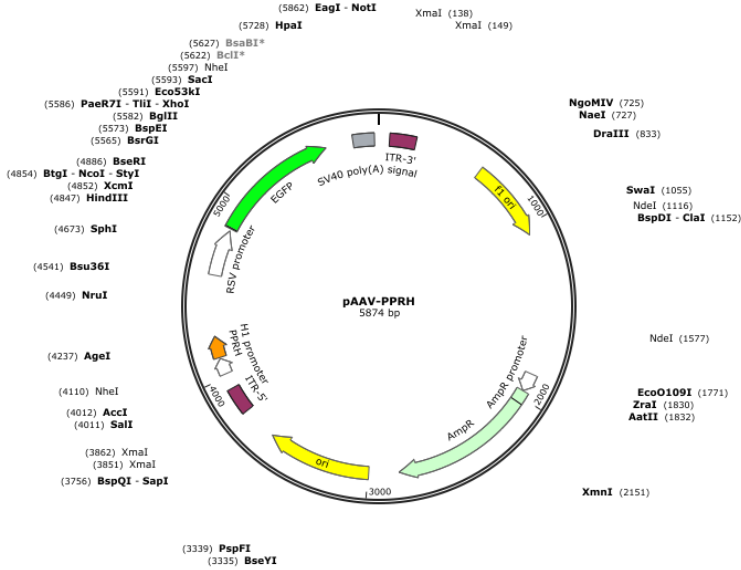


Figure 15. pAAV-HpsPr-C map. The HpsPr-C-WT sequence is under the control of the H1 promoter and contains the Ampicillin resistance gene and EGFP gene.

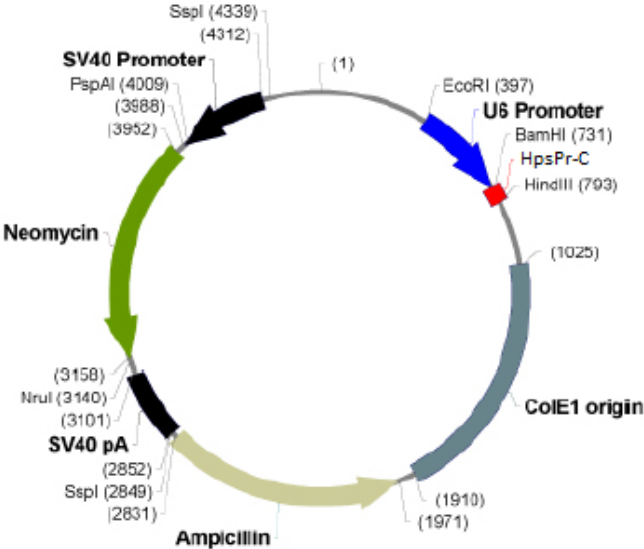


Figure 16. pSilencer-HpsPr-C map. The HpsPr-C-WT sequence is under the control of the human U6 promoter and contains the Ampicillin resistance and the Neomycin resistance genes. Image modified from (Thermo Fisher Scientific - ES 2003).

Primer	Sequence (5'-3')
Forward	5'- (P)TTTGACGTGAGGTAGGGAGGGGA <u>TTTTTGG</u> AAGCTTGGCG TAATCATGGTCATAGC-3
Reverse	5'-(P) AACTGCACTCCATCCCTCCCCT <u>C</u> GGATCCCGCGTCCTTTC CACAAAGATATATAAACC-3'

Table 6. Sequence of the primers used for pSilencer-HpsPr-C synthesis. The sequence corresponding to HpsPr-C-WT is indicated in bold, the starting sequence is underlined and in blue, the transcription terminator is underlined and in red, and the rest of the sequence hybridize to the pSilencer™ 2.1-U6 neo vector. Once the amplified vector was ligated, both parts of the PPRH were also linked, thus generating the complete PPRH structure in the vector.

3.5. Viral vector production

The batches of AAVs and AdV5 were produced in the viral vector production unit (UPV, autonomous university of Barcelona, UAB, Spain) in collaboration with Miguel Chillon, from the UAB.

The selection of the adequate viral vector for preliminary experiments was conducted with different AAV serotypes (AAV1, AAV8, AAV9) and AdVs expressing Green Fluorescence Protein (GFP) reporter gene. Then, PPRHs were cloned in the selected AAV serotypes or AdV genomes. In total, 3 viral vectors expressing the PPRH sequence were produced: AAV1-PPRH, AAV8-PPRH and AdV-PPRH.

The following sequence was cloned into the AAVs or the AdV genome:
 5'- **GT**CGACTAATATTTGCATGTAGCTATGTGTTCTGGGAAATCACCATAA
 ATGTGAAATGTCTTTGGATTGGGAATCTTATAAGTTCTGTATGAGACCAC
 GCTAGC**GG**AGGGGAGGGATGGAGTGCAGTTTTTGACGTGAGGTAGGGA
 GGGGA**TTTTTGG**TCAAGAGCCAAAAATCCCCTCCCTACCTCACGTCAAAA
 ACTGCACTCCATCCCTCCCCTC**TTTTTGGACCGGT**-3'. The colors indicate: in green the Sall site, in yellow H1 promoter, in grey the NheI site, red G for the beginning of transcription, in blue the PPRH, in fuchsia the stop sequence and in red the AgeI site.

The production of batches of AAVs were carried out in HEK293-AAV cells by triple transfection: (i) the plasmid with the PPRH sequence, (ii) the RepCap plasmid containing the AAV Rep and the Cap genes with the capsid proteins of the selected serotype, and (iii) the plasmid pXX6 which contains adenoviral genes needed as a helper virus. The AAV particles were purified by precipitation with PEG followed by ultracentrifugation by iodixanol gradient. The titration was evaluated by quantification by picogreen (Piedra *et al.* 2015).

The batches of AdV5 were produced transfecting the recombinant adenoviral plasmid in HEK293 cells. The AdV particles were purified by double cesium chloride gradient/ gel filtration chromatography. The titration was evaluated by Anti-Ad/Hexon Staining, and the quantification of Adenovirus Particles by Spectrophotometry (Puig *et al.* 2014).

3.6. Transfection of PPRHs

Cells were plated 24 hours before transfection. Transfection of PPRHs consisted in mixing DOTAP (Biontex, Germany) with the corresponding amount of the PPRH in serum-free medium up to 200 μ l. After 20 min of incubation at room temperature, the mixture was added to the cells in a final volume of 1 mL (full medium). Oligodeoxynucleotides PPRHs (DNA-PPRHs) were transfected with a final concentration of 10 μ M DOTAP in the cell culture media, whereas non-modified ribonucleotide PPRHs (RNA-PPRHs) were incubated with 15 μ M of DOTAP.

3.7. Transfection of vectors

Cells were plated in 6-well dishes one day before transfection. The transfection consisted in incubating FuGENE®6 (Promega Biotech Ibérica, S.L, Madrid, Spain) 5 min in serum-free medium, followed by the addition of plasmid DNA (5 μ g) and incubated 15 minutes. The ratio of FuGENE®6 (μ L) to DNA plasmid (μ g) was 3:1. The final volume for each reaction was 100 μ L. Then, the mixture was added to the cells in a final volume of 1 mL (full medium).

In the case of pAAV-HpSPr-C, plasmid transfection efficiency was monitored through EGFP expression using ZOE Fluorescent Cell Imager (Bio-Rad Laboratories, Inc, Spain).

3.8. Transduction of human cells

Different human cells (PC-3, HeLa, HepG2, A549, SH-SY5Y and HEK-293) were plated in 24-well dishes and infected with the corresponding AAV or AdV in a final volume of 300 μ L. The multiplicity of infection (MOI) used is indicated in each experiment. Six hours after infection, culture medium was added up to 1000 μ L. Viruses infection efficiency was monitored through GFP expression using ZOE Fluorescent Cell Imager (Bio-Rad Laboratories, Inc, Spain).

3.9. Cell viability

Cells were plated in 6-well dishes (10,000), or 24-well dishes (5,000 or 7,000) in F12 medium in assays conducted with viruses. Five days after transfection, or three after infection in the case of the viruses' tests, 0.63 mM of 3-(4,5-dimethylthiazol-2-yl)-2,5-diphenyltetrazolium bromide and 100 μ M sodium succinate (both from Merck, Madrid, Spain) were added to the culture media and incubated for 2.5 h at 37°C. After incubation, culture media were removed and the lysis solution (0.57% of acetic acid and 10% of sodium dodecyl sulfate (SDS) in dimethyl sulfoxide) (Merck, Madrid, Spain) was added. Absorbance was measured at 560 nm in a Modulus Microplate spectrophotometer (Turner BioSystems, Madrid, Spain). Cell viability results were expressed as the percentage of cell survival relative to the controls.

3.10. Annexin V Apoptosis Detection kit FITC

Cells (60,000) were plated in 24-well dishes in F12 medium. One day after transfection, the levels of apoptosis were analyzed using the eBioscience™ Annexin V Apoptosis Detection kit FITC (Thermo Fisher Scientific, Spain). Briefly, cells were collected by trypsinization, centrifuged at 800 x g at 4°C for 5 min and washed once in PBS and once in 1X Binding Buffer. The pellet was resuspended in 100 μ L of 1X Binding buffer and 5 μ L of fluorochrome-conjugated Annexin V was added. After 15 min of incubating at room temperature, cells were washed in 1X binding buffer, resuspended in 200 μ L of 1x binding buffer and 5 μ L of Propidium Iodide Staining solution was added. Then, flow cytometry analyses were performed in a Gallios flow cytometer (Beckman Coulter, Inc, Spain) at the Techno-Scientific facilities of the University of Barcelona. Annexin V-positive and IP-negative cells were considered as early-stage apoptotic cells, Annexin V-positive and IP-positive as late-stage apoptotic and necrotic cells, and Annexin V-negative and IP-negative as living cells.

3.11. RNA extraction

Total RNA was extracted from PC-3 and HeLa cells using TRIzol® (Life Technologies) following the manufacturer's specifications. RNA was quantified by measuring its absorbance at 260 nm using a NanoDrop ND-1000 spectrophotometer (Thermo Scientific).

3.12. Reverse transcription

cDNA was synthesized in a 20 µl reaction mixture containing 1 µg of total RNA, 125 ng of random hexamers (Roche, Spain), 500 µM of each dNTP (Bioline, Barcelona, Spain), 2 µL of buffer (10X), 20 units of RNase inhibitor and 200 units of Moloney murine leukemia virus reverse transcriptase (Last three from Lucigen, Wisconsin, USA). The reaction was incubated at 42 °C for 1h.

3.13. Real-time PCR for *survivin* detection

A QuantStudio 3 Real-Time PCR System (Applied Biosystems, Barcelona, Spain) was used to conduct these experiments. *Survivin* (BIRC5) mRNA TaqMan probe (Hs04194392_s1; Life Technologies, Barcelona, Spain) was used to determine *survivin* mRNA levels and TATA-binding protein (TBP) mRNA TaqMan probe (Hs00427620_m1, Life Technologies, Barcelona, Spain) was used as the endogenous control. The reaction was conducted in 20 µL containing 1x TaqMan Universal PCR Mastermix (Applied Biosystems), 0.5x TaqMan probe (Applied Biosystems) and 3 µL of cDNA. PCR cycling conditions were 10 min denaturation at 95 °C, followed by 40 cycles of 15 s at 95 °C and 1 min at 60 °C. mRNA quantification was performed using the $\Delta\Delta C_t$ method, where C_t is the threshold cycle that corresponds to the cycle when the amount of amplified mRNA reaches the fluorescence threshold.

3.14. Western blot analyses for *survivin* detection

Total protein extracts from PC-3 cells (30,000) were obtained 24 h after transfection, or from HeLa cells (15,000) 72h after transduction. Extracts were obtained using 100 µL of RIPA buffer (1% Igepal, 0.5% sodium deoxycholate, 0.1% SDS, 150 mM NaCl, 1 mM EDTA, 1 mM PMSF, 10 mM NaF and 50 mM Tris-HCl, pH 8.0) supplemented with Protease inhibitor cocktail (P8340) (all from Merck, Madrid, Spain). Extracts were incubated 5 min at 4°C and cell debris was removed by centrifugation (16,300 x g at 4°C for 10 min).

Whole-protein extracts (100 µg) were electrophoresed in 15% SDS-polyacrylamide gels and transferred to Immobilon-P polyvinylidene difluoride membranes (Merck, Madrid, Spain) using a semidry electroblotting system. Blocking was performed using a 5% skim milk solution. Then, membranes were probed with primary antibodies against survivin (5 µg/mL; AF886, Bio-Techne R&D Systems, S.L.U. Madrid, Spain), or α -Tubulin (1:100 dilution; CP06, Merck, Darmstadt, Germany). Secondary horseradish peroxidase-conjugated antibodies were anti-rabbit (1:2000 dilution; P0399, Dako, Denmark) for survivin, and anti-mouse (1:2500 dilution; sc-516102, Santa Cruz Biotechnology, Heidelberg, Germany) for α -tubulin detection. Chemiluminescence was detected with the ImageQuant LAS 4000 mini (GE Healthcare, Barcelona, Spain). Quantification was performed using the ImageQuant 5.2 software.

3.15. Transduction efficiency

PC-3 cells, HepG2 and HEK-293 cells (60,000) were plated the day before infection in 24-well dishes. Cells were infected with different AAV serotypes (10^5 MOI). Twenty-four hours after transduction, cell images for each condition were taken using a ZOE Fluorescent Cell Imager (Bio-Rad Laboratories, Inc, Spain). Then, cells were collected and assayed for GFP expression by flow cytometry in a Gallios flow cytometer (Beckman Coulter, Inc, Spain).

4. RESULTS

Informe dels directors

Els Drs. Verónica Noé Mata i Carlos J. Ciudad Gómez, directors de la tesi doctoral titulada “*Gene silencing of WEE1, CHK1 and Thymidylate Synthase using PPRHS. Non-viral and viral delivery of PPRHS*”.

INFORMEN

Del factor d'impacte de les revistes de publicació dels articles inclosos en aquesta tesi doctoral.

Que en els articles I i III la doctorand és la primera autora i no s'han utilitzat per la realització de cap tesi doctoral prèvia

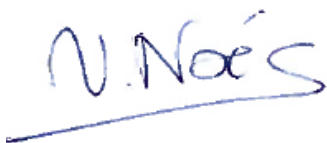
Que l'article II és un treball en co-autoria en què ambdós primers coautors han compartit el projecte i han realitzat els experiments per igual, i que no s'ha utilitzat per la realització de cap tesi doctoral prèvia.

Llistat de publicacions

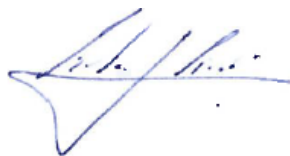
- **Article I.** Targeting replication stress response using PolyPurine Reverse Hoogsteen hairpins directed against *WEE1* and *CHK1* genes in human cancer cells.
Eva Aubets, Véronique Noé and Carlos J. Ciudad.
Biochemical Pharmacology. 2020;175:113911. (Impact factor: 4.960).
- **Article II.** Detection of a G-quadruplex as a regulatory element in Thymidylate synthase for gene silencing using Polypurine Reverse Hoogsteen Hairpins.
Eva Aubets[#], Alex J. Félix[#], Miguel Garavís, Laura Reyes, Anna Aviñó, Ramón Eritja, Carlos J. Ciudad and Véronique Noé.
[#]These authors contributed equally.
International Journal of Molecular Sciences. 2020;21(14):5028. (Impact factor: 4.556).

Results

- **Article III.** Synthesis and validation of DOPY: a new gemini dioleilybipyridinium based amphiphile for nucleic acid transfection. Eva Aubets, Rosa Griera, Alex J. Felix, Gemma Rigol, Chiara Sikorski, David Limón, Chiara Mastroso, Maria Antònia Busquets, Lluïsa Pérez-García, Véronique Noé and Carlos J. Ciudad. European Journal of Pharmaceutics and Biopharmaceutics. 2021;S0939-6411(21)00146-6. (Impact factor: 4.604).



Dra. Verònica Noé Mata



Dr. Carlos J. Ciudad Gómez

4.1. ARTICLE I

Targeting replication stress response using PolyPurine Reverse Hoogsteen hairpins directed against *WEE1* and *CHK1* genes in human cancer cells.

Eva Aubets, Véronique Noé and Carlos J. Ciudad

Biochemical Pharmacology. 2020;175:113911. (Impact factor: 4.960).

Background: RSR is one of the transduction pathways included in the intricate network of DNA damage response (Forment & O’connor 2018). Single-stranded DNA fragments produced by replication stress activate ATR kinase, which initiates a phosphorylation cascade that activates WEE1 and CHK1 kinases. The activation of the RSR kinases WEE1 and CHK1 results in cell cycle arrest, and the initiation of different mechanisms, such as DNA repair, senescence, or apoptosis, to maintain genomic integrity (Patil *et al.* 2014). Most cancer cells present high levels of replication stress (Macheret & Halazonetis, 2015) and a defective G1/S checkpoint, thus WEE1 and CHK1 inhibitors have been proposed as therapeutic agents for cancer not only as single agents but also in combination with radiation or other chemotherapy drugs that enhance replicative stress (Forment & O’connor 2018; Rundle *et al.* 2017).

Objectives: To test the effectiveness of PPRHs as a silencing tool for the RSR genes *WEE1* and *CHK1*, and to assess their effect when combined with other chemotherapies that promote replication stress.

Results: A total of seven PPRHs were designed, three directed against *WEE1* (HpWEE1Pr-T, HpWEE1I5-C, HpWEE1E11-C) and four against *CHK1* (HpCHK1I1-C, HpCHK1I1-T, HpCHK1I10-T, HpCHK1I13-C). All the designed PPRHs were able to reduce cell viability to a certain extent at 100 nM and none of the negative controls tested showed cytotoxicity. The most effective PPRHs against each gene (HpWEE1Pr-T and HpCHK1I1-C) were also effective in reducing cell viability in PC-3, MCF-7, SK-BR-3 and HepG2 cancer cells. In contrast, no reduction or a minor reduction on cell viability was observed in non-cancerous cells HEK-293 and ECV304 treated with these PPRHs. Moreover, both PPRHs were also tested in non-human cells from Chinese hamster ovary, whose DNA do not contain the target sequence of the PPRHs. We did not

Results

observe a decrease in cell viability, which highlight the specificity of these PPRHs.

Both PPRHs, HpWEE1Pr-T and HpCHK1I1-C, induced an increase of apoptosis and were capable of reducing the levels of mRNA and protein for their respective target genes in HeLa cells. When analyzing the levels of the two *CHK1* mRNA splicing variants, *CHK1* and *CHK1-S*, there was a proportional decrease of the two forms, thus maintaining the same expression ratio. Moreover, PPRHs targeting *WEE1* and *CHK1* also proved to disrupt cell cycle after 15 h of treatment.

Finally, we analyzed the effect of PPRHs targeting *WEE1* and *CHK1* when combined with methotrexate (MTX) or 5-Fluorouracil (5-FU), two agents that block the synthesis of dTTP de novo, and thus, increase replicative stress (Hagner & Joerger 2010; Longley *et al.* 2003). PPRHs showed a synergic effect when combined with either MTX or 5-FU.

Conclusions: This work validates *in vitro* the usage of PPRHs as a silencing tool against the RSR genes *WEE1* and *CHK1* and corroborates the potential of inhibiting these targets as a single agent or in combination with other chemotherapy agents in cancer therapy.



Targeting replication stress response using polypurine reverse hoogsteen hairpins directed against *WEE1* and *CHK1* genes in human cancer cells

Eva Aubets, Véronique Noé, Carlos J. Ciudad*

Department of Biochemistry and Physiology, School of Pharmacy and Food Sciences and Institute of Nanoscience and Nanotechnology (IN2UB), University of Barcelona (UB), 08028 Barcelona, Spain

ARTICLE INFO

Keywords:

PPRH
WEE1
CHK1
 Replication stress
 Cell cycle checkpoint
 DNA damage

ABSTRACT

In response to DNA damage, cell cycle checkpoints produce cell cycle arrest to repair and maintain genomic integrity. Due to the high rates of replication and genetic abnormalities, cancer cells are dependent on replication stress response (RSR) and inhibitors of this pathway are being studied as an anticancer approach. In this direction, we investigated the inhibition of *CHK1* and *WEE1*, key components of RSR, using Polypurine Reverse Hoogsteen hairpins (PPRHs) as gene silencing tool. PPRHs designed against *WEE1* or *CHK1* reduced the viability of different cancer cell lines and showed an increase of apoptosis in HeLa cells. The effect of the PPRHs on cell viability were dose- and time-dependent in HeLa cells. Both the levels of mRNA and protein for each gene were decreased after treatment with the PPRHs. When analyzing the levels of the two *CHK1* mRNA splicing variants, *CHK1* and *CHK1-S*, there was a proportional decrease of the two forms, thus maintaining the same expression ratio. PPRHs targeting *WEE1* and *CHK1* also proved to disrupt cell cycle after 15 h of treatment. Moreover, PPRHs showed a synergy effect when combined with DNA damaging agents, such as methotrexate or 5-Fluorouracil, widely used in clinical practice. This work validates *in vitro* the usage of PPRHs as a silencing tool against the RSR genes *WEE1* and *CHK1* and corroborates the potential of inhibiting these targets as a single agent therapy or in combination with other chemotherapy agents in cancer research.

1. Introduction

Genomic instability and mutation are one of the hallmarks of cancer. The high frequency of mutations enables cancer cells to develop the capability of surviving, proliferating, and disseminating [1]. Therefore, cells have evolved mechanisms to safeguard the integrity of the genome in response to DNA damage and to avoid cancer development [2].

Ataxia-telangiectasia mutated (ATM) and ataxia-telangiectasia and Rad3-related (ATR) kinases have a key role in initiating DNA damage response (DDR). In the presence of DNA damage, double-strand DNA breaks (DSBs) are detected by the MRE11-RAD50-NBS1 (MRN) complex, which activates the ATM/Checkpoint Kinase 2 (CHK2) pathway. In contrast, single-strand DNA breaks (ssDNA) are sensed by the Replication Protein A (RPA complex) leading to ATR/Checkpoint Kinase 1 (CHK1) pathway activation. Once ATM/CHK2 or ATR/CHK1 are activated, DDR is transduced to different effectors to produce either a cell cycle arrest or a cell cycle checkpoint activation and to repair DNA, or to activate programmed cell death [3–6].

Control of the G1/S checkpoint relies mainly on the ATM/CHK2

pathway, since there are not significant amounts of ssDNA. In contrast, S and G2/M checkpoints are under control of both pathways, ATM/CHK2 and ATR/CHK1 [5,7]. Most tumors cells have a deficient G1/S checkpoint; thus, cell cycle regulation relies on the G2/M checkpoint. Therefore, abrogation of the G2/M checkpoint using ATR-CHK1 pathway inhibitors has been proposed as an anticancer strategy in cancer cells, which have high rate of replication stress [2,8,9].

Activation of ATR and CHK1 kinases by DNA damage leads to *WEE1* protein kinase activation and CDC25 phosphatase inactivation. *WEE1* phosphorylates CDK1, which prevents the formation of the CDK1 – cyclin B complex. Furthermore, inhibition of CDC25 prevents the dephosphorylation of CDK1 and thus the formation of the CDK1 – cyclin B complex. The inactive form of the CDK1 – cyclin B complex activates G2/M checkpoint and prevents the entry into mitosis to facilitate DNA repair [2,8].

CHK1 kinase activity is also controlled by a splice variant of *CHK1* called *CHK1-short* or *CHK1-S*, which lacks exon 3. *CHK1-S* binds to *CHK1* leading to *CHK1* inhibition. In G2 phase, *CHK1* levels decrease while *CHK1-S* levels increase, in order to decrease *CHK1* activity and to promote mitotic entry. After DNA damage, the phosphorylation of

* Corresponding author at: Av. Juan XXIII # 27, 08028 Barcelona, Spain.
 E-mail address: cc Ciudad@ub.edu (C.J. Ciudad).

<https://doi.org/10.1016/j.bcp.2020.113911>

Received 2 January 2020; Accepted 10 March 2020

Available online 13 March 2020

0006-2952/© 2020 Elsevier Inc. All rights reserved.

Table 1
DNA sequences corresponding to the PPRHs used in the study.

Name	Sequence (5'-3')	Location
HpWEE1Pr-T	GGGACGAGGGGCAAGAAGCGG T T GGGACGAGGGGCAAGAAGCGG T T	Promoter
HpWEE1I5-C	GGGAGAGGAGGGAGAGACGACAAG T T GGGAGAGGAGGGAGAGACGACAAG T T	Intron 5
HpWEE1E11-C	GGGAGGTGGGAAAGGAGTAG T T GGGAGGTGGGAAAGGAGTAG T T	Exon 11
HpCHK1I1-T	GTGGATGAGATAGAAGGGGAAGG T T GTGGATGAGATAGAAGGGGAAGG T T	Intron 1
HpCHK1I1-C	GGGAAGGAGGAGGGAGAGGTGGG T T GGGAAGGAGGAGGGAGAGGTGGG T T	Intron 1
HpCHK1I10-T	AAGGAAGAAAGAGAGGAGGGAGG T T AAGGAAGAAAGAGAGGAGGGAGG T T	Intron 10
HpCHK1I13-C	AGGTGAGGAGGATAGGCAGA T T AGGTGAGGAGGATAGGCAGA T T	Intron 13
HpSC4	AGAGAAGAGGAAGAGAGGAAAGAGAGGAAGAGGA T T AGAGAAGAGGAAGAGAGGAAAGAGAGGAAGAGGA T T	-
HpWEE1Pr-T-WC	GGGACGAGGGGCAAGAAGCGG T T CCCTGCTCCCCGTTCTTCGCC T T	-
HpCHK1I1-C-WC	GGGAAGGAGGAGGGAGAGGTGGG T T CCCTTCTCCTCCCTCCTCCACCC T T	-

Name, sequence and location of the specific PPRHs designed against *WEE1* and *CHK1* and the negative controls (HpSC4, HpWEE1Pr-T-WC and HpCHK1I1-C-WC). C and T refers to the type of PPRHs used, either against the coding or the template strands, respectively.

CHK1 by ATR triggers the dissociation of CHK1-S from CHK1, which results in CHK1 activation and G2/M arrest [10,11].

Inhibitors of the ATR-CHK1 pathway have been proposed as therapeutic agents in cancer not only as single agents but also in combination with radiation or other chemotherapy drugs that enhance replicative stress. Since extensive preclinical data support this approach, different replication stress response (RSR) inhibitors have entered in clinical stages. In the case of CHK1 inhibitors, some failed to improve the efficacy in combination with other chemotherapies [12–14] or to prove safety because of the nonspecific targeting [15,16]. Encouragingly, LY2606368, MK8776, GDC-0575, SRA737 (CHK1 inhibitors) and AZD1775 (WEE1 inhibitor) [17,18] are currently being tested in clinical trials, some of them with positive results [19–22].

Given the importance of CHK1 and WEE1 kinases in DDR, we decided to design sequence specific Polypurine Reverse Hoogsteen hairpins (PPRHs) as a new approach to silence both replicative stress genes in a highly specific manner. The ability of PPRHs to inhibit different genes involved in the development of cancer has been proved *in*

vitro [23–25] and *in vivo* [26].

PPRHs are double stranded non-modified DNA molecules formed by two antiparallel polypurine mirror repeat sequences. These two specular domains are linked by a pentathymidine loop and bound intramolecularly by reverse-Hoogsteen bonds between the purines, thus producing a hairpin structure. A given PPRH can bind to a specific polypyrimidine sequence of double-stranded DNA (dsDNA) by Watson-Crick and form a triplex structure, which causes the displacement of the fourth strand of the dsDNA [27]. That complex interferes with DNA transcription, resulting in the specific inhibition of the target gene [25,28]. PPRHs can be directed either to the coding strand (C-PPRHs) or to the template strand (T-PPRHs) in the DNA.

We also aimed to assess the effect of PPRHs directed to RSR genes when combined with other chemotherapies that produce DNA damage. To this end, we chose methotrexate (MTX) and/or 5-Fluorouracil (5-FU), two agents widely used in the treatment of cancer. Both drugs have in common the blockage of *de novo* synthesis of dTTP, which results in an increase of dUTP levels and the imbalance of the dNTPs pool, thus

increasing DNA damage. While 5-FU inhibits thymidylate synthase (TYMS), enzyme that catalyze the conversion from dUMP to dTMP, MTX inhibits dihydrofolate reductase (DHFR), enzyme that catalyzes the reduction of dihydrofolate (DHF) to Tetrahydrofolate (THF), required for dTMP and purine synthesis [29,30].

The purpose of this study was to test the effectiveness of PPRHs as a new tool to inhibit replicative stress genes *WEE1* and *CHK1* in cancer therapy and to sensitize tumor cells to DNA-damaging agents.

2. Materials and methods

2.1. Cell culture

HeLa (human cervical carcinoma), PC-3 (human prostate adenocarcinoma cells), HepG2 (human liver hepatocellular carcinoma), MCF-7 (human breast adenocarcinoma), and SK-BR-3 (human breast adenocarcinoma), HEK-293 (Human embryonic kidney cells), ECV304 (Human endothelial cell) and CHO-DG44 (Chinese hamster ovary) obtained from cell bank resources from the UB, were grown in Ham F12 medium supplemented with 10% fetal bovine serum (GIBCO, Invitrogen, Barcelona, Spain) and incubated at 37 °C in a humidified 5% CO₂ atmosphere.

2.2. Design and usage of PPRHs

The PPRHs used in this study were made up of two antiparallel mirror repeats polypurine domains, bound by intramolecular reverse Hoogsteen bonds, and linked by a pentathymidine loop (T5). The Triplex-forming Oligonucleotide Target Sequence Search software (<http://utw10685.utweb.utexas.edu/tfo/>) MD Anderson cancer center, The University of Texas) was used to find the polypurine stretches, whose complementary sequence would be the polypyrimidine tracks of the target gene. Then, the PPRH sequences were designed by fusing the polypurine stretch to its mirror repeat using a T5 linker. BLAST analyses were performed to confirm the specificity of the designed PPRHs.

Three PPRHs were designed against *WEE1* (HpWEE1Pr-T, HpWEE1I5-C, HpWEE1E11-C) targeting polypyrimidine sequences in its promoter, intron 5 and exon 11, respectively; and 4 against *CHK1* (HpCHK1I1-C, HpCHK1I1-T, HpCHK1I10-T, HpCHK1I13-C), targeting sequences in introns 1, 10 and 13. As a negative control, we used a polypurine scrambled hairpin (HpSC4) and hairpins with intramolecular Watson–Crick bonds (WC-PPRH), HpWEE1Pr-T-WC and HpCHK1I1-C-WC, instead of Hoogsteen bonds. The PPRH sequences designed against *WEE1* and *CHK1* and the negative controls are shown in Table 1 and the mechanism of action for PPRHs illustrated in Fig. 1.

The sequences were synthesized as non-modified oligodeoxynucleotides by Sigma-Aldrich (Haverhill, United Kingdom) and then resuspended in sterile Tris-EDTA buffer (1 mM EDTA and 10 mM Tris, pH 8.0) (Sigma-Aldrich, Madrid, Spain) and stored at –20 °C.

2.3. Transfection of PPRHs

Cells were plated in 6-well dishes one day before transfection in F12 medium. The transfection procedure consisted in mixing N-[1-(1,2-Di-(9Z)-octadecenoyl)-3-trimethylammoniumpropane methyl sulfate in water (DOTAP; Biontix) with the corresponding PPRH in a molar ratio of 1:100 (PPRH/DOTAP), (100 nM/10 μM, unless stated otherwise) and serum free medium up to 200 μL. The mixture was incubated for 20 min at room temperature and added to the cells in a final volume of 1 mL of full medium.

2.4. Targeting RSR using PPRHs in combination with MTX or 5-FU

Cells were plated in 6-well dishes in RPMI medium one day before transfection. The transfection procedure was performed as indicated in 2.3 Transfection section. Either MTX or 5-FU were added to the cells

alone or simultaneously with the PPRH in a final volume of 1 mL. MTX (55 mM, Pfizer, Madrid, Spain) was diluted in RPMI medium and 5-FU (Sigma-Aldrich, Madrid, Spain) was prepared from powder as a 100 mM stock solution in DMSO and diluted in RPMI medium.

2.5. MTT assay

Cells (10,000) were plated in 6-well dishes in F12 medium. Five days after transfection or MTX or 5-FU treatment, 0.63 mM of 3-(4,5-dimethylthiazol-2-yl)-2,5-diphenyltetrazolium bromide and 100 μM sodium succinate (both from Sigma-Aldrich, Madrid, Spain) were added to the culture medium and incubated for 2,5h at 37 °C. After incubation, culture medium was removed and the lysis solution (0.57% of acetic acid and 10% of sodium dodecyl sulfate in dimethyl sulfoxide) (Sigma-Aldrich, Madrid, Spain) was added. Absorbance was measured at 570 nm in a Modulus Microplate spectrophotometer (Turner BioSystems). The results were expressed as the percentage of cell survival relative to the controls.

2.6. Apoptosis assay

Apoptosis was determined by the rhodamine method. Briefly, 60,000 HeLa cells were transfected with the selected PPRHs and after 20 h of incubation, rhodamine 123 (final concentration 5 μg/mL) (Sigma-Aldrich) was added to the cells for 30 min at 37 °C. Then, cells were collected by trypsinization, centrifuged at 800 × g at 4 °C for 5 min and washed once in PBS. The pellet was resuspended in 500 μL of PBS and Propidium Iodide was added to a final concentration of 5 mg/mL (Sigma-Aldrich). Flow cytometry analyses were performed in a CyAn™ ADP (Beckman Coulter, Inc, Spain) and data were analyzed using the software Summit v4.3. Rho123-positive and IP-negative cells were considered as living cells, Rho123-negative and IP-negative as apoptotic cells, and Rho123-negative and IP-positive as necrotic cells.

2.7. RNA extraction

Total RNA was extracted from 30,000 HeLa cells using TRIzol® (Life Technologies) following the manufacturer's specifications. RNA was quantified by measuring its absorbance at 260 nm using a NanoDrop ND-1000 spectrophotometer (Thermo Scientific).

2.8. Reverse transcription

cDNA was synthesized by reverse transcription in a 20 μL reaction mixture containing 1 μg of total RNA, 125 ng of random hexamers (Roche, Spain), 500 μM of each dNTP (Bioline, Barcelona, Spain), 2 μL of buffer (10×), 20 units of RNase inhibitor and 200 units of Moloney murine leukemia virus reverse transcriptase (Last three from Lucigen, Wisconsin, USA). The reaction was incubated at 42 °C for 1 h.

2.9. Real-time PCR

To determine *WEE1* and *CHK1* mRNA levels, a QuantStudio 3 Real-Time PCR System (Applied Biosystems, Barcelona, Spain) was used with the following TaqMan probes: *WEE1* (Hs01119384_g1), *CHK1* (Hs00967506_m1) and TATA-binding protein (TBP, used as endogenous control) (Hs00427620_m1). The reaction was conducted in 20 μL containing 1x TaqMan Universal PCR Mastermix (Applied Biosystems), 0.5x TaqMan probe (Applied Biosystems), 3 μL of cDNA and mQ H₂O. PCR cycling conditions were 10 min denaturation at 95 °C, followed by 40 cycles of 15 s at 95 °C and 1 min at 60 °C. mRNA quantification was calculated using the $\Delta\Delta C_T$ method, where C_T is the threshold cycle that corresponds to the cycle where the amount of amplified mRNA reaches the threshold of fluorescence.

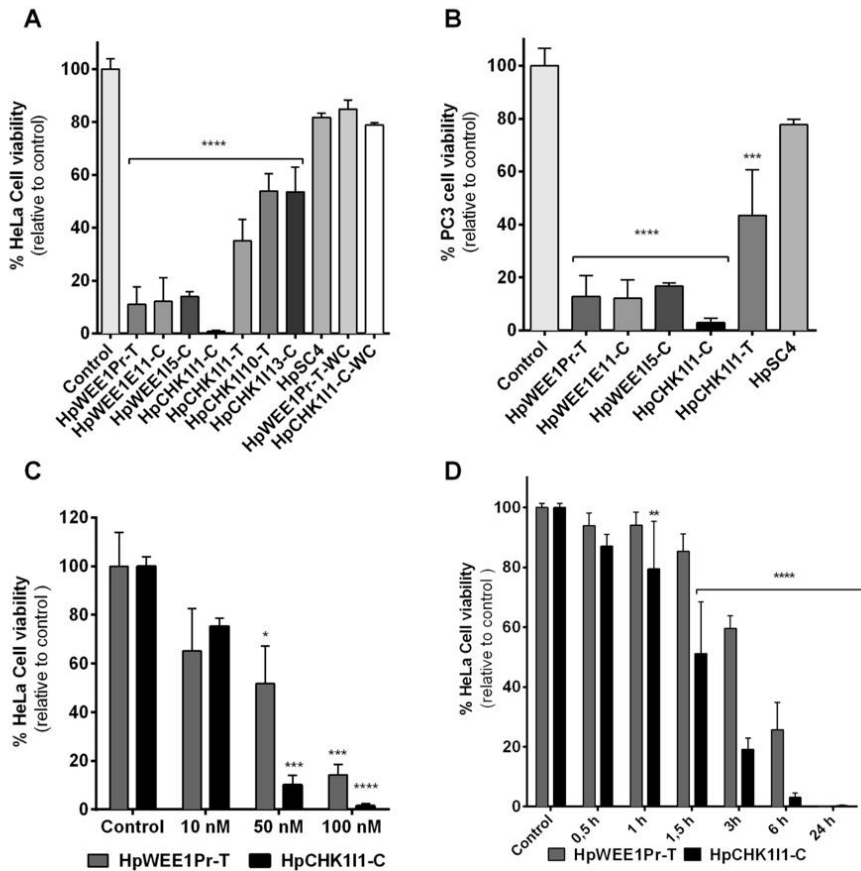


Fig. 2. Effect on cell viability by PPRHs directed against replicative stress response genes. All cell viability assays were conducted 5 days after transfection. (A) HeLa cells (10,000) viability upon treatment with all the PPRHs designed against *WEE1* and *CHK1*, and the negative controls (HpSC4, HpWEE1Pr-T-WC and HpCHK111-C-WC). (B) Viability of PC-3 cells (10,000) treated with the most effective PPRHs designed against *WEE1* and *CHK1* and the negative control. (C) Dose-response of HpWEE1Pr-T and HpCHK111-C in HeLa cells. The cationic liposome DOTAP was used to transfect the cells using a 1:100 PPRH/Liposome ratio. However, when transfecting PPRHs at 10 nM, 5 μ M DOTAP was used. (D) Time-course of HpWEE1Pr-T and HpCHK111-C in HeLa cells, after incubating cells with 100 nM of PPRHs. Changes of medium were conducted at 0.5, 1, 1.5, 3, 6 and 24 h and MTT assay was performed after 5 days of the transfection. Data represent the mean \pm SEM from 3 experiments. Statistical significance was determined using one-way ANOVA with Dunnett's multiple comparison test for figures A and B, two-ways ANOVA with Sidak's multiple comparisons test for dose-response and two-ways ANOVA with Dunnett's and time-course figures. (* $p < 0.05$, ** $p < 0.01$, *** $p < 0.001$, **** $p < 0.0001$).

expected to result in an increase in replicative stress leading to cell death. Therefore, all the PPRHs designed against *WEE1* and *CHK1* were tested in cell viability assays individually at 100 nM in HeLa cells to compare their effectiveness. All the PPRHs were able to reduce cell viability to a certain extent (Fig. 2A), standing out the decrease produced by HpCHK111-C. The five most effective PPRHs were also tested in the PC-3 cell line with similar results (Fig. 2B).

In addition, the most effective PPRH against each target were tested in three additional cells lines, namely MCF-7, SK-BR-3 and HepG2. HpCHK111-C was the most effective, causing a decrease in cell viability of 95%, 75% and 80%, respectively.

None of the negative controls tested showed cytotoxicity. Two kind of negative controls were used: a hairpin with a scrambled sequence maintaining the Hoogsteen bonds (HpSC4), and hairpins with intramolecular Watson-Crick bonds instead of Hoogsteen bonds (HpWEE1Pr-T-WC and HpCHK111-C-WC), which are not able to form triplexes. These negative controls were designed to prove that when the

triplex is not formed, there is no decrease in gene expression, even if the polypurine sequence is present. In this direction, no decrease on HeLa cell viability was observed in the presence of these controls, indicating that the cytotoxic effect after PPRHs treatment was due to a decrease in gene expression.

Furthermore, we conducted cell viability assays in HEK-293 and ECV304 cells to evaluate the PPRH-mediated viability effect in non-cancerous cells. In ECV304 cells, the specific PPRHs targeting *WEE1* did not affect cell viability and *CHK1* caused a decrease of 20%. In HEK293 cells the decrease caused by the PPRHs was 29% for *WEE1*, and 24% in the case of *CHK1*, when using the same concentrations that caused a more than 85% reduction in viability in HeLa cells. Additionally, we also tested PPRHs in a non-human cell line (CHO-DG44 from hamster) and we did not observe a significant effect on cell survival.

Then, we proceeded to perform dose- and time-dependent studies with the most effective PPRHs for each gene, HpWEE1Pr-T and HpCHK111-C, in HeLa cells. The concentrations used in dose-response

Results

E. Aubets, et al.

Biochemical Pharmacology 175 (2020) 113911

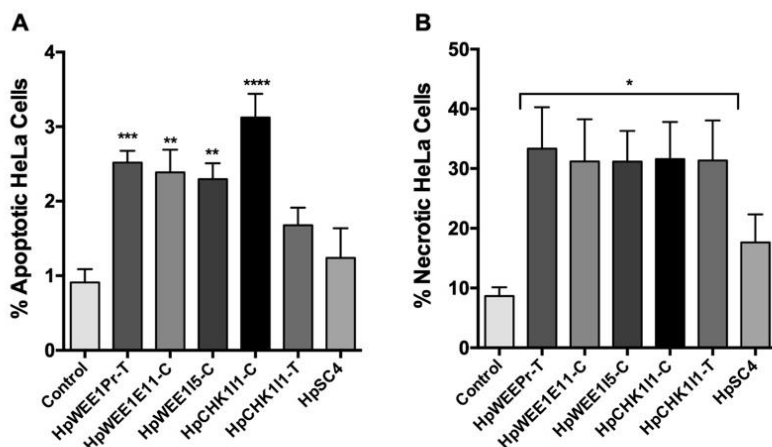


Fig. 3. Determination of apoptosis upon PPRH incubation for 20 h in HeLa cells (60,000). Percentages of apoptotic cells (A) and necrotic cells (B) after treatment with different PPRHs against *WEE1* and *CHK1* at 100 nM. The percentage of Rho-negative and IP-negative cells corresponded to the apoptotic population, whereas Rho123-negative and IP-positive represented necrotic cells. Data represent the mean \pm SEM from 3 experiments. Statistical significance was determined using a one-way ANOVA with Dunnett's multiple comparisons test (* $p < 0.05$, ** $p < 0.01$, *** $p < 0.001$, **** $p < 0.0001$).

were 10, 50 and 100 nM. Time-course assays were carried out using 100 nM of PPRHs and by changing the culture medium after 0.5, 1, 1.5, 3, 6 and 24 h upon transfection. Both PPRHs showed a dose-dependent effect in reducing cell viability. HpCHK1I11-C was the most cytotoxic with more than 85% reduction in cell viability at 50 nM. At this concentration, HpWEE1Pr-T reduced cell viability by almost a half compared to control (Fig. 2C). In addition, HpWEE1Pr-T and HpCHK1I11-C were already cytotoxic after only 3 h of cell incubation, reducing cell viability to 60% and 19%, respectively (Fig. 2D).

3.2. Effects of PPRHs on apoptosis levels

To get an insight into the mechanism that lead to cytotoxicity in cancer cells upon incubation with PPRHs against *WEE1* and *CHK1*, we determined the levels of apoptosis in these conditions. After 20 h of incubation with each PPRH, the apoptotic cell population increased between 2 and 3-fold (Fig. 3A). Furthermore, the necrotic cells population increased from 8% in the control cells to more than 30% in treated cells (Fig. 3B). The negative control did not show statistical differences compared to the control of untreated cells.

3.3. Effect of PPRHs on mRNA levels

To validate that the effects observed in cell viability and apoptosis were caused by a decrease in gene expression, mRNA levels after the treatment with the most effective PPRHs against *WEE1* and *CHK1* were determined in HeLa cells. HpWEE1Pr-T and HpCHK1I11-C were able to

decrease the mRNA levels of their target genes 1.6 and 1.9-fold respectively (Fig. 4). The negative HpSC4 control did not produce changes in the mRNA levels of neither *WEE1* nor *CHK1*.

3.4. Effect of PPRHs on different *CHK1* splicing variants

As *CHK1* presents several variants due to alternative splicing, we also examined the effect of HpCHK1I11-C on the different *CHK1* forms after 24 h of treatment. Accordingly, we amplified the cDNA from treated and not treated cells with different combinations of primers that annealed to specific exons. Since *CHK1-S* splicing variant lacks exon 3, amplification from exons 3 to 9 led to a single product of 771 pb (Fig. 5B) whereas amplification from exon 2 to exon 9 generated the two *CHK1* splicing variants, *CHK1-L* (841 bp) and *CHK1-S* (617 bp) (Fig. 5A). Quantification of the PCR products from exon 2 to exon 9 showed a decrease in the intensity of the two bands in treated cells when compared to those observed in untreated cells (Fig. 5C). This decrease was around 30–40% for both forms, resulting in no variation in the *CHK1-S/CHK1* mRNA splicing variants ratio. Quantification of the amplicon from exon 3 to 9 from treated cells also revealed a decrease of its intensity, which was of 57% relative to control cells (Fig. 5D).

3.5. Effects of PPRHs on *WEE1* and *CHK1* protein levels

The determination of protein levels in HeLa cells showed a decrease by 50% in *WEE1* protein levels after 24 h incubation with HpWEE1Pr-T

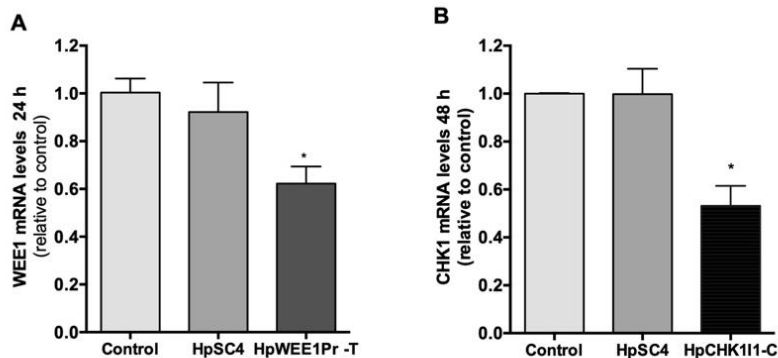


Fig. 4. Effect of PPRHs on *WEE1* and *CHK1* mRNA levels. HeLa cells (30,000) were incubated with 100 nM of PPRH and 10 μ M of DOTAP. Upon transfection, RNA extraction was conducted after 24 h for HpWEE1Pr-T (A), or after 48 h for HpCHK1I11-C (B). The levels of mRNA were determined by qRT-PCR and *TBP* was used to normalize the results. Data represent the mean \pm SEM from 3 experiments. Statistical significance was determined using a one-way ANOVA with Dunnett's multiple comparisons test (* $p < 0.05$).

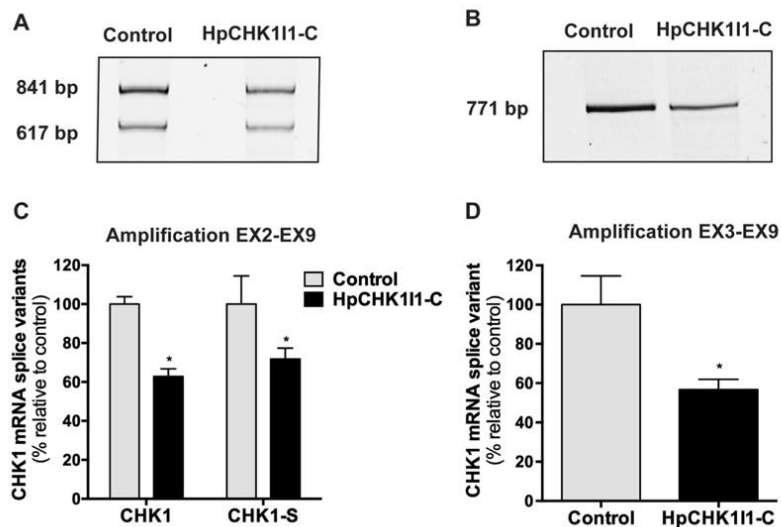


Fig. 5. Effect of HpCHK111-C on *CHK1* splicing variants in HeLa cells. PCR products obtained in control and treated cells upon amplification with primers Fw-EX2-CHK1 and Rv-EX9-CHK1 (A) and Fw-EX3-CHK1 and Rv-EX9-CHK1 (B). Quantification of the intensity of bands corresponding to the PCR products amplified with Fw-EX2-CHK1 and Rv-EX9-CHK1 (C) and Fw-EX3-CHK1 and Rv-EX9-CHK1 (D) and resolved by acrylamide gel electrophoresis. Data represent the mean \pm SEM from 3 experiments. Statistical significance was determined using χ^2 test and two-ways ANOVA with Sidak's multiple comparison test for Figure C and Unpaired Student's T test for Figure D (* $p < 0.05$).

(Fig. 5A) and a decrease by 45% in CHK1 protein levels after 15 h of incubation with HpCHK111-C (Fig. 6B).

3.6. Effect of HpWEE1Pr-T and HpCHK111-C on the cell cycle

Since WEE1 and CHK1 kinases play an important role in cell cycle regulation, we analyzed the effect of 100 nM HpWEE1Pr-T and HpCHK111-C on the different phases of the cell cycle upon 15 h of incubation (Fig. 7A). The values for HeLa control cells populations were 58%, 39% and 3% in G1, S and G2/M phases, respectively. HpWEE1Pr decreased the percentage of cells in G1 phase to 49% and increased G2/

M phase to 20.8%. In the same direction, HpCHK111-C reduced G1 phase to 47% and raised G2/M phase to 20.2% (Fig. 7B). Those results proved that PPRHs directed against RSR genes disrupted the cell cycle.

3.7. Sensitization of HeLa cells to methotrexate or 5-Fluorouracil using PPRHs

Once determined the effectivity of PPRHs to inhibit RSR genes and their capacity to kill cancer cells, we assessed the ability of these PPRHs to sensitize cancer cells to 5-FU or MTX. After performing a dose-response with 5-FU, we selected the concentration of 1 μ M (which

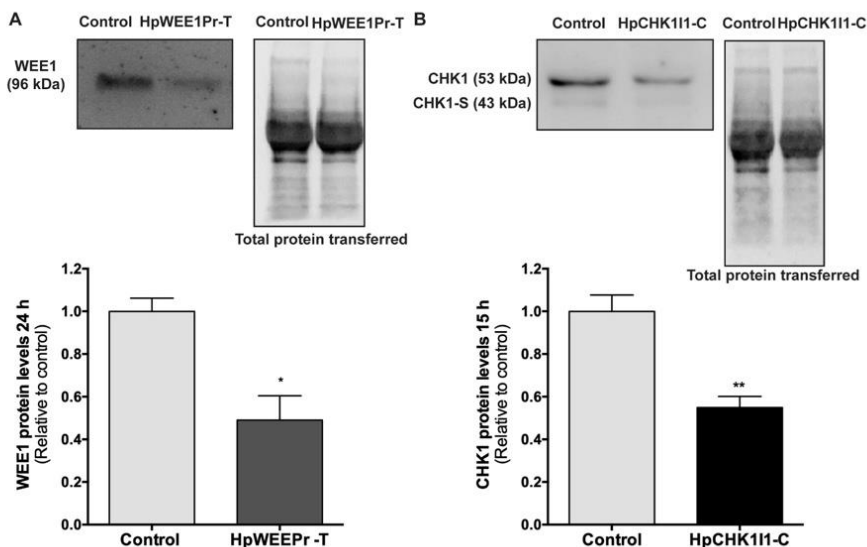


Fig. 6. Effect of PPRHs on WEE1 and CHK1 protein levels. Proteins extracts from HeLa cells (30,000) were obtained after 24 h of transfection with 100 nM of HpWEE1Pr-T (A) or 15 h after transfection with 100 nM of HpCHK111-C (B). Representative images of Western blots and total protein transferred to the membranes are shown. Protein levels were normalized using the quantification of the total protein transferred. Data represent the mean \pm SEM of at least 3 experiments. Statistical significance was determined using Unpaired Student's T test (* $p < 0.05$, ** $p < 0.01$).

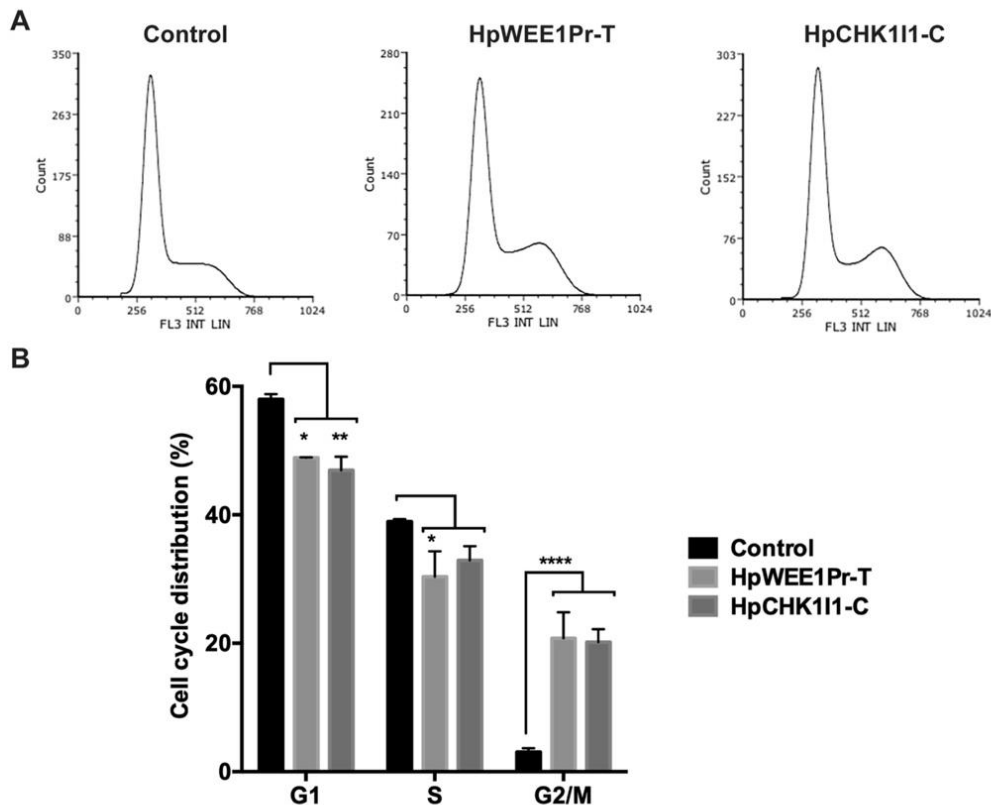


Fig. 7. Effect of HpWEE1Pr-T and HpCHK111-C on cell cycle distribution. Representative images (A) and percentages (B) of cell cycle distribution after 15 h of incubation with PPRHs. Data represent the mean \pm SEM of at least 3 experiments. Statistical significance was determined using two-way ANOVA with Dunnett's multiple comparison test (* $p < 0.05$, ** $p < 0.01$, **** $p < 0.0001$).

corresponded to IC30) to conduct the combination assays. In the case of MTX, we selected a range of concentrations between 10 and 15 nM (93–59% of remaining cell viability). For PPRHs, the concentrations selected were 50 nM for HpWEE1Pr-T and 30 nM for HpCHK111-C which by themselves produce a decrease in cell viability of < 35%. Both PPRHs, HpWEE1Pr-T and HpCHK111-C, when incubated with either 5-FU or MTX showed a synergic effect, as calculated by the CompusSyn software [31]. For instance, the combination of 5-FU 1 μ M and HpCHK111-C 30 nM decreased cell viability down to 25% (Fig. 8A). Similarly, 15 nM of MTX combined with 30 nM of HpCHK111-C reduced cell viability to 15% (Fig. 8B).

4. Discussion

In this study, we present PPRHs as a new approach to inhibit the replicative stress response (RSR) genes *WEE1* and *CHK1*. Different drugs targeting DDR have proved their effectivity *in vitro* and *in vivo* in preclinical assays as single agents or in combination with other therapies. Some *WEE1* or *CHK1* inhibitors are currently in clinical trials and most of them aim to sensitize different tumors to chemotherapy agents or radiation [19–21]. So far, only Poly-ADP-ribose polymerase inhibitors (olaparib, rucaparib, niraparib and talazoparib) have been approved by the Food and Drug Administration (FDA) and the European Medicines Agency (EMA) for cancer patients bearing a mutated *BRCA* gene. This fact encourages the development and the study of new agents targeting DDR in cancer treatments approaches [20,32–34]. In

this direction, as an alternative approach to target DDR genes, we explored the usage of PPRHs, whose effectivity as a gene silencing tool has been previously validated for other targets *in vitro* and *in vivo* [24,26,28]. These molecules work at nanomolar concentration, show a longer half-life than siRNAs, they do not activate the immunogenic response and present great advantages in terms of economy when compared to siRNA [35].

In the present work, we designed a set of PPRHs directed toward different regions of the *WEE1* and *CHK1* genes to produce the specific silencing of both genes. Of note, all the tested PPRHs were able to kill HeLa cancer cells at a final concentration of 100 nM. Although hypothetically an interaction between the DNA hairpin and cellular proteins could not be excluded, all negative controls tested did not produce a significant effect on HeLa cells viability, neither scrambled PPRHs nor WC-PPRH. Moreover, PPRHs did not cause a decrease on viability in cells lacking the target sequence such as CHO-DG44. Therefore, there are evidences to consider that PPRHs directed to RSR produced a specific effect on gene expression and that they might not interact with other elements that could produce a lethal effect on cells.

PPRHs produced cytotoxicity in a variety of cancer cell lines (HeLa, PC-3, HepG2, SK-BR-3, MCF-7). Originally, targeting RSR was a potential approach in p53 defective cancer cells, since G1 checkpoint is deficient and therefore the control of DNA damage relies on G2/M checkpoint. However, although in some studies RSR inhibitors showed greatest sensitivity in p53 deficient cells, some preclinical and clinical data proved effectiveness of DDR inhibitors regardless p53 status. Thus,

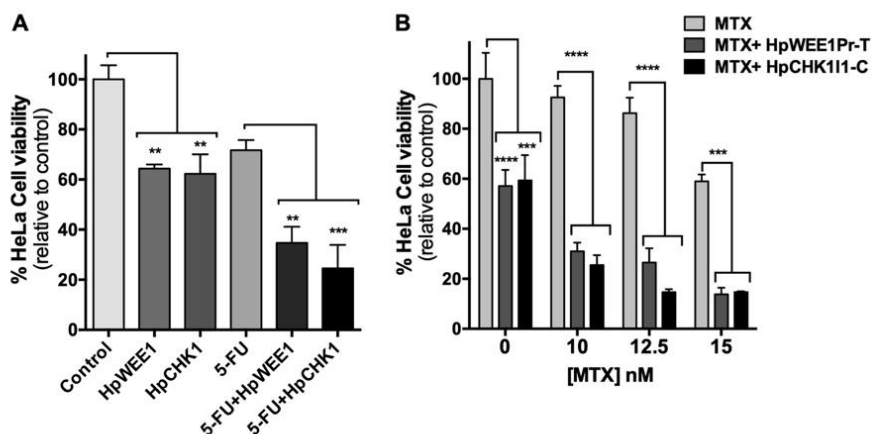


Fig. 8. Effect on cell viability when combining PPRHs directed against RSR genes with DNA-damaging agents. (A) HeLa cells (10,000) were incubated with 5-FU (1 μ M) in the absence or in the presence of HpWEE1Pr-T (50 nM) or HpCHK111-C (30 nM). (B) HeLa cells (10,000) were treated with MTX at different concentrations (0, 10, 12.5, 15 nM) in the absence or the presence of HpWEE1Pr-T (50 nM) or HpCHK111-C (30 nM). Cell viability assays were conducted 5 days either after transfection and/or after treatment with DNA-damaging agents. Data represent the mean \pm SEM of at least 3 experiments. Statistical significance was determined using one-way ANOVA with Dunnett's multiple comparison test for combinations with 5-FU and two-way ANOVA with Dunnett's multiple comparison test for MTX combinations (** p < 0.01, *** p < 0.001, **** p < 0.0001). Statistical significance was determined comparing PPRHs alone to control, and comparing the effect of DNA-damaging agent plus PPRHs to the DNA-damaging agent alone.

the role of p53 status is unclear and the efficacy of drugs targeting RSR is studied in different type of cancers [3,20]. Nevertheless, aside from p53, other aspects could affect the efficiency of targeting DDR. Cancer cells with higher rates of replication would be more responsive to this therapy relative to normal tissues, since loss of function of the ATR-CHK1 axis produces DNA damage in replicating cells. Furthermore, cancer cells with overexpression of oncogenes that enhance replication stress, or with an overexpressed ATR-CHK1-WEE1 pathway to overcome replication stress, would be potential candidates to be treated with this approach. Finally, RSR inhibitors would be favorable in cells with deficient DNA repair mechanisms, such as homologous recombination [20,36].

In cancer cells, the high rates of replication induce a stalled replication fork and fork collapses. It is proposed that to repair DNA by homologous recombination, stalled forks are cleaved, DSBs are detected by ATM and exposed ssDNA activates the ATR-CHK1-WEE1 pathway [36,37]. Therefore, inhibition of WEE1 and CHK1 produces an increase in CDK activity which induces S-phase entry, leading to a shortage of nucleotides and stalled replication forks. As a result, SLX4-MUS81 nuclease could generate DSBs to be detected by ATM-p53-p21 pathway. After G2/M checkpoint abrogation, the most sensitive cells can initiate apoptosis at S phase or early G2 phase, whereas the cells that are able to progress to G2/M phases die due to incomplete DNA replication, to unrepaired DNA damage and to accumulation of chromosomal breaks that results in mitotic catastrophe [36,38,39]. These observations would be in keeping with the accumulation in G2/M phase observed upon inhibition of WEE1 and CHK1 by PPRHs, due to a premature entry and prolonged mitosis with damaged DNA because of checkpoint failure, which is the mechanism attributed to WEE1 and CHK1 inhibitors [40,41], and in agreement with previous results reported on the inhibition of CHK1 [40,42] or WEE1 [40,43].

We also corroborate that inhibition of RSR genes induces apoptosis. As mentioned above and reported in other studies [40,44], inhibition of WEE1 and CHK1 induce cells to progress to apoptosis or to an anticipated mitosis without a previous DNA repair. This premature entry into mitosis results in a mitotic catastrophe and increased DNA damage that activates the apoptotic signaling cascade [45,46]. Accordingly, the

PPRHs producing the highest levels of apoptosis after 20 h of incubation were those with the highest values of cytotoxicity observed in cell viability assays.

The loss of functionality of CHK1 and WEE1 kinases results in an excess of replication stress exposure in cancer cells and death. Thus, the inhibition of WEE1 and CHK1 kinases could be considered as a single agent cancer therapy [36,39]. Moreover, since inhibition of WEE1 and CHK1 impairs mechanisms associated to DNA repair, such as homologous recombination, making cells more sensitive to DNA damage, RSR inhibitors are also used in combination with radiation or other chemotherapy agents that enhance replicative stress [36,47,48]. Different *in vitro*, *in vivo* and clinical studies, that combine RSR inhibitors with other chemotherapies, such as gemcitabine or radiotherapy, reported a synergic effect or are currently in progress [17,49,50]. In this direction, we show that PPRHs targeting RSR, either WEE1 or CHK1, can enhance the response to DNA-damaging agents, such as 5-FU or MTX.

Mechanistically, we show that PPRHs can decrease both mRNA and protein levels, which results in cell cycle impairment and an increase in apoptotic cells followed by cell death. These results are consistent with those reported in Yan Luo *et al.*, R. Russel *et al.* and Tang *et al.*, where decreases in expression produced very significant decreases in cell viability [51–53]. Moreover, to deepen into HpCHK111-C mechanism of action, we studied its effect on CHK1 mRNA and CHK1-S mRNA levels, the latter a shorter variant resulting from alternative splicing, whose role consists in repressing CHK1 and promoting mitotic entry [10,11]. The analysis of these two isoforms in HeLa cells treated with HpCHK111-C did not reveal any change in the CHK1-S/CHK1 mRNA splicing variants ratio. Since HpCHK111-C anneals to intron 1, it probably interferes with transcription of both isoforms with no distinction, resulting in a proportional decrease of both variants.

In conclusion, in this work we have validated *in vitro* the usage of PPRHs as a silencing tool for the replicative stress genes WEE1 and CHK1, both at the level of mRNA and protein, thus corroborating the potential of targeting the RSR machinery as a cancer therapeutic approach. Thereby, we demonstrated the feasibility of using PPRHs both as a tool for validating new targets and as pharmacological agents in cancer therapy.

Results

E. Aubets, et al.

Biochemical Pharmacology 175 (2020) 113911

CRedit authorship contribution statement

Eva Aubets: Investigation, Methodology, Validation, Formal analysis, Writing - original draft. **Véronique Noé:** Funding acquisition, Project administration, Writing - review & editing. **Carlos J. Ciudad:** Conceptualization, Visualization, Supervision.

Declaration of Competing Statement

The authors declare that they have no known competing financial interests or personal relationships that could have appeared to influence the work reported in this paper.

Acknowledgements

This work was supported by grant RTI2018-093901-B-I00 from Plan Nacional de Investigación Científica (Spain). Our group holds the Quality Mention from the Generalitat de Catalunya (2017-SGR-94). EA is the recipient of a FI fellowship from Generalitat de Catalunya.

References

- [1] D. Hanahan, R.A. Weinberg, Hallmarks of cancer: the next generation, *Cell* 144 (2011) 646–674, <https://doi.org/10.1016/j.cell.2011.02.013>.
- [2] C.S. Sorensen, R.G. Syljuåsen, Safeguarding genome integrity: the checkpoint kinases ATR, CHK1 and WEE1 restrain CDK activity during normal DNA replication, *Nucleic Acids Res.* 40 (2012) 477–486, <https://doi.org/10.1093/nar/gkr697>.
- [3] K. Do, J.H. Doroshov, S. Kummar, Wee1 kinase as a target for cancer therapy, *Cell Cycle*. 12 (2013) 3159–3164, <https://doi.org/10.4161/cc.26062>.
- [4] S.C. Lenzen, A. Loffreda, S.M.L. Barabino, RNA splicing: a new player in the DNA damage response, *Int. J. Cell Biol.* 2013 (2013) 153634, <https://doi.org/10.1155/2013/153634>.
- [5] A.N. Blackford, S.P. Jackson, ATM, ATR, and DNA-PK: the trinity at the heart of the DNA damage response, *Mol. Cell*. 66 (2017) 801–817, <https://doi.org/10.1016/j.molcel.2017.05.015>.
- [6] A. Maréchal, L. Zou, DNA damage sensing by the ATM and ATR kinases, *Cold Spring Harb. Perspect. Biol.* 5 (2013), <https://doi.org/10.1101/cshperspect.a012716>.
- [7] M.B. Kastan, J. Bartek, Cell-cycle checkpoints and cancer, *Nature* 432 (2004) 316–323, <https://doi.org/10.1038/nature03097>.
- [8] C.J. Matheson, D.S. Backos, P. Reigan, Targeting WEE1 Kinase in Cancer, *Trends Pharmacol. Sci.* 37 (2016) 872–881, <https://doi.org/10.1016/j.tips.2016.06.006>.
- [9] M. Dobbstein, C.S. Sorensen, Exploiting replicative stress to treat cancer, *Nat. Rev. Drug Discov.* 14 (2015) 405–423, <https://doi.org/10.1038/nrd4553>.
- [10] N. Pabla, K. Bhatt, Z. Dong, Checkpoint kinase 1 (Chk1)-short is a splice variant and endogenous inhibitor of Chk1 that regulates cell cycle and DNA damage checkpoints, *Proc. Natl. Acad. Sci.* 109 (2012) 197–202, <https://doi.org/10.1073/pnas.1104767109>.
- [11] M. Patil, N. Pabla, Z. Dong, Checkpoint kinase 1 in DNA damage response and cell cycle regulation, *Cell. Mol. Life Sci.* 70 (2014) 4009–4021, <https://doi.org/10.1007/s00018-013-1307-3>. Checkpoint.
- [12] B. Laquent, J. Lopez-Martin, D. Richards, G. Illerhaus, D.Z. Chang, G. Kim, et al., A phase II study to evaluate LY2603618 in combination with gemcitabine in pancreatic cancer patients, *BMC Cancer* 17 (2017) 137, <https://doi.org/10.1186/s12885-017-3131-x>.
- [13] G. Scagliotti, J.H. Kang, D. Smith, R. Rosenberg, K. Park, S.-W. Kim, et al., PHASE II STUDIES Phase II evaluation of LY2603618, a first-generation CHK1 inhibitor, in combination with pemetrexed in patients with advanced or metastatic non-small cell lung cancer, *Invest. New Drugs*. 34 (2016) 625–635, <https://doi.org/10.1007/s10637-016-0368-1>.
- [14] L.M. Krug, A.J. Wozniak, H.L. Kandler, R. Feld, M. Koczywas, J.L. Morero, et al., Randomized phase III trial of pemetrexed/cisplatin with or without CBP501 in patients with advanced malignant pleural mesothelioma, *Lung Cancer* 85 (2014) 429–434, <https://doi.org/10.1016/j.lungcan.2014.06.008>.
- [15] T. Seto, T. Esaki, F. Hirai, S. Arita, K. Nosaki, A. Makiyama, et al., Phase I, dose-escalation study of AZD7762 alone and in combination with gemcitabine in Japanese patients with advanced solid tumours, *Cancer Chemother. Pharmacol.* 72 (2013) 619–627, <https://doi.org/10.1007/s00280-013-2234-6>.
- [16] E. Sausville, P. Lorusso, M. Carducci, J. Carter, M.F. Quinn, L. Malburg, et al., Phase I dose-escalation study of AZD7762, a checkpoint kinase inhibitor, in combination with gemcitabine in US patients with advanced solid tumors, *Cancer Chemother. Pharmacol.* 73 (2014) 539–549, <https://doi.org/10.1007/s00280-014-2380-5>.
- [17] K.C. Cuneo, M.A. Morgan, V. Sahai, M.J. Schipper, L.A. Parsels, J.D. Parsels, et al., Dose escalation trial of the Wee1 inhibitor adavosertib (AZD1775) in combination with gemcitabine and radiation for patients With locally advanced pancreatic cancer, *J. Clin. Oncol.* (2019) JCO.19.00730. 10.1200/JCO.19.00730.
- [18] S. Leijen, R.M.J.M. Van Geel, A.C. Pavlick, R. Tibes, L. Rosen, A.R.A. Razak, et al., Phase I study evaluating WEE1 inhibitor AZD1775 as monotherapy and in combination with gemcitabine, cisplatin, or carboplatin in patients with advanced solid tumors, *J. Clin. Oncol.* 34 (2016) 4371–4380, <https://doi.org/10.1200/JCO.2016.67.5991>.
- [19] J. V. Forment, M.J. O'connor, Targeting the replication stress response in cancer, (2018). doi: 10.1016/j.pharmthera.2018.03.005.
- [20] S. Rundle, A. Bradbury, Y. Drew, N.J. Curtin, Targeting the ATR-CHK1 axis in cancer therapy, *Cancers (Basel)*. 9 (2017) 1–25, <https://doi.org/10.3390/cancers9050041>.
- [21] Z. Qiu, N.L. Oleinick, J. Zhang, ATR/CHK1 inhibitors and cancer therapy, *Radiother. Oncol.* 126 (2018) 450–464, <https://doi.org/10.1016/j.radonc.2017.09.043>.
- [22] Home - ClinicalTrials.gov. <https://clinicaltrials.gov/> (accessed September 5, 2019).
- [23] M.C. de Almagro, N. Mencia, V. Noé, C.J. Ciudad, Coding polypurine hairpins cause target-induced cell death in breast cancer cells, *Hum. Gene Ther.* 22 (2011) 451–463, <https://doi.org/10.1089/hum.2010.102>.
- [24] X. Villalobos, L. Rodríguez, A. Solé, C. Liberós, N. Mencia, C.J. Ciudad, et al., Effect of polypurine reverse Hoogsteen hairpins on relevant cancer target genes in different human cell lines, *Nucleic Acid Ther.* 25 (2015) 198–208, <https://doi.org/10.1089/nat.2015.0531>.
- [25] M.C. de Almagro, S. Coma, V. Noé, C.J. Ciudad, Polypurine hairpins directed against the template strand of DNA knock down the expression of mammalian genes, *J. Biol. Chem.* 284 (2009) 11579–11589, <https://doi.org/10.1074/jbc.M900981200>.
- [26] L. Rodríguez, X. Villalobos, S. Dakhel, L. Padilla, R. Hervas, J.L. Hernández, et al., Polypurine reverse Hoogsteen hairpins as a gene therapy tool against survivin in human prostate cancer PC3 cells in vitro and in vivo, *Biochem. Pharmacol.* 86 (2013) 1541–1554, <https://doi.org/10.1016/j.bcp.2013.09.013>.
- [27] S. Coma, V. Noé, R. Ertija, C.J. Ciudad, Strand displacement of double-stranded DNA by triplex-forming antiparallel purine-hairpins, *Oligonucleotides* 15 (2005) 269–283, <https://doi.org/10.1089/oli.2005.15.269>.
- [28] C.J. Ciudad, L. Rodríguez, X. Villalobos, A.J. Félix, V. Noé, Polypurine reverse Hoogsteen hairpins as a gene silencing tool for cancer, *Curr. Med. Chem.* 24 (2017), <https://doi.org/10.2174/0929867324666170301114127>.
- [29] D.B. Longley, D.P. Harkin, P.G. Johnston, 5-Fluorouracil: mechanisms of action and clinical strategies, *Nat. Rev. Cancer*. 3 (2003) 330–338, <https://doi.org/10.1038/nrc1074>.
- [30] N. Hagner, M. Joerger, Cancer chemotherapy: targeting folic acid synthesis, *Cancer Manag. Res.* 2 (2010) 293–301, <https://doi.org/10.2147/CMR.S100043>.
- [31] T.-C. Chou, Drug combination studies and their synergy quantification using the chou-talalay method, *Cancer Res.* 70 (2010) 440–446, <https://doi.org/10.1158/0008-5472.CAN-09-1947>.
- [32] X. Jiang, W. Li, X. Li, H. Bai, Z. Zhang, Current status and future prospects of PARP inhibitor clinical trials in ovarian cancer, (2019). doi: 10.2147/CMAR.S200524.
- [33] U.S. Food and Drug Administration. <https://www.fda.gov/> (accessed September 1, 2019).
- [34] European Medicines Agency. <https://www.ema.europa.eu/en> (accessed December 20, 2019).
- [35] X. Villalobos, L. Rodríguez, J. Prévot, C. Oleaga, C.J. Ciudad, V. Noé, Stability and immunogenicity properties of the gene-silencing polypurine reverse Hoogsteen hairpins, *Mol. Pharm.* 11 (2014) 254–264, <https://doi.org/10.1021/mp400431f>.
- [36] J. Benada, L. Macurek, Targeting the checkpoint to kill cancer cells, *Biomolecules*. 5 (2015) 1912, <https://doi.org/10.3390/Biom5031912>.
- [37] M. Macheret, T.D. Halazonetis, DNA replication stress as a hallmark of cancer, *Annu. Rev. Pathol. Mech. Dis.* 10 (2015) 425–448, <https://doi.org/10.1146/annurev-pathol-012414-040424>.
- [38] A.M. van Harten, M. Buijze, R. van der Mast, M.A. Roommans, S.R. Martens-de Kemp, C. Bachas, et al., Targeting the cell cycle in head and neck cancer by Chk1 inhibition: a novel concept of bimodal cell death, *Oncogenesis* 8 (2019), <https://doi.org/10.1038/s41389-019-0147-x>.
- [39] H. Beck, V. Nähse-Kumpf, M.S.Y. Larsen, K.A. O'Hanlon, S. Patzke, C. Holmberg, J. Mejlvang, A. Groth, O. Nielsen, R.G. Syljuåsen, C.S. Sorensen, Cyclin-dependent kinase suppression by WEE1 kinase protects the genome through control of replication initiation and nucleotide consumption, *Mol. Cell. Biol.* 32 (2012) 4226–4236, <https://doi.org/10.1128/MCB.00412-12>.
- [40] J.P.Y. Mak, W.Y. Man, H.T. Ma, R.Y.C. Poon, Pharmacological targeting the ATR-CHK1-WEE1 axis involves balancing cell growth stimulation and apoptosis, *Oncotarget* 5 (2014) 10546–10557, <https://doi.org/10.18632/oncotarget.2508>.
- [41] C.W. Lewis, Z. Jin, D. Macdonald, W. Wei, X.J. Qian, W.S. Choi, et al., Prolonged mitotic arrest induced by Wee1 inhibition sensitizes breast cancer cells to paclitaxel, *Oncotarget* 8 (2017) 73705–73722, <https://doi.org/10.18632/oncotarget.17848>.
- [42] F.-Z. Wang, H. Fei, Y.-J. Cui, Y.-K. Sun, Z.-M. Li, X.-Y. Wang, et al., The checkpoint 1 kinase inhibitor LY2603618 induces cell cycle arrest, DNA damage response and autophagy in cancer cells, *Apoptosis* 19 (2014) 1389–1398, <https://doi.org/10.1007/s10495-014-1010-3>.
- [43] J. Vera, Y. Raatz, O. Wolkenhauer, T. Kottek, A. Bhattacharya, J.C. Simon, et al., Chk1 and Wee1 control genotoxic-stress induced G2-M arrest in melanoma cells, *Cell. Signal.* 27 (2015) 951–960, <https://doi.org/10.1016/j.cellsig.2015.01.020>.
- [44] T. Kogiso, H. Nagahara, E. Hashimoto, S. Ariizumi, M. Yamamoto, K. Shiratori, Efficient induction of apoptosis by wee1 kinase inhibition in hepatocellular carcinoma cells, *e100495, PLoS One* 9 (2014), <https://doi.org/10.1371/journal.pone.0100495>.
- [45] M. Kimura, T. Yoshioka, M. Saio, Y. Banno, H. Nagaoka, Y. Okano, Mitotic catastrophe and cell death induced by depletion of centrosomal proteins, e603–e603, *Cell Death Dis.* 4 (2013), <https://doi.org/10.1038/cddis.2013.108>.
- [46] M. Castedo, J.-L. Perfettini, T. Roumier, K. Andreau, R. Medema, G. Kroemer, Cell death by mitotic catastrophe: a molecular definition, *Oncogene*. 23 (2004) 2825–2837, <https://doi.org/10.1038/sj.onc.1207528>.

- [47] M. Krajewska, A.M. Heijink, Y.J.W.M. Bisselink, R.I. Seinstra, H.H.W. Silljé, E.G.E. de Vries, et al., Forced activation of Cdk1 via wee1 inhibition impairs homologous recombination, *Oncogene* 32 (2013) 3001–3008, <https://doi.org/10.1038/onc.2012.296>.
- [48] T.B. Garcia, J.C. Snedeker, D. Baturin, L. Gardner, S.P. Fosmire, C. Zhou, et al., A small-molecule inhibitor of WEE1, AZD1775, synergizes with olaparib by impairing homologous recombination and enhancing DNA damage and apoptosis in acute leukemia, *Mol. Cancer Ther.* 16 (2017) 2058–2068, <https://doi.org/10.1158/1535-7163.MCT-16-0660>.
- [49] C.G. Engelke, L.A. Parsels, Y. Qian, Q. Zhang, D. Karnak, J.R. Robertson, et al., Sensitization of pancreatic cancer to chemoradiation by the Chk1 inhibitor MK8776, *Clin. Cancer Res.* 19 (2013), <https://doi.org/10.1158/1078-0432.CCR-12-3748>.
- [50] B. Sarcar, S. Kahali, A.H. Prabhu, S.D. Shumway, Y. Xu, T. Demuth, et al., Targeting radiation-induced G(2) checkpoint activation with the Wee-1 inhibitor MK-1775 in glioblastoma cell lines, *Mol. Cancer Ther.* 10 (2011) 2405–2414, <https://doi.org/10.1158/1535-7163.MCT-11-0469>.
- [51] Y. Luo, S.K. Rockow-Magnone, P.E. Kroeger, L. Frost, Z. Chen, E.K. Han, et al., Blocking Chk1 expression induces apoptosis and abrogates the G2 checkpoint mechanism, *Neoplasia* 3 (2001) 411–419, <https://doi.org/10.1038/sj.neo.7900175>.
- [52] M.R. Russell, K. Levin, J. Rader, L. Belcastro, Y. Li, D. Martinez, et al., Combination therapy targeting the Chk1 and Wee1 kinases shows therapeutic efficacy in neuroblastoma, *Cancer Res.* 73 (2013) 776–784, <https://doi.org/10.1158/0008-5472.CAN-12-2669>.
- [53] J. Tang, R.L. Erikson, X. Liu, Checkpoint kinase 1 (Chk1) is required for mitotic progression through negative regulation of polo-like kinase 1 (Plk1), *Proc. Natl. Acad. Sci. U.S.A.* 103 (2006) 11964–11969, <https://doi.org/10.1073/pnas.0604987103>.

Results

4.1.1. Additional results to Article I

The effect of 100 nM of both HpWEE1Pr-T and HpCHK111-C was also tested in three additional cancerous cell lines, HepG-2, SKBR-3 and MCF-7. HpCHK111-C was the most effective, causing a decrease in cell viability of 80%, 75% and 95%, respectively (Figure 17A).

Additionally, the effect of these PPRHs was also evaluated in non-cancerous cells lines (HEK-293 and ECV304) or in a non-human cell line (CHO-DG44 from hamster) (Figure 17B). No significant effect was observed in ECV304 or CHO-DG44 cells incubated with 100 nM of PPRHs targeting *WEE1* or *CHK1*. In HEK293 cells the decrease caused by the PPRHs was 29% for *WEE1*, and 24% for *CHK1*, when using the same concentrations that caused more than 85% reduction in viability in HeLa cells.

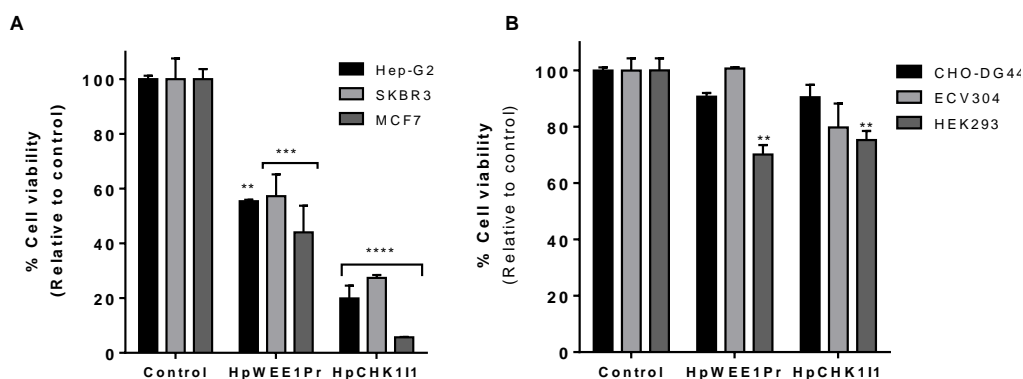


Figure 17. Effect on cell viability by PPRHs directed against the RSR genes *WEE1* and *CHK1* on cancer cells, non-human cells and non-cancerous human cells. Cell viability (10,000) assays were conducted 5 days after transfection. (A) HepG2, SKBR3 and MCF-7 cells viability upon treatment with 100 nM HpWEE1Pr-T (HpWEE1Pr) and 100 nM HpCHK111-C (HpCHK111). (B) CHO-DG44, ECV304 and HEK293 cell viability assay upon treatment with HpWEE1Pr-T (HpWEE1Pr) and HpCHK111-C (HpCHK111). In each condition 100 nM of the PPRH were used, except for HpCHK111-C in HEK293, where 50 nM was used. Data represent the mean \pm SEM from 3 experiments. Statistical significance was determined using two-way ANOVA with Dunnett's multiple comparisons test (Figure A) or one-way ANOVA with Dunnett's multiple comparisons test (Figure B) (** $p < 0.01$, *** $p < 0.001$, **** $p < 0.0001$).

Results

4.2. ARTICLE II

Detection of a G-quadruplex as a regulatory element in Thymidylate synthase for gene silencing using Polypurine Reverse Hoogsteen Hairpins

Eva Aubets[#], Alex J. Félix[#], Miguel Garavís, Laura Reyes, Anna Aviñó, Ramón Eritja, Carlos J. Ciudad and Véronique Noé.

[#] These authors contributed equally

International Journal of Molecular Sciences. 2020;21(14):5028. (Impact factor: 4.556).

Background: TYMS enzyme has been widely studied as an anti-cancer target given its role in DNA biosynthesis (Carreras & Santi 1995). Although different TYMS inhibitors (e.g. fluoropyrimidines or antifolates) have been developed, their effectivity in the clinical practice has been limited due to the development of drug resistance (Garg *et al.* 2010; Zhang *et al.* 2008). An autoregulatory mechanism at the translational level of TYMS protein that induce new synthesis of TYMS protein has been proposed as one of the processes that could induce drug resistance (Chu *et al.* 1991). In this direction, the regulatory elements G4s are potential candidates due to their role in gene regulation processes. G4s are nucleic acid secondary structures located in guanine-rich DNA or RNA sequences, which adopt square-planar arrangement of four guanines bound by Hoogsteen hydrogen bonds.

Objectives: We aimed to identify and validate regulatory elements in the *TYMS* gene that can be targeted by PPRHs, such as G-quadruplexes, as a novel approach to down-regulate *TYMS* expression. We also aimed to assess the effectiveness of a PPRH targeting the complementary strand of a G4 motif in the *TYMS* gene alone and in combination with the traditional TYMS inhibitor 5-Fluorouracil.

Results: We first search putative G4 forming sequences using the Quadruplex forming G-Rich Sequences (QGRS) mapper. The sequence with the highest score (G20) was located in the 5'-UTR of *TYMS*. Then, we corroborated the G4-folding of this G4-forming sequence (G4FS) in both DNA and mRNA by different spectroscopic approaches such as circular dichroism (CD), UV

Results

absorbance spectroscopy (UV), fluorescence and nuclear magnetic resonance (NMR) using synthetic oligonucleotides.

Furthermore, since TYMS protein has been reported to bind to at least two different sites located in its own mRNA (Chu *et al.* 1991, 1993), we evaluated the possible interaction between TYMS and the G4FS. EMSA revealed that TYMS protein could interact with the G4FS either in the form of DNA or mRNA, whereas 2 negative control proteins (DHFR and bovine serum albumin) did not produce any binding. Then, we designed a PPRH targeting the G4 region (HpTYMS-G4-T). Competition assays between HpTYMS-G4-T and the TYMS protein revealed that both compete with each other for the binding to the target sequence in the DNA. Furthermore, Thioflavin T gel staining showed that the PPRH bound to the corresponding dsDNA promoting G4 formation.

In HeLa cancer cells, the PPRH decreased both TYMS mRNA and protein levels in a specific manner. This down-regulation of TYMS expression led to a decrease in cell viability in a dose-dependent manner. It is noteworthy that the cytotoxic effect of HpTYMS-G4-T was lower when cells were incubated in medium containing thymidine. Furthermore, we demonstrated the synergic effect of HpTYMS-G4-T in HeLa cells treated concurrently with 5-FU.

Conclusions: In this work we identified and confirmed a G4 structure in the 5'UTR of the *TYMS* gene that could be involved in transcriptional and translational autoregulation of TYMS expression. We showed that the PPRH designed against the complementary strand of the G4FS presented therapeutic potential as a single agent or in combination with the traditional TYMS inhibitor 5-FU. Therefore, we validated the use of PPRHs to target G4 structures and we provided new strategies to down-regulate TYMS expression.



Article

Detection of a G-Quadruplex as a Regulatory Element in *Thymidylate synthase* for Gene Silencing Using Polypurine Reverse Hoogsteen Hairpins

Eva Aubets ^{1,†}, Alex J. Félix ^{1,†}, Miguel Garavís ^{2,3}, Laura Reyes ⁴, Anna Aviñó ⁴, Ramón Eritja ⁴, Carlos J. Ciudad ¹ and Véronique Noé ^{1,*}

¹ Department of Biochemistry and Physiology, School of Pharmacy and Food sciences, and IN2UB, University of Barcelona, 08028 Barcelona, Spain; eaubets@ub.edu (E.A.); alexjimenezf@ub.edu (A.J.F.); cciudad@ub.edu (C.J.C.)

² Instituto de Química y Física ‘Rocasolano’, CSIC, Serrano 119, 28006 Madrid, Spain; mgaravis@gmail.com

³ Department of Chemistry Pulp and Paper Building, McGill University, 3420 Rue University, Montréal, QC H3A 0C7, Canada

⁴ Institute for Advanced Chemistry of Catalonia (IQAC), CSIC, Networking Center on Bioengineering, Biomaterials and Biomedicine (CIBER-BBN), 08034 Barcelona, Spain; laura.reyes.fraile@gmail.com (L.R.); aaagma@cid.csic.es (A.A.); recgma@cid.csic.es (R.E.)

* Correspondence: vnoe@ub.edu; Tel.: +34-93-403-4455

† These authors contributed equally.

Received: 25 June 2020; Accepted: 15 July 2020; Published: 16 July 2020



Abstract: Thymidylate synthase (TYMS) enzyme is an anti-cancer target given its role in DNA biosynthesis. TYMS inhibitors (e.g., 5-Fluorouracil) can lead to drug resistance through an autoregulatory mechanism of TYMS that causes its overexpression. Since G-quadruplexes (G4) can modulate gene expression, we searched for putative G4 forming sequences (G4FS) in the *TYMS* gene that could be targeted using polypurine reverse Hoogsteen hairpins (PPRH). G4 structures in the *TYMS* gene were detected using the quadruplex forming G-rich sequences mapper and confirmed through spectroscopic approaches such as circular dichroism and NMR using synthetic oligonucleotides. Interactions between G4FS and TYMS protein or G4FS and a PPRH targeting this sequence (HpTYMS-G4-T) were studied by EMSA and thioflavin T staining. We identified a G4FS in the 5'UTR of the *TYMS* gene in both DNA and RNA capable of interacting with TYMS protein. The PPRH binds to its corresponding target dsDNA, promoting G4 formation. In cancer cells, HpTYMG-G4-T decreased TYMS mRNA and protein levels, leading to cell death, and showed a synergic effect when combined with 5-fluorouracil. These results reveal the presence of a G4 motif in the *TYMS* gene, probably involved in the autoregulation of TYMS expression, and the therapeutic potential of a PPRH targeted to the G4FS.

Keywords: G-quadruplex; PPRH; thymidylate synthase; anti-tumor therapy; 5-fluorouracil; gene silencing; gene regulation

1. Introduction

Thymidylate synthase (TYMS) has been widely studied as an anti-cancer target due to its essential role in the de novo synthesis of 2'-deoxythymidine-5'-monophosphate (dTMP), a critical precursor for DNA biosynthesis. TYMS catalyzes the conversion of 2'-deoxyuridine 5'-monophosphate (dUMP) to dTMP by transferring the methyl group from the 5,10-methylenetetrahydrofolate molecule (mTHF). Then, dTMP is successively phosphorylated to form 2'-deoxythymidine-5'-triphosphate (dTTP), generating one of the four fundamental nucleoside triphosphates involved in DNA synthesis [1,2].

TYMS inhibition affects highly proliferative cells (e.g., cancer cells) and has been established as a classic chemotherapeutic treatment during the last few decades [3]. Since its development in 1957, the nucleobase 5-fluorouracil (5-FU) has become one of the most widely used TYMS inhibitors for the treatment of different types of cancer, either as a single agent or in combination with other chemotherapeutics [2,4]. Intracellularly, 5-FU is converted to 5-fluoro-2'-deoxyuridine-5'-monophosphate (FdUMP), which is an analog of the endogenous ligand dUMP and binds to the nucleotide-binding domain of TYMS. This FdUMP-TYMS-mTHF ternary complex inhibits TYMS activity and leads to the suppression of dTMP synthesis, thus producing deoxynucleotide pool imbalance, increased levels of deoxyuridine triphosphate (dUTP) and, ultimately, DNA damage [4,5]. Nevertheless, the effectiveness of fluoropyrimidines or other TYMS inhibitors is compromised by the development of drug resistance. Some of these have been associated with high TYMS protein levels and are thought to be related to an autoregulatory mechanism of TYMS protein that modulates its own expression [6,7].

It has been proposed that the ligand-free TYMS protein is capable of binding to its own mRNA and represses its own translation. Two mRNA binding sites for TYMS have been identified so far in its mRNA: one located in the 5' untranslated region (5'UTR), containing the translational start site (binding site I), and the other in the mRNA-coding region (binding site II) [8,9]. When TYMS protein is bound to dUMP or TYMS inhibitors such as fluoropyrimidines or antifolates [10], it cannot bind to its own mRNA and TYMS mRNA translation is not inhibited. This mechanism of translational regulation would explain the increased TYMS protein levels observed in tumor resistance cells [8,10,11].

Different strategies to overcome drug resistance have been developed, including antisense oligodeoxynucleotides (ASO) targeting different TYMS mRNA regions such as the protein binding site I, which might be an important regulator of translation [10]. The goal in the present work was to target other regulatory elements located in the *TYMS* gene, such as G-quadruplex structures (G4s). In the last few decades, the interest in G4s as gene regulation elements for anti-tumor applications has increased considerably [12]. G4s are nucleic acid secondary structures formed by guanine-rich RNA or DNA sequences whose basic structural unit is called G-tetrad, a square-planar arrangement of four guanines held together through Hoogsteen type associations. [13,14]. Stacking a minimum of two of these G-tetrads produces the four-stranded G4 structure that is further stabilized by monovalent cations (especially K⁺) and presents a high thermodynamic stability under physiological conditions [15]. G4s may have an important role in controlling different biological processes such as DNA replication [16], telomere maintenance [17] and mRNA transcription, processing and translation [18,19]. For this reason, G4s are mainly found in regulatory regions such as promoters, 5'UTRs, splicing sites and telomeres [20].

Here, we targeted a G4 forming sequence (G4FS) in the 5'UTR of the *TYMS* gene using a gene silencing tool developed in our laboratory named polypurine reverse Hoogsteen (PPRH) hairpins [21]. These molecules are non-modified single-stranded oligodeoxynucleotides formed by two antiparallel polypurine mirror repeat domains linked by a five-thymidine loop (5T). The intramolecular linkage consists of reverse Hoogsteen bonds between the purines, forming the hairpin structure. PPRHs can bind in a sequence-specific manner to polypyrimidine targets in the double-stranded DNA (dsDNA) via Watson–Crick bonds, thus producing a triplex structure and displacing the fourth strand of the dsDNA. This local distortion of the dsDNA leads to a transcriptional disruption that provokes the knockdown of the targeted gene [22]. Therefore, it is essential for PPRH design to find polypyrimidine tracts within the target gene sequence, which are mainly present in promoter or intronic regions [23]. During the last decade, we have used PPRHs as gene silencing tools for anti-cancer therapy [22,24–27], immunotherapy approaches [28–30] and targeting genes involved in resistance to chemotherapeutic drugs like methotrexate [31].

In this work, we identified and validated a G4 structure in the *TYMS* gene that can be targeted by a PPRH as a new approach to down-regulate TYMS expression. Treatment with this DNA hairpin was very effective against human cancer cells, and it acted synergistically when administered together with 5-FU. Additionally, we aimed to study the role of this G4 structure in the modulation of TYMS expression.

2. Results

2.1. Detection of a G4 Structure in the 5'UTR of TYMS

We searched G4FSs that could modulate TYMS expression using the quadruplex forming G-rich sequences (QGRS) mapper (Figure 1A). The sequence with the highest score (G20) was found in the 5'UTR of this gene (Figure 1B), according to reference [32] and in agreement with the human TYMS mRNA sequence NM_001071.3. However, in the last sequence version available in the NCBI gene database (NM_001071.4), the 5'UTR has been shortened (−69 nt) and the G4FS is excluded from the 5'UTR. Therefore, we carried out PCR reactions from either genomic or reverse transcribed DNA in order to test whether this G4FS was positioned in this untranslated region. Both genomic DNA (gDNA) and cDNA samples originated a main product of 184 bp (Figure 1C), thus confirming that the identified G4FS was actually located within the 5'UTR of the *TYMS* gene and not in the promoter. Moreover, we confirmed by sequencing that the 184 bp PCR product amplified from the cDNA sample corresponded to the 5'UTR sequence containing the G4FS. The human TYMS mRNA sequence (NM_001071.3) was subjected to the Triplex-Forming Oligonucleotide (TFO) searching tool [33]. The output (Figure 1D) was confronted with the list obtained with the QGRS mapper (Figure 1A). The matching sequence was used to design the PPRH targeting the G4FS (HpTYMS-G4-T) to decrease TYMS expression (Figure 1E). The mechanism of action of HpTYMS-G4-T is depicted in Figure 1F.

2.2. G4 Structure Confirmation in Both RNA and DNA

Next, we proceeded to confirm whether the G4FS (ssDNA-G4-Fw and RNA-G4) could form a G4 structure using different spectroscopic approaches such as circular dichroism (CD), UV absorbance spectroscopy (UV) and fluorescence and nuclear magnetic resonance (NMR) using synthetic oligonucleotides. UV absorbance and CD spectroscopies have played important roles in the verification of G-quadruplex folding [34,35]. Denaturation or melting curves recorded at 295 nm are commonly used to determine the thermodynamic properties of G-quadruplex [34]. In addition, a thermal difference spectrum (TDS) (absorption difference between unfolded and folded form) is applied in order to confirm the existence of G-quadruplex structures and differentiate them from other DNA structures such as duplexes or triplexes [36].

Oligonucleotides ssDNA-G4-Fw and RNA-G4 (Table 1) contain the G4FS identified by the QGRS mapper (Figure 1A,B) in both DNA and RNA backbones. The melting curves of these oligonucleotides were recorded in two different buffers. One of them, K⁺ solution, contains a relatively large amount of potassium, which has been described to stabilize the G-quadruplex structure. The other is a phosphate-buffered solution (PBS) containing sodium cations. The thermal denaturation profiles exhibited hypochromism at 295 nm with increasing temperature, indicating the denaturation of a potential G-quadruplex structure. Both denaturation curves showed similar melting profiles with similar melting temperatures, being 37 °C in K⁺ solution, which is slightly higher than in PBS (35 °C) for ssDNA-G4-Fw. RNA-G4 showed similar behavior, with increased stability compared to ssDNA-G4-Fw, 47 °C in K⁺ buffer and 40 °C in PBS. TDS, especially in K⁺ buffer, showed the spectra profile assigned to a G-quadruplex with maxima around 243 and 273 and minima at around 295 nm [36] (Figure S1).

CD spectra were recorded using the same buffers (Figure 2A,B). Spectra were indicative of hybrid G-quadruplex, with positive bands at ~260 and 295 nm and a negative band at 245 nm for ssDNA-G4-Fw (Figure 2A), and a parallel G-quadruplex structure with positive bands ~260 and a negative band at 245 nm for RNA-G4 (Figure 2B). A schematic illustration of the possible G-quadruplex structure of RNA-G4 is shown in Figure 2C.

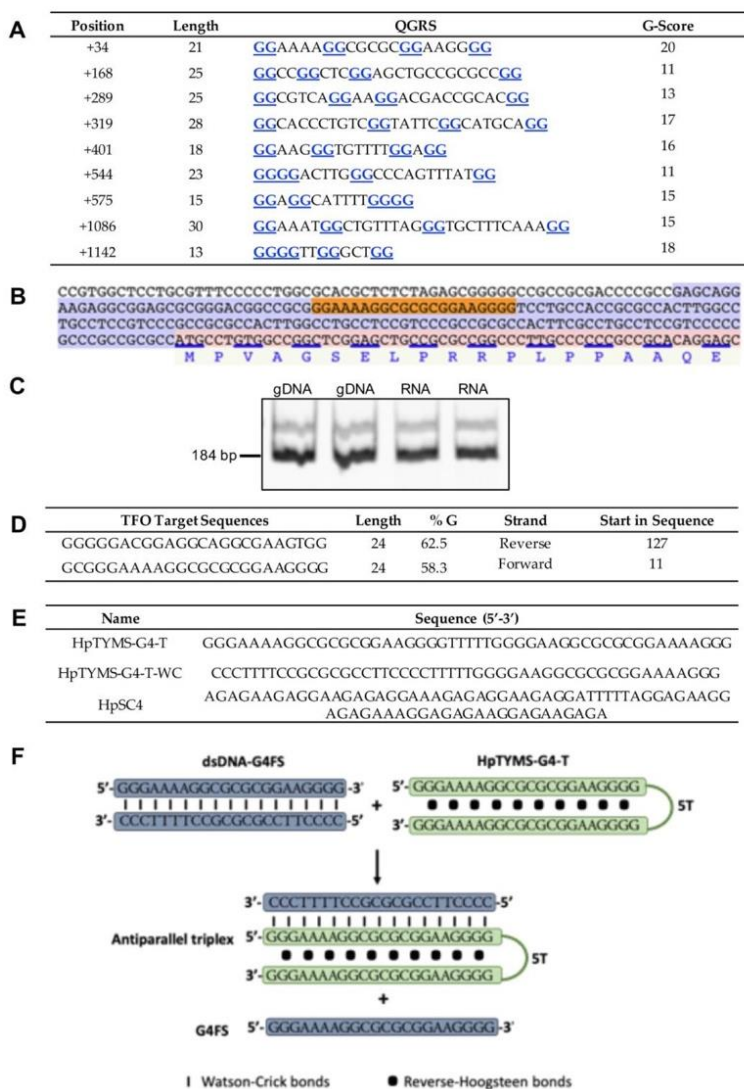


Figure 1. Identification of a G4FS in the TYMS gene and design of a PPRH targeting this site. (A) Putative G4-forming sequences detected in the TYMS gene using the QGRS mapper. The positions of the identified G4FS are referred to as the transcription start site considering the TYMS mRNA sequence NM_001071.3. The blue underlined Guanines (Gs) represent the ones implicated in G4 formation. (B) Localization of the G4FS with the higher G-score in the TYMS gene sequence (NM_001071.3). The orange highlighted sequence corresponds to G4FS. (C) The G4FS is located in the 5'UTR of the TYMS gene. PCR products (184 bp) obtained after amplification with primers 5'UTR-TYMS-Fw and 5'UTR-TYMS-Rv of both gDNA and cDNA/RNA samples. PCR products were resolved in a 6% polyacrylamide gel electrophoresis. (D) The first two polypurine sequences found in TYMS mRNA using the TFO searching tool. (E) Sequence of the specific PPRH targeting the G4FS (HpTYMS-G4-T), its corresponding Watson–Crick negative control (HpTYMS-G4-T-WC) and a scramble negative control (HpSC4). (F) Scheme showing the potential strand displacement produced when the PPRH (HpTYMS-G4-T) is mixed with dsDNA-G4FS. The formation of the antiparallel triplex by binding of the PPRH to the polypyrimidine oligonucleotide dissociates the polypurine oligonucleotide.

Table 1. Oligonucleotides used in this study.

Name	Sequence (5'-3')	Length	Assay
5'UTR-TYMS-Fw	GAGCAGGAAGAGGCGGAGCG	20	PCR
5'UTR-TYMS-Rv	GCAGCTCCGAGCCGGCCACAGG	22	PCR
APRT-Ex1-Fw	CACCCCAGGCGTGGTATCA	20	PCR
APRT-Ex2-Rv	CTGCGATGTAGTTCGATGCGG	20	PCR
TYMS-Fw	CCTCGGTGTGCCTTTC AACATC	22	qPCR
TYMS-Rv	GGTCTGGGTTCGCTGAAGC	21	qPCR
PPIB-Fw	GGAGATGGCACAGGAGGAAA	20	qPCR
PPIB-Rv	CGTAGTGCTTCAGTTTGAAGTTCTCA	26	qPCR
RNA-G4	GGGAAAAGGCGCGGGAAGGGG	22	EMSA, CD, UV, Flu
ssDNA-G4-Fw-E	GGGAAAAGGCGCGGGAAGGGG	22	EMSA
ssDNA-G4-Rv-E	CCCCTTCCGCGCGCCTTTTCCC	22	EMSA
ssDNA-G4-Fw	CGGGAAAAGGCGCGGGAAGGGGT	24	TGS, CD, UV, Flu, NMR
ssDNA-G4-Rv	ACCCCTTCCGCGCGCCTTTTCCC	24	TGS

PCR (polymerase chain reaction), qPCR (quantitative PCR), EMSA (electrophoretic mobility shift assay), CD (circular dichroism), UV (UV absorbance spectroscopy), Flu (thioflavin T fluorescence spectroscopy), Thioflavin T gel staining (TGS), NMR (nuclear magnetic resonance).

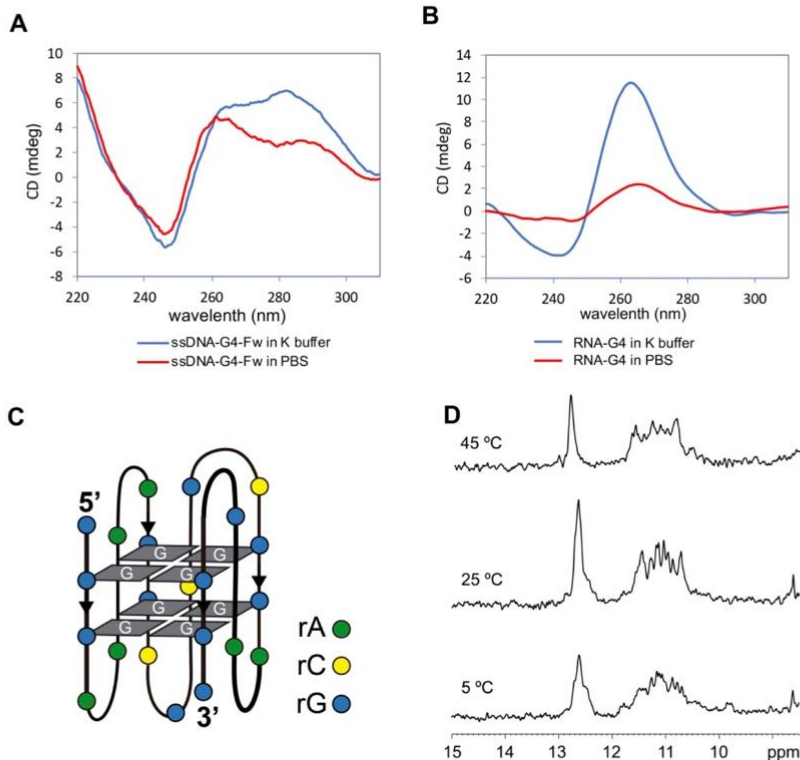


Figure 2. Structural characterization of G4FS in both RNA and DNA oligonucleotides. CD spectra of ssDNA-G4-Fw (A) and RNA-G4 (B) in K^+ buffer (blue line) and PBS (red line) at 20 °C, showing a shape consistent with the formation of G-quadruplex structures. (C) Illustration representing the G-quadruplex folding of the G4-RNA sequence. Each color dot represents a ribonucleotide: adenine (rA), cytosine (rC) and guanine (rG). (D) Imino region of monodimensional 1H -NMR spectra of ssDNA-G4-Fw in H_2O/D_2O (90:10) at different temperatures. The spectra show signals between 10 and 12 ppm, characteristic of imino protons taking part in G-tetrads. Buffer conditions: 25 mM KPi pH 7, 100 mM KCl.

The imino region of the one-dimensional $^1\text{H-NMR}$ spectrum (Figure 2D) of ssDNA-G4-Fw showed signals between 10 and 12 ppm, which are within the range of the chemical shifts of guanine imino protons involved in G-tetrads. The signals observed between 12 and 13 ppm belong to imino protons forming GC Watson–Crick base pairs. Most probably, these signals are due to the formation of G:C:G:C tetrads within the G-quadruplex. Such tetrads, resulting from the association of two G:C base pairs, are not unusual and accommodate well between G:G:G:G tetrads [37]. All the imino signals remained visible at 45 °C (Figure 2D), indicating the remarkable thermal stability of the structure, which is frequent for G-quadruplexes [15].

Thioflavin T (ThT) is an efficient fluorescent sensor of G-quadruplex and it has been used to discriminate G-quadruplex structures from other structures [38]. To this end, we carried out fluorescence spectra titrations by adding the oligonucleotide (ODN) dissolved in PBS to a solution of ThT. We observed an increase in fluorescence with increasing concentrations of the ODN, which enables us to determine an association constant following the method described in the literature [39]. The association constants for ssDNA-G4-Fw were found to be 2.72×10^6 and 2.90×10^6 for RNA-G4, both in the range of the values described for other G-quadruplexes [38] (Figure S2).

2.3. TYMS Protein Binds to the G4FS

To study the possible binding of the TYMS protein to the G4FS contained in the 5'UTR of the TYMS gene, we performed different electrophoretic mobility shift assays (EMSA) using radioactively labeled ssDNA-G4-Fw-E or RNA-G4 oligonucleotides (Table 1).

In the case of ssDNA-G4-Fw-E, we observed three shifted bands—two with high molecular weight—when incubating the probe with purified TYMS protein (Figure 3A, lane 2). In a similar way, incubation of a nuclear extract from cervical carcinoma cells (HeLa) with the probe produced the same shifted bands (Figure 3A, lane 3–4) that could correspond to the binding of the TYMS protein present in the nuclear extract. In contrast, the incubation of the ssDNA-G4-Fw-E probe with either bovine serum albumin (BSA) or dihydrofolate reductase (DHFR) proteins as negative controls did not show any shifted bands (Figure 3A, lane 5–6). Therefore, TYMS protein specifically binds to the G4FS located in the 5'UTR of the TYMS gene.

Since we observed the binding of the TYMS protein to the ssDNA-G4-Fw-E probe, we checked whether this binding could occur using the RNA sequence corresponding to the same G4FS. The incubation of TYMS protein with the RNA probe (RNA-G4) showed three shifted bands (Figure 3B, lane 2), thus demonstrating that TYMS protein binds to this particular G4FS located in the 5'UTR of its own mRNA. The incubation of the probe with the BSA protein did not produce any binding (Figure 3B, lane 3).

2.4. TYMS Protein and HpTYMS-G4-T Compete to Bind to the G4FS in the dsDNA

Since TYMS protein can also be found in the cell nucleus, we explored the possible binding of this protein to the dsDNA corresponding to the G4FS. In these experiments, we observed a unique shifted band when incubating the dsDNA-G4-E probe (prepared by hybridization of ssDNA-G4-Fw-E and ssDNA-G4-Rv-E, Table 1) with TYMS protein (Figure 4A, lane 2). The intensity of this shifted band was increased when a higher amount of TYMS protein was added to the reaction (Figure 4A, lane 3). Additionally, the incubation of the probe with a HeLa nuclear extract (2 μg) produced a shifted band with the same mobility as the one obtained with purified TYMS protein (Figure 4A, lane 4). We confirmed that the binding of TYMS protein to the G4FS was specific since incubation with BSA or DHFR proteins did not produce any shifted bands (Figure 4A, lane 5–6).

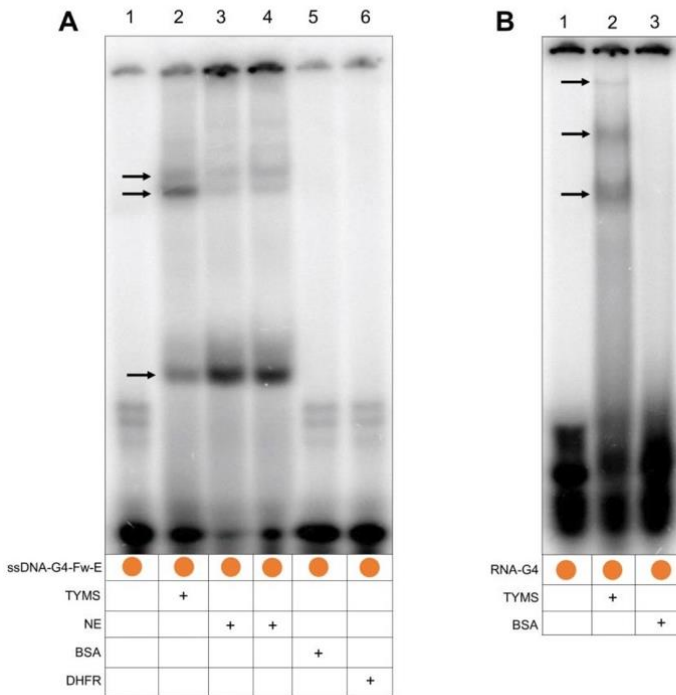


Figure 3. Binding of TYMS protein to the G4FS mRNA. EMSAs using ³²P-radiolabeled ssDNA (A) or RNA (B) probes corresponding to the G4FS. (A) Lane 1, ssDNA-G4-Fw-E probe alone; lane 2, ssDNA-G4-Fw-E plus TYMS protein (1.5 µg); lane 3 and 4, ssDNA-G4-Fw-E plus nuclear protein extract (2 µg) in duplicate; lane 5, ssDNA-G4-Fw-E plus BSA protein (2 µg); lane 6, ssDNA-G4-Fw-E plus DHFR protein (2 µg). (B) Lane 1, RNA-G4 probe alone; lane 2, RNA-G4 plus TYMS protein (1.5 µg); lane 3, RNA-G4 plus BSA protein (2 µg). Arrows indicate the shifted bands corresponding to the different molecular species.

Next, we designed the PPRH sequence (HpTYMS-G4-T) against the homopyrimidine complementary sequence of G4FS (Figure 1E). Then, we demonstrated that this PPRH oligonucleotide was able to bind the dsDNA-G4-E probe, observing one shifted band whose intensity increased depending on the amount of HpTYMS-G4-T added to the reaction (10, 30 or 60 ng) (Figure 4B, lane 2–4). We also performed a competition assay between HpTYMS-G4-T and TYMS protein. To do so, different amounts of HpTYMS-G4-T (10, 30 and 60 ng) were added to the binding reaction, together with a fixed amount of TYMS protein, showing a decrease in the intensity of the shifted band, corresponding to the binding of TYMS protein to the probe (Figure 4B, lane 5–8). Interestingly, the shifted band corresponding to the binding of HpTYMS-G4-T to the probe reappeared, and its intensity was proportional to the amount of HpTYMS-G4-T added to the reaction (Figure 4B, lane 5–8). Therefore, we demonstrated that HpTYMS-G4-T and TYMS protein bind to the same G4FS site in the dsDNA.

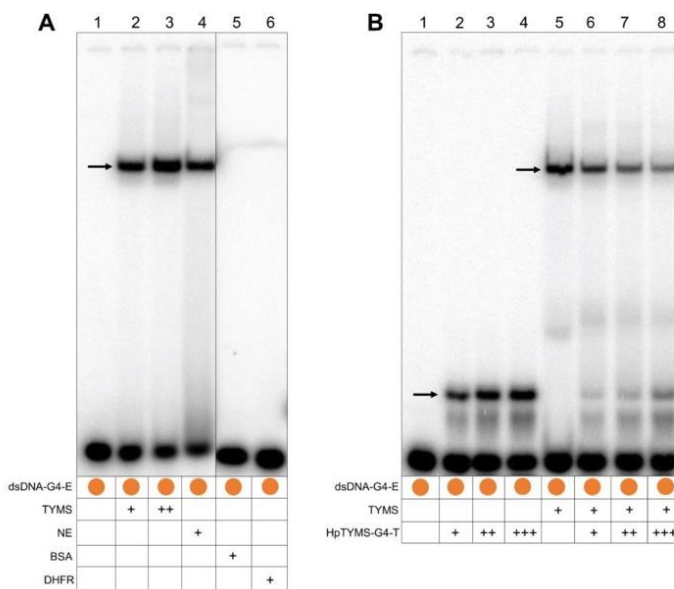


Figure 4. Binding of TYMS protein to the ³²P-radiolabeled dsDNA probe corresponding to the G4FS. (A) Lane 1, dsDNA-G4-E probe alone; lane 2, dsDNA-G4-E plus TYMS protein (1.5 μg); lane 3, dsDNA-G4 plus TYMS protein (3 μg); lane 4, dsDNA-G4-E plus HeLa nuclear protein extract (NE) (2 μg); lane 5, dsDNA-G4-E plus BSA protein (2 μg); lane 6, dsDNA-G4-E plus DHFR protein (2 μg). (B) Competition assay between the TYMS protein and the HpTYMS-G4-T for the binding to the G4FS in the dsDNA. Lane 1, dsDNA-G4-E probe alone; lane 2, dsDNA-G4-E plus HpTYMS-G4-T (10 ng); lane 3, dsDNA-G4-E plus HpTYMS-G4-T (30 ng); lane 4, dsDNA-G4-E plus HpTYMS-G4-T (60 ng); lane 5, dsDNA-G4-E plus TYMS protein (1.5 μg); lane 6, dsDNA-G4-E plus TYMS protein (1.5 μg) competed with HpTYMS-G4-T (10 ng); lane 7, dsDNA-G4-E plus TYMS protein (1.5 μg) competed with HpTYMS-G4-T (30 ng); lane 8, dsDNA-G4-E plus TYMS protein (1.5 μg) competed with HpTYMS-G4-T (60 ng). Arrows indicate the shifted bands corresponding to the different molecular species.

2.5. HpTYMS-G4-T Promotes the Formation of the G4 Structure

HpTYMS-G4-T was designed to bind to its polypyrimidine target sequence in the dsDNA and form a DNA triplex. This would displace the G-rich sequence of the duplex that consequently could fold into a G4 structure (Figure 1F). To verify this possibility, the products of different binding assays were separated on a non-denaturing gel (Figure 5), which was then stained with ThT to detect the G4 structures formed [40]. The ssDNA-G4-Fw sequence was stained by ThT, as expected for a G4 structure (Figure 5A, lane 1), while dsDNA-G4 (hybrid from ssDNA-G4-Fw and ssDNA-G4-Rv) did not (Figure 5A, lane 2). The PPRH HpTYMS-G4-T was also detected by ThT staining, which is consistent with the fact that its sequence contains two repeats of G4-Fw and thus is able to fold into G4 structures. The PPRH samples showed a strong band and a shadow since they can adopt different conformations [24,41] (Figure 5A, lane 3). Incubation of dsDNA-G4 concurrently with the PPRH led to the formation of two extra bands, the upper corresponding to the ssDNA-G4-Rv/PPRH DNA triplex and the lower corresponding to the ssDNA-G4-Fw strand displaced from dsDNA-G4, which did form a G4 structure (Figure 5A, lane 4). As a negative control, we incubated ssDNA-G4-Rv, which is not a G4FS and, consequently, was not stained with ThT (Figure 5A, Lane 5). In addition, we used HpTYMS-G4-T-WC, a hairpin intramolecularly bound by Watson–Crick base pairs and thus not able to produce the DNA triplex and to displace the fourth strand. Accordingly, we did not observe the formation of the triplex between HpTYMS-G4-T-WC and the dsDNA-G4 (Figure 5A, lane 7). However,

since one of the domains of HpTYMS-G4-T-WC still contains a G4FS, the oligonucleotide was also stained by ThT (Figure 6A, lane 6). Then, after staining the same gel with ethidium bromide (EthBr), the species corresponding to dsDNA-G4 (Figure 5B, lane 2, lane 4 and lane 7) and ssDNA-G4-Rv (Figure 5B, lane 5) were visualized. G4 structures were also detected when ThT was directly added to the different binding assays incubations instead of electrophoresing the samples and staining the gel afterwards (Figure 5C).

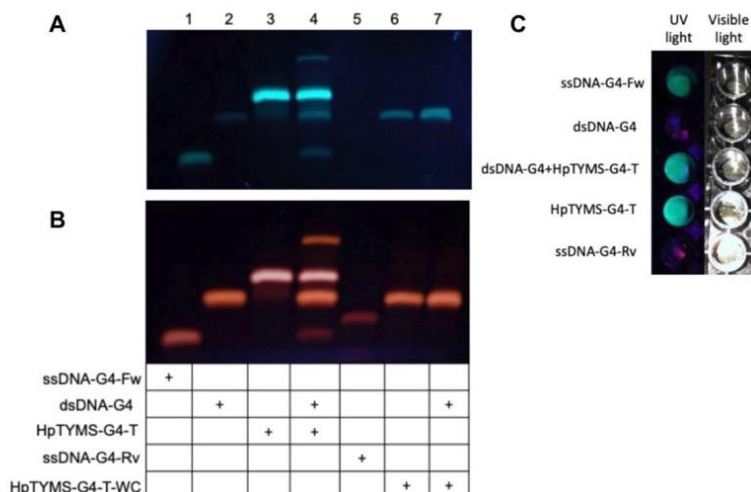


Figure 5. DNA binding assays and G4 structure detection using ThT. Samples incubated at 90 °C were cooled down slowly to room temperature and loaded in a nondenaturing 12% acrylamide gel supplemented with 10 mM KCl. The gel was visualized under UV light after ThT staining (A) and EthBr staining. (B) Lane 1, ssDNA-G4-Fw alone; lane 2, dsDNA-G4 alone; lane 3, HpTYMS-G4-T alone; lane 4, dsDNA-G4-2 plus HpTYMS-G4-T; lane 5, ssDNA-G4-Rv alone; lane 6, HpTYMS-G4-T-WC alone; lane 7, dsDNA-G4 plus HpTYMS-G4-T-WC. (C) G4 detection in samples directly incubated with ThT and visualized under UV light. Samples were prepared as indicated in Section 4.11 of Materials and Methods but containing 1 μ M of each oligonucleotide. When samples reached room temperature, 8 μ M of ThT was added and samples were visualized under UV light lamp or visible light.

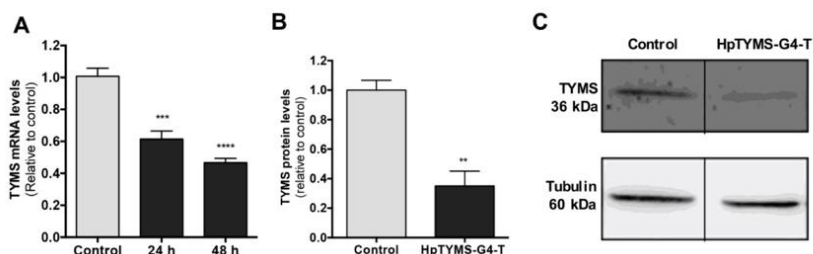


Figure 6. Effect of HpTYMS-G4-T on the levels of TYMS mRNA and protein. HeLa cells (30,000) were incubated with 100 nM of HpTYMS-G4-T. (A) TYMS mRNA levels 24 h and 48 h after transfection; RNA levels determined by RT-qPCR. Cyclophilin B (PPIB) was used to normalize the results. Statistical significance was determined using one-way ANOVA with Dunnett's multiple comparisons test (** $p < 0.001$, **** $p < 0.0001$). (B) TYMS protein levels in HeLa cells after 24 h of transfection. Statistical significance was determined using an unpaired Student's T test (** $p < 0.01$). Tubulin protein levels were used to normalize the results. (C) Representative images of Western blots.

2.6. Effect of HpTYMS-G4-T on the Levels of TYMS mRNA and Protein

To confirm a specific decrease in *TYMS* gene expression, *TYMS* mRNA levels in cervical carcinoma cells (HeLa) treated with HpTYMS-G4-T for 24 h or 48 h were analyzed. Cells incubated with HpTYMS-G4-T showed a decrease in *TYMS* gene expression, both at 24 h and 48 h (1.6–2.1-fold decrease relative to control) (Figure 6A). In addition, a 65% decrease in *TYMS* protein levels was observed after 24 h of incubation with the HpTYMS-G4-T (Figure 6B,C).

2.7. Effect of HpTYMS-G4-T as a Single Agent or Combined with 5-FU on HeLa Cell Viability

Since *TYMS* is involved in the de novo synthesis of dTTP, inhibition of *TYMS* expression using HpTYMS-G4-T was expected to reduce the viability of cancer cells and to produce a higher effect when the incubation was carried out in thymidine deficient medium. Therefore, HpTYMS-G4-T was incubated either in the presence or in the absence of thymidine. The PPRH was cytotoxic in a dose-dependent manner in both media, whereas HpSC4 did not produce any effect on cell viability. The highest cytotoxicity was reached at 100 nM in the absence of thymidine, with less than 5% of the viable cells remaining (Figure 7A). Once the effectiveness of HpTYMS-G4-T was established, we studied the effects of combining this specific PPRH with 5-FU, a classic inhibitor of *TYMS* protein. The PPRH (15 nM) presented a synergic effect when combined with different doses of 5-FU (0.3, 1 and 3 μ M), reducing cell viability down to 38%, 30%, and 14%, respectively (combination index calculated by the CompusSyn software [42]) (Figure 7B).

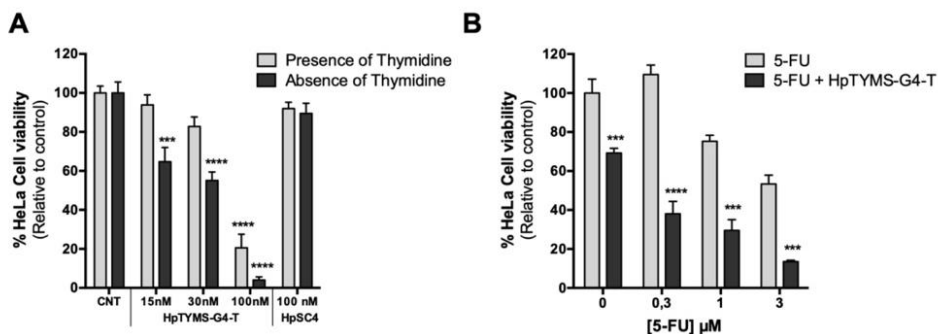


Figure 7. Effect on HeLa cell viability of HpTYMS-G4-T. (A) Dose–response of HeLa cell viability upon treatment with the HpTYMS-G4 and the HpSC4 in the absence (RPMI medium) or presence of thymidine (F12 medium). (B) Effect on cell viability when combining HpTYMS-G4-T with 5-FU. HeLa cells were treated with 5-FU at different concentrations (0.3, 1, 3 μ M) in the absence or presence of HpTYMS-G4-T (15 nM). Statistical significance was determined using two-way ANOVA with Sidak’s multiple comparisons test (*** $p < 0.001$, **** $p < 0.0001$). When combining the PPRH with 5-FU, statistical significance was estimated by comparing the effect of the PPRH alone to the control or comparing the effect of 5-FU plus PPRH to 5-FU alone. When transfecting the PPRH at 100 nM, 10 μ M of DOTAP was used, whereas for 15 nM or 30 nM of PPRH, 5 μ M DOTAP was employed.

As a control, the influence of 5-FU as a single agent on *TYMS* expression was also addressed. HeLa cells incubated for 24 h with 3 μ M of 5-FU showed a slight increase in *TYMS* mRNA levels, which were re-established after 48 h. At the protein level, a three-fold increase in total *TYMS* protein was observed after 24 h (Figure S3). These results are in agreement with [43–45].

2.8. Effect of HpTYMS-G4-T on PC-3 Cell Viability and mRNA Levels

We further examined whether the antiproliferative effect of HpTYMS-G4-T on HeLa cells was reproducible in other human cancer cell lines. HpTYMS-G4-T also produced a decrease in the viability of prostate adenocarcinoma cells (PC-3) in a dose–response manner, with only 4% of the viable cells

remaining at a concentration of 100 nM of PPRH (Figure 8A). In addition, after 24 h of transfection, PC-3 cells treated with 30 nM or 100 nM of HpTYMS-G4-T showed a 45% and 60% decrease in TYMS mRNA levels relative to the control, respectively (Figure 8B).

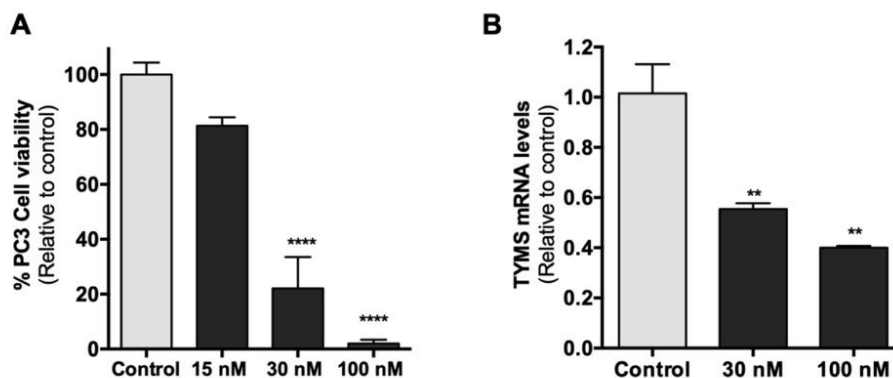


Figure 8. Effect of HpTYMS-G4-T on cell viability and TYMS mRNA levels in PC-3 cells. (A) Dose–response of PC-3 cell viability upon treatment of HpTYMS-G4-T in the presence of thymidine. (B) TYMS mRNA levels. After 24 h of transfection, RNA extraction was conducted and RNA levels determined by RT-qPCR. PPIB was used to normalize the results. Statistical significance was determined using one-way ANOVA with Dunnett’s multiple comparisons test (** $p < 0.01$, **** $p < 0.0001$).

3. Discussion

In this work, we describe the effects of a PPRH targeting a polypyrimidine strand complementary to a newly identified G4 motif present in the 5’UTR of the *TYMS* gene, whose encoded protein is a classical anti-cancer target due to its role in DNA synthesis [2]. Since it is known that G4 structures can be important gene regulatory elements, we searched for G4 structures in the *TYMS* gene using the QGRS mapper, a computational tool for the prediction of quadruplex forming G-rich sequences [12,46]. The spectroscopic experiments carried out in this work confirmed that the G4FS detected in the 5’UTR of the *TYMS* gene by the QGRS mapper fold into a G4 structure as both RNA and DNA.

Since there was a discrepancy in the extension of the 5’UTR sequence of the human *TYMS* mRNA in the last two accession numbers (NM_001071.4 and NM_001071.3) available in the NCBI database, we verified by PCR and RT-PCR that the G4FS identified in this work was actually located in the 5’UTR of the *TYMS* gene and not in its promoter sequence, in agreement with the original sequence for the *TYMS* gene reported in [32].

Interestingly, some metabolic enzymes have been described as multifunctional proteins performing distinct biochemical functions in the cytoplasm and nucleus, which are involved in transcriptional, posttranscriptional and translational regulation. Among them, we find glyceraldehyde 3-phosphate dehydrogenase, arg 5,6, enoyl-CoA hydratase, lactate dehydrogenase, threonyl-tRNA-synthetase, dihydrofolate reductase and Thymidylate synthase [47–49]. Moreover, it has been demonstrated that G4FS are putative protein binding regions that can act as regulatory elements of gene expression [12]. For these reasons, we aimed to study whether *TYMS* protein could directly interact with the G4FS present in its own 5’UTR (*TYMS*-G4FS). Since *TYMS* is a self-mRNA targeting protein binding to at least two different sites and inhibiting its own translation [8,9], we also evaluated the possible interaction between *TYMS* and the G4FS as mRNA species. This was confirmed by EMSA, thus proving that this protein has another binding site in its own mRNA that could also correspond to a translational regulator.

In addition, we explored whether *TYMS* protein was also interacting with the dsDNA formed by the *TYMS*-G4FS and its complementary strand, as this interaction could be important for the regulation of gene expression at the transcriptional level. EMSAs showed the specific binding of *TYMS* protein to the G4FS site, both as dsDNA and ssDNA. The same G4FS site, through its polypyrimidine

tract, was targeted by the binding of the designed PPRH (HpTYMS-G4-T), which caused a decrease in the expression of TYMS. These results suggest that TYMS protein could be involved in its own transcriptional regulation upon binding to this G4FS site.

Altogether, the observed interactions between TYMS protein and G4FS, either as mRNA or DNA, highlight that this site could be involved in translational and transcriptional regulation. Moreover, it has been previously demonstrated that C-MYC [50], p53 [51,52] and IFN-induced 15 kDa protein [53] mRNA translation is also controlled by TYMS, highlighting the important role of TYMS protein regulating not only its own expression but also that of other proteins.

Furthermore, in this work, we uncover the importance of the TYMS-G4FS region in the regulation of TYMS expression. Whether G4 structures promote or inhibit transcriptional or translational processes is a discrepant issue. While some studies indicate that G4s may positively contribute to gene expression through protein binding, others maintain that G4 structures may act as obstacles [54]. For instance, it has been reported that a G4 located in the C-MYC promoter interacts with the nucleic acid binding protein (CNBP) and NM23-H2, contributing to the enhancement of its own transcription [55]. In contrast, Kumari et al. reported that a G4 structure located in the 5'UTR of the NRAS mRNA inhibited its own translation [56]. This could also be the function of the G4FS identified in the 5'UTR of TYMS. One hypothesis is that the interaction that we observed between TYMS protein and the G4FS, either as DNA or RNA, could be preventing the function of the transcriptional or translational machineries. According to this premise, when TYMS is bound by its substrates (mTHF and dUMP) or by TYMS inhibitors, it does not interact with G4FS, thus increasing TYMS expression and leading to resistance to inhibitors. This proposition is in concordance with the currently postulated TYMS autoregulatory mechanism [8,9], but with an additional self-mRNA binding site and extrapolating the effect at the transcriptional level.

In view of the relevant role of G4 motifs in the regulation of gene expression, a wide range of G4 ligands have been developed for anti-tumor applications, such as ligands that stabilize G4 structures in the telomere region to block telomerase activity [57,58] and those targeting G4 structures located in promoters, 5'UTRs or 3'UTRs to regulate different cancer-related genes [12,59–62]. Several G4 ligands have demonstrated their potential in vivo [63] and some have reached clinical trials [64–67]. However, one of the main problems with these compounds is their lack of specificity and the possible off-target effects due to the high number of putative G4 structures present in the human genome [20,68].

In contrast, PPRHs can be designed to bind specifically to a polypyrimidine sequence that is complementary to a given G4FS. In fact, we proved that HpTYMS-G4-T binds in a specific manner to its target sequence, located in the complementary polypyrimidine strand of G4FS. Accordingly, our binding assays with ThT staining showed that even in conditions in which a PPRH can fold into a G4 structure, this does not impair its binding to the dsDNA, thus confirming our previous data [41]. In addition, dsDNA/PPRH triplex formation promoted the displacement of the polypurine strand and its folding into a G4 structure, thus the PPRH may contribute to stabilizing the formation of the G4 structure and would regulate transcription of this gene. We also corroborated the notion that Hoogsteen bonds stabilizing the PPRH are essential for triplex formation, since the Watson–Crick hairpin HpTYMS-G4-WC was not able to form the triplex.

One of the goals of this work was to demonstrate the effect of HpTYMS-G4-T on cancer cells. In this regard, we demonstrated that the PPRH targeting G4FS decreased both TYMS mRNA and protein levels in a specific manner. This down-regulation of TYMS expression led to a decrease in cell viability in a dose-dependent manner in both HeLa and PC3 cancer cells. It is worth noting that the cytotoxic effect of HpTYMS-G4-T was lower when cells were incubated in medium containing thymidine. Similarly, Schmitz et al. also reported that the effect of a siRNA targeting TYMS mRNA was reversed with 10 μ M of thymidine [69]. These data suggest that the cytotoxic effect of HpTYMS-G4-T results from the inhibition of thymidylate biosynthesis, caused by the specific inhibition of TYMS expression.

Other gene silencing molecules such as siRNAs [10,69], ASOs [70–72] or peptides [73] targeting TYMS mRNA also succeeded in down-regulating TYMS expression. However, PPRHs present some

advantages compared to other silencing tools. PPRHs are nonmodified DNA molecules that inhibit gene expression at lower concentrations than those needed for ASOs [22], they are more economical, less immunogenic and have a longer half-life than siRNAs [74]. Recently, we also demonstrated in a pharmacogenomic study that PPRHs do not present hepatotoxicity or nephrotoxicity *in vitro* [75].

In addition, since TYMS's autoregulatory translation mechanism has been associated with traditional TYMS inhibitor resistance [6–8], we evaluated the effect of HpTYMS-G4-T in combination with 5-FU. We demonstrated the synergic effect of HpTYMS-G4-T in HeLa cells treated concurrently with 5-FU. Our results are in accordance with others proving that strategies focused on reducing TYMS gene expression can sensitize cells to traditional TYMS inhibitors [69,72].

Overall, in this work, we identified and confirmed a G4 structure in the 5'UTR of the TYMS gene that could be involved in transcriptional and translational autoregulation of TYMS expression. We also showed that a PPRH designed against this G4FS presented therapeutic potential as a single agent or in combination with 5-FU treatment. Therefore, we provide new insights for the design of strategies that improve the effect of traditional TYMS inhibitors.

4. Materials and Methods

4.1. Bioinformatic Detection of G4-Forming Sequences

Putative G4FS were analyzed using the QGRS mapper (<http://bioinformatics.ramapo.edu/QGRS/index.php>). This software program generates information on the composition and distribution of putative QGRS in nucleotide sequences and is based on published algorithms for the recognition and mapping of putative QGRS [46].

4.2. Design of Polypurine Reverse Hoogsteen Hairpins

The search of polypurine sequences that serve to design PPRH hairpins was performed using the Triplex-Forming Oligonucleotide Target Sequence Search software (<http://utw10685.utweb.utexas.edu/tfo/> MD Anderson Cancer Center, University of Texas) [33]. The design consisted of two antiparallel mirror repeats of polypurine stretches, intramolecularly bound by reverse Hoogsteen bonds and linked by a loop of five thymidines (5T). As negative controls, we designed a hairpin with intramolecular Watson–Crick bonds instead of Hoogsteen bonds (HpTYMS-G4-T-WC) and a scrambled hairpin (HpSC4) (Figure 1E). The sequences were synthesized as non-modified oligodeoxynucleotides by Sigma-Aldrich (Haverhill, UK), resuspended in sterile Tris-EDTA buffer (1 mM EDTA and 10 mM Tris, pH 8.0) (Sigma-Aldrich, Madrid, Spain) and stored at $-20\text{ }^{\circ}\text{C}$ until use.

4.3. RNA and gDNA Extraction

Total RNA was extracted from cells using TRIzol® (Life Technologies, Barcelona, Spain), following the manufacturer's specifications. RNA intended for PCR assays was treated with DNase I, RNase-free (ThermoFisher, Barcelona, Spain). Total gDNA was extracted using the Wizard genomic DNA purification kit (Promega, Madrid, Spain), following the manufacturer's instructions. RNA and gDNA concentrations were determined by measuring its absorbance at 260 nm using a NanoDrop ND-1000 spectrophotometer (ThermoFisher, Barcelona, Spain).

4.4. Reverse Transcription

cDNA was synthesized in a 20 μL reaction mixture containing 1 μg of total RNA, 125 ng of random hexamers (Roche, Spain), 500 μM of each deoxynucleotide triphosphate (Biolone, Barcelona, Spain), 2 μL of buffer (10 \times), 20 units of RNase inhibitor and 200 units of Moloney murine leukemia virus reverse transcriptase (Last three from Lucigen, WI, USA). The reaction was carried out at $42\text{ }^{\circ}\text{C}$ for 1 h.

4.5. PCR

gDNA and cDNA samples from HeLa cells were used as templates to perform PCR reactions in order to locate sequences corresponding to the 5'UTR. Reactions were performed in a final volume of 50 μ L containing either 500 ng of gDNA or 250 ng of cDNA, 5 μ L of buffer 5 \times , 500 ng forward primer, 500 ng reverse primer, 200 μ M dNTPs (Bioline, Barcelona, Spain), 1.25 U OneTaq DNA polymerase (New England Biolabs, Barcelona, Spain) and H₂O mQ. Cycling conditions were as follows: 3 min denaturation at 94 °C, followed by 30 cycles of 30 s at 94 °C, 1 min at 59 °C and 1 min at 68 °C, and a final extension step of 5 min at 68 °C. PCR products were resolved in a non-denaturing 6% polyacrylamide gel electrophoresis in 1 \times TBE buffer. Gels were visualized using Gel Doc™ EZ and the Image Lab Software, Version 6.0 (Bio-Rad, Madrid, Spain). Forward (5'UTR-TYMS-Fw) and reverse primers (5'UTR-TYMS-Rv) were designed to hybridize to a sequence located 32 nt upstream and 109 nt downstream from the G4FS, respectively. The 5'UTR-TYMS-Rv primer covers 25 nt of the translating mRNA. The 184 bp PCR product was sequenced in Macrogen (Amsterdam, the Netherlands).

We confirmed that the DNase digestion was completely achieved by performing a PCR with primers located in exon 1 (APRT-Ex1-Fw) and exon 2 (APRT-Ex2-Rv) of the human *APRT* gene, intervened by a short intron of 163 bp. The amplification of the gDNA sample led to a product of 291 bp (including intron 1), whereas in the case of the RNA (treated with DNase), the product had a length of 128 bp (excluding intron 1). Primer sequences are shown in Table 1.

4.6. CD and UV Absorbance Spectroscopy

The CD spectra were recorded on a JASCO spectropolarimeter J-810 at 20 °C with a scanning speed of 100 nm/min, a response time of 4 s, 0.5 nm data pitch and 1 nm bandwidth. The samples (4 μ M) were dissolved in the above buffers, annealed and slowly cooled to room temperature and left at 4 °C for at least one night.

The thermal melting curves were obtained following the absorption change at 295 nm for the ODN from 15 °C to 70 °C, with a linear temperature ramp of 0.5°/min in Teflon-stoppered 1-cm path-length quartz cells, on a JASCO V-650 spectrophotometer equipped with a Peltier temperature control. UV spectra of the oligonucleotides were recorded at 15° (folded) and 80 °C (unfolded) to calculate the TDS. The measurements were conducted in either 10 mM sodium cacodylate buffer plus 100 mM KCl (pH 7.0) or PBS.

4.7. Thioflavin T Fluorescence Spectroscopy

ThT titrations were carried out with a JASCO FP-6200 spectrofluorometer with a temperature-controlled circulator JASCO ETC-272T. The fluorescence spectra were acquired using a quartz cuvette with a 10-mm path length. In the fluorescence measurements, both the excitation and emission slits were 10 nm, the excitation wavelength was set to 430 nm, and the scan speed was 250 nm/min. Fluorescence spectra were recorded between 450 to 650 nm. ThT (3 μ M) was titrated with increasing concentrations of ODN (0–6 μ M) to measure the binding constant. The fluorescence intensity at 491 nm was plotted as a function of the oligonucleotide concentration. The data were fitted according to a 1:1 binding model.

4.8. Nuclear Magnetic Resonance

The sample for NMR was prepared by dissolving the oligonucleotide at 180 μ M concentration in 25 mM K₂HPO₄; pH7, 100 mM KCl buffer containing 10% D₂O. NMR spectra were acquired with a Bruker QANUC 800 MHz spectrometer equipped with a cryoprobe and processed with TOPSPIN 2.1 software. An excitation sculpting pulse program was used to suppress the water signal while detecting rapid interchangeable imino protons.

4.9. RT-qPCR

To determine TYMS mRNA levels, a QuantStudio 3 Real-Time PCR System (Applied Biosystems, Barcelona, Spain) was used. The reaction was performed in a final volume of 20 μ L, containing 1 \times SYBR Universal PCR Master mix (Applied Biosystems, Barcelona, Spain), 0.25 μ M of reverse and forward primers (Sigma- Aldrich, Madrid, Spain), 3 μ L of cDNA and H₂O mQ. PCR cycling conditions were 10 min denaturation at 95 °C, followed by 40 cycles of 15 s at 95 °C and 1 min at 60 °C. The mRNA quantification was performed using the $\Delta\Delta$ Ct method, where Ct is the threshold cycle that corresponds to the cycle where the amount of amplified mRNA reaches the threshold of fluorescence. Cyclophylin B (PPIB) was used as an endogenous control to normalize the results. Primer sequences for RT-qPCR are detailed in Table 1.

4.10. Electrophoretic Mobility Shift Assay

To perform EMSA analyses, the dsDNA probe corresponding to G4FS was obtained by mixing equal amounts of each single-stranded oligodeoxynucleotide in a 150 mM NaCl solution. After incubation at 90 °C for 5 min, the solution was allowed to cool down slowly to room temperature. The duplex was resolved in a nondenaturing 20% polyacrylamide gel, visualized using UV shadowing and purified from the gel. DNA concentration was measured as stated in Section 4.3 of Materials and Methods.

dsDNA, ssDNA and RNA probes (200 ng) were 5'-end-labeled with (γ -³²P)-ATP (3000 Ci/mmol) (Perkin Elmer, Madrid, Spain) using T4 polynucleotide kinase (New England BioLabs, MA, USA) in a 10 μ L reaction mixture, according to the manufacturer's instructions. After incubation at 37 °C for 1 h, 90 μ L of Tris-EDTA buffer (1 mM EDTA and 10 mM Tris, pH 8.0; Sigma-Aldrich, Madrid, Spain) was added to the reaction mixture, which was subsequently filtered through a Sephadex G-25 (Sigma-Aldrich, Madrid, Spain) spin-column to eliminate the unincorporated (γ -³²P)-ATP.

Radio-labeled probes (100,000 cpm, [γ -³²P]-ATP) were incubated with either HeLa nuclear protein extracts, purified TYMS or HpTYMS-G4-T PPRH. Both BSA and DHFR proteins were used as negative controls. Poly(dI:dC) (3 μ g) was added to each reaction as an unspecific competitor. Binding reactions were performed in the presence of a binding buffer (5% glycerol, 0.5 mM DTT, 4 mM MgCl₂, 36 mM KCl, 0.5 mM EDTA, 25 mM Tris-HCl, pH 8.0; all reagents were purchased from Sigma-Aldrich). The products of the binding reactions were electrophoretically resolved in 5% polyacrylamide and 5% glycerol native gels in 0.5 \times TBE buffer, at a fixed voltage of 220 V and 4 °C. Gels were dried at 80 °C and scanned on a Storm 840 PhosphorImager (Molecular Dynamics, GE Healthcare Life Sciences, Barcelona, Spain). ImageQuant software v5.2 was used to visualize and quantify the results (GE Healthcare, Barcelona, Spain).

4.11. Detection of G4 Structures with ThT upon DNA Binding Assays

To detect G4 structures after DNA binding assays, 1.5 μ g of each oligonucleotide, alone or combined with the indicated oligonucleotide, was incubated at 90 °C for 5 min in water, then diluted with a buffer containing 100 mM KCl and 100 mM Tris/HCl (pH 7.5) in a final volume of 100 μ L and slowly cooled to room temperature (2 h).

Samples (75 μ L) were loaded on nondenaturing 12% polyacrylamide gels (10 cm) containing 10 mM KCl in 1 \times TBE buffer and electrophoresed for 1–2 h at 150 V. After electrophoresis, gels were stained with 5 μ M of ThT solution for 15 min under agitation, briefly washed in water, and exposed to a UV light lamp to obtain images. Then, the same gels were further stained with 1 μ g/mL ethidium bromide solution for 10 min under agitation and washed for 10 min in water. Images were captured under a UV light lamp or using the Gel DocTM EZ with the Image Lab Software, Version 6.0.

4.12. Cell Culture

HeLa and PC-3 cell lines obtained from the cell bank resources from University of Barcelona were grown in Ham's F12 medium supplemented with 10% fetal bovine serum (GIBCO, Invitrogen,

Barcelona, Spain) or in Roswell Park Memorial Institute medium (RPMI), which is deficient in thymidine, supplemented with 7% dialyzed fetal bovine serum and incubated at 37 °C in a humidified 5% CO₂ atmosphere.

4.13. Transfection of the PPRH

One day before transfection, cells were plated in 6-well dishes in 800 µL of either F12 or RPMI medium. The transfection consisted of mixing N-[1-(1,2-Di-(9Z-octadecenoyl)-3-trimethylammoniumpropane methyl sulfate (DOTAP; Biontex, Germany) with the PPRH and serum-free medium in volumes of up to 200 µL. Unless stated otherwise, the molar ratio of PPRH/DOTAP was 1:100 (100 nM/10 µM). After 20 min of incubation at room temperature, the mixture was added to the cells to attain a final volume of 1 mL.

4.14. Western Blot Analyses

Total protein extracts from HeLa cells (30,000) were obtained using 100 µL of RIPA buffer (1% Igepal, 0.5% sodium deoxycholate, 0.1% SDS, 150 mM NaCl, 1 mM EDTA, 1 mM PMSF, 10 mM NaF and 50 mM Tris-HCl, pH 8, containing additionally the Protease inhibitor cocktail (P8340-5ML); all the above were purchased from Sigma Aldrich, Madrid, Spain, but Tris-HCl was from PanReac AppliChem, Barcelona, Spain). Extracts were incubated for 5 min at 4 °C and cell debris was removed by centrifugation (16,300× g at 4 °C for 10 min). Protein concentrations were determined using a Bio-Rad protein assay based on the Bradford method and using bovine serum albumin as a standard.

Protein extracts were electrophoresed in 10% SDS-polyacrylamide gels and transferred to polyvinylidene difluoride membranes. Blocking of membranes was performed using 5% Blotto. In the case of primary antibody against TYMS (1:100 dilution; sc-376161, Santa Cruz Biotechnology, Heidelberg, Germany), membranes were probed overnight at 4 °C, whereas primary antibody against α-Tubulin (1:100 dilution; CP06, Merck, Darmstadt, Germany) membranes were probed for 90 min at room temperature. Signals of both proteins were detected by secondary horseradish peroxidase-conjugated anti-mouse antibody (1:2500 dilution; sc-516102, Santa Cruz Biotechnology, Heidelberg, Germany). Chemiluminescence was detected with the ImageQuant LAS 4000 mini imager (GE Healthcare, Barcelona, Spain). Quantification was performed using the ImageQuant 5.2 software.

4.15. Combination Treatment of 5-FU plus HpTYMS-G4-T

Cells were plated in 6-well dishes in RPMI medium one day before transfection or 5-FU treatment. The 5-FU (Sigma-Aldrich, Madrid, Spain) was prepared from powder as a 100 mM stock solution in DMSO and diluted in RPMI medium. The transfection was performed as indicated in the Section 4.13, Transfection. Cells were incubated with 5-FU alone or combined concurrently with the PPRH in a final volume of 1 mL.

4.16. MTT Assay

Cells (10,000) were plated in 6-well dishes in F12 medium or RPMI medium. Five days after transfection or 5-FU treatment, 3-(4,5-dimethylthiazol-2-yl)-2,5-diphenyltetrazolium bromide and sodium succinate (both from Sigma-Aldrich, Madrid, Spain) were added to the culture medium (final concentration 0.63 mM and 100 µM, respectively) and incubated for 2.5 h at 37 °C. Then, the culture medium was removed and the lysis solution (0.57% of acetic acid and 10% of SDS in DMSO) (Sigma-Aldrich, Madrid, Spain) was added. Absorbance was measured at 570 nm in a Modulus Microplate spectrophotometer (Turner BioSystems, Madrid, Spain). Cell viability results were expressed as the percentage of cell survival relative to the controls.

4.17. Statistical Analyses

Statistical analyses were performed using GraphPad Prism 6 (GraphPad Software, CA, USA). All data are shown as the mean \pm SEM of at least three independent experiments. The levels of statistical significance were denoted as follows: $p < 0.05$ (*), $p < 0.01$ (**), $p < 0.001$ (***) or $p < 0.0001$ (****).

5. Conclusions

In this work, we identified a G4FS in the 5'UTR of the *TYMS* gene and confirmed its folding into a G4 structure in both DNA and RNA backbones. Additionally, we determined that TYMS protein directly interacts with G4FS either as dsDNA, ssDNA or RNA, which may be involved in transcriptional and translational autoregulation of TYMS expression. Finally, the HpTYMS-G4-T PPRH targeting the complementary strand of the G4FS decreased both TYMS mRNA and protein levels in cancer cells, leading to cell death and showing a synergic effect in combination with 5-FU.

Supplementary Materials: Supplementary materials can be found at <http://www.mdpi.com/1422-0067/21/14/5028/s1>.

Author Contributions: Conceptualization, C.J.C. and V.N.; methodology, E.A. and A.J.F.; software, E.A. and A.J.F.; validation, E.A. and A.J.F.; formal analysis, E.A. and A.J.F.; investigation, E.A., A.J.F., M.G., L.R. and A.A.; resources, V.N.; data curation, E.A. and A.J.F.; writing—original draft preparation, E.A. and A.J.F.; writing—review and editing, M.G., A.A., R.E., C.J.C. and V.N.; supervision, C.J.C. and V.N.; project administration, V.N.; funding acquisition, C.J.C. and V.N. All authors have read and agreed to the published version of the manuscript.

Funding: This research was funded by grant RTI2018-093901-B-I00 from Plan Nacional de Investigación Científica (Spain). Group holding the Quality Mention from Generalitat de Catalunya 2017-SGR-94. AJF, EA and MG were awarded with fellowships from Ministerio de Educación (FPU), Generalitat de Catalunya (FI), and Marie Skłodowska-Curie (GA799693), respectively.

Acknowledgments: We thank Carme Plasencia for providing TYMS protein, Carlos Gonzalez for helpful suggestions and Masad J. Damha for providing the laboratory resources for NMR characterization of DNA oligonucleotides.

Conflicts of Interest: The authors declare no conflict of interest.

Abbreviations

TYMS	Thymidylate synthase
5-FU	5-fluorouracil
ASO	Antisense oligodeoxynucleotides
G4	G-quadruplex structures
G4FS	G4 forming sequence
PPRH	Polypurine reverse Hoogsteen hairpins
ThT	Thioflavin T
DOTAP	N-(1-(1,2-Di-(9Z-octadecenyl)-3-trimethylammoniumpropane methyl sulfate

References

1. Carreras, C.W.; Santi, D.V. The Catalytic Mechanism and Structure of Thymidylate Synthase. *Annu. Rev. Biochem.* **1995**, *64*, 721–762. [[CrossRef](#)] [[PubMed](#)]
2. Rose, M.G.; Farrell, M.P.; Schmitz, J.C. Thymidylate synthase: A critical target for cancer chemotherapy. *Clin. Colorectal Cancer* **2002**, *1*, 220–229. [[CrossRef](#)] [[PubMed](#)]
3. Gmeiner, W. Novel Chemical Strategies for Thymidylate Synthase Inhibition. *Curr. Med. Chem.* **2012**, *12*, 191–202. [[CrossRef](#)] [[PubMed](#)]
4. Longley, D.B.; Harkin, D.P.; Johnston, P.G. 5-Fluorouracil: Mechanisms of action and clinical strategies. *Nat. Rev. Cancer* **2003**, *3*, 330–338. [[CrossRef](#)] [[PubMed](#)]
5. Zhang, N.; Yin, Y.; Xu, S.J.; Chen, W.S. 5-Fluorouracil: Mechanisms of resistance and reversal strategies. *Molecules* **2008**, *13*, 1551–1569. [[CrossRef](#)]
6. Berger, S.H.; Jenh, C.H.; Johnson, L.F.; Berger, F.G. Thymidylate synthase overproduction and gene amplification in fluorodeoxyuridine-resistant human cells. *Mol. Pharmacol.* **1985**, *28*, 461–467.

7. Rooney, P.H.; Stevenson, D.A.J.; Marsh, S.; Johnston, P.G.; Haites, N.E.; Cassidy, J.; McLeod, H.L. Comparative genomic hybridization analysis of chromosomal alterations induced by the development of resistance to thymidylate synthase inhibitors. *Cancer Res.* **1998**, *58*, 5042–5045.
8. Chu, E.; Koeller, D.M.; Casey, J.L.; Drake, J.C.; Chabner, B.A.; Elwood, P.C.; Zinn, S.; Allegra, C.J. Autoregulation of human thymidylate synthase messenger RNA translation by thymidylate synthase. *Proc. Natl. Acad. Sci. USA* **1991**, *88*, 8977–8981. [[CrossRef](#)]
9. Chu, E.; Voeller, D.; Koeller, D.M.; Drake, J.C.; Takimoto, C.H.; Maley, G.F.; Maley, F.; Allegra, C.J. Identification of an RNA binding site for human thymidylate synthase. *Proc. Natl. Acad. Sci. USA* **1993**, *90*, 517–521. [[CrossRef](#)]
10. Garg, D.; Henrich, S.; Salo-Ahen, O.M.H.; Myllykallio, H.; Costi, M.P.; Wade, R.C. Novel approaches for targeting thymidylate synthase to overcome the resistance and toxicity of anticancer drugs. *J. Med. Chem.* **2010**, *53*, 6539–6549. [[CrossRef](#)]
11. Brunn, N.D.; Dibrov, S.M.; Kao, M.B.; Ghassemian, M.; Hermann, T. Analysis of mRNA recognition by human thymidylate synthase. *Biosci. Rep.* **2014**, *34*, 905–913. [[CrossRef](#)]
12. Tian, T.; Chen, Y.Q.; Wang, S.R.; Zhou, X. G-Quadruplex: A Regulator of Gene Expression and Its Chemical Targeting. *Chem* **2018**, *4*, 1314–1344. [[CrossRef](#)]
13. Gellert, M.; Lipsett, M.N.; Davies, D.R. Helix formation by guanylic acid. *Proc. Natl. Acad. Sci. USA* **1962**, *48*, 2013–2018. [[CrossRef](#)] [[PubMed](#)]
14. Davis, J.T. G-Quartets 40 Years Later: From 5'-GMP to Molecular Biology and Supramolecular Chemistry. *Angew. Chem. Int. Ed.* **2004**, *43*, 668–698. [[CrossRef](#)] [[PubMed](#)]
15. Lane, A.N.; Chaires, J.B.; Gray, R.D.; Trent, J.O. Stability and kinetics of G-quadruplex structures. *Nucleic Acids Res.* **2008**, *36*, 5482–5515. [[CrossRef](#)]
16. Hänsel-Hertsch, R.; di Antonio, M.; Balasubramanian, S. DNA G-quadruplexes in the human genome: Detection, functions and therapeutic potential. *Nat. Rev. Mol. Cell Biol.* **2017**, *18*, 279–284. [[CrossRef](#)]
17. Rhodes, D.; Lipps, H.J. Survey and summary G-quadruplexes and their regulatory roles in biology. *Nucleic Acids Res.* **2015**, *43*, 8627–8637. [[CrossRef](#)]
18. Bugaut, A.; Balasubramanian, S. 5'-UTR RNA G-quadruplexes: Translation regulation and targeting. *Nucleic Acids Res.* **2012**, *40*, 4727–4741. [[CrossRef](#)]
19. Song, J.; Perreault, J.-P.; Topisirovic, I.; Richard, S. RNA G-quadruplexes and their potential regulatory roles in translation. *Translation* **2016**, *4*, e1244031. [[CrossRef](#)]
20. Chambers, V.S.; Marsico, G.; Boutell, J.M.; di Antonio, M.; Smith, G.P.; Balasubramanian, S. High-throughput sequencing of DNA G-quadruplex structures in the human genome. *Nat. Biotechnol.* **2015**, *33*, 877–881. [[CrossRef](#)]
21. Ciudad, C.J.; Rodríguez, L.; Villalobos, X.; Félix, A.J.; Noé, V. Polypurine Reverse Hoogsteen Hairpins as a Gene Silencing Tool for Cancer. *Curr. Med. Chem.* **2017**, *24*, 2809–2826. [[CrossRef](#)] [[PubMed](#)]
22. De Almagro, M.C.; Coma, S.; Noé, V.; Ciudad, C.J. Polypurine hairpins directed against the template strand of DNA knock down the expression of mammalian genes. *J. Biol. Chem.* **2009**, *284*, 11579–11589. [[CrossRef](#)] [[PubMed](#)]
23. Goñi, J.R.; de la Cruz, X.; Orozco, M. Triplex-forming oligonucleotide target sequences in the human genome. *Nucleic Acids Res.* **2004**, *32*, 354–360. [[CrossRef](#)]
24. Rodríguez, L.; Villalobos, X.; Dakhel, S.; Padilla, L.; Hervas, R.; Hernández, J.L.; Ciudad, C.J.; Noé, V. Polypurine reverse Hoogsteen hairpins as a gene therapy tool against survivin in human prostate cancer PC3 cells in vitro and in vivo. *Biochem. Pharmacol.* **2013**, *86*, 1541–1554. [[CrossRef](#)]
25. De Almagro, M.C.; Mencia, N.; Noé, V.; Ciudad, C.J. Coding polypurine hairpins cause target-induced cell death in breast cancer cells. *Hum. Gene Ther.* **2011**, *22*, 451–463. [[CrossRef](#)]
26. Villalobos, X.; Rodríguez, L.; Solé, A.; Lliberós, C.; Mencia, N.; Ciudad, C.J.; Noé, V. Effect of polypurine reverse Hoogsteen hairpins on relevant cancer target genes in different human cell lines. *Nucleic Acid Ther.* **2015**, *25*, 198–208. [[CrossRef](#)]
27. Aubets, E.; Noé, V.; Ciudad, C.J. Targeting replication stress response using polypurine reverse Hoogsteen hairpins directed against WEE1 and CHK1 genes in human cancer cells. *Biochem. Pharmacol.* **2020**, *175*, 113911. [[CrossRef](#)] [[PubMed](#)]

28. Bener, G.; Félix, A.J.; de Diego, C.S.; Fabregat, I.P.; Ciudad, C.J.; Noé, V. Silencing of CD47 and SIRP α by Polypurine reverse Hoogsteen hairpins to promote MCF-7 breast cancer cells death by PMA-differentiated THP-1 cells. *BMC Immunol.* **2016**, *17*, 32. [[CrossRef](#)]
29. Ciudad, C.J.; Enriquez, M.M.M.; Félix, A.J.; Bener, G.; Noé, V. Silencing PD-1 and PD-L1: The potential of PolyPurine Reverse Hoogsteen hairpins for the elimination of tumor cells. *Immunotherapy* **2019**, *11*, 369–372. [[CrossRef](#)]
30. Enríquez, M.M.M.; Félix, A.J.; Ciudad, C.J.; Noé, V. Cancer immunotherapy using PolyPurine Reverse Hoogsteen hairpins targeting the PD-1/PD-L1 pathway in human tumor cells. *PLoS ONE.* **2018**, *13*, e0206818.
31. Mencia, N.; Selga, E.; Noé, V.; Ciudad, C.J. Underexpression of miR-224 in methotrexate resistant human colon cancer cells. *Biochem. Pharm.* **2011**, *82*, 1572–1582. [[CrossRef](#)] [[PubMed](#)]
32. Kaneda, S.; Nalbantoglu, J.; Takeishi, K.; Shimizu, K.; Gotoh, O.; Seno, T.; Ayusawa, D. Structural and functional analysis of the human thymidylate synthase gene. *J. Biol. Chem.* **1990**, *265*, 20277–20284.
33. Gaddis, S.S.; Wu, Q.; Thames, H.D.; Digiovanni, J.; Walborg, E.F.; Macleod, M.C.; Vasquez, K.M. A web-based search engine for triplex-forming oligonucleotide target sequences. *Oligonucleotides* **2006**, *16*, 196–201. [[CrossRef](#)]
34. Mergny, J.-L.; Phan, A.-T.; Lacroix, L. Following G-quartet formation by UV-spectroscopy. *FEBS Lett.* **1998**, *435*, 74–78. [[CrossRef](#)]
35. Paramasivan, S.; Rujan, I.; Bolton, P.H. Circular dichroism of quadruplex DNAs: Applications to structure, cation effects and ligand binding. *Methods* **2007**, *43*, 324–331. [[CrossRef](#)] [[PubMed](#)]
36. Mergny, J.-L.; Li, J.; Lacroix, L.; Amrane, S.; Chaires, J.B. Thermal difference spectra: A specific signature for nucleic acid structures. *Nucleic Acids Res.* **2005**, *33*, e138. [[CrossRef](#)] [[PubMed](#)]
37. Kettani, A.; Kumar, R.A.; Patel, D.J. Solution structure of a DNA quadruplex containing the fragile X syndrome triplet repeat. *J. Mol. Biol.* **1995**, *254*, 638–656. [[CrossRef](#)]
38. Mohanty, J.; Barooah, N.; Dhamodharan, V.; Harikrishna, S.; Pradeepkumar, P.I.; Bhasikuttan, A.C. Thioflavin T as an Efficient Inducer and Selective Fluorescent Sensor for the Human Telomeric G-Quadruplex DNA. *J. Am. Chem. Soc.* **2013**, *135*, 367–376. [[CrossRef](#)] [[PubMed](#)]
39. Maiti, S.; Chaudhury, N.K.; Chowdhury, S. Hoechst 33258 binds to G-quadruplex in the promoter region of human c-myc. *Biochem. Biophys. Res. Commun.* **2003**, *310*, 505–512. [[CrossRef](#)]
40. De la Faverie, A.R.; Guédin, A.; Bedrat, A.; Yatsunyk, L.A.; Mergny, J.L. Thioflavin T as a fluorescence light-up probe for G4 formation. *Nucleic Acids Res.* **2014**, *42*, e65. [[CrossRef](#)]
41. Solé, A.; Delagoutte, E.; Ciudad, C.J.; Noé, V.; Alberti, P. Polypurine reverse-Hoogsteen (PPRH) oligonucleotides can form triplexes with their target sequences even under conditions where they fold into G-quadruplexes. *Sci. Rep.* **2017**, *7*, 1–11. [[CrossRef](#)]
42. Chou, T.-C. Drug Combination Studies and Their Synergy Quantification Using the Chou-Talalay Method. *Cancer Res.* **2010**, *70*, 440–446. [[CrossRef](#)] [[PubMed](#)]
43. Ligabue, A.; Marverti, G.; Liebl, U.; Myllykallio, H. Transcriptional Activation and Cell Cycle Block Are the Keys for 5-Fluorouracil Induced Up-Regulation of Human Thymidylate Synthase Expression. *PLoS ONE* **2012**, *7*, e47318. [[CrossRef](#)] [[PubMed](#)]
44. Peters, G.J.; Backus, H.H.J.; Freemantle, S.; van Triest, B.; Codacci-Pisanelli, G.; van der Wilt, C.L.; Smid, K.; Lunec, J.; Calvert, A.H.; Marsh, S.; et al. Induction of thymidylate synthase as a 5-fluorouracil resistance mechanism. *Biochim. Biophys. Acta Mol. Basis Dis.* **2002**, *1587*, 194–205. [[CrossRef](#)]
45. Peters, G.J.; van Triest, B.; Backus, H.H.J.; Kuiper, C.M.; van der Wilt, C.L.; Pinedo, H.M. Molecular downstream events and induction of thymidylate synthase in mutant and wild-type p53 colon cancer cell lines after treatment with 5-fluorouracil and the thymidylate synthase inhibitor raltitrexed. *Eur. J. Cancer* **2000**, *36*, 916–924. [[CrossRef](#)]
46. Kikin, O.; D’Antonio, L.; Bagga, P.S. QGRS Mapper: A web-based server for predicting G-quadruplexes in nucleotide sequences. *Nucleic Acids Res.* **2006**, *34*, W676–W682. [[CrossRef](#)]
47. Chu, E.; Takimoto, C.H.; Voeller, D.; Grem, J.L.; Allegra, C.J. Specific Binding of Human Dihydrofolate Reductase Protein to Dihydrofolate Reductase Messenger RNA in Vitro. *Biochemistry* **1993**, *32*, 4756–4760. [[CrossRef](#)]
48. Bhardwaj, A.; Wilkinson, M.F. A metabolic enzyme doing double duty as a transcription factor. *BioEssays* **2005**, *27*, 467–471. [[CrossRef](#)]

49. Zheng, L.; Roeder, R.G.; Luo, Y. S Phase Activation of the Histone H2B Promoter by OCA-S, a Coactivator Complex that Contains GAPDH as a Key Component. *Cell* **2003**, *114*, 255–266. [[CrossRef](#)]
50. Chu, E.; Takechi, T.; Jones, K.L.; Voeller, D.M.; Copur, S.M.; Maley, G.F.; Maley, F.; Segal, S.; Allegra, C.J. Thymidylate synthase binds to c-myc RNA in human colon cancer cells and in vitro. *Mol. Cell. Biol.* **1995**, *15*, 179–185. [[CrossRef](#)]
51. Ju, J.; Pedersen-Lane, J.; Maley, F.; Chu, E. Regulation of p53 expression by thymidylate synthase. *Proc. Natl. Acad. Sci. USA* **1999**, *96*, 3769–3774. [[CrossRef](#)] [[PubMed](#)]
52. Chu, E.; Copur, S.M.; Ju, J.; Chen, T.; Khleif, S.; Voeller, D.M.; Mizunuma, N.; Patel, M.; Maley, G.F.; Maley, F.; et al. Thymidylate Synthase Protein and p53 mRNA Form an In Vivo Ribonucleoprotein Complex. *Mol. Cell. Biol.* **1999**, *19*, 1582–1594. [[CrossRef](#)]
53. Chu, E. Identification of in vivo target RNA sequences bound by thymidylate synthase. *Nucleic Acids Res.* **1996**, *24*, 3222–3228. [[CrossRef](#)]
54. Cogo, S.; Shchekotikhin, A.E.; Xodo, L.E. HRAS is silenced by two neighboring G-quadruplexes and activated by MAZ, a zinc-finger transcription factor with DNA unfolding property. *Nucleic Acids Res.* **2014**, *42*, 8379–8388. [[CrossRef](#)] [[PubMed](#)]
55. Chen, S.; Su, L.; Qiu, J.; Xiao, N.; Lin, J.; Tan, J.H.; Ou, T.M.; Gu, L.Q.; Huang, Z.S.; Li, D. Mechanistic studies for the role of cellular nucleic-acid-binding protein (CNBP) in regulation of c-myc transcription. *Biochim. Biophys. Acta Gen. Subj.* **2013**, *1830*, 4769–4777. [[CrossRef](#)] [[PubMed](#)]
56. Kumari, S.; Bugaut, A.; Huppert, J.L.; Balasubramanian, S. An RNA G-quadruplex in the 5' UTR of the NRAS proto-oncogene modulates translation. *Nat. Chem. Biol.* **2007**, *3*, 218–221. [[CrossRef](#)]
57. Kim, M.Y.; Vankayalapati, H.; Shin-Ya, K.; Wierzba, K.; Hurley, L.H. Telomestatin, a potent telomerase inhibitor that interacts quite specifically with the human telomeric intramolecular G-quadruplex. *J. Am. Chem. Soc.* **2002**, *124*, 2098–2099. [[CrossRef](#)]
58. Zahler, A.M.; Williamson, J.R.; Cech, T.R.; Prescott, D.M. Inhibition of telomerase by G-quartet DNA structures. *Nature* **1991**, *350*, 718–720. [[CrossRef](#)]
59. Asamitsu, S.; Obata, S.; Yu, Z.; Bando, T.; Sugiyama, H. Recent progress of targeted G-quadruplex-preferred ligands toward cancer therapy. *Molecules* **2019**, *24*, 429. [[CrossRef](#)]
60. Siddiqui-Jain, A.; Grand, C.L.; Bearss, D.J.; Hurley, L.H. Direct evidence for a G-quadruplex in a promoter region and its targeting with a small molecule to repress c-MYC transcription. *Proc. Natl. Acad. Sci. USA* **2002**, *99*, 11593–11598. [[CrossRef](#)]
61. Wang, S.K.; Wu, Y.; Wang, X.Q.; Kuang, G.T.; Zhang, Q.; Lin, S.L.; Liu, H.Y.; Tan, J.H.; Huang, Z.S.; Ou, T.M. Discovery of Small Molecules for Repressing Cap-Independent Translation of Human Vascular Endothelial Growth Factor (hVEGF) as Novel Antitumor Agents. *J. Med. Chem.* **2017**, *60*, 5306–5319. [[CrossRef](#)]
62. Beaudoin, J.D.; Perreault, J.P. Exploring mRNA 3'-UTR G-quadruplexes: Evidence of roles in both alternative polyadenylation and mRNA shortening. *Nucleic Acids Res.* **2013**, *41*, 5898–5911. [[CrossRef](#)] [[PubMed](#)]
63. Che, T.; Wang, Y.Q.; Huang, Z.L.; Tan, J.H.; Huang, Z.S.; Chen, S.B. Natural alkaloids and heterocycles as G-quadruplex ligands and potential anticancer agents. *Molecules* **2018**, *23*, 493.
64. Xu, H.; di Antonio, M.; McKinney, S.; Mathew, V.; Ho, B.; O'Neil, N.J.; Santos, N.D.; Silvester, J.; Wei, V.; Garcia, J.; et al. CX-5461 is a DNA G-quadruplex stabilizer with selective lethality in BRCA1/2 deficient tumours. *Nat. Commun.* **2017**, *8*, 14432. [[CrossRef](#)]
65. Khot, A.; Brajanovski, N.; Cameron, D.P.; Hein, N.; Maclachlan, K.H.; Sanij, E.; Lim, J.; Soong, J.; Link, E.; Blombery, P.; et al. First-in-human RNA polymerase I transcription inhibitor CX-5461 in patients with advanced hematologic cancers: Results of a phase I dose-escalation study. *Cancer Discov.* **2019**, *9*, 1036–1049. [[CrossRef](#)]
66. Drygin, D.; Siddiqui-Jain, A.; O'Brien, S.; Schwaebe, M.; Lin, A.; Bliesath, J.; Ho, C.B.; Proffitt, C.; Trent, K.; Whitten, J.P.; et al. Anticancer activity of CX-3543: A direct inhibitor of rRNA biogenesis. *Cancer Res.* **2009**, *69*, 7653–7661. [[CrossRef](#)] [[PubMed](#)]
67. Local, A.; Zhang, H.; Benbatoul, K.D.; Folger, P.; Sheng, X.; Tsai, C.Y.; Howell, S.B.; Rice, W.G. APTO-253 stabilizes G-quadruplex DNA, inhibits MYC expression, and induces DNA damage in acute myeloid leukemia cells. *Mol. Cancer Ther.* **2018**, *17*, 1177–1186. [[CrossRef](#)] [[PubMed](#)]
68. Huppert, J.L.; Balasubramanian, S. Prevalence of quadruplexes in the human genome. *Nucleic Acids Res.* **2005**, *33*, 2908–2916. [[CrossRef](#)]

69. Schmitz, J.C.; Chen, T.M.; Chu, E. Small Interfering Double-Stranded RNAs as Therapeutic Molecules to Restore Chemosensitivity to Thymidylate Synthase Inhibitor Compounds. *Cancer Res.* **2004**, *64*, 1431–1435. [[CrossRef](#)]
70. Jason, T.L.H.; Berg, R.W.; Vincent, M.D.; Koropatnick, J. Antisense targeting of Thymidylate Synthase (TS) mRNA increases TS gene transcription and TS protein: Effects on human tumor cell sensitivity to TS enzyme-inhibiting drugs. *Gene Expr.* **2007**, *13*, 227–239. [[CrossRef](#)]
71. Ferguson, P.J.; Collins, O.; Dean, N.M.; DeMoor, J.; Sha-Li, C.; Vincent, M.D.; Koropatnick, J. Antisense down-regulation of thymidylate synthase to suppress growth and enhance cytotoxicity of 5-FUdR, 5-FU and Tomudex in HeLa cells. *Br. J. Pharmacol.* **1999**, *127*, 1777–1786. [[CrossRef](#)] [[PubMed](#)]
72. Berg, R.W.; Ferguson, P.J.; Vincent, M.D.; Koropatnick, D.J. A “combination oligonucleotide” antisense strategy to downregulate thymidylate synthase and decrease tumor cell growth and drug resistance. *Cancer Gene Ther.* **2003**, *10*, 278–286. [[CrossRef](#)] [[PubMed](#)]
73. Yan, S.; Niu, R.L.; Wang, Z.; Lin, X.K. In vitro selected peptides bind with thymidylate synthase mRNA and inhibit its translation. *Sci. China Ser. C Life Sci.* **2007**, *50*, 630–636. [[CrossRef](#)]
74. Villalobos, X.; Rodríguez, L.; Prévot, J.; Oleaga, C.; Ciudad, C.J.; Noé, V. Stability and immunogenicity properties of the gene-silencing polypurine reverse Hoogsteen hairpins. *Mol. Pharm.* **2014**, *11*, 254–264. [[CrossRef](#)]
75. Félix, A.J.; Ciudad, C.J.; Noé, V. Functional pharmacogenomics and toxicity of PolyPurine Reverse Hoogsteen hairpins directed against survivin in human cells. *Biochem. Pharmacol.* **2018**, *155*, 8–20. [[CrossRef](#)]

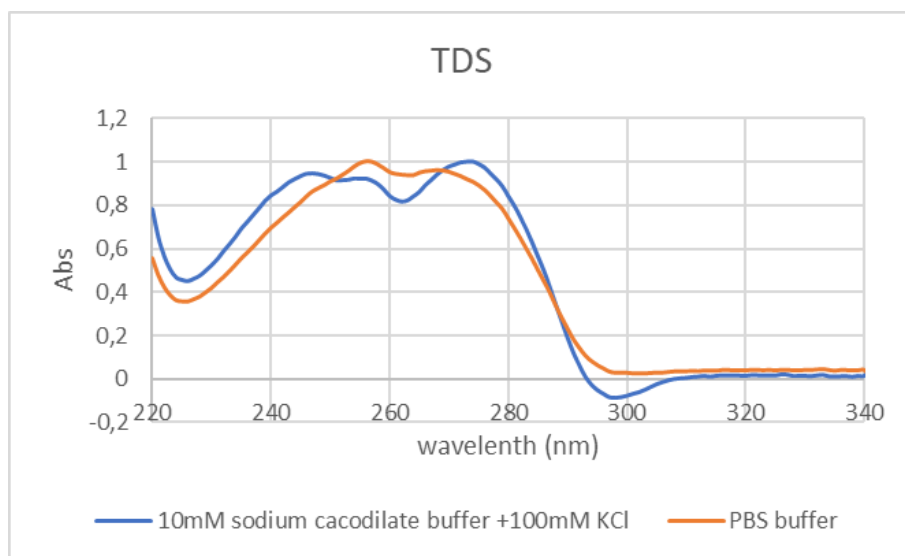


© 2020 by the authors. Licensee MDPI, Basel, Switzerland. This article is an open access article distributed under the terms and conditions of the Creative Commons Attribution (CC BY) license (<http://creativecommons.org/licenses/by/4.0/>).

Results

Supplementary data

A)



B)

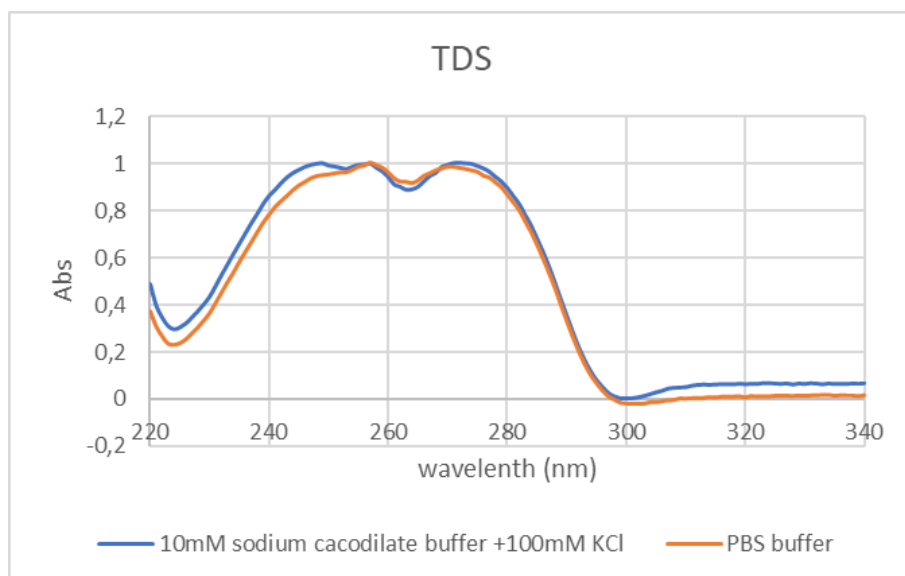
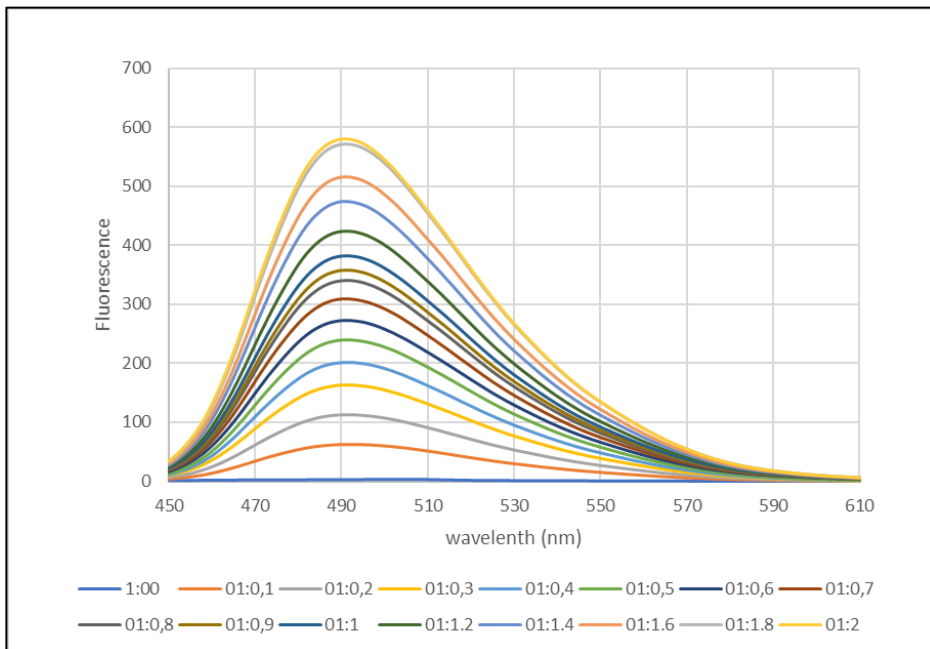


Figure S1: Thermal Differentiation Spectra of ssDNA-G4-Fw (A) and RNA-G4 (B) in two different buffers.

Results

A)



B)

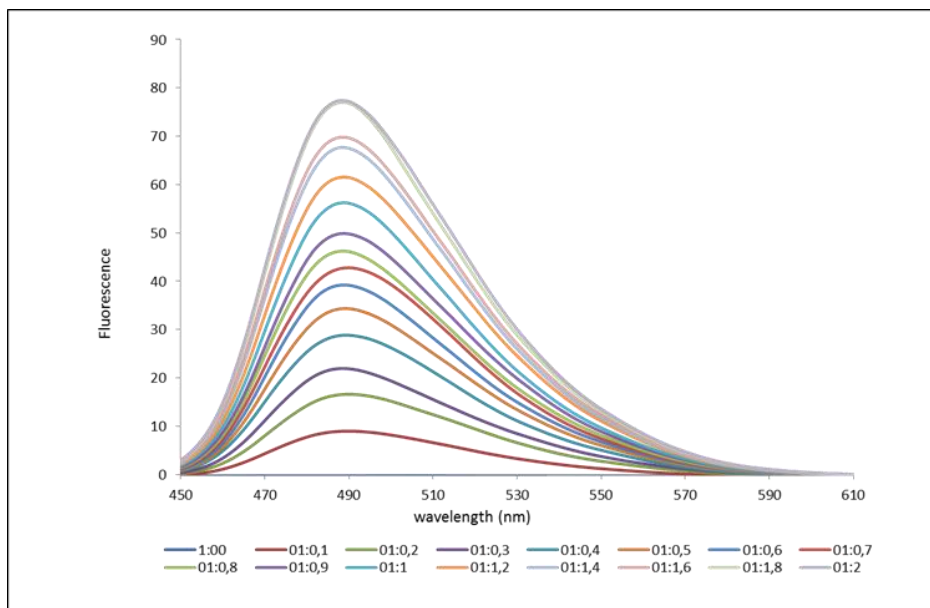


Figure S2: Fluorescence spectra of ThT with increasing concentrations of ssDNA-G4-Fw (A) and RNA-G4 (B) ODN. Initial 1: 0 (3 μ M ThT: 0 ODN). Final 1: 2 (3 μ M ThT: 6 μ M ODN).

The data were fitted according to a 1:1 binding model. The following equation was used to calculate the association constant (K_a)

$$\Delta F_{calc} = \left(\frac{\Delta F_{max}}{2C_t} \right) \left[\left\{ [Q_o] + [C_o] + \frac{1}{K_a} \right\} - \left\{ \sqrt{\left([Q_o] + [C_o] + \frac{1}{K_a} \right)^2 - 4[Q_o][C_o]} \right\} \right]$$

$[Q_o]$ is the concentration of the oligonucleotide, $[C_o]$ and C_t are the concentrations of the initial free and final ligand respectively. Finally, ΔF_{max} corresponds to the maximum increment of fluorescence. Note that the model (ODN + ligand \rightarrow complex) assumes two states, and the fluorescence is the sum of the free and the complex ligand.

Results

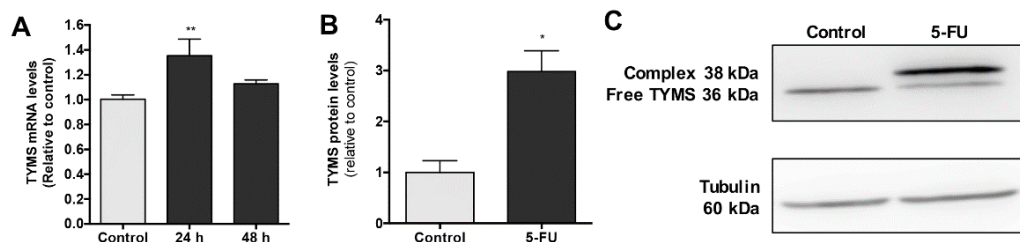


Figure S3: Effect of 5-FU on the levels of TYMS mRNA and protein. HeLa cells (30,000) were incubated with 3 μ M of 5-FU in RPMI medium. (A) TYMS mRNA levels were determined by RT-qPCR 24 h and 48 h after 5-FU treatment. Cyclophilin B (PPIB) was used to normalize the results. Statistical significance was determined using one-way ANOVA with Dunnett's multiple comparisons test (** $p < 0.01$). (B) Total TYMS protein levels on HeLa cells after 24h of treatment. The total amount of TYMS protein levels were quantified (free TYMS protein, corresponding to 36 kDa band, plus the ternary complex FdUMP-TYMS-mTHF, corresponding to 38 kDa band). Statistical significance was determined using an Unpaired Student's T test (* $p < 0.05$). Tubulin protein levels were used to normalize the results. (C) Representative images of Western blots.

4.2.1. Additional results to Article II

In this work we demonstrate that G4s are targetable by PPRHs. One of the objectives of our research group is to expand the use of PPRHs and to find new types of targets, such as long non-coding RNA (lncRNA) or microRNAs. To do so, we decided to introduce different modifications in the PPRH structure, seeking to improve the properties mentioned below, and then, to evaluate their effect on the binding to their target sequence (ssDNA and dsDNA) and on cell viability upon incubation in PC-3 cells.

First, to increase PPRH stability we added PS linkages in the minimal modification fashion (Anusch & Eugen 1996), that is, the 3 first nucleotides in the 5' and the 2 last nucleotides in the 3' ends of the oligonucleotide sequence, and in between pyrimidines to get an enhanced protection against nucleases (HpsPr-C-PS).

Secondly, although pyrimidine tracts in the genome are more frequently than expected, the polypurine arms of PPRHs are limited to 3 interruptions. Pursuing to overcome this limitation, we studied the possibility to establish other triplets, involving inosine nucleosides or C·TA/T·CG triplets (HpsPr-C-I and HpsPr-C-S, respectively).

Finally, we also studied the effect of varying the loop size of the hairpin (3T, 4T or 5T-loop), and that of introducing Watson and Crick bonds in the loop by replacing the 5T-loop by TATTA or TTAA sequence (HpsPr-C-TATTA and HpsPr-C-TTAA, respectively).

4.2.2. DNA-PPRH binding analysis

We started conducting binding experiments to determine if PPRHs with internal modifications targeting *survivin* were able to bind to the ssDNA or the dsDNA of its target sequence. The modifications tested were: (I) PS backbone, HpsPr-C-PS; (II) pyrimidines substituted for Inosines, HpsPr-C-I; or (III) T>C and C>T substitutions, HpsPr-C-Subs. The incubation of different amounts of each modified PPRH with the ssDNA or the dsDNA target sequence led to the appearance of a shifted band, thus indicating that PPRHs were still able to bind to its target even in the presence of the above mentioned modifications. Moreover, the intensity of the shifted band increased in a dose dependent manner for all PPRHs in both ssDNA and dsDNA binding assays (Figures 18A

Results

and 18B). The intensity of the shifted bands produced by HpsPr-C-I and HpsPr-C-Subs when incubated with the ssDNA probe were lower than those produced by HpsPr-C-WT and HpsPr-C-PS (Figure 18C), suggesting less affinity. In contrast, HpsPr-C-PS showed the lowest affinity when incubated with the dsDNA (Figure 18D). No shifted band was originated by the scrambled negative control HpSC6 with neither ssDNA (Figure 18A, Lane 14) nor dsDNA (Figure 18B, Lane 14).

We also confirmed that replacing the 5T loop that links the two arms of the PPRH by TATTA or TTTAA sequences did not alter the binding to ssDNA (Figure 19A) or the dsDNA (Figure 19B), obtaining similar results for the triplex band intensity (Figure 19C and 19D).

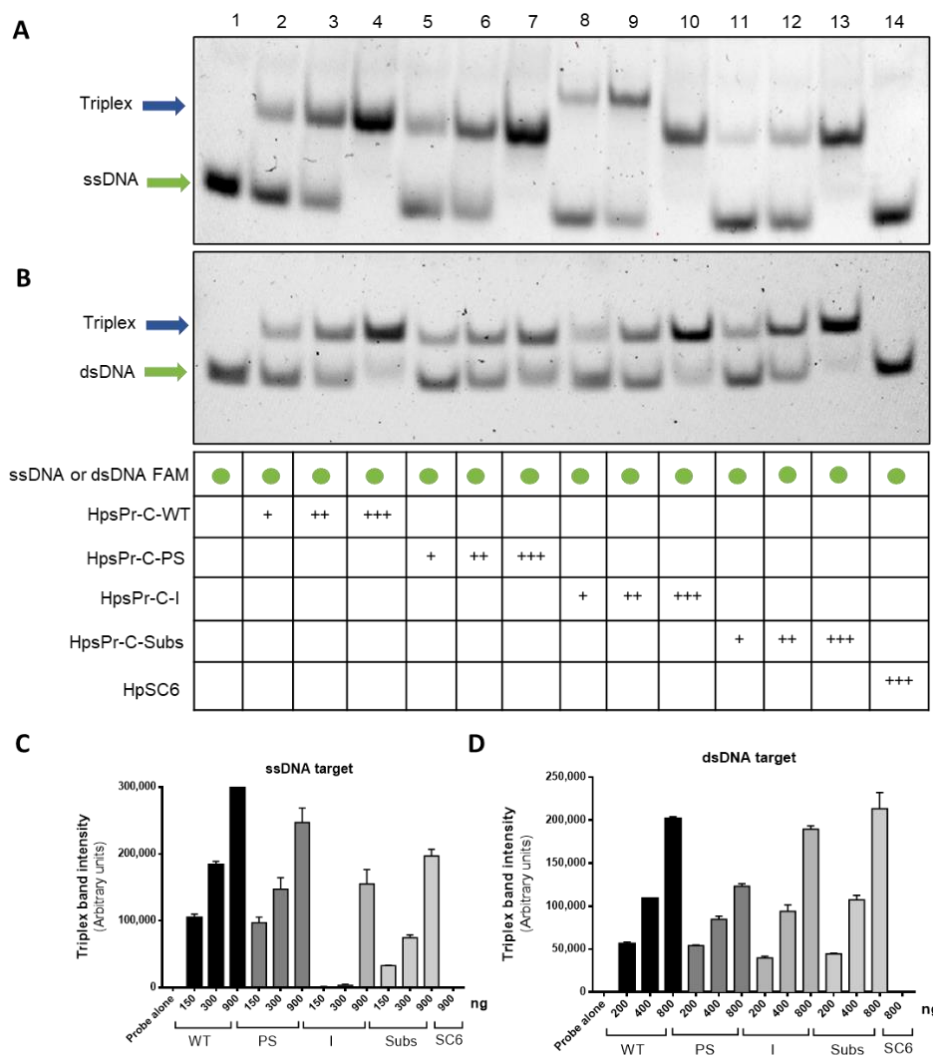


Figure 18. Binding of modified PPRHs to their target sequence. Gel-shift assays using 300 ng of a 5' FAM labeled ssDNA probe (ssDNA-FAM) or 200 ng of a 5' FAM labeled dsDNA probe (dsDNA-FAM) corresponding to the target sequence. The unlabeled oligodeoxynucleotides present in each binding reaction are indicated. (A) Lane 1, ssDNA-FAM probe alone; lane 2, ssDNA-FAM plus HpsPr-C-WT (150 ng); lane 3, ssDNA-FAM plus HpsPr-C-WT (300 ng); lane 4, ssDNA-FAM plus HpsPr-C-WT (900 ng); lane 5, ssDNA-FAM plus HpsPr-C-PS (150 ng); lane 6, ssDNA-FAM plus HpsPr-C-PS (300 ng); lane 7, ssDNA-FAM plus HpsPr-C-PS (900 ng); lane 8, ssDNA-FAM plus HpsPr-C-I (150 ng); lane 9, ssDNA-FAM plus HpsPr-C-I (300 ng); lane 10, ssDNA-FAM plus HpsPr-C-I (900 ng); lane 11, ssDNA-FAM plus HpsPr-C-Subs (150 ng); lane 12, ssDNA-FAM plus HpsPr-C-Subs (300 ng); lane 13, ssDNA-FAM plus HpsPr-C-Subs

Results

(900 ng); lane 14, ssDNA-FAM plus HpSC6 (900 ng). (B) Lane 1, dsDNA-FAM probe alone; lane 2, dsDNA-FAM plus HpsPr-C-WT (200 ng); lane 3, dsDNA-FAM plus HpsPr-C-WT (400 ng); lane 4, dsDNA-FAM plus HpsPr-C-WT (800 ng); lane 5, dsDNA-FAM plus HpsPr-C-PS (200 ng); lane 6, dsDNA-FAM plus HpsPr-C-PS (400 ng); lane 7, dsDNA-FAM plus HpsPr-C-PS (800 ng); lane 8, dsDNA-FAM plus HpsPr-C-I (200 ng); lane 9, dsDNA-FAM plus HpsPr-C-I (400 ng); lane 10, dsDNA-FAM plus HpsPr-C-I (800 ng); lane 11, dsDNA-FAM plus HpsPr-C-Subs (200 ng); lane 12, dsDNA-FAM plus HpsPr-C-Subs (400 ng); lane 13, dsDNA-FAM plus HpsPr-C-Subs (800 ng); lane 14, dsDNA-FAM plus HpSC6 (800 ng). The Intensity of the triplex band produced by the PPRH incubated with either the ssDNA (Figure C) or the dsDNA (Figure D) target sequence was quantified with the GelQuant.NET software provided by Biochemlabolutions.com. Abbreviations used: Hp, hairpin; Pr, promoter; s, survivin; -C, Coding-PPRH; WT, wild type; PS, phosphorothioate; I, Inosine; Subs, Substitution; SC, scrambled.

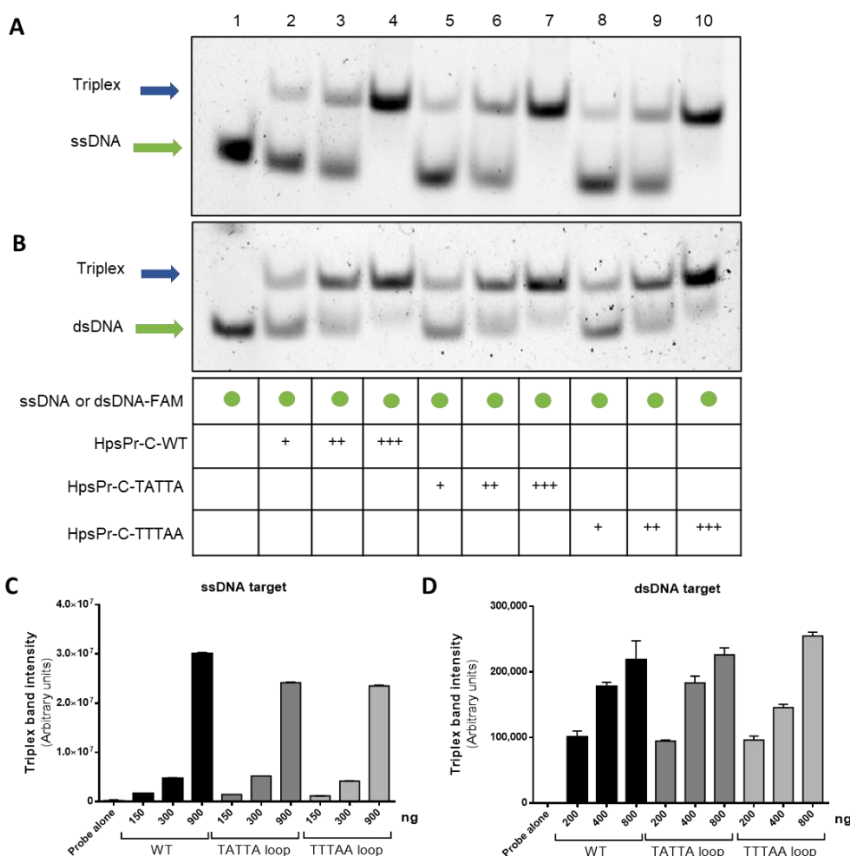


Figure 19. Binding of modified PPRHs to their target sequence. Gel-shift assays using 300 ng of a 5' FAM labeled ssDNA probe (ssDNA-FAM) or 200 ng of a 5' FAM labeled

dsDNA probe (dsDNA-FAM) corresponding to the target. The unlabeled oligodeoxynucleotides present in each binding reaction are indicated. (A) Lane 1, ssDNA-FAM probe alone; lane 2, ssDNA-FAM plus HpsPr-C-WT (150 ng); lane 3, ssDNA-FAM plus HpsPr-C-WT (300 ng); lane 4, ssDNA-FAM plus HpsPr-C-WT (900 ng); lane 5, ssDNA-FAM plus HpsPr-C-TATTAA (150 ng); lane 6, ssDNA-FAM plus HpsPr-C-TATTAA (300 ng); lane 7, ssDNA-FAM plus HpsPr-C-TATTAA (900 ng); lane 8, ssDNA-FAM plus HpsPr-C-TTTAA (150 ng); lane 9, ssDNA-FAM plus HpsPr-C-TATTAA (300 ng); lane 10, ssDNA-FAM plus HpsPr-C-TATTAA (900 ng). (B) Lane 1, dsDNA-FAM probe alone; lane 2, dsDNA-FAM plus HpsPr-C-WT (200 ng); lane 3, dsDNA-FAM plus HpsPr-C-WT (400 ng); lane 4, dsDNA-FAM plus HpsPr-C-WT (800 ng); lane 5, dsDNA-FAM plus HpsPr-C-TATTAA (200 ng); lane 6, dsDNA-FAM plus HpsPr-C-TATTAA (400 ng); lane 7, dsDNA-FAM plus HpsPr-C-TATTAA (800 ng); lane 8, dsDNA-FAM plus HpsPr-C-TTTAA (200 ng); lane 9, dsDNA-FAM plus HpsPr-C-TTTAA (400 ng); lane 10, dsDNA-FAM plus HpsPr-C-TTTAA (800 ng).). The Intensity of the triplex band produced by the PPRH incubated with either the ssDNA (Figure C) or the dsDNA (Figure D) target sequence was quantified with the GelQuant.NET software provided by Biochemlabsolutions.com. Nomenclature used: Hp, hairpin; Pr, promoter; s, survivin; -C, Coding-PPRH; WT, wild type. The sequence of the loop is indicated.

4.2.3. Effect on cell viability upon transfection with modified PPRHs

Once we had determined that all modified PPRHs were able to bind to the ssDNA and the dsDNA of its target sequence, we analyzed their effect on PC-3 cell viability. PC-3 cells were incubated with different concentrations of each modified PPRH (30, 60 and 100 nM) (Figure 20A). PS PPRH (HpsPr-C-PS, PS) showed a decrease on cell viability at 60 nM of 44%, which was higher than the 20% caused by the wild type PPRH (HpsPr-C-WT, WT) at the same concentration, while at 100 nM the effect observed was very similar. The PPRH with Inosine substitutions (HpsPr-C-I, I) also showed a decrease on cell viability of 63% at 100 nM. However, the PPRH with C·TA/T·CG triplets (HpsPr-C-Subs) presented a low decrease on cell viability, even at 100 nM.

We further studied the effect of varying the size of the T-loop that links the two arms of the PPRH on PC-3 cell viability. First, we calculated *in silico* the ΔG to establish a hairpin by intramolecular bonds with the sequence of HpsPr-C-WC and varying the number of thymidine residues, using the Mfold web server for nucleic acid folding and hybridization prediction (Zuker 2003). The best results were obtained with hairpins with 4T (-26.82 Kcal/mol), followed by 5T (-26.52 Kcal/mol) and 3T (-25.42 Kcal/mol). Then, we analyzed PC-3 cell viability upon transfection with different concentrations of these PPRHs (30, 60 and 100

Results

nM) (Figure 20B). Similar viabilities were obtained with all the PPRHs (<17% of cell viability), thus suggesting that the PPRH structure is viable even with 3 or 4 residues. Furthermore, we analyzed the effect on cell viability when linking the two arms of the HpsPr-C hairpin with the TATTA or TTAA sequences instead of 5T (Figure 20B). The highest decrease on cell viability at 100 nM was achieved by HpsPr-C-WT (84%), followed by HpsPr-C-TATTA (70%), and then, HpsPr-C-TTAA (54%).

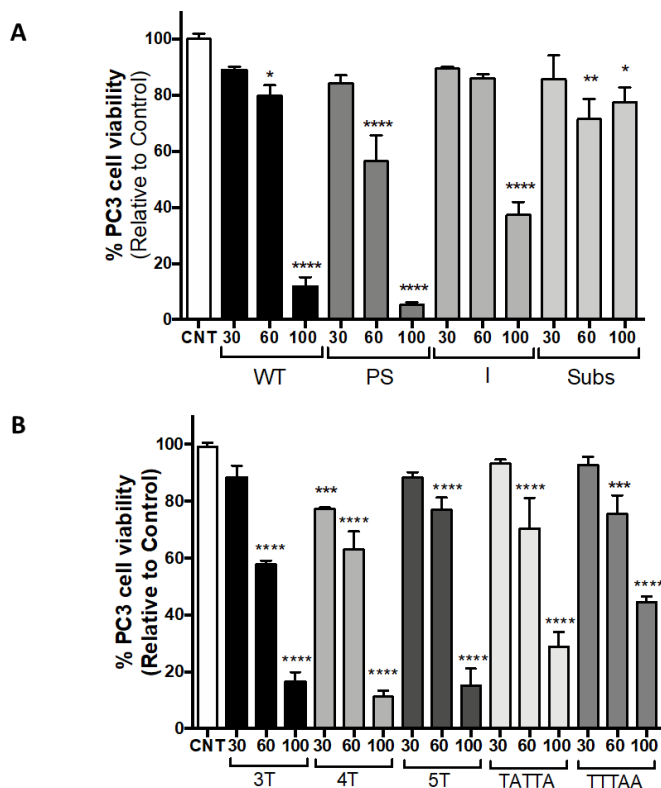


Figure 20. Effect of different modifications in HpsPr-C-WT structure on PC-3 cell viability. (A) Effect on PC-3 cell viability upon transfection of HpsPr-C-WT (WT), HpsPr-C-PS (PS), HpsPr-C-I (I), HpsPr-C-Subs (Subs) at 30 nM, 60 nM or 100 nM. (B) Effect on PC-3 cell viability upon transfection of HpsPr-C-WT (30 nM, 60 nM or 100 nM) varying the T-loop length: HpsPr-C-3T (3T), HpsPr-C-4T (4T) and HpsPr-C-WT; or replacing the 5T loop by TATTA or TTAA sequences: HpsPr-C-TATTA (TATTA) and HpsPr-C-TTAA (TTTAA), respectively. Error bars represent the standard error of the mean of at least three experiments. Statistical significance was calculated using one-way ANOVA with Dunnett's multiple comparisons test (* $p < 0.05$, ** $p < 0.01$, *** $p < 0.001$, **** $p < 0.0001$).

4.3. DELIVERY OF PPRHs USING VIRAL VECTORS

Background: Several technologies have been developed seeking to increase the efficiency and tissue specificity of nucleic acids delivery. Among them, viral vectors present high transduction efficiencies on a variety of cells. Several types of viruses for gene therapy have been studied with different properties, such as AdVs and AAVs (Bulcha *et al.* 2021). AdVs and AAVs are capable of infecting dividing and non-dividing cells, without integrating with the host genome. AdVs have higher packaging capacity than AAVs although they can activate immune response. In contrast, AAVs have a smaller transgene size capacity, but their infection triggers low levels of immune system response. Both of those viral vectors are promising gene delivery systems studied in either preclinical or clinical trials. Indeed, several gene therapies using viral vectors have been approved around the world, which highlight the potential of these vectors for nucleic acids delivery (Lundstrom & Slade 2018; Rodrigues *et al.* 2018).

Objectives: The main aim of this work was to demonstrate the efficiency of viral vectors as a delivery system for a PPRH directed against the anti-apoptotic gene *survivin*. To do so, since in viral vectors the PPRH sequence would be transcribed into RNA, we also intended to evaluate the effect of a PPRH targeting *survivin* as an RNA species (synthetic RNA-PPRH) and that intracellularly generated upon transfection of a plasmid vector.

Results: First, we demonstrated the ability of the RNA-PPRH to bind to its ssDNA or dsDNA target sequence. Then, we showed that the RNA-PPRH induced a decrease on cell viability in a dose-dependent manner and an increase of apoptosis in PC-3 cells. We also determined that two plasmids encoding the PPRH sequence under the control of either the U6 or H1 promoters were able to reduce cell viability. Furthermore, *survivin* mRNA and protein levels were reduced in PC-3 cells incubated with either the RNA-PPRH or the plasmid encoding the RNA-PPRH.

Once validated that RNA-PPRHs induced *survivin* silencing, we tested the biological response produced by the infection of AAV or AdV5 encoding the PPRH against *survivin*. Two different AAV serotypes (AAV1 and AAV9) were tested. Both showed low transduction efficiencies, and no effect in cell viability or *survivin* mRNA levels in none of the tested cell lines were observed. In

Results

contrast, we demonstrated that an AdV vector containing the PPRH sequence (AdV-PPRH) was able to reduce HeLa cell viability, while no significant decrease on cell viability was observed in cells infected with the negative control AdV-GFP, an adenovirus encoding the GFP gene. We also confirmed that AdV-PPRH induced a decrease in *survivin* mRNA and protein levels in a specific manner.

Conclusions: In this work we validated the ability of RNA-PPRHs to produce gene silencing. Furthermore, we established the proof of principle of an adenoviral vector as a new viral strategy for PPRHs delivery.

In this part of the thesis, we studied viral vectors as a delivery system for PPRHs. However, beforehand, we proceeded to test the ability of an RNA-PPRH (PPRH made out of non-modified ribonucleotides) to bind to its ssDNA or dsDNA target sequence. Then, we determined the molecular effect produced by the RNA-PPRH made out of non-modified ribonucleotides and that of an RNA-PPRH transcribed from a vector. Afterwards, the capacity of viral vectors to transduce this RNA-PPRH was analyzed.

4.3.1. RNA-PPRH binding analysis

As stated before, previous work in our laboratory had validated HpsPr-C (DNA-PPRH) as a silencing tool for *survivin*, both *in vitro* and *in vivo* (Rodríguez *et al.* 2013). Therefore, since in viral vectors PPRHs would be transcribed to RNA from a plasmid, we first tested if the RNA sequence of HpsPr-C (HpsPr-C-RNA, RNA-PPRH) was able to bind to its target sequence in ssDNA or dsDNA. Incubation of increasing amounts of the RNA-PPRH with ssDNA resulted in a progressive disappearance of the band corresponding to the ssDNA signal (Figure 21A, lane 2, lane 5, 6 and 7) compared to ssDNA alone (Figure 21A, lane 1) and produced two shifted bands. Accordingly, incubation of increasing amounts of the RNA-PPRH with dsDNA also resulted in a progressive disappearance of the band corresponding to the dsDNA signal (Figure 21B, lane 2, 4, 5, 6, 8, 9 and 10) compared to dsDNA alone (Figure 21B, lane 1, 3, 7 and 13) and produced two shifted bands, thus indicating that the RNA-PPRH was able to bind to its target sequence in both ssDNA and dsDNA. Furthermore, no shifted band was originated by the negative control HpSC6 with neither ssDNA (Figure 21A, Lane 4) nor dsDNA (Figure 21B, Lane 12). As a positive control, we incubate the ssDNA and the dsDNA probes with the DNA-PPRH (Figure 21A, lane 3, and Figure 21B, lane 11, respectively).

Results

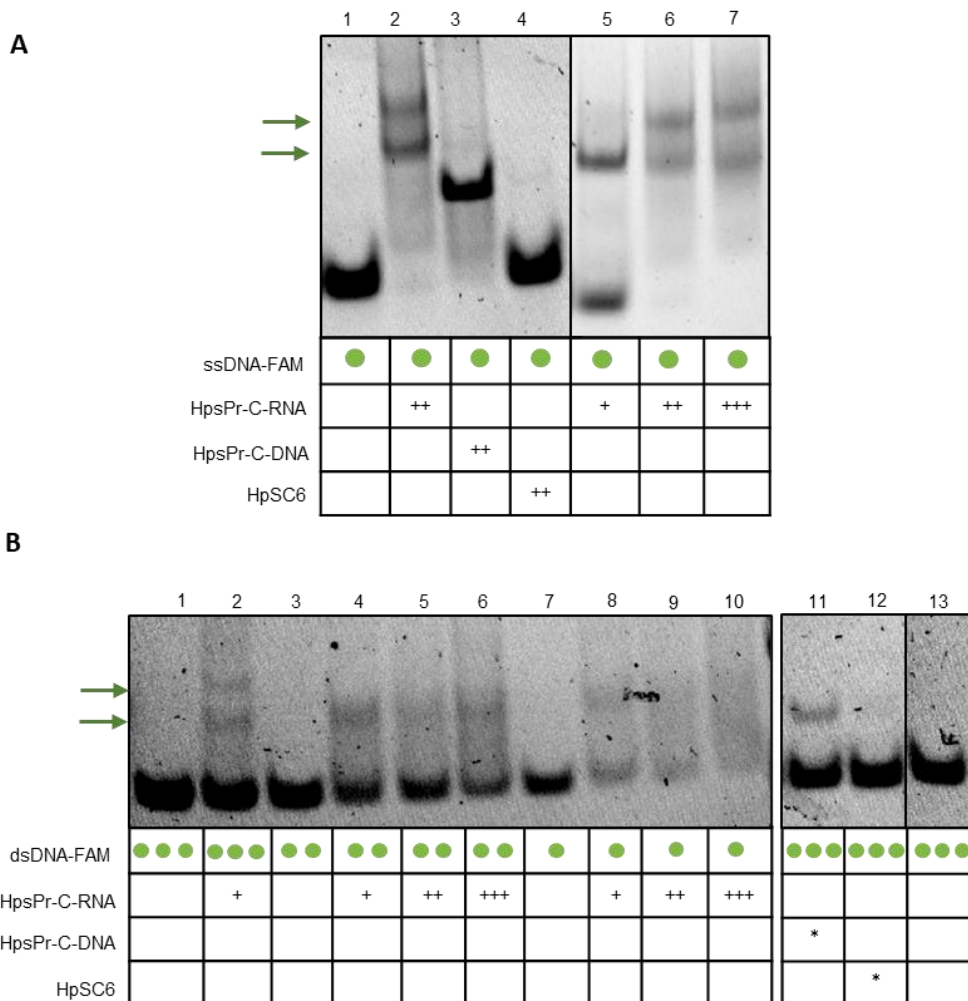


Figure 21. Binding of the RNA-PPRH to its ssDNA or dsDNA target sequence. (A) Gel-shift assays using 300 ng of a 5' FAM labeled ssDNA probe (ssDNA-FAM). The unlabeled oligonucleotides present in each binding reaction are indicated. Lane 1, ssDNA-FAM probe alone; lane 2, ssDNA-FAM plus HpsPr-C-RNA (600 ng); lane 3, ssDNA-FAM plus HpsPr-C-DNA (600 ng); lane 4, ssDNA-FAM plus HpSC6 (600 ng); lane 5, ssDNA-FAM plus HpsPr-C-RNA (300 ng); lane 6, ssDNA-FAM plus HpsPr-C-RNA (600 ng); lane 7, ssDNA-FAM plus HpsPr-C-RNA (1200 ng) (B) Gel-shift assays using 200 ng, 100 or 50 ng of a 5' FAM labeled dsDNA probe (dsDNA-FAM). The unlabeled oligonucleotides present in each binding reaction are indicated. Lane 1, dsDNA-FAM probe alone (200 ng); lane 2, dsDNA-FAM (200 ng) plus HpsPr-C-RNA (200 ng); lane 3, dsDNA-FAM probe alone (100 ng); lane 4, dsDNA-FAM (100 ng) plus HpsPr-C-RNA (200 ng); lane 5, dsDNA-FAM (100 ng) plus HpsPr-C-RNA (600 ng); lane 6, dsDNA-FAM (100 ng) plus HpsPr-C-RNA (1200 ng); lane 7, dsDNA-FAM probe alone (50 ng); lane 8, dsDNA-FAM (50 ng) plus HpsPr-C-RNA (200 ng); lane 9, dsDNA-FAM (50 ng) plus HpsPr-C-RNA (600 ng); lane 10, dsDNA-FAM (50 ng) plus HpsPr-C-RNA (1200 ng); lane 11, dsDNA-FAM probe alone (200 ng); lane 12, dsDNA-FAM (200 ng) plus HpsPr-C-RNA (200 ng); lane 13, dsDNA-FAM (200 ng) plus HpsPr-C-RNA (1200 ng). Asterisks (*) indicate non-specific binding.

(50 ng); lane 8, dsDNA-FAM (50 ng) plus HpsPr-C-RNA (200 ng); lane 9, dsDNA-FAM (50 ng) plus HpsPr-C-RNA (600 ng); lane 10, dsDNA-FAM (50 ng) plus HpsPr-C-RNA (1200 ng); lane 11, dsDNA-FAM (200 ng) plus HpsPr-C-DNA (200 ng); lane 12, dsDNA-FAM (200 ng) plus HpSC6 (200 ng); Lane 13, dsDNA-FAM probe alone (200 ng).

4.3.2. Effect of an RNA-PPRH targeting *survivin* on PC-3 cell viability and apoptosis

Our previous results demonstrated that the suppression of the antiapoptotic *survivin* gene using HpsPr-C resulted in a decrease of cell survival and an increase of apoptosis in prostate cancer cells (Rodríguez *et al.* 2013). Therefore, the effect of the RNA-PPRH on cell viability and apoptosis was tested in PC-3 cells. Transfection of HpsPr-C-RNA reduced PC-3 cell viability in a dose-dependent manner, with a decrease of 89% relative to control at 800 nM (Figure 22A). As previously reported, 100 nM of HpsPr-C-WT (DNA-PPRH) decreased PC-3 cell viability more than 95%.

Furthermore, 24h after transfection, both HpsPr-C-WT-DNA and HpsPr-C-RNA led to an increase in apoptosis levels in PC-3 cells of 1.4-fold and 1.6-fold, respectively (Figure 22B). In contrast, cells treated with the negative control SC4 did not showed an increment in apoptosis.

Once verified the effect of the RNA-PPRH, we also tested the effect of the PPRH when transcribed from a plasmid on PC-3 cell viability. First, the presence of the PPRH sequence in the plasmids was confirmed by sequencing (Figure 23). 5 µg of pAAV-HpsPr-C and pSilencer-HpsPr-C reduced cell viability by 75% and 50%, respectively. In contrast, cell viability of cells incubated with FuGENE®6 only or the plasmid containing a non-related sequence was reduced less than 27% (Figure 22C). Fluorescence microscopy images of cells to verify pAAV expression were taken (Figure 22D).

Results

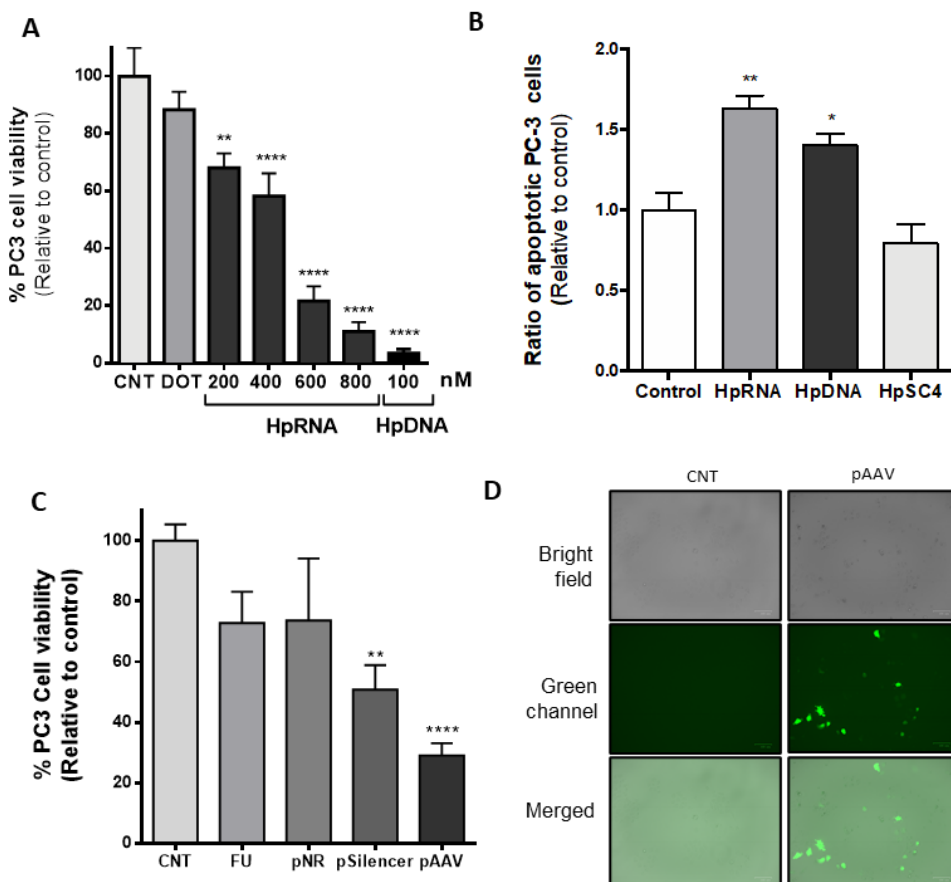


Figure 22. Effect of the RNA-PPRH on viability and apoptosis in PC-3 cells. (A) Effect on viability in PC-3 cells upon transfection of the RNA-PPRH HpsPr-C-RNA (HpRNA, 200-800 nM) or the DNA-PPRH HpsPr-C (HpDNA, 100 nM). Cell viability assays (10,000) were conducted 5 days after transfection. (B) Effect of RNA-PPRH on apoptosis levels in PC-3 cells. PC-3 cells (60,000) were transfected with 800 nM of the RNA-PPRH HpsPr-C-RNA (HpRNA), 100 nM of the DNA-PPRH HpsPr-C (HpDNA) or 100 nM of a DNA-PPRH negative control HpSC4. 24 h after transfection, cells were collected and processed as specified in eBioscience™ Annexin V Apoptosis Detection kit FITC. The percentage of cells corresponds to Annexin V-positive/IP-negative (early-stage apoptotic cells). (C) Effect on viability upon incubation of PC-3 cells with the transfection reagent FuGENE®6, 5 µg of pSilencer-NR (pNR), pSilencer-HpsPr-C (pSilencer) or pAAV-HpsPr-C (pAAV). Cell viability assays (10,000) were conducted 5 days after transfection. (D) PC-3 cells (30,000) images were acquired 48 h after transfection of pAAV-HpsPr-C (pAAV). Other abbreviations: CNT, control; DOT, DOTAP 15 µM; FU, FuGENE®6. Data represent the mean ± SEM from 3 experiments. Statistical significance was determined using a one-way ANOVA with Dunnett's multiple comparisons test (* $p < 0.05$, ** $p < 0.01$, *** $p < 0.001$, **** $p < 0.0001$).

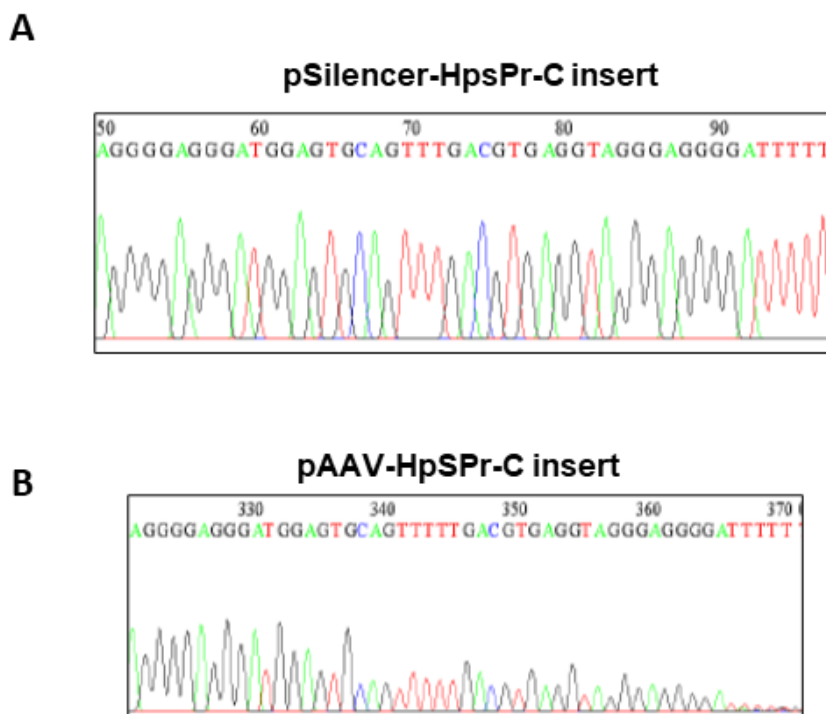


Figure 23. DNA sequences of pSilencer-HpsPr-C (A) and pAAV-HpsPr-C (B) confirming the presence of the HpsPr-C sequence in the two recombinant plasmids.

4.3.3. Effect on the levels of *survivin* mRNA and protein upon RNA-PPRH transfection

To confirm that the decrease in cell viability and the increase of apoptosis were due to the inhibition of *survivin*, we analyzed its mRNA and protein levels. In terms of *survivin* mRNA levels (Figure 24A), cells treated with HpsPr-C-RNA showed a decrease of nearly 70% relative to the control. In the case of pAAV-HpsPr-C, mRNA levels were reduced by 25% relative to the control. Moreover, the positive control HpsPr-C-DNA also reduced mRNA levels around 56%, whereas the scrambled negative control did not show a reduction in mRNA levels of PC-3 cells.

In the case of *survivin* protein levels (Figure 24B and 24C), PC-3 cells transfected with HpsPr-C-RNA showed a decrease of 50 %, while cells treated with pAAV-HpsPr-C presented a reduction of 30 % relative to the control.

Results

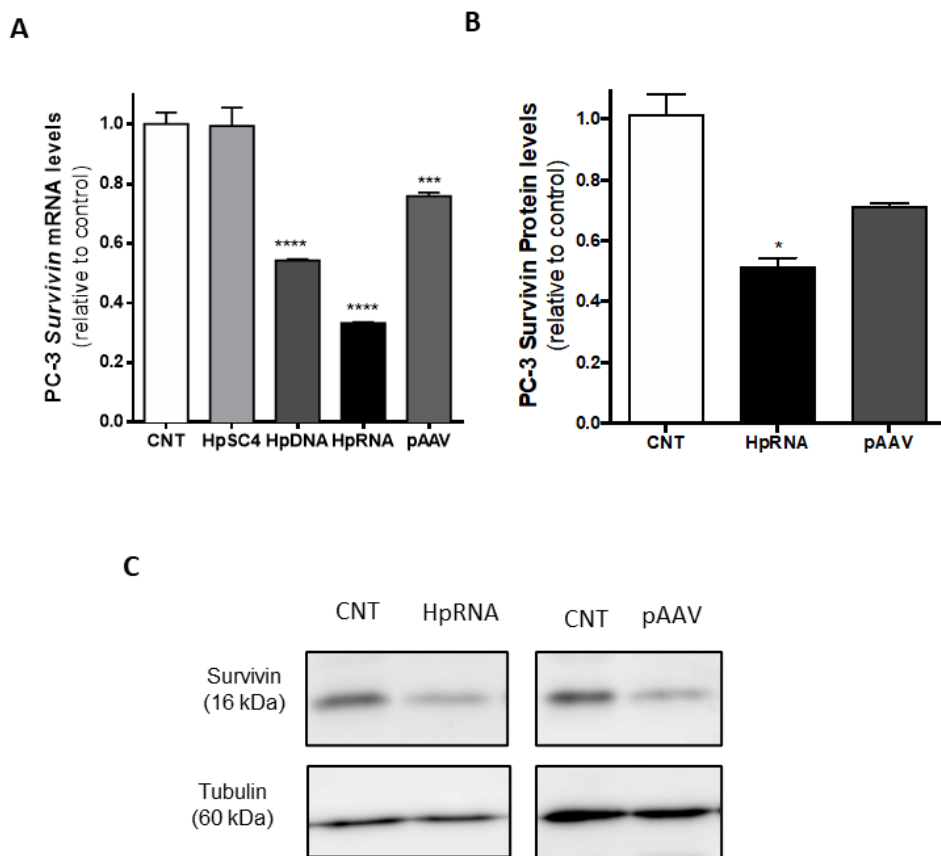


Figure 24. Effect of RNA-PPRH on survivin mRNA and protein levels in PC-3 cells. (A) Effect of RNA-PPRH on *survivin* mRNA levels. PC-3 cells (30,000) were transfected with 100 nM of a DNA-PPRH negative control HpSC4, 100 nM of the DNA-PPRH HpsPr-C (HpDNA), 800 nM of the RNA-PPRH HpsPr-C-RNA (HpRNA) or with 5 μ g of pAAV-HpsPr-C (pAAV). 24 h after transfection, or 48 h in the case of pAAV, *survivin* mRNA levels were determined by RT-qPCR. TATA-binding protein (TBP) was used to normalize the results. (B) Effect of RNA-PPRH on survivin protein levels. PC-3 cells (30,000) were treated 24h with 800 nM of the specific RNA-PPRH HpsPr-C (HpRNA) or 48h with 5 μ g of pAAV-HpsPr-C (pAAV), then protein extracts were obtained to analyze survivin protein levels. (C) Representative images of Western blots. Tubulin protein levels were used to normalize the results. Data represent the mean \pm SEM from 3 experiments. Statistical significance was determined using a one-way ANOVA with Tukey's multiple comparisons test (* $p < 0.05$, ** $p < 0.01$, *** $p < 0.001$, **** $p < 0.0001$).

4.3.4. Effect of an RNA-PPRH targeting *survivin* on HeLa cell viability and apoptosis

The effect of the RNA-PPRH in viability and apoptosis levels was also tested in HeLa cells. Similarly to PC-3 cells, transfection of HpsPr-C-RNA in HeLa cells led to a decrease in viability in a dose-dependent manner (Figure 25A). Moreover, HeLa cells treated with HpsPr-C-WT-DNA or HpsPr-C-RNA also showed a 2.3-fold or 3-fold increase in apoptosis, respectively (Figure 25B), while the negative control SC4 did not produce an increment in the apoptotic cell population.

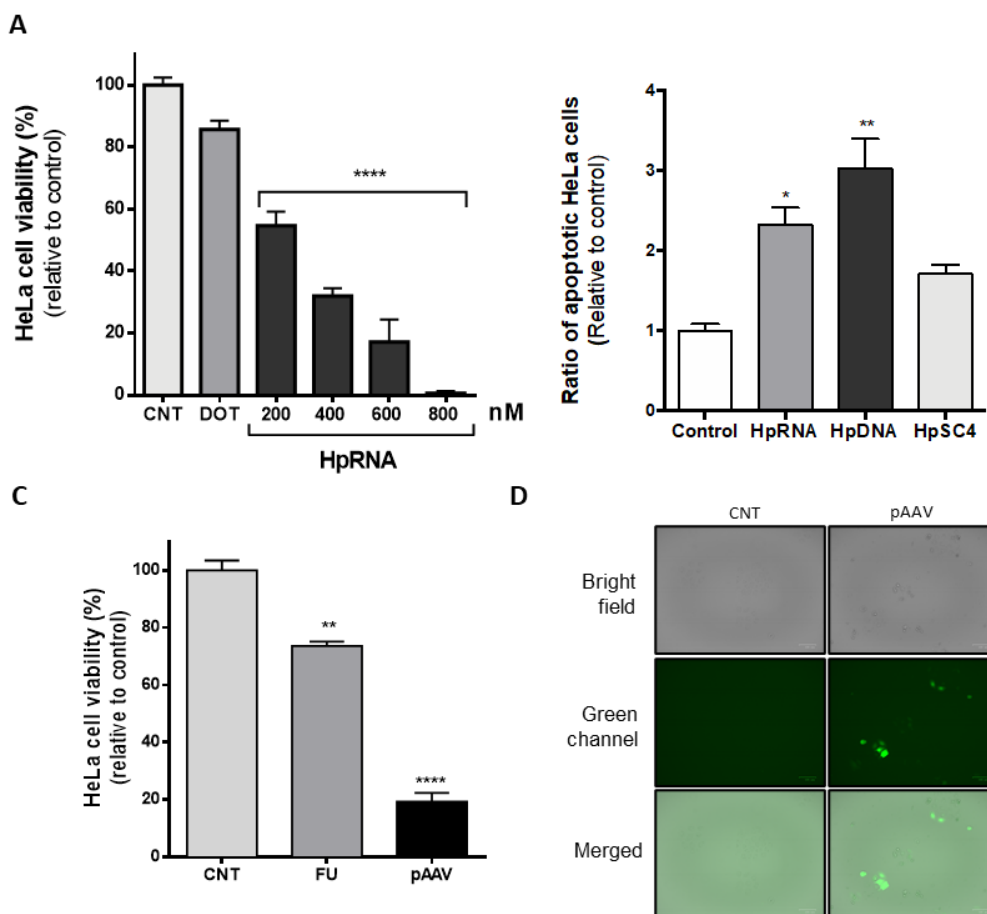


Figure 25. Effect of the RNA-PPRH on cell viability and apoptosis in HeLa cells. (A) Effect on viability in HeLa cells upon transfection with HpsPr-C-RNA (HprRNA, 200-800 nM). Cell viability assays (10,000) were conducted 5 days after transfection (B) Effect of RNA-PPRH on apoptosis levels in HeLa cells. HeLa cells (60,000) were transfected with

Results

800 nM of the RNA-PPRH HpsPr-C-RNA (HpRNA), 100 nM of the DNA-PPRH HpsPr-C (HpDNA) or 100 nM of a DNA-PPRH negative control HpSC4. 24 h after transfection, cells were collected and processed as specified in eBioscience™ Annexin V Apoptosis Detection kit FITC. The percentage of cells corresponds to Annexin V-positive/IP-negative (early-stage apoptotic cells). (C) Effect on viability after incubating HeLa cells (10,000) with the transfection reagent FuGENE®6 or 5 µg pAAV-HpsPr-C (pAAV). Cell medium was changed 48h after transfection and cell viability assays were conducted 5 days after transfection. D) HeLa cells (30,000) images were acquired 48 h after transfection of pAAV-HpsPr-C (pAAV). Other abbreviations: CNT, control; DOT, DOTAP 15 µM; FU, FuGENE®6. Data represent the mean ± SEM from 3 experiments. Statistical significance was determined using a one-way ANOVA with Dunnett's multiple comparisons test (*p < 0.05, **p < 0.01, ***p < 0.001, ****p < 0.0001).

In the case of the PPRH transcribed from a vector, a reduction of 80% was observed in HeLa cells incubated with 5 µg of pAAV-HpsPr-C, whereas FuGENE®6 only reduced 26% cell viability (Figure 25C). Fluorescence microscopy images of cells to verify pAAV expression were taken 48h after plasmid transfection (Figure 25D).

4.3.5. Effect of a PPRH delivered into cells using viral vectors

4.3.5.1. Results with AAV vectors

Once verified that RNA-PPRHs induced *survivin* silencing, we tested the biological response produced by the infection of AAV or AdV5 encoding the PPRH against *survivin* HpsPr-C under the H1 promoter control. Different parameters were analyzed, including transduction efficiency, cell death, mRNA or protein levels.

Initial experiments with AAV8-PPRH in different cell lines (PC-3, HepG-2, A549, HEK-293) revealed that the PPRH was ineffective in reducing viability or reducing mRNA levels (Table 7). Moreover, cell images obtained 24h (Figure 26) after infection or longer times (Data not shown), showed that GFP expression in infected cells was low or null. Therefore, we evaluated the transduction efficiency of AAV8-PPRH and other AAV serotypes (AAV1 and AAV9) in PC-3, HepG2 and HEK-293 cells. We analyzed the fluorescence produced by GFP protein expression by flow cytometry 24h after infection (Table 8) (10⁵ MOI). AAV1 achieved the highest values of percentage of fluorescence cells and fluorescence mean in all cell lines. These results were in accordance with the images acquired just before flow cytometer analyses (Figure 26).

Then, AAV1 vectors expressing the PPRH sequence (AAV1-PPRH) were generated to conduct further analyses. Nevertheless, no decrease in viability was observed neither in PC-3, HEK-293 nor SH-SY5Y cells infected with AAV1-PPRH (Table 7). Furthermore, cell images acquired 24h after infection, showed a decrease of GFP expression in HEK-293 or null expression in PC-3 cells transduced with AAV1-PPRH (Figure 27) compared to AAV1 (Figure 26). Even 48h upon transduction, there was no expression of GFP in PC-3 cells (Figure 28), indicating a reduction of GFP expression when the PPRH was cloned in the viral genome.

Viral vector	Cell line	Number of cells	Cytotoxicity (Relative to control)	mRNA levels (Relative to control)
AAV8-PPRH	PC-3	10,000	0%	ND
		30,000	5.30%	91%*, 91%*
		60,000	ND	ND
	HepG-2	10,000	0%	ND
		30,000	5.20%	100%*, 88%*
		60,000	1.34%	ND
	A549	10,000	5,34%	ND
		30,000	0%	ND
	HEK293	10,000	ND	ND
		30,000	ND	100%*
		60,000	ND	ND
	AAV1-PPRH	PC-3	10,000	0%*
30,000			0.5%*	ND
HEK293		10,000	4.13%*	ND
		30,000	3.56%*	ND
SH-SY5Y		10,000	1.06%*	ND
		30,000	13.17%*	ND

Table 7. Compendium of the different conditions conducted to evaluate AAV-PPRH effect in distinct cancer cell lines on cytotoxicity (72 h after infection) and mRNA levels (24h after infection). All experiments were carried out using a MOI of 10^4 except for the results marked with * corresponding to 10^5 MOI, ** 10^6 .

Results

Cell line	Condition	% Fluorescence cells	Fluorescence mean
PC3	Control	5,45	3,14
	AAV1	69,45	168
	AVV9	74,18	6,61
	AAV8-PPRH	14,43	7,03
HepG-2	Control	6,38	3,1
	AAV1	13,27	14,1
	AVV9	6,9	3,86
	AAV8-PPRH	4,62	2,64
HEK293	Control	1,66	3,05
	AAV1	93,93	274
	AVV9	44,15	43,1
	AAV8-PPRH	73,44	35,6

Table 8. Percentage of fluorescent cells and the mean fluorescence for each cell line determined by flow cytometry. Cells were infected with 10^5 MOI, incubated for 24h and collected for flow cytometry analyses.

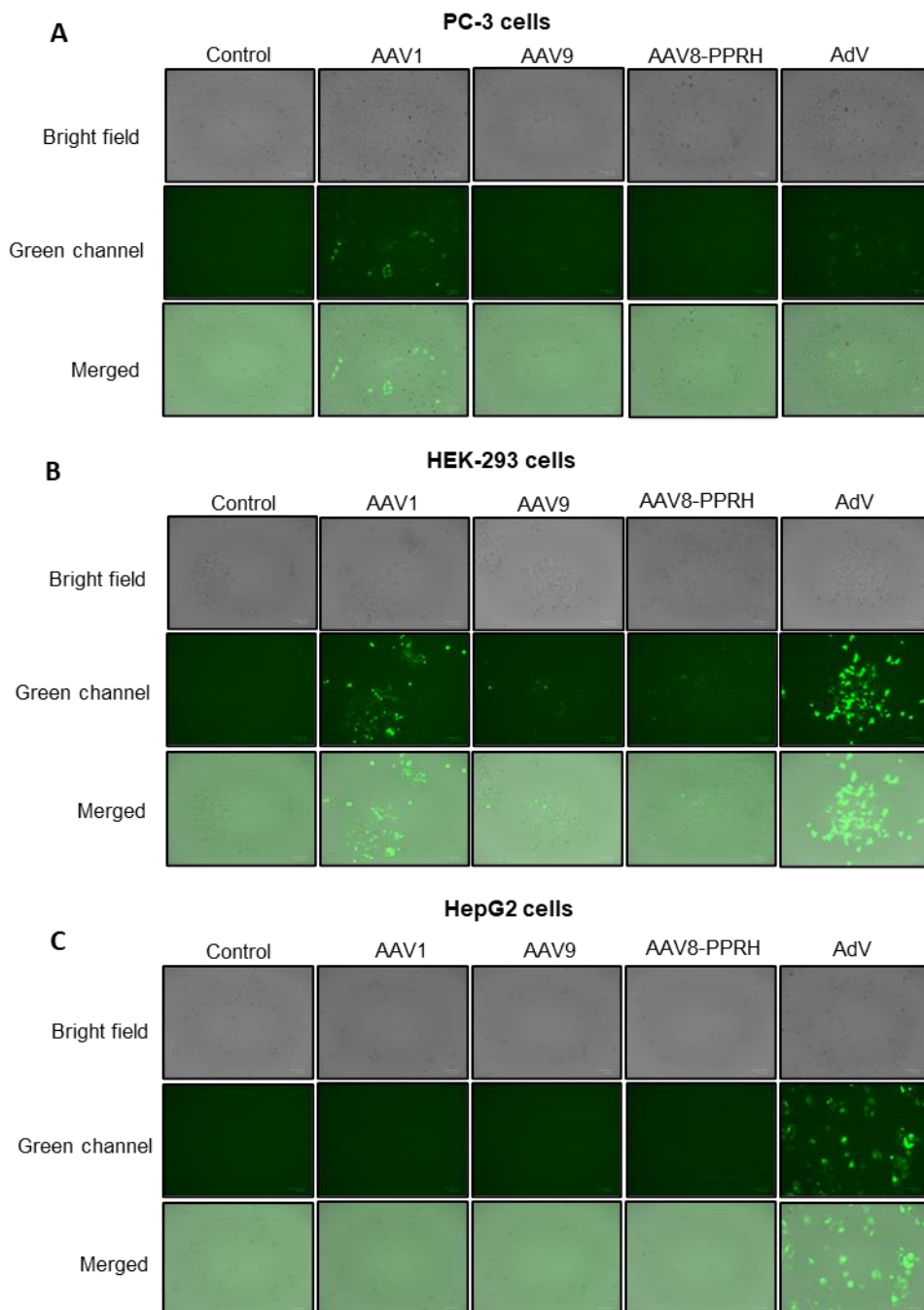


Figure 26. Fluorescence microscopy images of PC-3 (A), HEK-293 (B) and HepG2 (C) were taken 24 h after transduction of AAV1, AAV9, AAV8-PPRH or AdV. For AAV infection, 10^5 MOI was used, whereas for AdV vectors 100 MOI was employed.

Results

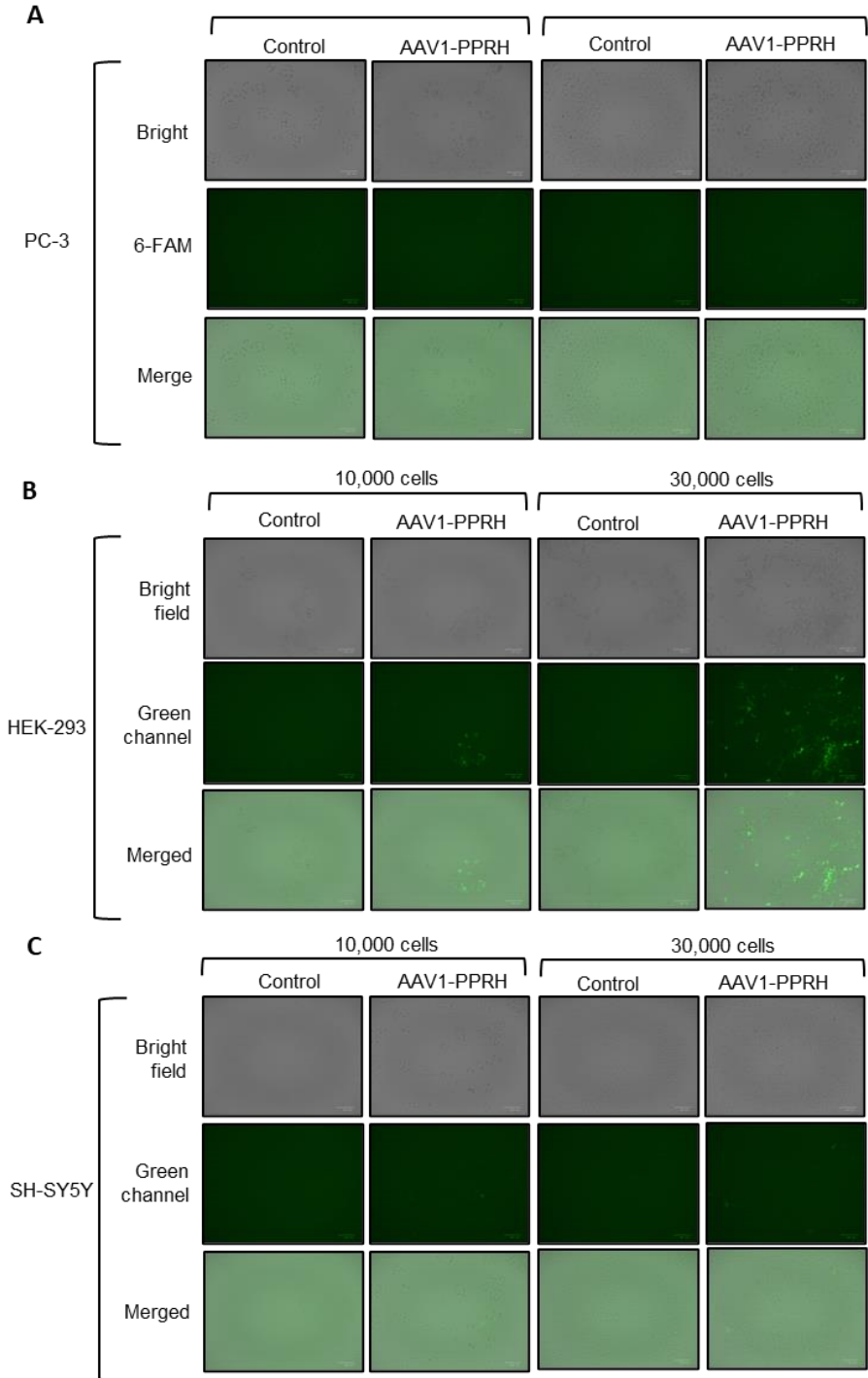


Figure 27. Fluorescence microscopy images of PC-3 (A), HEK-293 (B) and SH-SY5Y (C) cells taken 24 h after AAV1-PPRH transduction (10^5 MOI).

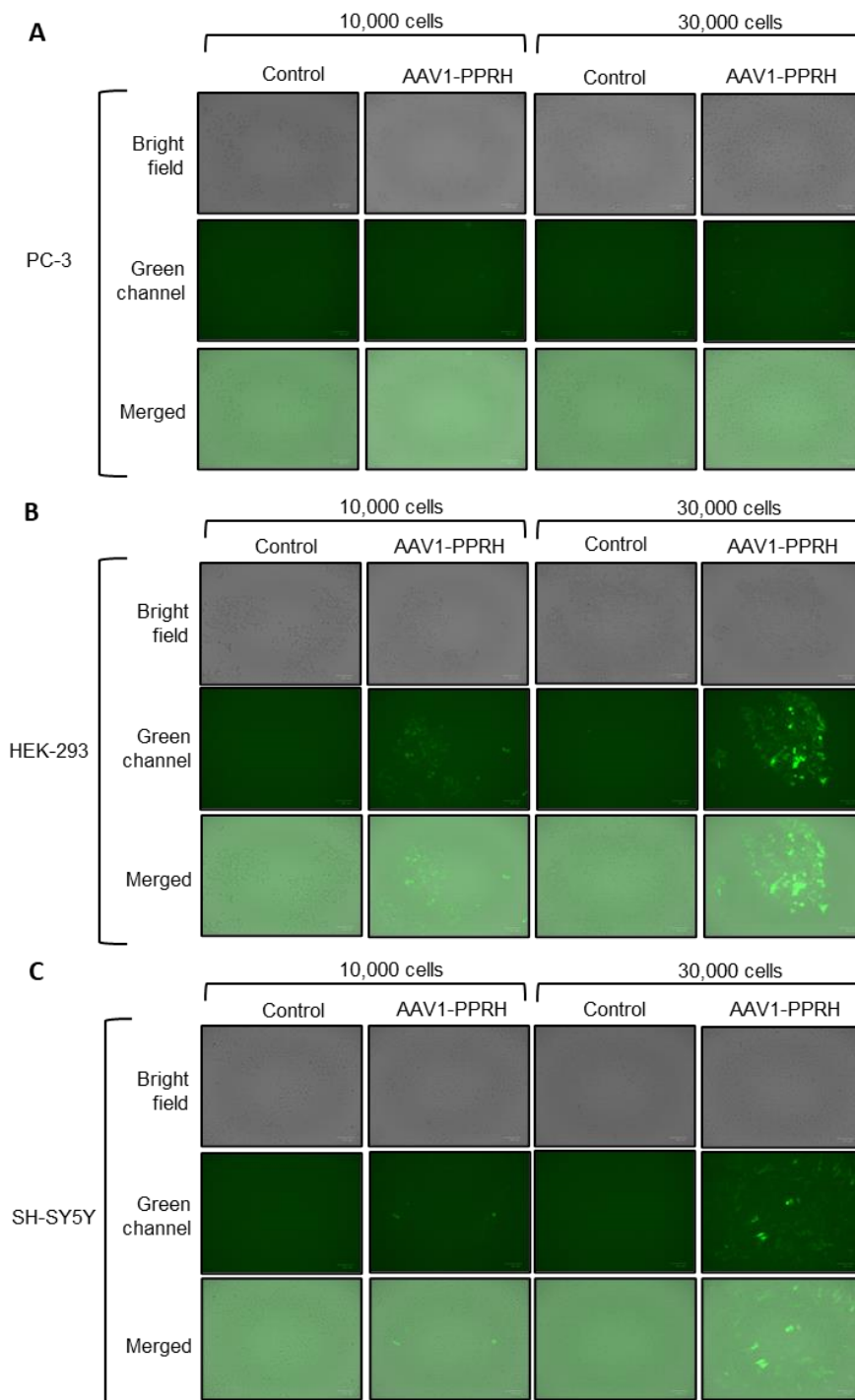


Figure 28. Fluorescence microscopy images of PC-3 (A), HEK-293 (B) and SH-SY5Y (C) cells taken 48 h after AAV1-PPRH transduction (10^5 MOI).

4.3.5.2. Results with AdV vectors

Since AAV vectors were ineffective in transducing PPRH, we decided to generate AdV vectors as PPRHs carriers (AdV-PPRH). After 72h of AdV-PPRH transduction, viability assays conducted with HeLa cells showed a reduction of 34% and 48%, starting with 5,000 or 7,000 cells, respectively (Figure 29A and 29B). Moreover, no significant decrease on viability was observed in cells infected with the negative control AdV-GFP, an adenovirus encoding GFP. Nevertheless, PC-3 cells infected with AdV-PPRH did not show a significant decrease on viability (Figure 29C and figure 29D).

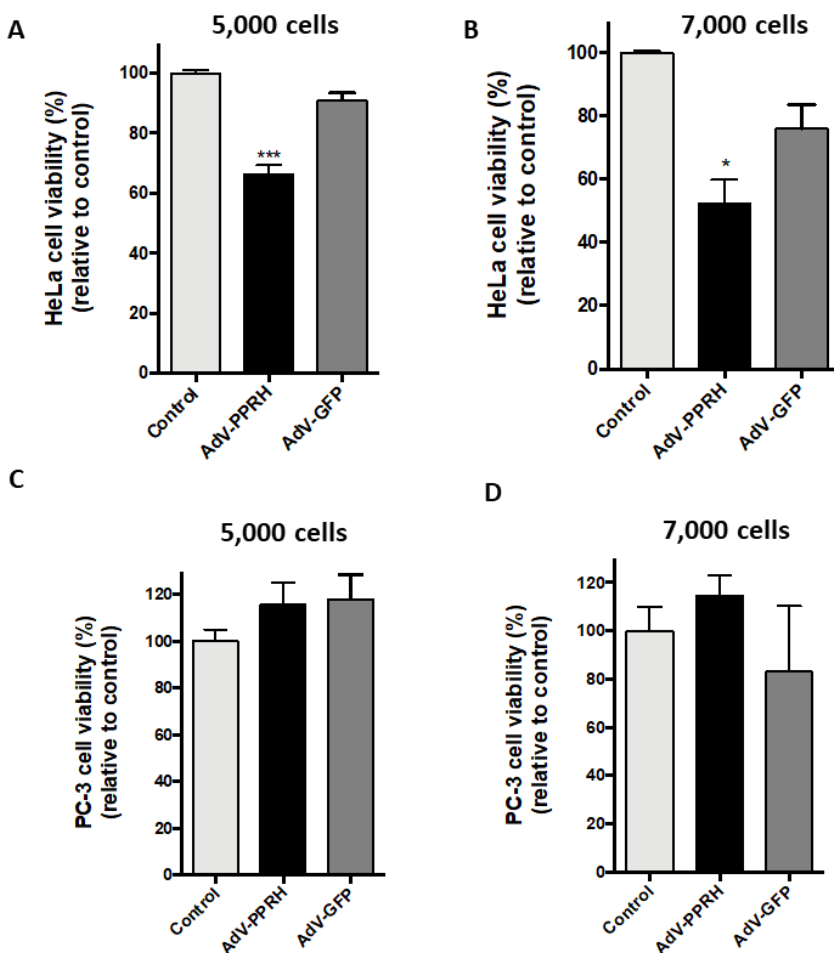


Figure 29. Cell viability effect of AdV-PPRH on HeLa and PC-3 cells. HeLa (A and B) or PC-3 cells (C and D) cells were plated the day before infection (100 MOI). Error bars represent the standard error of the mean of three experiments. Statistical significance

was calculated using one-way ANOVA with Tukey's multiple comparisons test (* $p < 0.05$, *** $p < 0.001$).

Then, to confirm that the decrease on HeLa cell viability was the result of a specific inhibition of *survivin* expression caused by AdV-PPRH, we analyzed the levels of both *survivin* mRNA and protein in HeLa cells 72h after infection (Figure 30). HeLa cells infected with AdV-PPRH showed a decrease on *survivin* mRNA levels of 30% relative to controls (Figure 30A), whereas the negative control AdV-GFP did not decrease mRNA levels. Furthermore, survivin protein levels in HeLa cells infected with AdV-PPRH were reduced by 50% compared to the control (Figure 30B and 30C), while its levels in cells treated with the negative control AdV-GFP were unaltered in comparison with the control. The infection of cells was monitored through GFP expression using ZOE Fluorescent Cell Imager (Bio-Rad Laboratories, Inc, Spain). Cell images acquired just before RNA or protein expression are shown in Figure 30D.

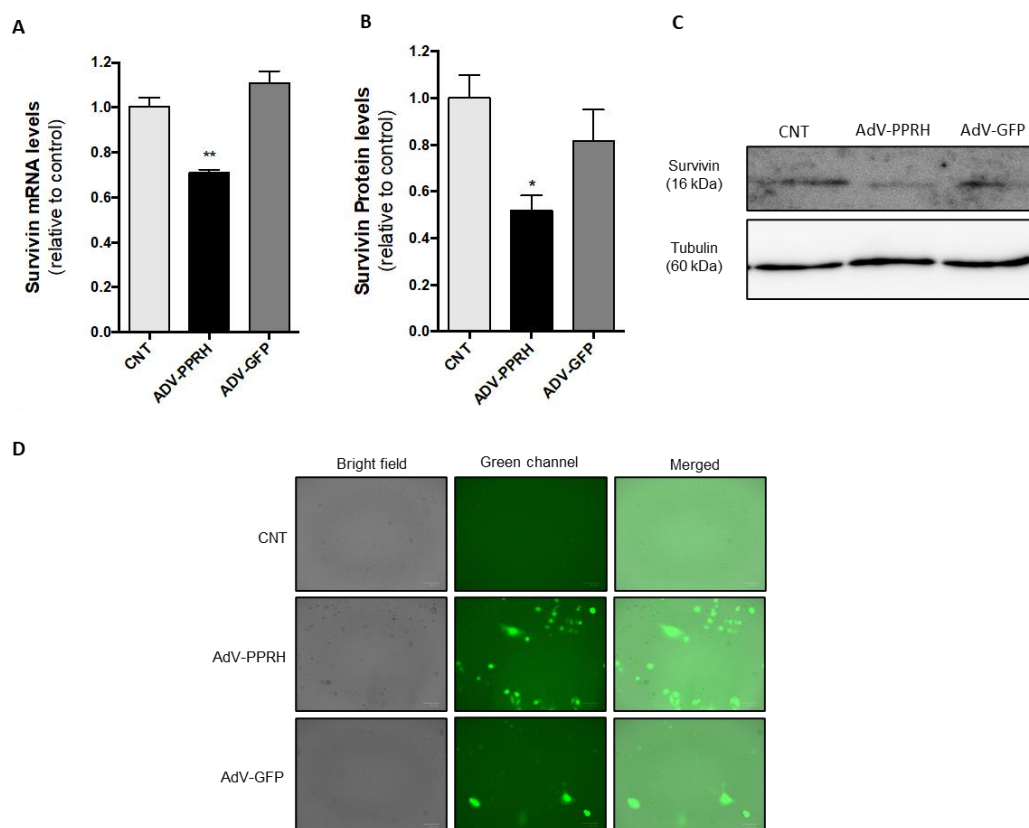


Figure 30. Effect of AdV-PPRH on *survivin* mRNA and protein levels in HeLa cells. HeLa cells (15,000) were plated the day before infection (100 MOI). mRNA levels (A) and

Results

protein levels (B) were analyzed 72h after infection. *survivin* mRNA levels were determined by RT-qPCR. TATA-binding protein (TBP) was used to normalize the results. (C) Representative images of Western blots are shown. Tubulin protein levels were used to normalize the results. (D) Fluorescence microscopy images of each condition were taken before each analysis. Error bars represent the standard error of the mean of three experiments. Statistical significance was calculated using one-way ANOVA with Dunnett's multiple comparisons test (* $p < 0.05$, ** $p < 0.01$). Abbreviation: CNT, control.

4.3. ARTICLE III

Synthesis and validation of DOPY: a new gemini dioleilybispyridinium based amphiphile for nucleic acid transfection

Eva Aubets, Rosa Griera, Alex J. Felix, Gemma Rigol, Chiara Sikorski, David Limón, Chiara Mastrosera, Maria Antònia Busquets, Lluïsa Pérez-García, Véronique Noé and Carlos J. Ciudad

European Journal of Pharmaceutics and Biopharmaceutics. 2021;S0939-6411(21)00146-6. (Impact factor: 4.604).

Background: One of the major issues of nucleic acids therapeutics is the development of a safe, specific, and efficient delivery systems. The N-[1-(2,3-Dioleoyloxy)propyl]-N,N,N-trimethylammonium methylsulfate (DOTAP) cationic liposome has routinely been used as a transfection agent of PPRHs in *in vitro* assays (Villalobos *et al.* 2015). However, the delivery of PPRHs in hard-to-transfect SH-SY5Y neuroblastoma cells has been unsuccessful. An alternative lipid-based delivery system is the new family of cationic gemini surfactants created by Pérez-García and co-workers (Alea-Reyes *et al.* 2017; Giraldo *et al.* 2020; Sporer *et al.* 2009). The ability of these compounds as anion nanocarriers has been studied over the years, with promising results (Casal-Dujat *et al.* 2012; Penon *et al.* 2017; Rodrigues *et al.* 2014a). Therefore, in this work, we studied one member of this family of surfactants, the (1,3-bis[(4-oleyl-1-pyridinio)methyl]benzene dibromide (DOPY), as a non-viral vector for the delivery of PPRHs.

Objectives: One of the aims of this work was to characterize the complexes formed between PPRHs and the novel liposome formulation DOPY. Additionally, we wanted to study the efficiency of DOPY/PPRHs complexes in cellular uptake, gene silencing, and gene repair applications.

Results: First, the ability of DOPY to interact with a FAM-labeled PPRH was confirmed by gel retardation assays, thus demonstrating the formation of DOPY/PPRH complexes. The size of these lipoplexes was determined by dynamic light scattering (DLS), obtaining 155 nm in diameter with a dispersion index of 0.25. The Z-potential of DOPY/PPRH complexes was $67.53 \text{ mV} \pm 1.08$

Results

mV, in accordance with the cationic nature of the lipoplexes, and indicated high stability. Transmission Electron Microscopy experiments allowed the visualization of the fibrillar structures of the PPRH molecules covered by DOPY, thus corroborating the interaction between DOPY and the PPRH, and confirmed the hydrodynamic diameters obtained by DLS.

Regarding the cellular uptake, we obtained high efficiencies of PPRH internalization using DOPY compared to other chemical vehicles in SH-SY5Y, PC-3 and DF42 cells. The decrease in DOPY/PPRH cellular uptake after the treatment with clathrin-mediated or caveolae-mediated endocytosis inhibitors indicated the implication of these two pathways in the internalization of DOPY/PPRHs complexes.

In gene silencing experiments conducted with a specific PPRH against *survivin*, DOPY/PPRH complexes decreased survivin protein levels and cell viability more effectively than complexes with DOTAP in both SH-SY5Y and PC-3 cells. Moreover, we aimed to correct a point mutation in the endogenous *locus* of the *dhfr* gene using a repair-PPRH in DF42 cells. Higher repair frequencies were obtained with DOPY/repair-PPRH complexes compared with other vehicles. The correction of the mutation was confirmed by DNA sequencing, protein expression, and DHFR enzymatic activity.

Conclusions: This work demonstrated successful cellular uptake, efficient *survivin* gene silencing and correction of the *dhfr* gene using DOPY/PPRHs complexes. Therefore, we show the potential of DOPY as a new gemini cationic lipid-based vector suitable for the delivery of therapeutic oligonucleotides *in vitro*.



Contents lists available at ScienceDirect

European Journal of Pharmaceutics and Biopharmaceutics

journal homepage: www.elsevier.com/locate/ejpb

Synthesis and validation of DOPY: A new gemini dioleilylpyridinium based amphiphile for nucleic acid transfection

Eva Aubets^{a,d}, Rosa Grieria^b, Alex J. Felix^{a,d}, Gemma Rigol^a, Chiara Sikorski^{a,1}, David Limón^{b,d}, Chiara Mastrorosa^{a,2}, Maria Antònia Busquets^{c,d}, Lluïsa Pérez-García^{b,d,*}, Véronique Noé^{a,d}, Carlos J. Ciudad^{a,d,*}

^a Department of Biochemistry and Physiology, School of Pharmacy and Food Sciences, University of Barcelona, 08028 Barcelona, Spain

^b Department of Pharmacology, Toxicology and Therapeutic Chemistry, School of Pharmacy and Food Sciences, University of Barcelona, 08028 Barcelona, Spain

^c Department of Pharmacy and Pharmaceutical Technology and Physical, Chemistry, School of Pharmacy and Food Sciences, University of Barcelona, 08028 Barcelona, Spain

^d Nanoscience and Nanotechnology Institute, IN2UB, University of Barcelona, Spain

ARTICLE INFO

Keywords:

PPRHs
DOPY
Cationic liposome
Gene delivery
Transfection
Gene silencing
Gene repair
Nucleic acids
Lipid-based vector
Cancer therapy

ABSTRACT

Nucleic acids therapeutics provide a selective and promising alternative to traditional treatments for multiple genetic diseases. A major obstacle is the development of safe and efficient delivery systems. Here, we report the synthesis of the new cationic gemini amphiphile 1,3-bis[(4-oleyl-1-pyridinio)methyl]benzene dibromide (DOPY). Its transfection efficiency was evaluated using PolyPurine Reverse Hoogsteen hairpins (PPRHs), a nucleic acid tool for gene silencing and gene repair developed in our laboratory. The interaction of DOPY with PPRHs was confirmed by gel retardation assays, and it forms complexes of 155 nm. We also demonstrated the prominent internalization of PPRHs using DOPY compared to other chemical vehicles in SH-SY5Y, PC-3 and DF42 cells. Regarding gene silencing, a specific PPRH against the *survivin* gene delivered with DOPY decreased survivin protein levels and cell viability more effectively than with *N*-[1-(2,3-Dioleoyloxy)propyl]-*N,N,N*-trimethylammonium methylsulfate (DOTAP) in both SH-SY5Y and PC-3 cells. We also validated the applicability of DOPY in gene repair approaches by correcting a point mutation in the endogenous *locus* of the *dhfr* gene in DF42 cells using repair-PPRHs. All these results indicate both an efficient entry and release of PPRHs at the intracellular level. Therefore, DOPY can be considered as a new lipid-based vehicle for the delivery of therapeutic oligonucleotides.

1. Introduction

The use of nucleic acids therapeutics has emerged as a promising gene therapy approach to modulate any gene of interest for the treatment of multiple diseases such as cancer [1,2] neurological [3–6], cardiovascular [7,8] or hematological [9,10] disorders, among others. The advances in this field have eventually led to the approval by the Food and Drug administration (FDA) of several nucleic acid tools [11], including antisense oligonucleotides (ASOs) [12–18], small interfering RNAs (siRNAs) [19–21], aptamers [22] or the very recent mRNA vaccines against COVID-19 [23,24].

Despite the great efforts made during the last decades, the

development of safe, efficient and tissue-specific delivery systems still remains as one of the major limitations of gene therapies. In general, delivery vectors can be classified into viral, physical or chemical systems [25]. On the one hand, although viral vectors exhibit high transduction efficiencies, they can generate mutations in the DNA or undesired immunogenic responses. Moreover, the laborious production and the restriction on the transgene size also represent some of the limitations of viral vectors [26]. On the other hand, physical systems, which perturb the cell membrane to enforce the entry of nucleic acids into the cell, are safer but present lower efficiency than viral vectors and they are difficult to implement for internal organs [27]. Finally, chemical systems (e.g., calcium phosphate, lipoplexes or polyplexes) are safer than viral vectors,

* Corresponding authors at: School of Pharmacy and Food Sciences, University of Barcelona, 08028 Barcelona, Spain.

E-mail addresses: mperez@ub.edu (L. Pérez-García), cciuudad@ub.edu (C.J. Ciudad).

¹ Present address: Dipartimento di Medical Affairs, Novartis Farma, Via Saronno 1, 21042, Origgio, Varese, Italy.

² Present address: Merck Serono Spa, Via Einaudi 11, 00012, Guidonia, Roma, Italy.

<https://doi.org/10.1016/j.ejpb.2021.05.016>

Received 22 February 2021; Received in revised form 15 April 2021; Accepted 18 May 2021

Available online 24 May 2021

0939-6411/© 2021 Elsevier B.V. All rights reserved.

easier to produce and susceptible to modifications to enhance targeting specificity. However, some of these chemical alternatives present low levels of internalization or some toxicity [28–30].

During the last decade, our laboratory of Biochemistry and Molecular biology has developed a new nucleic acid tool called PolyPurine Reverse Hoogsteen hairpins (PPRHs) [31,32]. PPRHs are non-modified DNA hairpins, whose structure is formed by two antiparallel polypurine mirror repeat domains linked by a five-thymidine loop (5T) and bound intramolecularly by Hoogsteen bonds. PPRHs are designed to hybridize to a specific polypyrimidine sequence in the dsDNA by Watson–Crick bonds, thus producing a triplex structure. This conformation displaces the fourth strand of the complex and leads to the inhibition of the target gene. The ability of PPRHs as gene silencing tools has been validated in a wide range of target genes involved in cancer progression both *in vitro* [33–42] and *in vivo* [35]. Furthermore, PPRHs have also demonstrated their potential to correct point mutations in the gDNA. The design of these PPRHs, called repair-PPRHs, consists of a polypurine hairpin that bears at its 5'-end an extension sequence homologous to the sequence to be repaired but containing the wild-type nucleotide instead of the mutated one [43,44]. Repair-PPRHs were able to correct at the endogenous level two collections of Chinese Hamster Ovary (CHO) cell lines bearing different mutations in either the *dihydrofolate reductase* (*dhfr*) [45] or *adenine phosphoribosyltransferase* (*aprt*) [46] loci.

As in other gene therapy methods, internalization of PPRHs is vital to obtain the desired effect. Regarding *in vitro* gene silencing approaches, we have routinely been delivering PPRHs in various cancer cell lines [35,36] using the *N*-[1-(2,3-Dioleoyloxy)propyl]-*N,N,N*-trimethylammonium methylsulfate (DOTAP) cationic liposome, which is commercially available [47,48]. However, the delivery of PPRHs in hard-to-transfect SH-SY5Y neuroblastoma cells was unsuccessful.

More than a decade ago our Organic Chemistry group created a new family of cationic gemini surfactants. The dicationic amphiphiles are formed by two cationic heterocycles –either imidazolium [49], pyridinium [50] or bipyridinium rings [51] linked by a 1,3-dimethylene-phenylene spacer, where the cationic rings incorporate long alkyl chains of different lengths and functionality, their properties being driven by their specific structural composition. Over the years we have reported the ability of this class of amphiphiles to behave as ionic liquid crystals [52], their self-assembly into micelles as anion nanocarriers [53], as well as their use for the synthesis and stabilization of gold nanoparticles for drug delivery [54,55]. The bis cationic amphiphiles self-assemble to form nanostructured supramolecular hydrogels [56] for the topical treatment of Psoriasis and delivery in skin diseases [57,58] able to act as enhancers of skin permeation [59]. Both cationic amphiphilic incorporating nanoparticles [60] and hydrogels [61] have proven to be efficient deliverers of photosensitizers and their selective phototoxicity in cancer cells makes them promising nanomaterials for targeted photodynamic therapy [62].

The present work exemplifies the synergy created by the combination of the expertise of our two groups. Thus, with the aim to develop a non-viral vehicle capable of delivering PPRHs in hard-to-transfect cells, we designed and synthesized a new liposome formulation called 1,3-bis [(4-oleyl-1-pyridinio)methyl]benzene dibromide (DOPY) testing its capacity to form complexes with PPRH molecules. Due to its gemini cationic nature, the assemblies from DOPY are able to interact with polyanionic PPRH molecules, with the oleyl moieties aiding their cell uptake. In addition, we analyzed the efficiency of DOPY in gene silencing approaches by inhibiting the *survivin* gene in both PC3 and SH-SY5Y cancer cells using PPRHs. Finally, we validated DOPY as a transfection agent for gene repair applications by correcting a point mutation in the *dhfr* gene in CHO cells using repair-PPRHs.

2. Materials and methods

2.1. Chemicals and instrumentation

Oleyl alcohol, 4-chloropyridine hydrochloride, sodium hydride (NaH), α,α' -dibromo-*m*-xylene, dimethyl sulfoxide (DMSO), acetonitrile and deuteriochloroform (CDCl_3) were purchased from Sigma-Aldrich. Ethyl acetate (AcOEt), hexane, sodium sulfate anhydrous (Na_2SO_4) and silica gel 60 were purchased from Carlo Erba. All chemicals were analytical grade and used directly without any further modification.

Evaporation of solvent was accomplished with a rotatory evaporator. Thin-layer chromatography was done on SiO_2 (silica gel 60 F254), and the spots were located by either an UV light or a 1% KMnO_4 solution. Flash column chromatography was carried out on SiO_2 (silica gel 60, 230–400 mesh).

NMR spectra were recorded at 400 MHz (^1H) and 100.6 MHz (^{13}C) on a Varian Mercury in the Scientific and Technologic Center of the University of Barcelona (CCIT-UB); chemical shifts are reported in δ values, in parts per million (ppm) relative to Me_4Si (0 ppm) or relative to residual chloroform (7.26 ppm, 77.00 ppm) as an internal standard. Data are reported in the following manner: chemical shift, multiplicity, coupling constant (*J*) in hertz (Hz), integrated intensity.

The hydrodynamic diameter of the liposomes was determined by dynamic light scattering (DLS) at a fixed scattering angle of 90° with a Zetasizer Nano (Malvern, United Kingdom) at 25°C . To perform this measurement, lipoplexes were formed by mixing aqueous solutions of DOPY (2.1 μM) and PPRH against survivin (100 nM), mimicking the conditions of transfection. Nanoparticles were dissolved in 200 μL water and brought to 1 mL for the measurements. Particle size distribution was determined by the polydispersity index (PI). The ζ -potential was measured by Doppler microelectrophoresis using a Zetasizer Nano (Malvern, United Kingdom). For this measurement, the final volume of the lipoplexes was 1.2 mL.

Transmission Electron Microscopy (TEM) images were obtained in the CCITUB. Samples of DOPY, PPRH, and DOPY-PPRH complexes were prepared in the same molar proportions used in transfection experiments. Copper grids with carbon coating were irradiated with a UV glow discharge during 30 s under vacuum. The grid was placed onto a 5 μL drop of the sample for 1 min. The grid was then placed onto a 20 μL drop of milli Q water for 1 min to rinse excess sample and then placed onto a 20 μL drop of a 2% uranyl acetate solution in water for 1 min. Excess solution was then removed with filter paper and allowed to dry overnight in a desiccator at 24°C . Samples were observed in a Tecnai Spirit microscope (FEI, The Netherlands) equipped with a LaB6 cathode. Images were acquired at 120 kV and at room temperature with a 1376×1024 -pixel Megaview CCD camera.

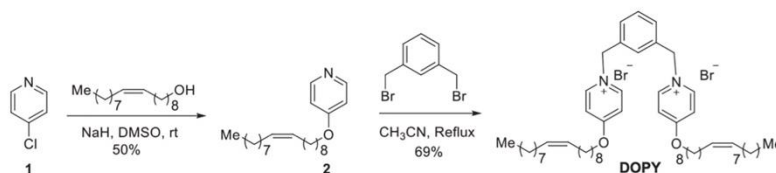
2.2. Preparation of 4-Oleyloxy-pyridine

Oleyl alcohol (1.3 mL, 4.09 mmol) was added dropwise to a stirring suspension of NaH (115 mg, 4.55 mmol, 95%) in dry DMSO (3 mL). After 45 min, crude 4-chloropyridine (800 mg, 7.05 mmol) (compound 1, Fig. 1A), freshly liberated using KOH (2 N) from its hydrochloride salt, was added at once. The stirring was continued overnight at room temperature. Water was added and the mixture was extracted with AcOEt (3 \times 10 mL). The combined organic extracts were dried over Na_2SO_4 , filtered and concentrated at reduced pressure. Flash chromatography (from 3:2 to 1:1 hexane–EtOAc) afforded 4-oleylpyridine (510 mg, 50%) as a colourless oil. The structure of the 4-oleylpyridine (compound 2, Fig. 1A) was characterized and confirmed by ^1H NMR and ^{13}C NMR spectroscopy (Figure S1).

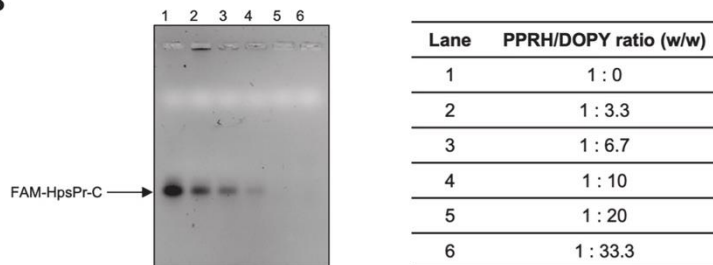
^1H NMR (400 MHz, CDCl_3) δ : 8.39 (d, *J* = 5.0 Hz, 2H), 6.77 (d, *J* = 5.0 Hz, 2H), 5.30–5.38 (m, 2H), 3.98 (t, *J* = 6.6 Hz, 2H), 1.93–2.04 (m, 4H), 1.78 (quint, *J* = 6.6 Hz, 2H, H-6), 1.40–1.47 (m, 2H), 1.20–1.37 (m, 20H), 0.87 (t, *J* = 7.0 Hz, 3H).

^{13}C NMR (100.6 MHz, CDCl_3) δ : 165.1, 150.9, 129.98, 129.7, 110.2,

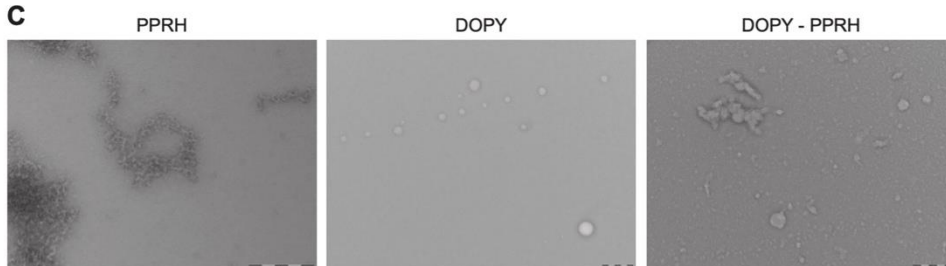
A



B



C



D

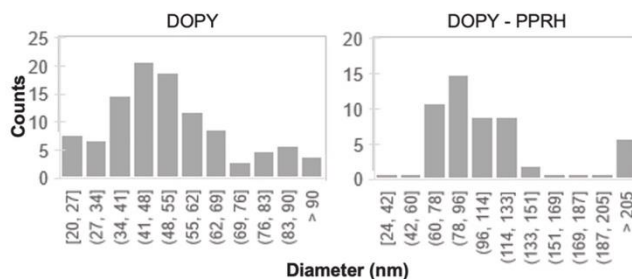


Fig. 1. DOPY synthesis and binding properties. (A) Schematic representation of the synthesis of 1,3-bis(4-oleyl-1-pyridiniummethyl)benzene dibromide (DOPY). Compounds 1 and 2 correspond to free pyridine and its oleyl ether, respectively. (B) Gel retardation assay with increasing amounts of DOPY, which binds to 150 ng of FAM-HpsPr-C and generates DOPY/PPRH complexes. (C) TEM images of PPRH (left), DOPY (center), and DOPY-PPRH lipoplexes (right). (D) Size distribution by half-open intervals of DOPY vesicles (left) ($n = 109$) and DOPY-PPRH lipoplexes (right) ($n = 57$) as observed by TEM.

67.9, 31.9, 29.7, 29.7, 29.5, 29.4, 29.3, 29.27, 29.2, 28.9, 27.2, 27.1
25.90, 22.7, 14.1.

2.3. Preparation of DOPY

α,α' -Dibromo-*m*-xylene (166 mg, 0.61 mmol) was added to a solution

of 4-oleylpyridine (423 mg, 1.22 mmol) in acetonitrile (7 mL), and the mixture was heated at reflux for 24 h. After cooling at room temperature, the suspension was filtered off, and the resulting gum was washed with acetonitrile affording 1,3-bis(4-oleyl-1-pyridiniummethyl)benzene dibromide (DOPY) (400 mg, 69%, MW 956 g/mol), as a sticky yellowish solid (Fig. 1A). The structure of DOPY (Figure S2) was

Results

characterized and confirmed by ¹H NMR and ¹³C NMR spectroscopy.

¹H NMR (400 MHz, CDCl₃) δ 9.77 (d, J = 7 Hz, 4H), 8.36 (s, 1H), 7.69 (d, J = 8 Hz, 2H), 7.35 (d, J = 7 Hz, 4H), 7.00 (t, J = 8 Hz, 1H), 5.94 (s, 4H), 5.39–5.30 (m, 4H), 4.21 (t, J = 6 Hz, 4H), 2.05–1.94 (m, 8H), 1.84 (quint, J = 7 Hz, 4H), 1.47–1.39 (m, 4H), 1.38–1.22 (m, 40H), 0.87 (t, J = 7 Hz, 6H).

¹³C NMR (100.6 MHz, CDCl₃) δ: 170.0, 146.3, 134.5, 130.7, 129.9, 129.6, 129.3, 113.8, 71.2, 60.9, 32.2, 31.5, 29.4, 29.3, 29.2, 29.1, 29.0, 28.9, 28.8, 28.7, 28.1, 26.8, 26.7, 26.7, 25.3, 22.3.

2.4. Design and usage of PPRHs

For gene silencing experiments, a PPRH directed against the *survivin* promoter previously validated in our laboratory was selected [35,63]. The polypurine stretches that conform the hairpin structure of the PPRH were found using the Triplex-forming Oligonucleotide Target Sequence Search software (<http://utw10685.utweb.utexas.edu/tfo/>) MD Anderson cancer center, The University of Texas) [64]. BLAST analyses were performed to confirm the specificity of the designed PPRH. As negative control, we used a hairpin with intramolecular Watson-Crick bonds instead of Hoogsteen bonds (HpWC), thus preventing triplex formation with the target DNA.

Regarding the gene repair approach, repair-PPRHs were designed by attaching an extension sequence (repair domain) at the 5'-end of the PPRH. This repair domain is homologous to the mutation site but containing the corrected nucleotide instead. As negative control, a scrambled repair-PPRH was used. This negative repair-PPRH contained the specific repair domain to correct the mutation but a scrambled polypurine hairpin core, which cannot bind to the polypyrimidine target sequence near the mutation in the dsDNA.

All hairpins were synthesized as non-modified oligodeoxynucleotides by Merck (Haverhill, United Kingdom), resuspended in sterile Tris-

EDTA buffer (1 mM EDTA and 10 mM Tris, pH 8.0) (Merck, Madrid, Spain) and stored at -20 °C until use. All the sequences of the hairpins used in this study are shown in Table 1.

2.5. Agarose gel retardation assay

Binding reactions were conducted in a final volume of 10 μL containing 150 ng of FAM-HpsPr-C PPRH, increasing amounts of DOPY and H₂O mQ. After 20 min of incubation at room temperature, binding reactions were electrophoresed in 0.8% agarose gels. Gels were visualized on a Gel Doc™ EZ (Bio-Rad Laboratories, Inc, Spain).

2.6. Cell culture

For gene silencing experiments, SH-SY5Y neuroblastoma and PC-3 prostate cancer cells, obtained from the cell bank resources from University of Barcelona, were grown in Ham's F12 medium supplemented with 10% fetal bovine serum (GIBCO, Invitrogen, Barcelona, Spain) and incubated at 37 °C in a humidified 5% CO₂ atmosphere. Subculture was performed using 0.05% Trypsin (Merck, Madrid, Spain).

For gene correction experiments, the DF42 Chinese Hamster Ovary (CHO) mutant cell line was used. This cell line contained a single-point mutation in the endogenous *dhfr* gene bearing a G > T substitution in c.541 (exon 6), thus generating a premature STOP codon and a nonfunctional DHFR enzyme. The DF42 cell line was obtained using a variety of mutagens in UA21 cells [65], which is a CHO cell line hemizygous for the *dhfr* gene [66]. Cells were grown as stated previously.

2.7. Transfection of PPRHs

Regarding gene silencing experiments, cells were plated in 6-well dishes one day before transfection in F12 medium. Transfection

Table 1

Oligodeoxynucleotides used in this study.

Name	Sequence (5'-3')
FAM-HpsPr-C	[6FAM] AGGGGAGGGATGGAGTGCAG T T AGGGGAGGGATGGAGTGCAG T T
HpsPr-C	AGGGGAGGGATGGAGTGCAG T T AGGGGAGGGATGGAGTGCAG T T
HpWC	GACGTGAGGTAGGGAGGGGA T T AGGGGAGGGATGGAGTGCAG T T
HpE6rep-L	GAAGTCCAGGAGGAAAAAGGCATCAAGTATAAAATTTGAAGTCTATGAGAAGAAAGGCTAACAGAAAGA T T GAGAAGAAAGGCTAACAGAAAGA T T
HpE6rep-L-Sc	GAAGTCCAGGAGGAAAAAGGCATCAAGTATAAAATTTGAAGTCTATAGAGGAGGAATCGGTGAGGGAG T T AGAGGAGGAATCGGTGAGGGAG T T

Name and sequence of the PPRHs used for gel retardation and cellular uptake assays (FAM-HpsPr-C), gene silencing experiments (HpsPr-C and the negative control HpWC) and gene repair approaches (HpE6rep-L and the negative control HpE6rep-L-Sc). The corrected nucleotide in the repair-PPRHs is represented in bold and underlined. The abbreviations used for the nomenclature of the PPRHs are: Hp, hairpin; Pr, promoter; s, *survivin*; -C, Coding-PPRH; -WC, Watson-Crick; E6, exon 6; rep, repair- PPRH; Sc, scramble.

consisted in mixing the corresponding amount of the transfection agent with the PPRH in serum-free medium up to 200 μ L. After 20 min of incubation at room temperature, the mixture was added to the cells in a final volume of 1 mL (full medium). Transfection agents used were the newly synthesized compound DOPY or the commercially available cationic liposome DOTAP (Biont, Germany).

For gene correction experiments, DF42 cells (300,000) were plated in 100-mm plates the day before transfection. Transfections were performed using either calcium phosphate, DOTAP or DOPY. Calcium phosphate transfections were carried out using the original method [67], and similarly to our previous works [43,45,46]. DOTAP transfections were performed by mixing 12 μ g of DOTAP with 10 μ g of repair-PPRH in serum-free medium up to 600 μ L. After 20 min of incubation, DOTAP/repair-PPRH complexes were added to cells in a final volume of 6 mL (full medium) (Final concentration of DOTAP 2.6 μ M). DOPY transfections were performed by mixing 12 μ g of DOPY with 10 μ g of repair-PPRH in serum-free medium up to 600 μ L. After 20 min of incubation, DOPY/repair-PPRH complexes were added to cells in a final volume of 6 mL (full medium) (Final concentration of DOPY 2.1 μ M). In all types of transfections, cells were incubated during 48 h with repair-PPRHs before selection.

2.8. Cellular uptake

SH-SY5Y cells (60,000), PC-3 cells (60,000) or DF42 cells (300,000) were plated the day before transfection. Transfections were carried out as stated previously in the transfection section of M&M, but in this case using FAM-HpsPr-C PPRH. After 24 h of incubation, cell images for each condition were taken using a ZOE Fluorescent Cell Imager (Bio-Rad Laboratories, Inc, Spain). Then, cells were trypsinized and collected, centrifuged at 800g at 4 °C for 5 min and washed once in PBS. The pellet was resuspended in 500 μ L of PBS and Propidium Iodide was added to a final concentration of 5 μ g/mL (Merck, Madrid, Spain). Flow cytometry analyses were performed in a Gallios flow cytometer (Beckman Coulter, Inc, Spain).

To study the internalization mechanism of DOPY, SH-SY5Y and PC-3 cells (120,000) were plated in 6-well dishes in F12 medium. After 24 h, cells were preincubated with 75 μ M of the clathrin-dependent endocytosis inhibitor Dynasore [68], 185 μ M of the caveolin-mediated endocytosis inhibitor Genistein [69], or 33 μ M of the micropinosytosis inhibitor 5-(*N*-ethyl-*N*-isopropyl) amiloride (EIPA) [70], all from Merck, Madrid, Spain, for 60 min at 37 °C. Then, transfection mixes containing FAM-HpsPr-C were added to cells for 4 h and processed for flow cytometry analyses as described above in this section.

2.9. MTT assay

Cells (10,000) were plated in 6-well dishes in F12 medium. Five (PC-3 cells) or four (SH-SY5Y cells) days after transfection, 0.63 mM of 3-(4,5-dimethylthiazol-2-yl)-2,5-diphenyltetrazolium bromide and 100 μ M sodium succinate (both from Merck, Madrid, Spain) were added to the culture medium and incubated for 2.5 h at 37 °C. After incubation, culture medium was removed and the lysis solution (0.57% of acetic acid and 10% of sodium dodecyl sulfate (SDS) in dimethyl sulfoxide) (Merck, Madrid, Spain) was added. Absorbance was measured at 560 nm in a Modulus Microplate spectrophotometer (Turner BioSystems, Madrid, Spain). Cell viability results were expressed as the percentage of cell survival relative to the controls.

2.10. Western blot analyses

Total protein extracts from PC-3 and SH-SY5Y cells (30,000) were obtained 24 h after transfection using 100 μ L of RIPA buffer (1% Igepal, 0.5% sodium deoxycholate, 0.1% SDS, 150 mM NaCl, 1 mM EDTA, 1 mM PMSF, 10 mM NaF and 50 mM Tris-HCl, pH 8.0) supplemented with Protease inhibitor cocktail (P8340) (all from Merck, Madrid, Spain).

Extracts were incubated 5 min at 4 °C and cell debris was removed by centrifugation (16,300g at 4 °C for 10 min).

In the case of DF42 protein extracts, cells were harvested by trypsinization and treated with Lysis buffer (0.5 M NaCl, 1.5 mM MgCl₂, 1 mM EDTA, 10% glycerol, 1% Triton X-100, 50 mM HEPES, pH 7.2), supplemented with Protease Inhibitor Mixture (P8340) (all from Merck, Madrid, Spain). Whole-protein extracts were maintained at 4 °C for 1 h with vortexing every 15 min. Cell debris was removed by centrifugation (16,300g for 10 min).

Protein concentrations were determined using a Bio-Rad protein assay based on the Bradford method and using bovine serum albumin as a standard. Whole-protein extracts (100 μ g) were electrophoresed in 15% or 12% SDS-polyacrylamide gels for survivin or DHFR detection, respectively, and transferred to Immobilon-P polyvinylidene difluoride membranes (Merck, Madrid, Spain) using a semidry electroblotting system. Blocking was performed using a 5% skim milk solution. Then, membranes were probed with the primary antibody against survivin (5 μ g/mL; AF886, Bio-Techne R&D Systems, S.L.U. Madrid, Spain), DHFR (1:250 dilution; Pocono Rabbit Farm & Lab, Canadensis, PA, USA) or α -Tubulin (1:100 dilution; CP06, Merck, Darmstadt, Germany). Secondary horseradish peroxidase-conjugated antibodies were anti-rabbit (1:2000 dilution; P0399, Dako, Denmark) for primary antibodies against survivin and DHFR, and anti-mouse (1:2500 dilution; sc-516102, Santa Cruz Biotechnology, Heidelberg, Germany) for α -tubulin detection. Chemiluminescence was detected with the ImageQuant LAS 4000 mini (GE Healthcare, Barcelona, Spain). Quantification was performed using the ImageQuant 5.2 software.

2.11. Selection of repaired cells

DHFR selection was applied to transfected cells after 48 h of incubation with the repair-PPRH. Selection was performed using RPMI 1640 selective medium (Gibco) lacking glycine, hypoxanthine and thymidine (-GHT medium), which are the final products of DHFR activity, and containing 7% dialyzed FBS (Gibco). Each experimental condition was performed in triplicate, and a minimum of three colonies were analyzed for each condition.

2.12. Gene correction frequency

After 14 days of selection in -GHT medium, surviving cell colonies were fixed in 6% formaldehyde, stained with crystal violet (both from Merck, Madrid, Spain) and manually counted. Gene correction frequency values were calculated as the ratio between the number of surviving colonies and the total number of cells initially plated.

2.13. DNA sequencing

Total genomic DNA was isolated from either DF42 mutant or DF42 repaired cells using the Wizard genomic DNA purification kit (Promega, Madrid, Spain) following the manufacturer's recommendations. PCRs were carried out to amplify the target site using OneTaq polymerase (New England Biolabs, Ipswich, MA, USA) following the PCR cycling conditions recommended by the manufacturer. Primer sequences were 5'-GTGATGTGCTTCAATGGGGT-3' and 5'-TCTAAAGCCAACA-CAAGTCCC-3'. PCR-amplified products (227 bp) were run in 5% polyacrylamide gel electrophoresis, purified and sequenced by MacroGen (Amsterdam, the Netherlands).

2.14. DHFR activity assay

The method is based on the incorporation of radioactive deoxyuridine into cellular DNA. This depends on the reductive methylation of deoxyuridylate to thymidylate by tetrahydrofolate, which is generated by DHFR from folate supplied in the medium. Therefore, incorporation of radioactive dTTP into DNA relies on DHFR activity, and it can be

Results

detected by DNA isolation [71].

Mutant or repaired DF42 cells (1×10^5) were seeded in 6-well plates in 1 mL of selective medium (-GHT). Next day, $2 \mu\text{Ci}$ of 6- ^3H deoxyuridine (18.9 Ci/mmol, Hartmann Analytic, Germany) were added for 24 h. Cells were lysed in 100 μL of 0.1% SDS. The lysate was placed onto 31ET chromatography paper (Whatman) and dried at room temperature. Finally, papers were washed three times for 30 min in constant

agitation with 66% cold ethanol containing 250 mM NaCl, dried, and counted in a scintillation counter.

2.15. Statistical analyses

Statistical analyses were performed using GraphPad Prism 6 (GraphPad Software, CA, USA). Data are represented as the mean \pm SEM

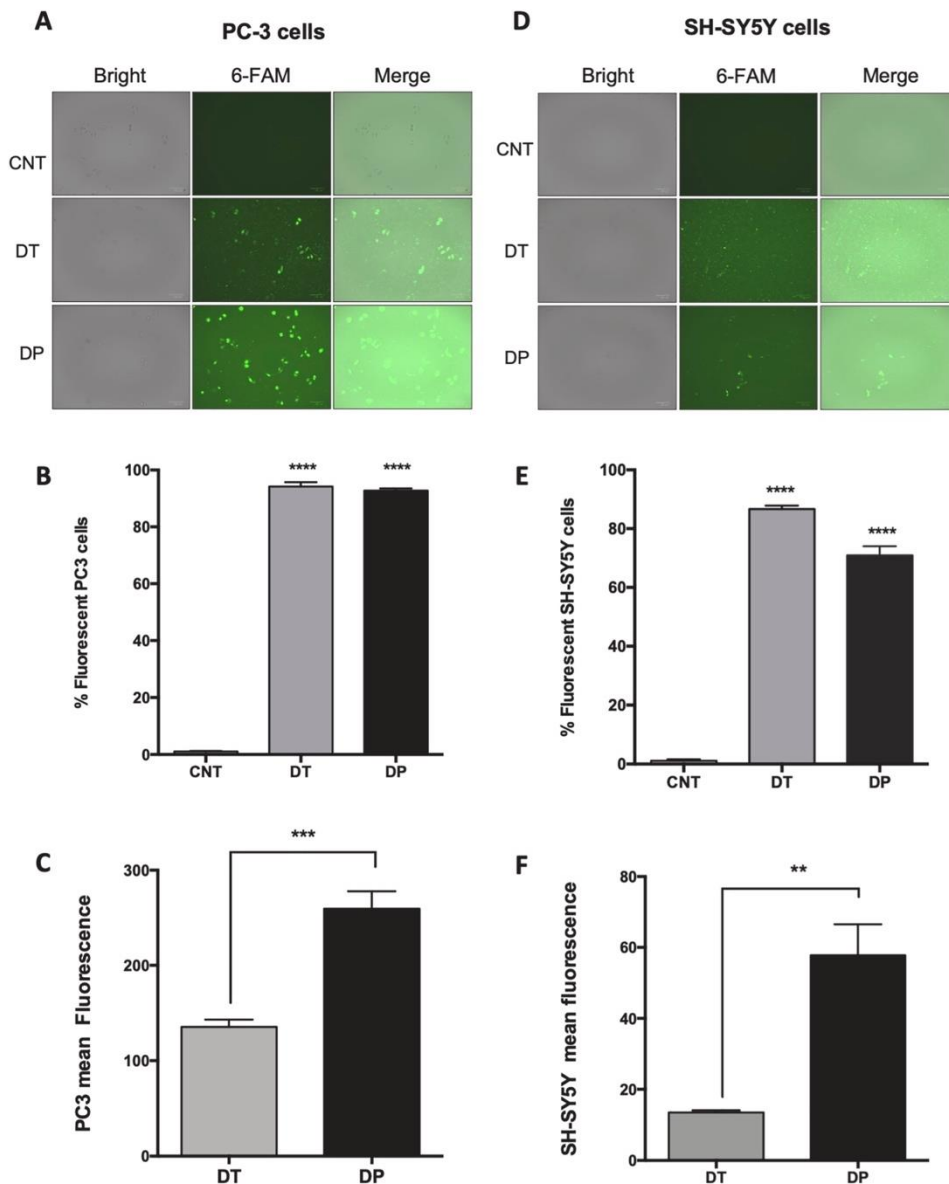


Fig. 2. Cellular uptake of PPRHs for gene silencing applications. Fluorescence microscopy images of PC-3 (A) and SH-SY5Y (D) cells were taken 24 h after transfection with 100 nM of FAM-HpsPr-C using either DOTAP (10 μM) or DOPY (2.1 μM). Then, the percentage of fluorescent cells (B and E) and the mean fluorescence (C and F) for each cell line were determined by flow cytometry. Error bars represent the standard error of the mean of three experiments. Statistical significance was calculated using one-way ANOVA with Dunnett's multiple comparisons test for the percentage fluorescent cells or Unpaired T test for the mean fluorescence (** $p < 0.01$, *** $p < 0.001$, **** $p < 0.0001$). Abbreviations: CNT, control; DT, DOTAP; DP, DOPY.

of at least three independent experiments. The levels of statistical significance were denoted as follows: $p < 0.05$ (*), $p < 0.01$ (**), $p < 0.001$ (***) or $p < 0.0001$ (****).

3. Results

3.1. DOPY/PPRH complexes characterization

First, the ability of DOPY to interact with FAM-HpsPr-C PPRH was assessed by gel retardation assays. Incubation of increasing amounts of DOPY with 150 ng of the PPRH resulted in a progressive disappearance of the band corresponding to the PPRH signal compared to the PPRH alone (Fig. 1B), thus demonstrating the formation of DOPY/PPRH complexes. Then, we analyzed the size of DOPY/PPRH complexes, which show a hydrodynamic diameter of 155 nm, with a dispersion index of 0.25 (Figure S3A), as analyzed by DLS, a value significantly increased respect the DOPY vesicles (ca. 100 nm) upon complexation. Furthermore, the Z-potential of DOPY/PPRH complexes 67.53 ± 1.08 mV (Figure S3B), is not significantly different from that of DOPY vesicles (ca. 57 mV), in accordance with the cationic nature of the lipoplexes, and indicates the excellent stability of the lipoplexes.

Transmission Electron Microscopy (TEM) was used to study the morphology of the materials. As shown in Fig. 1C, the FAM-HpsPr-C PPRH molecules intertwine forming fibrillar structures, whereas DOPY forms vesicles of 52.4 ± 18.2 nm in diameter (Fig. 1D). In contrast, when DOPY vesicles come in contact with PPRH, the fibers of PPRH are completely covered by DOPY as a consequence of their strong interaction, leading to a combined morphology. Most of the lipoplexes formed are less than 133 nm in diameter (Fig. 1D), which is also in accordance with the hydrodynamic diameters observed in aqueous colloidal dispersion.

3.2. Transfection efficiency for gene silencing

Once verified the capacity of DOPY to interact with PPRHs, we compared the cellular uptake of FAM-HpsPr-C PPRH (100 nM) when cells were transfected using either DOPY or the validated transfection agent DOTAP, which is widely used in our laboratory for gene silencing approaches, and thus useful for comparison purposes in the different assays. Cells were transfected using either 2.1 μ M of DOPY or 10 μ M of DOTAP (standard conditions used for PPRH transfection in gene silencing approaches: molar ratio of 1:100 PPRH/DOTAP). The percentage of fluorescent cells and their mean fluorescence intensity were determined 24 h after transfection using flow cytometry. The cellular uptake was analyzed in PC-3 cells, in which we had previous experience transfecting PPRHs using DOTAP, and in SH-SY5Y cells, which are difficult to transfect using DOTAP in standardized conditions. According to our previous results using HpsPr-C PPRH [35], high percentages of fluorescent PC-3 cells were observed when using DOTAP (94%) (Fig. 2A and B). Similar values of fluorescent cell percentages were obtained when using DOPY (93%) (Fig. 2B). However, the mean values were 2-fold higher in DOPY transfections than those of DOTAP (Fig. 2C). In the case of hard-to-transfect SH-SY5Y cells, the percentages of fluorescent cells were 87% using DOTAP and 71% using DOPY (Fig. 2D and E), but the fluorescence mean was 4.3 times higher in DOPY transfections than that of DOTAP transfections (Fig. 2F). Fluorescence microscopy cell images acquired just before flow cytometer analyses were in accordance with the results described in this section (Fig. 2A and D).

We also analyzed the mechanisms involved in the internalization of DOPY/PPRH complexes by transfecting cells with FAM-HpsPr-C either in the presence or the absence of different endocytic pathways inhibitors (Fig. 3) [68–70]. After 4 h of transfection, DOPY/PPRH complexes internalization was significantly reduced with either the clathrin-dependent endocytosis inhibitor Dynasore (75 μ M) or the caveolin-mediated endocytosis inhibitor Genistein (185 μ M), in both PC-3 and SH-SY5Y cells. The treatment with Dynasore presented a decrease of

51% and 35% of fluorescent cells, in PC-3 and SH-SY5Y respectively, in comparison with untreated cells (Fig. 3A and C). Furthermore, the fluorescence mean values were reduced by 24.5 and 3.4-fold in PC-3 and SH-SY5Y cells, respectively, relative to untreated cells (Fig. 3B and D). In the case of Genistein treatment, the decrease of fluorescent cells was of 23% in PC-3 and 21% in SH-SY5Y (Fig. 3A and C), and the fluorescence mean values were reduced by 20-fold and 2.7-fold in PC-3 and SH-SY5Y cells, respectively (Fig. 3B and D). No significant decrease was observed in neither the percentage of fluorescent cells nor the fluorescent mean in neither of the two cell lines treated with the micropinocytosis inhibitor EIPA (33 μ M) (Fig. 3). These results indicate that both the clathrin-mediated endocytosis and the caveolin-mediated endocytosis are involved in DOPY/PPRH complexes internalization. Fluorescence microscopy cell images are shown in Figure S4.

3.3. Cell viability assays

Previous work in our laboratory demonstrated that the inhibition of the antiapoptotic gene *survivin* using PPRHs led to a decrease in prostate cancer cell survival both *in vitro* and *in vivo* [33,35]. Therefore, we used PC-3 cells as a positive control since we had evidence of the effectiveness of transfecting the HpsPr-C PPRH using DOTAP in this type of cells [35]. In this work, we searched for a non-toxic amount of DOPY for each cell line. The optimum concentration in PC-3 cells was ranging from 0.52–1.05 μ M (Fig. 4A), whereas SH-SY5Y cells could be incubated with higher doses of DOPY (1.05–2.1 μ M) (Fig. 4B). Then, 100 nM of HpsPr-C PPRH was transfected using either DOTAP or DOPY to compare the effect on cell viability caused by the PPRH. PC-3 cells transfected with DOTAP/HpsPr-C complexes showed a decrease in cell viability of 90% (Fig. 4A). Similarly, cells transfected using 0.52 μ M and 1.05 μ M of DOPY showed a reduction in cell viability of 97% and 99%, respectively (Fig. 4A).

However, in the case of SH-SY5Y cells, incubations with DOTAP/HpsPr-C complexes at standard conditions did not reduce cell viability, whereas cells treated with DOPY/HpsPr-C complexes showed a decrease in cell viability of 36% and 84% using 1.05 μ M and 2.1 μ M of DOPY, respectively (Fig. 4B). Transfections with the negative control hairpin (HpWC) did not produce any effect on cell viability in PC-3 and SH-SY5Y cells (Fig. 4A and B).

3.4. Survivin protein analyses

To confirm that the detrimental effect on cell viability was caused by a specific decrease of *survivin* expression triggered by 100 nM of HpsPr-C PPRH, we analyzed survivin protein levels in both PC-3 and SH-SY5Y cells. After 24 h of incubation, PC-3 cells transfected using either DOTAP (10 μ M) or DOPY (1.05 μ M) presented a 75% reduction on survivin protein levels (Fig. 5A). In contrast, SH-SY5Y cells transfected with DOTAP (10 μ M) did not show a significant decrease in protein expression (Fig. 5B), while cells transfected using DOPY (2.1 μ M) showed a decrease of 85% on survivin protein levels.

3.5. Transfection efficiency for gene repair

One of the goals of this work was to demonstrate the versatility of transfection of DOPY. For that reason, we also used DOPY for gene correction applications. In this regard, repair-PPRHs were delivered into the DF42 CHO mutant cell line to correct a point mutation in the endogenous locus of the *dhfr* gene. The HpE6rep-L repair-PPRH was designed to correct the c.541 G > T mutation in this gene (Table 1). HpE6rep-L consisted in (i) a 23 nt polypurine core complementary to its polypyrimidine target sequence located 9 nt downstream from the mutation, and (ii) a 45 nt repair domain homologous to the mutation region but containing the desired nucleotide (G) instead of the mutation (T).

First, the delivery of PPRHs into DF42 cells was assessed by fluorescence microscopy (Fig. 6A) and flow cytometry (Fig. 6B and C) using

Results

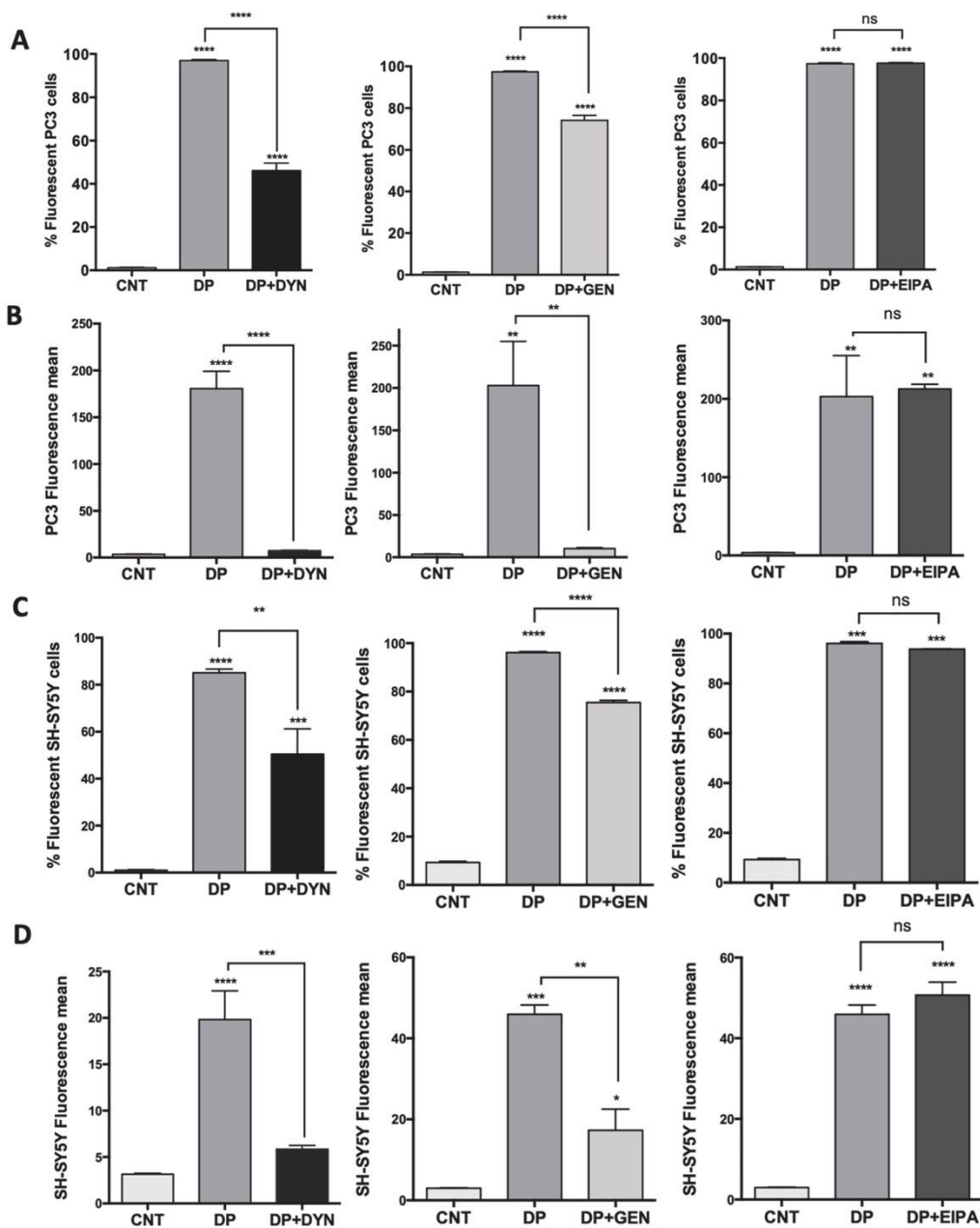


Fig. 3. Study of the endocytic pathways involved in DOPY/PPRH complexes internalization. PC-3 and SH-SY5Y cells were incubated for 1 h with 75 μ M of Dynasore, 185 μ M Genistein, or 33 μ M EIPA and subsequently transfected with 100 nM of the FAM-HpsPr-C PPRH using 2.1 μ M of DOPY. After 4 h of incubation, the percentage of fluorescent cells (A and C) and the mean fluorescence (B and D) for each cell line were determined by flow cytometry. Error bars represent the standard error of the mean of three experiments. Statistical significance was calculated using one-way ANOVA with Tukey's multiple comparisons test for the percentage fluorescent cells and the mean fluorescence (* $p < 0.05$, ** $p < 0.01$, *** $p < 0.001$, **** $p < 0.0001$). Abbreviations: CNT, control; DP, DOPY; DYN, Dynasore; GEN, Genistein; EIPA, 5-(*N*-ethyl-*N*-isopropyl)amiloride; ns, not statistically significant.

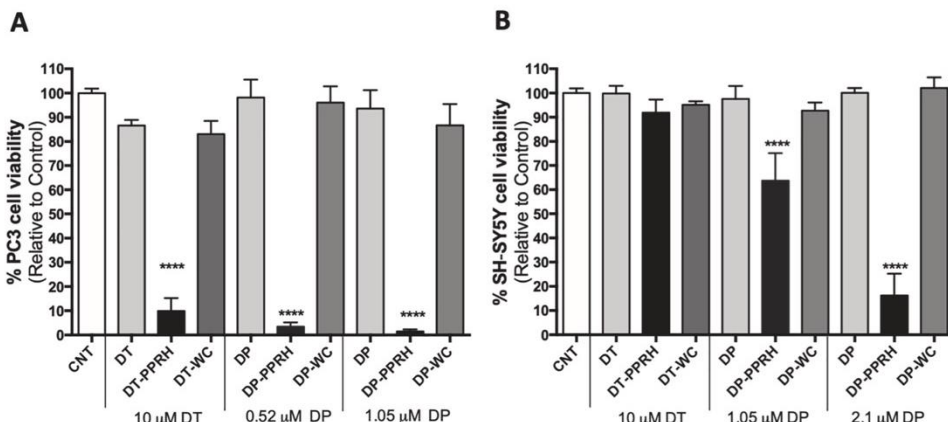


Fig. 4. Effect of HpsPr-C on cell viability in PC-3 and SH-SY5Y cells. Effect on cell viability in PC-3 (A) and SH-SY5Y (B) upon transfection of 100 nM the HpsPr-C PPRH or the negative control hairpin (HpwC) using DOTAP (DT) or DOPY (DP). The concentrations for each transfection agent are indicated in the figure. Error bars represent the standard error of the mean of three experiments. Statistical significance was calculated using one-way ANOVA with Dunnett’s multiple comparisons test (**** $p < 0.0001$).

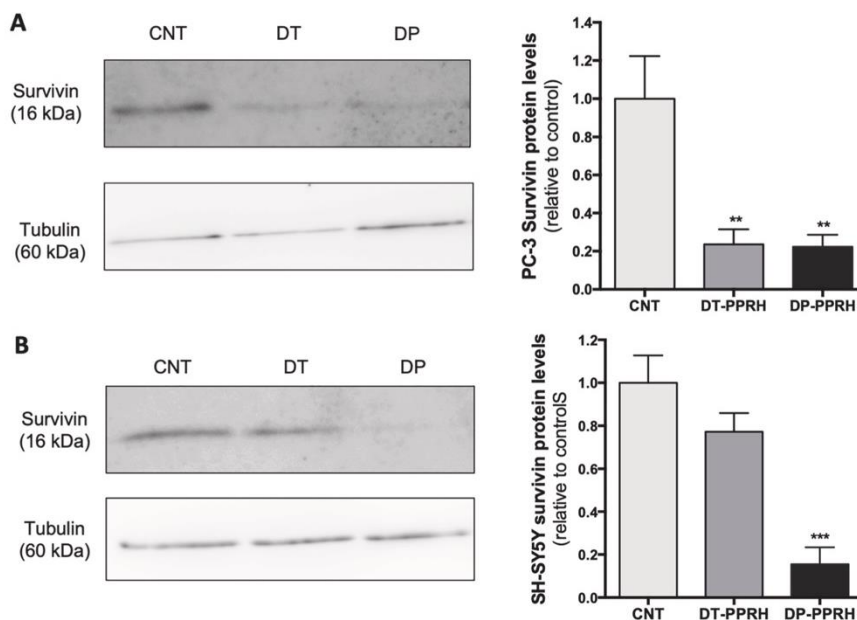


Fig. 5. Comparison of the effect of HpsPr-C on survivin protein levels using either DOTAP or DOPY as transfection agent. PC-3 (A) and SH-SY5Y (B) cells were transfected with 100 nM of the HpsPr-C PPRH using either DOTAP (10 μM) or DOPY (1.05 μM for PC-3 cells and 2.1 μM for SH-SY5Y cells) and incubated for 24 h. Representative images of Western blots (left) and quantification of survivin protein levels relative to the control (right) are shown. Tubulin protein levels were used to normalize the results. Error bars represent the standard error of the mean of three experiments. Statistical significance was calculated using one-way ANOVA with Dunnett’s multiple comparisons test (** $p < 0.01$, *** $p < 0.001$). Abbreviations: CNT, control; DT, DOTAP; DP, DOPY.

FAM-HpsPr-C PPRH. The efficiency of transfection of DOPY in DF42 cells was compared to that of calcium phosphate or DOTAP, since both methodologies are standardly used in our laboratory for the delivery of repair-PPRHs. Both DOTAP and DOPY transfections were able to deliver PPRHs to more than 80% of the total cell population, whereas calcium phosphate transfections only achieved 50% of transfection efficiency (Fig. 6B). However, mean fluorescence values showed that the highest

internalization was obtained using DOPY (Fig. 6C). It is worth noting that calcium phosphate transfections presented lower internalization values than those of DOPY, but higher than those of DOTAP (Fig. 6C). Fluorescence microscopy cell images acquired just before flow cytometer analyses were in accordance with the results described in this section (Fig. 6A).

Results

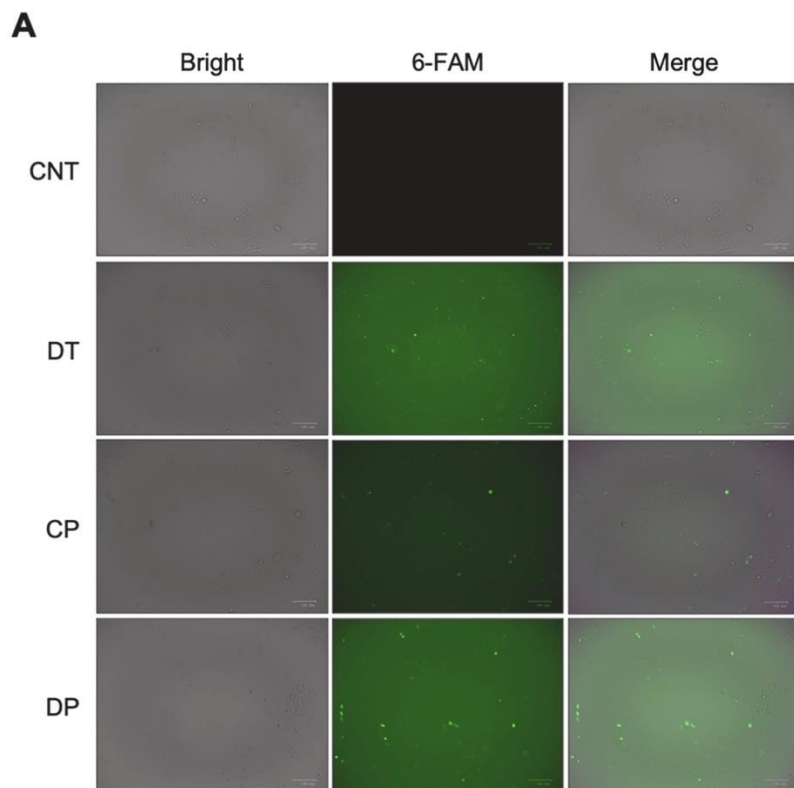
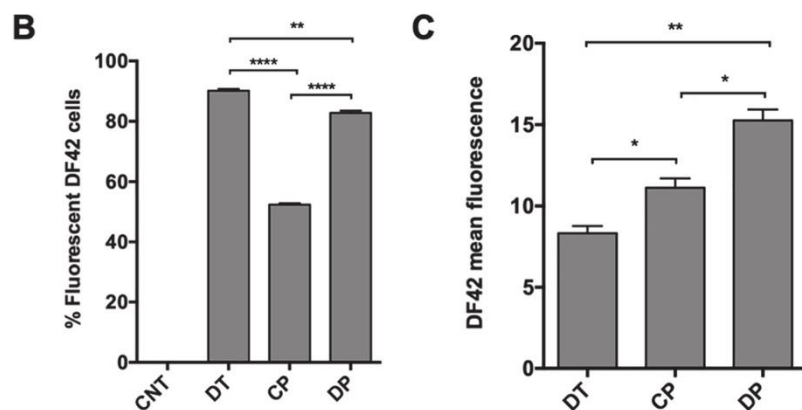


Fig. 6. Cellular uptake of PPRHs for gene repair applications. (A) DF42 cells were transfected with 10 μ g of FAM-HpsPr-C (112 nM) using DOTAP (2.6 μ M), calcium phosphate or DOPY (2.1 μ M) and visualized under a fluorescence microscope after 24 h of incubation. Then, cells were harvested and analyzed by flow cytometry to determine the (B) percentage of DF42 fluorescent cells and (C) the mean fluorescence. Error bars represent the standard error of the mean of three experiments. Statistical significance was calculated using Unpaired T test comparing the effect of the different transfection agents (* $p < 0.05$, ** $p < 0.01$, **** $p < 0.0001$). Abbreviations: CNT, control; DT, DOTAP; CP, calcium phosphate; DP, DOPY.



3.6. Gene correction frequency

After 48 h of incubation with repair-PPRHs, selective medium (-GHT) was applied during 14 days. At this point, cell colonies were stained and counted to determine gene repair frequencies for each transfection method. In these experimental conditions, no cell colonies were obtained when transfecting using DOTAP (Fig. 7A). However,

calcium phosphate transfections generated a 0.2% of corrected cells, while DOPY transfections led to repair frequencies of 0.4%, which represented a 2-fold increase compared to calcium phosphate frequencies (Fig. 7B).

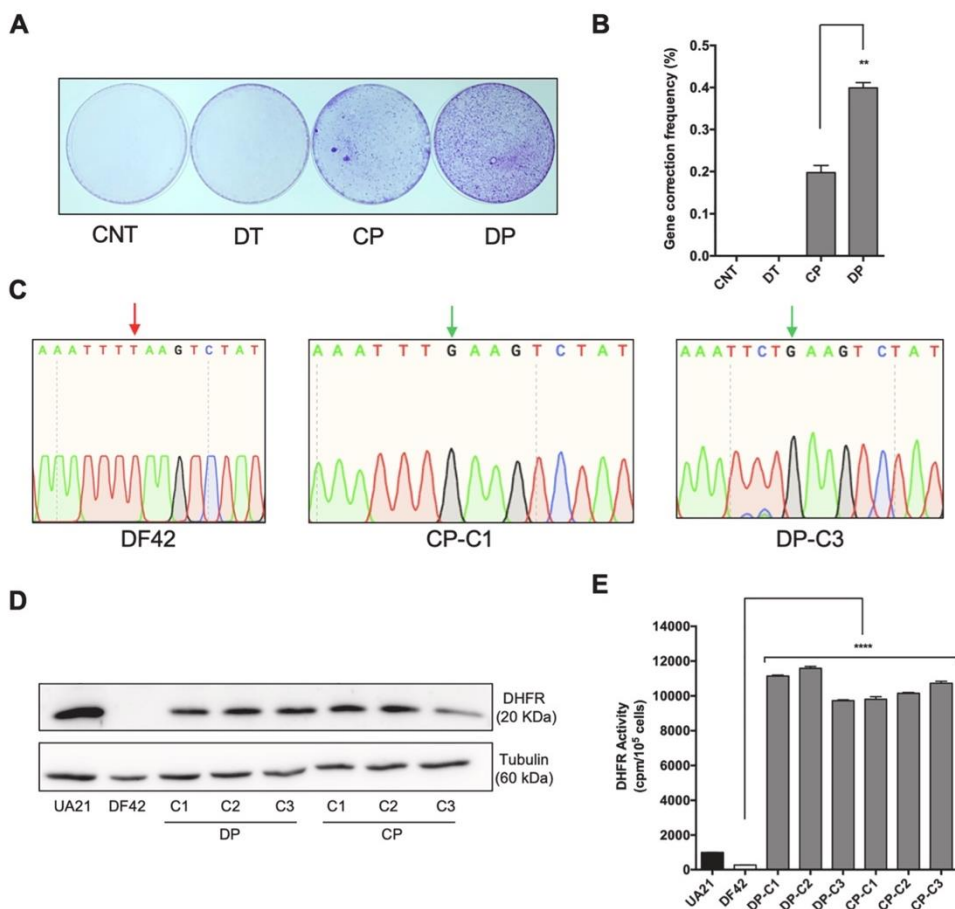


Fig. 7. Gene correction frequency and characterization of DF42 repaired clones. (A) Representative image of the number of DF42 repaired colonies obtained after transfection with 10 µg of the HpE6rep-L repair-PPRH (55 nM) using DOTAP (2.6 µM), calcium phosphate or DOPY (2.1 µM). After selection, surviving cell colonies were fixed and stained with crystal violet. (B) Gene correction frequency values were calculated as the ratio between the number of DF42 surviving colonies and the total number of cells initially plated. (C) DNA sequences from DF42 mutant and DF42 repaired cells after treatment with the HpE6rep-L repair-PPRH using calcium phosphate or DOPY are shown. Red and green arrows indicate the mutated and corrected nucleotide, respectively. (D) Western blotting of DHFR protein in DF42 mutant cells and DF42 repaired clones. Tubulin protein was used as endogenous control. (E) DHFR enzymatic activity was determined in DF42 mutant cells and DF42 repaired clones. UA21 parental cells were used as positive control. Error bars represent the standard error of the mean of three experiments. Statistical significance was calculated using Unpaired T test in (B) and ordinary one-way ANOVA in (E). (**p < 0.01, ****p < 0.0001). Abbreviations: CNT, control; DT, DOTAP; CP, calcium phosphate; DP, DOPY.

3.7. Characterization of dhfr repaired clones

After selection, a representative number of cell colonies from each transfection condition were expanded individually and analyzed at the DNA level to confirm the correction of the mutation. As shown in Fig. 7C, both calcium phosphate and DOPY transfections of the HpE6rep-L repair-PPRH were able to correct the c.541 G > T mutation at the genomic level in DF42 cells, thus restoring the wild-type sequence of the *dhfr* gene.

In addition, we corroborated that the restoration of the wild type *dhfr* sequence in the DNA of the repaired clones led to the production of DHFR protein. Western blot assays showed the presence of DHFR protein in all the analyzed clones derived from both calcium phosphate and DOPY transfections (Fig. 7D). DHFR protein was also present in the wild-type UA21 cell line, used as positive control (Fig. 7D).

Finally, we demonstrated the functionality of the DHFR protein by determining its enzymatic activity. All the repaired clones derived from both calcium phosphate and DOPY transfections showed a similar enzymatic activity, which represented a 50-fold increase compared to that of mutant DF42 cells (Fig. 7E).

4. Discussion

In this work, we describe DOPY as a new gemini cationic liposome-based formulation for PPRH delivery and evaluate its transfection efficiency for both gene silencing and gene repair applications. We chose PPRH delivery since these molecules represent an economical biotechnological tool with advantages compared to other therapeutic oligonucleotides [31,32]. PPRHs are more stable than siRNAs due to its clamp structure composed of deoxynucleotides instead of ribonucleotides [72].

Results

E. Aubets et al.

European Journal of Pharmaceutics and Biopharmaceutics 165 (2021) 279–292

Furthermore, PPRHs are effective at lower concentrations than ASOs [33] and they bind with higher affinity to the target dsDNA than Triplex-Forming Oligonucleotides (TFOs) [37]. In terms of safety, PPRHs have demonstrated their lack of immunogenicity [72], nephrotoxicity and hepatotoxicity *in vitro* [63]. Moreover, pharmacogenomic studies demonstrated the specificity of PPRHs and the absence of off-target effects [63].

It is known that cationic lipid-based delivery systems form electrostatic complexes with DNA. This condensation protects DNA from nuclease degradation and confers desirable physicochemical properties in terms of size and charge to facilitate DNA entry into cells [73]. In several chemical vectors, the positive charge is provided by a pyridinium salt [74–76]. Following this approach, in the present work we designed DOPY, a gemini amphiphilic bis-pyridinium salt connected through a 1,3-xylyl spacer and bearing hydrophobic oleyl moieties on the position 4 of the pyridinium rings, to study its ability as DNA carrier. In solution, these complexes have ca. 155 nm in diameter, as determined by DLS. Accordingly, gel retardation assays demonstrated that DOPY can form complexes with PPRHs, thus pairing their negative charges. Transmission Electron Microscopy experiments also corroborate this interaction and allows the visualization of the fibrillar structures of the PPRH molecules covered by DOPY.

To achieve the desired effect of PPRHs within the cell, a successful transfection requires their internalization into the cytoplasm and their transportation into the nucleus. Regarding PPRHs internalization, DOPY has demonstrated high delivery efficiencies in PC-3, SH-SY5Y and DF42 cells. Interestingly, the amount of PPRH internalized by DOPY complexes was higher than that of other chemical vehicles routinely used in our laboratory such as DOTAP or calcium phosphate. These higher values of internalization can explain the superior effects obtained in both gene silencing and gene repair approaches using PPRHs compared to that of other transfection agents. Additionally, the decrease in DOPY/PPRH cellular uptake after Dynasore or Genistein treatment in both PC-3 and SH-SY5Y cells suggests that the clathrin-mediated endocytosis and the caveolae-dependent endocytosis are involved in the internalization of PPRHs mediated by DOPY.

In gene silencing experiments, we targeted the antiapoptotic gene survivin, which has been correlated with different types of cancer such as prostate [77], breast [78], gastric [79,80], osteosarcoma [81] or neuroblastoma [82,83]. Since we faced difficulties in transfecting neuroblastoma SH-SY5Y cells with commercially available agents, we transfected the HpsPr-C PPRH directed against survivin in SH-SY5Y cells using DOPY. DOPY/HpsPr-C complexes successfully decreased survivin protein levels and cell viability in hard-to-transfect SH-SY5Y cells, even using nearly 4-fold less amount of DOPY than that of DOTAP. These results are in accordance with other studies showing the inhibition of SH-SY5Y cell proliferation due to an increase of apoptosis after suppressing survivin expression [84]. In contrast, the transfection of DOTAP/HpsPr-C complexes in SH-SY5Y cells did not reduce survivin protein levels nor cell viability, which corroborates the greater internalization capacity of DOPY. In the case of PC-3 cells, our previous studies transfecting HpsPr-C using DOTAP showed an effective delivery and survivin gene silencing [35]. In this work, we showed a great reduction on protein levels and cell viability using 7.75-fold less amount of DOPY than that of DOTAP. Therefore, DOPY/PPRH complexes are more effective in terms of inhibiting survivin expression and reducing cell viability in both SH-SY5Y and PC-3 cells.

In gene correction experiments, the HpE6rep-L repair-PPRH transfected using DOPY in DF42 mutant cells achieved higher correction frequencies than that of DOTAP or calcium phosphate transfection agents, which are the chemical vehicles routinely used in our laboratory for gene correction strategies [45,46]. The HpE6rep-L repair-PPRH was able to specifically correct the c.541 G > T mutation in the endogenous locus of the dhfr gene, thus restoring its wild-type sequence. In addition, we confirmed that DF42 corrected cells were able to produce a full DHFR protein with restored enzymatic activity, thus proving the effectivity of

DOPY as a transfection agent also in gene repair approaches.

Overall, the successful cellular uptake, the efficient survivin gene silencing and the correction of the dhfr gene are evidence that DOPY enables both an efficient entry and release of PPRHs at the intracellular level, thus allowing them to exert their action in the target dsDNA. Although further studies to demonstrate safety and efficacy of DOPY *in vitro* and *in vivo* should be performed, the results to date indicate that DOPY can be considered as a new gemini cationic lipid-based delivery vector suitable for the delivery of therapeutic oligonucleotides.

Declaration of Competing Interest

The authors declare that they have no known competing financial interests or personal relationships that could have appeared to influence the work reported in this paper.

Acknowledgements

This research was funded by grant RTI2018-093901-B-I00 from MICINN (Spain), by EU ERDF (FEDER) funds and the Spanish Government grant TEC2017-85059-C3-2-R, and by *Ajut a la Recerca Transversal 2018* from IN2UB, and the Serra Hunter programme (RG). Groups holding the Quality Mention from Generalitat de Catalunya 2017-SGR-94 and 2017-SGR-1277. AJF and EA are awarded with fellowships from Ministerio de Educación (FPU) and Generalitat de Catalunya (FI), respectively, and CS and CM obtained fellowships from the Erasmus program.

Appendix A. Supplementary data

Supplementary data to this article can be found online at <https://doi.org/10.1016/j.ejpb.2021.05.016>.

References

- [1] M.H. Amer, Gene therapy for cancer: present status and future perspective, *Mol. Cell. Ther.* 2 (2014) 27, <https://doi.org/10.1186/2052-8426-2-27>.
- [2] S.M. Parsel, J.R. Grandis, S.M. Thomas, Nucleic acid targeting: Towards personalized therapy for head and neck cancer, *Oncogene*. 35 (2016) 3217–3226, <https://doi.org/10.1038/onc.2015.424>.
- [3] T.T. Nielsen, J.E. Nielsen, Antisense gene silencing: Therapy for neurodegenerative disorders? *Genes (Basel)*. 4 (2013) 457–484, <https://doi.org/10.3390/genes4030457>.
- [4] E.A. Burton, J.C. Glorioso, D.J. Fink, Gene therapy progress and prospects: Parkinson's disease, *Gene Ther.* 10 (2003) 1721–1727, <https://doi.org/10.1038/sj.gt.3302116>.
- [5] J.M. Alisky, B.L. Davidson, Gene therapy for amyotrophic lateral sclerosis and other motor neuron diseases, *Hum. Gene Ther.* 11 (2000) 2315–2329, <https://doi.org/10.1089/104303400750038435>.
- [6] A.M. Winkelsas, K.H. Fischbeck, Nucleic acid therapeutics in neurodevelopmental disease, *Curr. Opin. Genet. Dev.* 65 (2020) 112–116, <https://doi.org/10.1016/j.gde.2020.05.022>.
- [7] E.G. Nabel, Gene therapy for cardiovascular diseases, *J. Nucl. Cardiol.* 6 (1999) 69–75, [https://doi.org/10.1016/S1071-3581\(99\)90066-1](https://doi.org/10.1016/S1071-3581(99)90066-1).
- [8] U. Landmesser, W. Poller, S. Tsimikas, P. Most, F. Paneni, T.F. Lü Scher, From traditional pharmacological towards nucleic acid-based therapies for cardiovascular diseases, *Eur. Heart J.* 41 (2020) 3884–3899, <https://doi.org/10.1093/eurheartj/ehaa229>.
- [9] C.E. Walsh, Gene therapy progress and prospects: Gene therapy for the hemophilias, *Gene Ther.* 10 (2003) 999–1003, <https://doi.org/10.1038/sj.gt.3302024>.
- [10] I. Hazan-Halevy, D. Landesman-Milo, D. Rosenblum, S. Mizrahy, B.D. Ng, D. Peer, Immunomodulation of hematological malignancies using oligonucleotides based-nanomaterials, *J. Control. Release*. 244 (2016) 149–156, <https://doi.org/10.1016/j.jconrel.2016.07.052>.
- [11] T.C. Roberts, R. Langer, M.J.A. Wood, Advances in oligonucleotide drug delivery, *Nat. Rev. Drug Discov.* 19 (2020) 673–694, <https://doi.org/10.1038/s41573-020-0075-7>.
- [12] FDA News Release, FDA grants accelerated approval to first targeted treatment for rare Duchenne muscular dystrophy mutation | FDA, FDA. (2019). <https://www.fda.gov/news-events/press-announcements/fda-grants-accelerated-approval-first-targeted-treatment-rare-duchenne-muscular-dystrophy-mutation> (accessed January 18, 2021).
- [13] IONIS press release, Akcea and Ionis Receive FDA Approval of TEGSEDTM (inotersen) for the Treatment of the Polyneuropathy of Hereditary Transthyretin-

- Mediated Amyloidosis in Adults | Ionis Pharmaceuticals, Inc., IONIS. (2018). <https://ir.ionispharma.com/news-releases/news-release-details/akcea-and-ionis-receive-fda-approval-tesgeditm-intotersen> (accessed January 18, 2021).
- [14] FDA News Release, FDA approves first drug for spinal muscular atrophy | FDA, FDA. (2016). <https://www.fda.gov/news-events/press-announcements/fda-approves-first-drug-spinal-muscular-atrophy> (accessed January 18, 2021).
- [15] FDA News Release, FDA grants accelerated approval to first drug for Duchenne muscular dystrophy | FDA, FDA. (2016). <https://www.fda.gov/news-events/press-announcements/fda-grants-accelerated-approval-first-drug-duchenne-muscular-dystrophy> (accessed January 18, 2021).
- [16] FDA News Release, FDA approves first treatment for rare disease in patients who receive stem cell transplant from blood or bone marrow, FDA. (2016). <https://www.fda.gov/NewsEvents/Newsroom/PressAnnouncements/ucm493225.htm> (accessed January 18, 2021).
- [17] P. Hair, F. Cameron, K. McKeage, Mipomersen sodium: First global approval, *Drugs*. 73 (2013) 487–493, <https://doi.org/10.1007/s40265-013-0042-2>.
- [18] L. Hightleyman, FDA approves fomivirsen, famciclovir, and Thalidomide. Food and Drug Administration - PubMed, BETA. (1998). <https://pubmed.ncbi.nlm.nih.gov/11365993/> (accessed January 18, 2021).
- [19] D. Adams, A. Gonzalez-Duarte, W.D. O'Riordan, C.C. Yang, M. Ueda, A.V. Kristen, I. Tourneir, H.H. Schmidt, T. Coelho, J.L. Berk, K.P. Lin, G. Vita, S. Attarian, V. Planté-Bordenave, M.M. Mezei, J.M. Campistol, J. Buades, T.H. Brannagan, B. J. Kim, J. Oh, Y. Parman, Y. Sekijima, P.N. Hawkins, S.D. Solomon, M. Polydefkis, P.J. Dyck, P.J. Gandhi, S. Goyal, J. Chen, A.L. Strahs, S.V. Nocher, M.T. Sweetser, P.P. Garg, A.K. Vaishnav, J.A. Gollob, O.B. Suhr, Patisiran, an RNAi therapeutic, for hereditary transthyretin amyloidosis, *N. Engl. J. Med.* 379 (2018) 11–21, <https://doi.org/10.1056/NEJMoa1716153>.
- [20] L.J. Scott, Givosiran: First Approval, *Drugs*. 80 (2020) 335–339, <https://doi.org/10.1007/s40265-020-01269-0>.
- [21] FDA News Release, FDA Approves First Drug to Treat Rare Metabolic Disorder | FDA, FDA. (2020). <https://www.fda.gov/news-events/press-announcements/fda-approves-first-drug-treat-rare-metabolic-disorder> (accessed December 9, 2020).
- [22] S.A. Doggrell, Pegaptanib: The first antiangiogenic agent approved for neovascular macular degeneration, *Expert Opin. Pharmacother.* 6 (2005) 1421–1423, <https://doi.org/10.1517/14656566.6.8.1421>.
- [23] FDA News Release, Pfizer-BioNTech COVID-19 Vaccine | FDA, FDA. (2020). <https://www.fda.gov/emergency-preparedness-and-response/coronavirus-disease-2019-covid-19/pfizer-biontech-covid-19-vaccine> (accessed January 7, 2021).
- [24] FDA News Release, Moderna COVID-19 Vaccine | FDA, FDA. (2020). <https://www.fda.gov/emergency-preparedness-and-response/coronavirus-disease-2019-covid-19/moderna-covid-19-vaccine> (accessed January 7, 2021).
- [25] N. Nayerossadat, P. Ali, T. Maedeh, Viral and nonviral delivery systems for gene delivery, *Adv. Biomed. Res.* 1 (2012) 27, <https://doi.org/10.4103/2277-9175.98152>.
- [26] N. Slade, Viral vectors in gene therapy, *Period. Biol.* 103 (2001) 139–143, <https://doi.org/10.3390/diseases6020042>.
- [27] M. Alsaggar, D. Liu, Physical Methods for Gene Transfer, *Adv. Genet.* 89 (2015) 1–24, <https://doi.org/10.1016/b978-0-12-410011-0.001>.
- [28] D.W. Pack, A.S. Hoffman, S. Pun, P.S. Stayton, Design and development of polymers for gene delivery, *Nat. Rev. Drug Discov.* 4 (2005) 581–593, <https://doi.org/10.1038/nrd1775>.
- [29] M.C. Filion, N.C. Phillips, Major limitations in the use of cationic liposomes for DNA delivery, *Int. J. Pharm.* 162 (1998) 159–170, [https://doi.org/10.1016/s0378-5173\(97\)00423-7](https://doi.org/10.1016/s0378-5173(97)00423-7).
- [30] B.L. Florea, C. Meaney, H.E. Junginger, G. Borchard, Transfection efficiency and toxicity of polyethylenimine in differentiated Calu-3 and nondifferentiated COS-1 cell cultures, *AAPS PharmSci.* 4 (2002) 1, <https://doi.org/10.1208/ps040312>.
- [31] C.J. Ciudad, L. Rodríguez, X. Villalobos, A.J. Félix, V. Noé, PolyPurine Reverse Hoogsteen Hairpins as a Gene Silencing Tool for Cancer, *Curr. Med. Chem.* 24 (2017), <https://doi.org/10.2174/0929867324666170301114127>.
- [32] V. Noé, E. Aubets, A.J. Félix, C.J. Ciudad, Nucleic acids therapeutics using PolyPurine Reverse Hoogsteen hairpins, *Biochem. Pharmacol.* (2020) 114371, <https://doi.org/10.1016/j.bcp.2020.114371>.
- [33] M.C. de Almagro, S. Coma, V. Noé, C.J. Ciudad, PolyPurine hairpins directed against the template strand of DNA knock down the expression of mammalian genes, *J. Biol. Chem.* 284 (2009) 11579–11589, <https://doi.org/10.1074/jbc.M900981200>.
- [34] M.C. De Almagro, N. Mencia, V. Noé, C.J. Ciudad, Coding polyPurine hairpins cause target-induced cell death in breast cancer cells, *Hum. Gene Ther.* 22 (2011) 451–463, <https://doi.org/10.1089/hum.2010.102>.
- [35] L. Rodríguez, X. Villalobos, S. Dakhel, L. Padilla, R. Hervas, J.L. Hernández, C. J. Ciudad, V. Noé, PolyPurine reverse Hoogsteen hairpins as a gene therapy tool against survivin in human prostate cancer PC3 cells in vitro and in vivo, *Biochem. Pharmacol.* 86 (2013) 1541–1554, <https://doi.org/10.1016/j.bcp.2013.09.013>.
- [36] X. Villalobos, L. Rodríguez, A. Solé, C. Lliberós, N. Mencia, C.J. Ciudad, V. Noé, Effect of polyPurine reverse Hoogsteen hairpins on relevant cancer target genes in different human cell lines, *Nucleic Acid Ther.* 25 (2015) 198–208, <https://doi.org/10.1089/nat.2015.0531>.
- [37] L. Rodríguez, X. Villalobos, A. Solé, C. Lliberós, C.J. Ciudad, V. Noé, Improved design of PPRHs for gene silencing, *Mol. Pharm.* 11 (2015) 867–877, <https://doi.org/10.1021/mp5007008>.
- [38] G. Bener, A.J. Félix, C. Sánchez de Diego, I. Pascual Fabregat, C.J. Ciudad, V. Noé, Silencing of CD47 and SIRP α by PolyPurine reverse Hoogsteen hairpins to promote MCF-7 breast cancer cells death by PMA-differentiated THP-1 cells, *BMC Immunol.* 17 (2016) 1–12, <https://doi.org/10.1186/s12865-016-0170-z>.
- [39] M.M.M. Enriquez, A.J. Félix, C.J. Ciudad, V. Noé, Cancer immunotherapy using PolyPurine Reverse Hoogsteen hairpins targeting the PD-1/PD-L1 pathway in human tumor cells, *PLoS One*. 13 (2018), <https://doi.org/10.1371/journal.pone.0206818>.
- [40] C.J. Ciudad, M.M.M. Enriquez, A.J. Félix, G. Bener, V. Noé, Silencing PD-1 and PD-L1: The potential of PolyPurine Reverse Hoogsteen hairpins for the elimination of tumor cells, *Immunotherapy*. 11 (2019) 369–372, <https://doi.org/10.2217/imt-2018-0215>.
- [41] E. Aubets, V. Noé, C.J. Ciudad, Targeting replication stress response using polyPurine reverse Hoogsteen hairpins directed against WEE1 and CHK1 genes in human cancer cells, *Biochem. Pharmacol.* 175 (2020), <https://doi.org/10.1016/j.bcp.2020.113911>.
- [42] E. Aubets, A.J. Félix, M. Garavís, L. Reyes, A. Avinó, R. Eritja, C.J. Ciudad, V. Noé, Detection of a g-quadruplex as a regulatory element in thymidylate synthase for gene silencing using polyPurine reverse Hoogsteen hairpins, *Int. J. Mol. Sci.* 21 (2020) 1–22, <https://doi.org/10.3390/ijms21145028>.
- [43] A. Solé, X. Villalobos, C.J. Ciudad, V. Noé, Repair of single-point mutations by polyPurine reverse Hoogsteen hairpins, *Hum. Gene Ther. Methods*. 25 (2014) 288–302, <https://doi.org/10.1089/hgtb.2014.049>.
- [44] A.J. Félix, A. Solé, V. Noé, C.J. Ciudad, Gene Correction of Point Mutations Using PolyPurine Reverse Hoogsteen Hairpins Technology, *Front. Genome Ed.* 2 (2020), 583577, <https://doi.org/10.3389/fgene.2020.583577>.
- [45] A. Solé, C.J. Ciudad, L.A. Chasin, V. Noé, Correction of point mutations at the endogenous locus of the dihydrofolate reductase gene using repair-PolyPurine Reverse Hoogsteen hairpins in mammalian cells, *Biochem. Pharmacol.* 110–111 (2016) 16–24, <https://doi.org/10.1016/j.bcp.2016.04.002>.
- [46] A.J. Félix, C.J. Ciudad, V. Noé, Correction of the apt Gene Using Repair-PolyPurine Reverse Hoogsteen Hairpins in Mammalian Cells, *Mol. Ther. - Nucleic Acids*. 19 (2020) 683–695, <https://doi.org/10.1016/j.omtn.2019.12.015>.
- [47] S. Falsini, S. Ristori, Lipoplexes from non-viral cationic vectors: DOTAP-DOPE liposomes and gemini micelles, in: *Methods Mol. Biol.*, Humana Press Inc., 2016, pp. 33–43, https://doi.org/10.1007/978-1-4939-3718-9_3.
- [48] R. Leventis, J.R. Silvius, Interactions of mammalian cells with lipid dispersions containing novel metabolizable cationic amphiphiles, *BBA - Biomembr.* (1990), [https://doi.org/10.1016/0005-2736\(90\)90017-1](https://doi.org/10.1016/0005-2736(90)90017-1).
- [49] C. Sporer, L. Casal, D. Caballero, J. Samitier, A. Errachid, L. Pérez-García, Novel anionophores for biosensor applications: nano characterisation of SAMS based on amphiphilic imidazolium protophanes and cyclophanes on gold surfaces, *Sens. Lett.* 7 (2009) 757–764, <https://doi.org/10.1166/sl.2009.1144>.
- [50] M.E. Alca-Reyes, A. González, A.C. Calpena, D. Ramos-López, J. de Lapuente, L. Pérez-García, Gemini pyridinium amphiphiles for the synthesis and stabilization of gold nanoparticles for drug delivery, *J. Colloid Interface Sci.* 502 (2017) 172–183, <https://doi.org/10.1016/j.jcis.2017.04.064>.
- [51] S. Giraldo, M.E. Alca-Reyes, D. Limón, A. González, M. Duch, J.A. Plaza, D. Ramos-López, J. de Lapuente, A. González-Campo, L. Pérez-García, π -Donor/ π -Acceptor interactions for the encapsulation of neurotransmitters on functionalized polysilicon-based microparticles, *Pharmaceutics*. 12 (2020) 1–19, <https://doi.org/10.3390/pharmaceutics12080724>.
- [52] L. Casal-Dujat, O. Penon, C. Rodríguez-Abreu, C. Solans, L. Pérez-García, Macrocytic ionic liquid crystals, *New J. Chem.* 36 (2012) 558–561, <https://doi.org/10.1039/c2nj20934a>.
- [53] L. Casal-Dujat, P.C. Griffiths, C. Rodríguez-Abreu, C. Solans, S. Rogers, L. Pérez-García, Nanocarriers from dicationic bis-imidazolium amphiphiles and their interaction with anionic drugs, *J. Mater. Chem. B*. 1 (2013) 4963–4971, <https://doi.org/10.1039/c3tb20289e>.
- [54] L. Casal-Dujat, M. Rodrigues, A. Yagüe, A.C. Calpena, D.B. Amabilino, J. González-Linares, M. Borrás, L. Pérez-García, Gemini imidazolium amphiphiles for the synthesis, stabilization, and drug delivery from gold nanoparticles, *Langmuir*. 28 (2012) 2368–2381, <https://doi.org/10.1021/la203601n>.
- [55] M. Rodrigues, A.C. Calpena, D.B. Amabilino, D. Ramos-López, J. de Lapuente, L. Pérez-García, Water-soluble gold nanoparticles based on imidazolium gemini amphiphiles incorporating piroxicam, *RSC Adv.* 4 (2014) 9279–9287, <https://doi.org/10.1039/c3ra44578j>.
- [56] M. Samperi, L. Pérez-García, D.B. Amabilino, Quantification of energy of activation to supramolecular nanofiber formation reveals enthalpic and entropic effects and morphological consequence, *Chem. Sci.* 10 (2019) 10256–10266, <https://doi.org/10.1039/c9sc03280k>.
- [57] M. Rodrigues, A.C. Calpena, D.B. Amabilino, M.L. Garduño-Ramírez, L. Pérez-García, Supramolecular gels based on a gemini imidazolium amphiphile as molecular material for drug delivery, *J. Mater. Chem. B*. 2 (2014) 5419–5429, <https://doi.org/10.1039/c4tb00450g>.
- [58] D. Limón, C. Jiménez-Newman, A.C. Calpena, A. González-Campo, D.B. Amabilino, L. Pérez-García, Microscale coiling in bis-imidazolium supramolecular hydrogel fibres induced by the release of a cationic serine protease inhibitor, *Chem. Commun.* 53 (2017) 4509–4512, <https://doi.org/10.1039/c6cc09392b>.
- [59] N.J. Starr, K. Abdul Hamid, J. Wibawa, I. Marlow, M. Bell, L. Pérez-García, D. A. Barrett, D.J. Scurr, Enhanced vitamin C skin permeation from supramolecular hydrogels, illustrated using in situ ToF-SIMS 3D chemical profiling, *Int. J. Pharm.* 563 (2019) 21–29, <https://doi.org/10.1016/j.ijpharm.2019.03.028>.
- [60] M.E. Alca-Reyes, J. Soriano, I. Mora-Espí, M. Rodrigues, D.A. Russell, L. Barrios, L. Pérez-García, Amphiphilic gemini pyridinium-mediated incorporation of Zn(II) meso-tetrakis(4-carboxyphenyl)porphyrin into water-soluble gold nanoparticles for photodynamic therapy, *Colloids Surfaces B Biointerfaces*. 158 (2017) 602–609, <https://doi.org/10.1016/j.colsurfb.2017.07.033>.
- [61] M. Samperi, D. Limón, D.B. Amabilino, L. Pérez-García, Enhancing Singlet Oxygen Generation by Self-Assembly of a Porphyrin Entrapped in Supramolecular Fibers,

Results

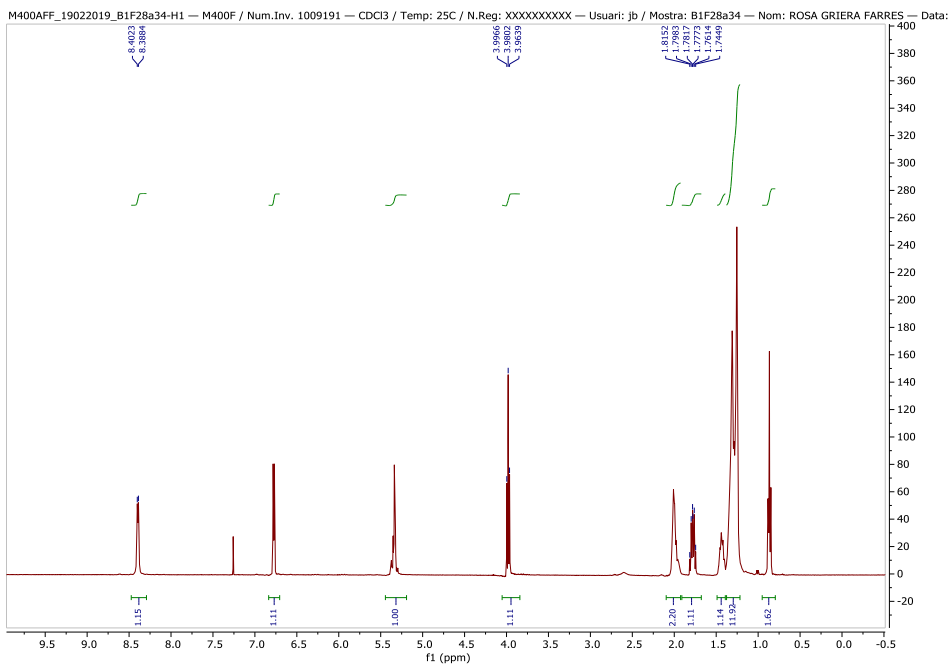
E. Aubets et al.

European Journal of Pharmaceutics and Biopharmaceutics 165 (2021) 279–292

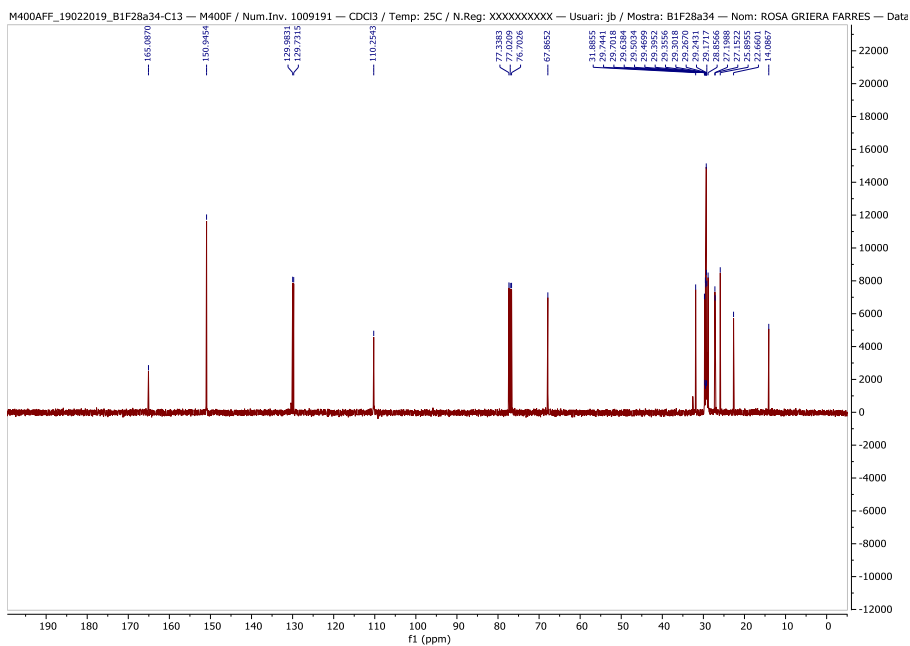
- Cell Reports Phys. Sci. 1 (2020), 100030, <https://doi.org/10.1016/j.xcrp.2020.100030>.
- [62] O. Penon, M.J. Marín, D.A. Russell, L. Pérez-García, Water soluble, multifunctional antibody-porphyrin gold nanoparticles for targeted photodynamic therapy, *J. Colloid Interface Sci.* 496 (2017) 100–110, <https://doi.org/10.1016/j.jcis.2017.02.006>.
- [63] A.J. Félix, C.J. Ciudad, V. Noé, Functional pharmacogenomics and toxicity of PolyPurine Reverse Hoogsteen hairpins directed against survivin in human cells, *Biochem. Pharmacol.* 155 (2018) 8–20, <https://doi.org/10.1016/j.bcp.2018.06.020>.
- [64] S.S. Gaddis, Q. Wu, H.D. Thames, J. Digiovanni, E.F. Walborg, M.C. Macleod, K. M. Vasquez, A web-based search engine for triplex-forming oligonucleotide target sequences, *Oligonucleotides*. 16 (2006) 196–201, <https://doi.org/10.1089/oli.2006.16.196>.
- [65] A.M. Carothers, G. Urlaub, R.W. Steigerwalt, L.A. Chasin, D. Grunberger, Characterization of mutations induced by 2-(N-acetoxy-N-acetyl)aminofluorene in the dihydrofolate reductase gene of cultured hamster cells, *Proc. Natl. Acad. Sci. USA* 83 (1986) 6519–6523, <https://doi.org/10.1073/pnas.83.17.6519>.
- [66] G. Urlaub, E. Käs, A.M. Carothers, L.A. Chasin, Deletion of the diploid dihydrofolate reductase locus from cultured mammalian cells, *Cell*. 33 (1983) 405–412, [https://doi.org/10.1016/0092-8674\(83\)90422-1](https://doi.org/10.1016/0092-8674(83)90422-1).
- [67] M. Wigler, A. Pellicer, S. Silverstein, R. Axel, G. Urlaub, L. Chasin, DNA-mediated transfer of the adenine phosphoribosyltransferase locus into mammalian cells, *Proc. Natl. Acad. Sci. USA* 76 (1979) 1373–1376, <https://doi.org/10.1073/pnas.76.3.1373>.
- [68] E. Macia, M. Ehrlich, R. Massol, E. Boucrot, C. Brunner, T. Kirchhausen, Dynasore, a Cell-Permeable Inhibitor of Dynamins, *Dev. Cell*. 10 (2006) 839–850, <https://doi.org/10.1016/j.devcel.2006.04.002>.
- [69] D. Vercauteren, R.E. Vandenbroucke, A.T. Jones, J. Rejman, J. Demeester, S.C. De Smedt, N.N. Sanders, K. Braeckmans, The use of inhibitors to study endocytic pathways of gene carriers: Optimization and pitfalls, *Mol. Ther.* 18 (2010) 561–569, <https://doi.org/10.1038/mt.2009.281>.
- [70] H.-P. Lin, B. Singla, P. Ghoshal, J.L. Faulkner, M. Cherian-Shaw, P.M. O'Connor, J.-X. She, E.J. Belin de Chantemele, G. Csányi, Identification of novel macropinocytosis inhibitors using a rational screen of Food and Drug Administration-approved drugs, *Br. J. Pharmacol.* 175 (2018) 3640–3655, <https://doi.org/10.1111/bph.14429>.
- [71] C.J. Ciudad, G. Urlaub, L.A. Chasin, Deletion analysis of the Chinese hamster dihydrofolate reductase gene promoter, *J. Biol. Chem.* 263 (1988) 16274–16282, <http://www.jbc.org/content/263/31/16274.short>.
- [72] X. Villalobos, L. Rodríguez, J. Prévot, C. Oleaga, C.J. Ciudad, V. Noé, Stability and Immunogenicity Properties of the Gene-Silencing Polypurine Reverse Hoogsteen Hairpins, *Mol. Pharm.* 11 (2014) 254–264, <https://doi.org/10.1021/mp400431f>.
- [73] C. Pichon, L. Billiet, P. Midoux, Chemical vectors for gene delivery: uptake and intracellular trafficking, *Curr. Opin. Biotechnol.* 21 (2010) 640–645, <https://doi.org/10.1016/j.copbio.2010.07.003>.
- [74] P. Dubrue, B. Christiaens, B. Vanloo, K. Bracke, M. Rosseneu, J. Vandekerckhove, E. Schacht, Physicochemical and biological evaluation of cationic polymethacrylates as vectors for gene delivery, *Eur. J. Pharm. Sci.* 18 (2003) 211–220, [https://doi.org/10.1016/S0928-0987\(02\)00280-4](https://doi.org/10.1016/S0928-0987(02)00280-4).
- [75] O. Petrichenko, M. Rucins, A. Vezane, I. Timofejeva, A. Sobolev, B. Cekavicus, K. Pajuste, M. Plotniece, M. Gosteva, T. Kozlovska, A. Plotniece, Studies of the physicochemical and structural properties of self-assembling cationic pyridine derivatives as gene delivery agents, *Chem. Phys. Lipids*. 191 (2015) 25–37, <https://doi.org/10.1016/j.chemphyslip.2015.08.005>.
- [76] K. Pajuste, Z. Hyvönen, O. Petrichenko, D. Kaldre, M. Rucins, B. Cekavicus, V. Ose, B. Skrivele, M. Gosteva, E. Morin-Picardat, M. Plotniece, A. Sobolev, G. Duburs, M. Ruponen, A. Plotniece, Gene delivery agents possessing antiradical activity: Self-assembling cationic amphiphilic 1,4-dihydropyridine derivatives, *New J. Chem.* 37 (2013) 3062–3075, <https://doi.org/10.1039/c3nj00272a>.
- [77] M. Zhang, J.J. Coen, Y. Suzuki, M.R. Siedow, A. Niemierko, L.Y. Khor, A. Pollack, Y. Zhang, A.L. Zietman, W.U. Shipley, A. Chakravarti, Survivin is a potential mediator of prostate cancer metastasis, *Int. J. Radiat. Oncol. Biol. Phys.* 78 (2010) 1095–1103, <https://doi.org/10.1016/j.ijrobp.2009.09.007>.
- [78] X. Cai, S. Ma, M. Gu, C. Zu, W. Qu, X. Zheng, Survivin regulates the expression of VEGF-C in lymphatic metastasis of breast cancer, *Diagn. Pathol.* 7 (2012) 52, <https://doi.org/10.1186/1746-1596-7-52>.
- [79] G.H. Lee, Y.E. Joo, Y.S. Koh, I.J. Chung, Y.K. Park, J.H. Lee, H.S. Kim, S.K. Choi, J. S. Rew, C.S. Park, S.J. Kim, Expression of survivin in gastric cancer and its relationship with tumor angiogenesis, *Eur. J. Gastroenterol. Hepatol.* 18 (2006) 957–963, <https://doi.org/10.1097/01.meg.0000230086.83792.5e>.
- [80] K. Miyachi, K. Sasaki, S. Onodera, T. Taguchi, M. Nagamachi, H. Kaneko, M. Sunagawa, Correlation between survivin mRNA expression and lymph node metastasis in gastric cancer, *Gastric Cancer*. 6 (2003) 217–224, <https://doi.org/10.1007/s10120-003-0255-2>.
- [81] L. Zhang, Y. Ye, D. Yang, J. Lin, Survivin and vascular endothelial growth factor are associated with spontaneous pulmonary metastasis of osteosarcoma: Development of an orthotopic mouse model, *Oncol. Lett.* 8 (2014) 2577–2580, <https://doi.org/10.3892/ol.2014.2556>.
- [82] T. Azuhata, D. Scott, S. Takamizawa, J. Wen, A. Davidoff, M. Fukuzawa, A. Sandler, The inhibitor of apoptosis protein survivin is associated with high-risk behavior of neuroblastoma, *J. Pediatr. Surg.* 36 (2001) 1785–1791, <https://doi.org/10.1053/jpsu.2001.28839>.
- [83] R. Ito, S. Asami, S. Motohashi, S. Ootsuka, Y. Yamaguchi, M. Chin, H. Shichino, Y. Yoshida, N. Nemoto, H. Mugishima, T. Suzuki, Significance of survivin mRNA expression in prognosis of neuroblastoma, *Biol. Pharm. Bull.* 28 (2005) 565–568, <https://doi.org/10.1248/bpb.28.565>.
- [84] H. Liang, L. Zhang, R. Xu, X.L. Ju, Silencing of survivin using YM155 induces apoptosis and chemosensitization in neuroblastomas cells, *Eur. Rev. Med. Pharmacol. Sci.* 17 (2013) 2909–2915 (accessed January 5, 2021), <https://www.europeanreview.org/article/5826>.

Supplementary

A

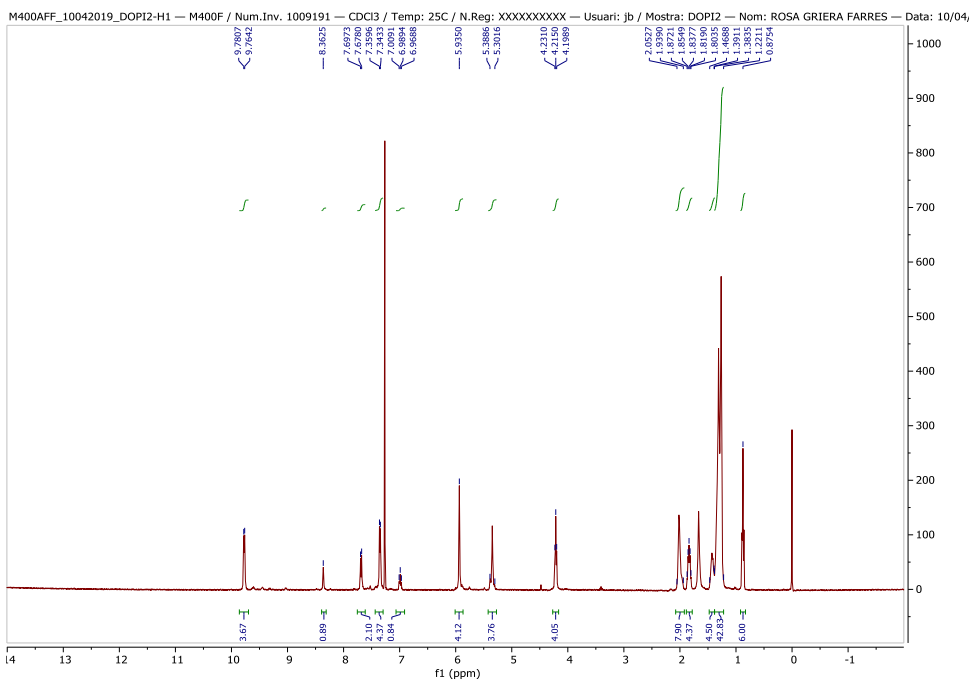


B

Figure S1. ¹H-NMR (A) and ¹³C NMR (B) spectra of 4-Oleyloxy pyridine.

Results

A



B

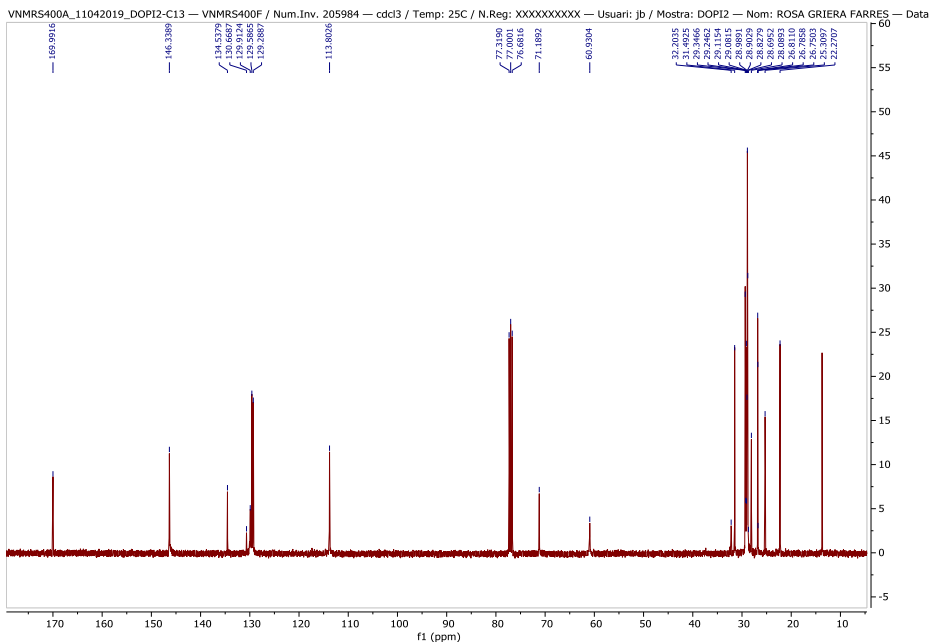
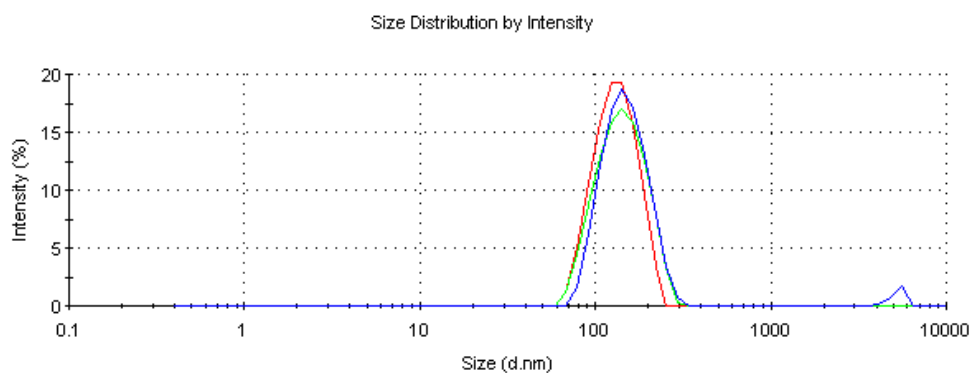


Figure S2. ^1H -NMR (A) and ^{13}C NMR (B) spectra of DOPIY.

A

	Diam. (nm)	% Intensity	Width (nm)
Z-Average (d.nm): 155,6	Peak 1: 151,4	97,6	43,23
Pdl: 0,249	Peak 2: 5299	2,4	402,6
Intercept: 0,849	Peak 3: 0,000	0,0	0,000



B

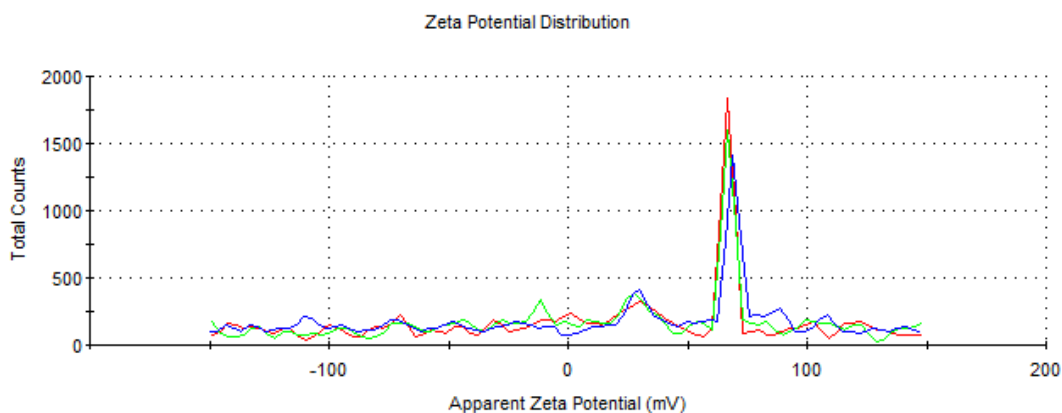


Figure S3. Hydrodynamic diameter analyzed using DLS (A) and Zeta Potential (B) of DOPY/PPRH complexes. Triplicate measures of DOPY/PPRH complexes 1:1.3 (w/w) in deionized water are indicated.

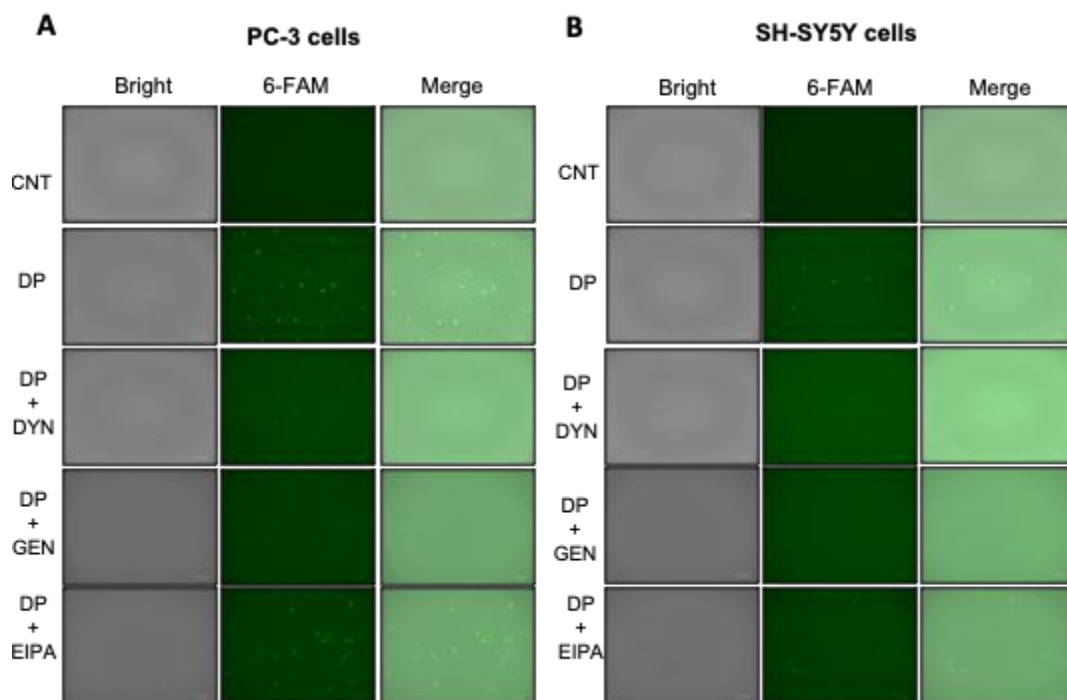


Figure S4. Fluorescence microscopy images of PC-3 (A) and SH-SY5Y (B) cells after the treatment with different endocytic pathways inhibitors. PC-3 and SH-SY5Y cells were incubated for 1h with 75 μ M of Dynasore, 185 μ M Genistein, or 33 μ M EIPA and subsequently transfected with 100 nM of the FAM-HpsPr-C PPRH using 2.1 μ M of DOPY. Fluorescence microscopy images were taken 4h after transfection. Abbreviations: CNT, control; DP, DOPY; DYN, Dynasore; GEN, Genistein; EIPA, 5-(*N*-ethyl-*N*-isopropyl)amiloride.

4.3.5. Additional results to Article III

Besides protein levels, we also analyzed the effect on *survivin* mRNA levels in PC-3 cells transfected with 100 nM HpsPr-C-WT using DOPY. Cells transfected with either DOPY or DOTAP showed a decrease on mRNA levels of around 50% (Figure 31). The negative control transfected with DOPY did not show a decrease on mRNA levels.

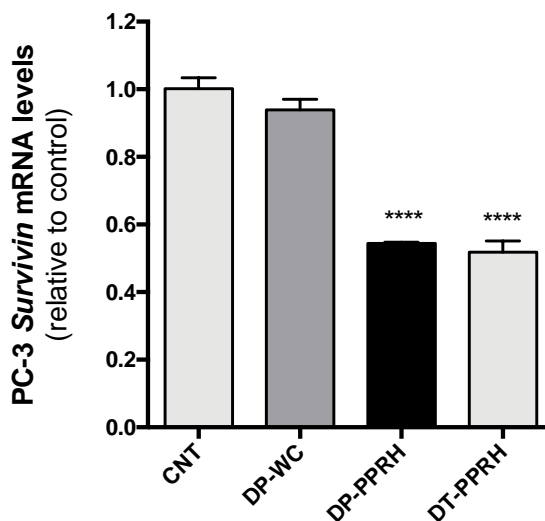


Figure 31. Effect of HpsPr-C-WT transfected with DOPY on mRNA levels in PC-3 cells. PC-3 cells (30.000) were transfected with 100 nM of HpsPr-C (PPRH) or the negative control HpsPr-C-WC (WC) using 1.05 μ M DOPY (DP) or 10 μ M DOTAP (DT). 24 h after transfection, *survivin* mRNA levels were determined by RT-qPCR. TATA-binding protein (TBP) was used to normalize the results. Statistical significance was determined using one-way ANOVA with Dunnett's multiple comparisons test (**** $p < 0.0001$).

5. DISCUSSION

A long-term goal of our laboratory is to keep developing the PolyPurine Reverse Hoogsteen (PPRH) hairpins for possible applications in gene therapy. Therefore, in this work we aim to expand their use in cancer therapy as a gene silencing tool, targeting the RSR genes *WEE1* and *CHK1*, and a G-quadruplex located in *TYMS*. Moreover, in an effort to improve the pharmacokinetic and pharmacodynamic properties of PPRHs, we intend to evaluate different modifications in the PPRH structure and to test alternative methods of delivery, including non-viral and viral vectors.

5.3. PPRHs as gene silencing tool

One of the main limitations of traditional cancer therapies is the low specificity, affecting both healthy and cancer cells, and thus, resulting in severe side effects (Pucci *et al.* 2019). Furthermore, despite the great efforts to develop effective targeted therapies, many proteins are still undruggable (Meric-Bernstam & Mills 2012). Due to their pharmacological properties, PPRHs are promising therapeutic oligonucleotides that could overcome these limitations.

PPRHs can be designed to hybridize selectively to polypyrimidine regions of any target gene. Polypyrimidines regions are abundant in the genome, especially in crucial regulatory regions for gene expression, indicating that many genes can be targets for triplex formation (Goñi *et al.* 2004, 2006). Accordingly, during the last decade, PPRHs have proved to specifically silence different targets involved in cancer progression both *in vitro* and *in vivo* (Ciudad *et al.* 2017; Rodríguez *et al.* 2013; Villalobos *et al.* 2015).

Compared to other gene silencing nucleic acids, PPRHs present several advantages in terms of stability, safety, and effectivity. PPRHs have showed longer half-life than siRNAs in different types of sera and in PC-3 cells (Villalobos, 2013). This fact could be explained by the nature of the structure of PPRHs. Their backbone composed by deoxynucleotides and their hairpin structure probably contribute to increase their stability. Furthermore, PPRHs are more economical to synthesize than siRNAs since no modifications to increase stability are needed. Regarding safety, PPRHs molecules present a low immunogenic profile. Unlike siRNAs, PPRHs do induce neither the Toll-like Receptor nor the inflammasome activation pathways, thus they are considered to be less immunogenic than siRNAs (Villalobos, 2013). Additionally, pharmacogenomic studies have demonstrated the specificity of a PPRH directed against the *survivin* gene (HpsPr-C) and the lack of off-target effects of an

unspecific hairpin (AJF,2020). This negative hairpin did not cause toxicity in viability assays conducted in HepG2 or 786-O cells, and produced minor changes in gene expression, indicating the lack of hepatotoxicity and nephrotoxicity of PPRHs (AJF,2020). Moreover, it is noteworthy that in the two *in vivo* efficacy assays administering HpsPr-C, the mice body weight loss was approximately 2%, denoting the lack of toxicity (Laura, 2013). In respect of gene silencing effect, PPRHs bind with higher affinity to their target dsDNA than TFOs (Rodríguez *et al.* 2015) and exert a more potent effect compared with ASOs (de Almagro *et al.* 2009) or TFOs (Rodríguez *et al.* 2015). Hence, PPRHs are capable of inhibiting gene expression at lower concentrations. It is also important to consider that PPRHs are targeting the gene itself, which present several advantages compared to other oligonucleotides that are directed only to the mRNA (e.g. ASOs, siRNAs or ribozymes). For instance, there are only two targets per cell corresponding to the two alleles of the targeted gene, while there may be multiples copies of a mRNA. Furthermore, inhibition of translation does not prevent the formation of new mRNA, thus inhibition of gene expression is expected to be more efficient (Praseuth *et al.* 1999). All these particularities make PPRHs a potential alternative for gene silencing, and thus in this work we demonstrate their use in other relevant targets for cancer therapy.

5.3.5. Targeting Replication Stress Response gene *WEE1* and *CHK1*

In this work, we explored the usage of PPRHs as a new approach to downregulate the expression of *WEE1* and *CHK1*. In response to replication stress, *CHK1* and *WEE1* are required for checkpoint-mediated cell cycle arrest at the G2/M transition and for the activation of mechanisms to protect genome integrity. In cancer cells, the high levels of replication stress and/or the lack of functionality of other DDR components such as *TP53*, *ATM*, *BRCA1* or *BRCA2*, suggests that tumors rely heavily on a functional RSR, and thus, *WEE1* and *CHK1* represent potential targets in cancer therapy (Forment & O'connor 2018). Therefore, we designed a set of PPRHs directed toward different regions of *WEE1* and *CHK1* to produce a specific downregulation of each gene. First, to confirm their antitumor activity, we analyzed their effect on viability in cancer cells. All the PPRHs demonstrated to decrease cell survival to a certain extent and none of the negative controls tested, neither scrambled PPRHs nor WC-PPRH, showed cytotoxicity on HeLa cells. These determinations are also in agreement with Yan Luo *et al.*, R. Russel *et al.* and Tang *et al.*, in which inhibition of *WEE1* or *CHK1* using other therapeutic oligonucleotides produced very significant decreases in cell viability (Luo *et al.* 2001; Russell *et al.* 2013; Tang

et al. 2006). Interestingly, the most effective PPRH against each gene (HpWEE1Pr-T and HpCHK111-C) did not cause a decrease on viability in non-human cells CHO-DG44. Since these cells do not possess the target sequence of the PPRHs, these results suggest that the detrimental effect on viability produced by PPRHs on human cancer cells is caused by a specific effect on gene expression. Furthermore, HpWEE1Pr-T and HpCHK111-C were also effective in reducing viability in other cancer cell lines (PC-3, MCF-7, SK-BR-3 and HepG2), whereas no reduction or a minor reduction on viability was observed in non-cancerous cells HEK-293 and ECV304, thus, supporting the hypothesis that cancer cells would be more responsive to this therapy than normal tissues (Zhu *et al.* 2020).

We validated that the effects observed in cell viability were caused by a specific decrease in both mRNA and protein levels of WEE1 and CHK1. Furthermore, since previous results in our laboratory had demonstrated that PPRHs could alter the splicing of their target genes (Almagro 2011), we also analyzed the effect of HpCHK111-C on CHK1-S, a shorter variant lacking exon 3. This alternative splice variant represses CHK1 and promotes mitotic entry (Pabla *et al.* 2012; Patil *et al.* 2014). We did not observe differences in CHK1-S/CHK1 mRNA splicing variants ratio, indicating that HpCHK111-C interferes with transcription of both isoforms with no distinction, resulting in a proportional decrease of both variants.

Loss of functionality of CHK1 and WEE1 kinases has been described to provoke an excess of replication stress that induce cancer cells to initiate apoptosis or to progress to an anticipated mitosis without a previous DNA repair (Beck *et al.* 2012; Benada & Macurek 2015; van Harten *et al.* 2019). As a result of extensive DNA damage at this phase, cells undergo mitotic catastrophe and apoptosis (Castedo *et al.* 2004; Qiu *et al.* 2018). Therefore, we studied the effect produced by PPRHs on cell cycle and apoptosis levels. In agreement with other studies conducted with CHK1 inhibitors (Mak *et al.* 2014; Wang *et al.* 2014) or WEE1 inhibitors (Chen *et al.* 2021; Mak *et al.* 2014; Vera *et al.* 2015), we found that inhibition of *WEE1* and *CHK1* using PPRHs induce an accumulation in G2/M phase, which can be explained by premature entry and prolonged mitosis with damaged DNA (Lewis *et al.* 2017; Mak *et al.* 2014). Furthermore, we also observed an increase in apoptosis and necrosis levels in cells transfected with those PPRHs, in agreement with other WEE1 and CHK1 inhibitors (Chen *et al.* 2021; Kogiso *et al.* 2014; Mak *et al.* 2014).

Most of the current anticancer agents induce DNA damage, and thus, enhance replicative stress directly or indirectly (Dobbelstein & Sørensen 2015). Therefore, the combination of WEE1 and CHK1 inhibitors with radiotherapy or other chemotherapy agents has been proposed to further boost replicative stress. In agreement with several pre-clinical and clinical studies (Cuneo *et al.* 2019; Engelke *et al.* 2013; Sarcar *et al.* 2011), we also corroborated that inhibition of either WEE1 or CHK1 using PPRHs can enhance the response to DNA-damaging agents, such as 5-FU or MTX.

To date, multiple CHK1 inhibitors have been developed and tested in clinical trials (e.g. UCN-01, CBP501, AZD7762, LY2603618, MK8776, PF-00477736, LY2606368, SRA737, GDC-0575 or SRA737) (Forment & O'connor 2018; Huang & Zhou 2020; Qiu *et al.* 2018). However some failed to improve the efficacy in combination with other chemotherapies (Krug *et al.* 2014; Laquente *et al.* 2017; Scagliotti *et al.* 2016) or induced serious adverse events because of the nonspecific targeting (Sausville *et al.* 2014; Seto *et al.* 2013). In the case of WEE1 inhibitors, PD0166285 was the first reported drug (Panek *et al.* 1997) and AZD1775 (Adavosertib) is a promising candidate currently tested in a large number of preclinical and clinical studies (Cuneo *et al.* 2019; Ghelli Luserna Di Rorà *et al.* 2020; Leijen *et al.* 2016). Nevertheless, despite extensive research, there is no drug targeting the RSR currently available in the market. Indeed, only Poly-ADP-ribose polymerase inhibitors (olaparib, rucaparib, niraparib and talazoparib), which target DDR, have been approved by the Food and Drug Administration (FDA) and the European Medicines Agency (EMA) for cancer patients bearing a mutated BRCA gene (Faraoni & Graziani 2018). Thus, as an alternative pharmacological agent for the inhibition of the RSR genes *WEE1* and *CHK1*, we explored the usage of PPRHs against these targets, finding out that they were able to decrease the mRNA and protein levels of their targets causing a very significant decrease in the viability of a variety of human cancer cells. Therefore, these hairpin molecules could be envisioned as possible novel inhibitors of these targets involved in RSR.

5.3.6. Targeting the regulatory element G-quadruplex in *Thymidylate Synthase* gene

TYMS inhibitors (e.g. fluoropyrimidines or antifolates) have been widely used as an anti-cancer strategy due to the key role of TYMS in DNA synthesis (Chu *et al.* 2003; Rahman *et al.* 2004). However, their effectivity have been limited by the development of drug resistance (Zhang *et al.* 2008). In an

autoregulatory manner, TYMS can regulate its own translation and induces new synthesis of TYMS protein when is inhibited by fluoropyrimidines, thus promoting drug resistance (Berger *et al.* 1985; Rooney *et al.* 1998). Therefore, in this work we searched for regulatory regions of TYMS that could be targetable using PPRHs, as an alternative approach to down-regulate TYMS expression.

Since G4s motifs have been described to act as regulatory elements in both DNA and RNA of several protooncogenes (Kim 2017), we searched putative G4FSs located in the *TYMS* gene using the web-based server QGRS (Kikin *et al.* 2006). We identified a putative G4FS in the 5'-UTR of *TYMS* (G4-TYMS), and then, we confirmed the G4 folding in both DNA and RNA using different spectroscopic approaches, including CD, UV absorbance, fluorescence or NMR. To note, there was a discrepancy regarding the location of the G4FS between the last two accession numbers of *TYMS* in the NCBI Gene database (NM_001071.4 and NM_001071.3). While the G4FS was located in the 5'UTR in NM_001071.3, in NM_001071.4, the G4FS was excluded from the 5'-UTR and included in the promoter. Therefore, we verified that the G4FS was actually included in 5'UTR of *TYMS* by PCR and RT-PCR, in agreement with the original sequence (Kaneda *et al.* 1990).

G4s can be high-affinity binding sites for certain proteins and act as regulatory element of gene expression (Tian *et al.* 2018). Besides that, TYMS protein act as an RNA binding protein and regulates mRNA translation of different genes, including its own (Chu *et al.* 1991, 1993), *C-MYC* (Chu *et al.* 1995), *TP53* (Chu *et al.* 1999; Ju *et al.* 1999) and the gene encoding human IFN-induced 15 kDa protein (Chu 1996). For those reasons, we evaluated the possible interaction between TYMS and the G4FS as mRNA. EMSA confirmed the binding of TYMS protein to the G4FS as mRNA, thus revealing that this protein has another binding site, in addition to the two binding sites already known (Chu *et al.* 1991, 1993). Moreover, we also verified that TYMS protein also interacts with the G4FS as dsDNA, which could indicate that TYMS protein, aside from its translational control, could also regulate gene expression at the transcriptional level through the binding to this newly discovered site located in the 5'-UTR.

At this point, we designed a PPRH targeting the polypyrimidine sequence that is complementary to G4-TYMS (HpTYMS-G4-T). EMSA assays confirmed the binding of the PPRH to its target sequence and demonstrated that TYMS protein and the PPRH competed for the binding to the G4FS. We hypothesized

that a PPRH could form a triplex with the complementary strand of G4-TYMS, which would displace the G-rich sequence of the duplex enabling its folding into a G4 structure. To verify this, we performed binding assays with Tht, a fluorescence sensor that can detect G4 structures (De La Faverie *et al.* 2014). Those assays showed that the formation of a dsDNA/PPRH triplex promoted the displacement of the polypurine strand and its folding into a G4 structure, thus supporting our hypothesis. Interestingly enough, the PPRH itself, on each one of its two arms, forms a G4 structure. Nevertheless, in accordance with our previous results, we corroborated that conditions in which a PPRH can fold into a G4 structure do not impair its binding to the dsDNA (Solé *et al.* 2017).

Then, we proceeded to test the activity of HpTYMS-G4-T in cancer cells. We demonstrated that the PPRH targeting G4-TYMS decreased both TYMS mRNA and protein levels in a specific manner, which led to a decrease in viability in a dose-dependent manner in HeLa and PC3 cancer cells. It is remarkable that the detrimental effect in viability produced by HpTYMS-G4-T was lower when cells were incubated in medium containing thymidine. The fact that the cytotoxic effect is reversed by thymidine, also corroborates that HpTYMS-G4-T impairs specifically TYMS activity. Similar results have been described by Schmitz *et al.*, whose studies demonstrated that the effect of a siRNA targeting TYMS mRNA was reversed with 10 μ M of thymidine (Schmitz *et al.* 2004).

Therapies targeted to downregulate TYMS expression have been proposed for tackling the resistance produced by the autoregulatory mechanism of TYMS protein (Garg *et al.* 2010). Therefore, we also evaluated the effect of HpTYMS-G4-T in combination with the traditional TYMS inhibitor 5-FU. We demonstrated that HpTYMS-G4-T present a synergic effect in reducing viability when was combined with 5-FU in HeLa cells. Other studies have also demonstrated that inhibition of TYMS using gene silencing oligonucleotides can inhibit tumor cell proliferation and enhance the efficacy of traditional TYMS inhibitors (Berg *et al.* 2003; Ferguson *et al.* 1999; Schmitz *et al.* 2004). As a control, we verified that 5-FU as a single agent induce an increase of total TYMS protein, as reported in (Ligabue *et al.* 2012; Peters *et al.* 2000, 2002).

All the results obtained in this work uncover the importance of the new identified G4s structure in *TYMS*. However, its regulatory function in TYMS expression remains unclear. While some G4 structures have been described to positively contribute to gene expression through protein binding (Chen *et al.* 2013), others sustain that G4 structures may act as obstacles (Cogoi *et al.* 2014;

Kumari *et al.* 2007). In accordance with the currently postulated TYMS translational autoregulatory mechanism (Chu *et al.* 1991, 1993), we hypothesize that this G4 can act as an additional binding site of TYMS protein in either its mRNA or DNA, preventing the function of either the transcriptional or translational machineries.

G4s have been related to the regulation of the transcription of several tumor-related genes, including *C-MYC* (Chen *et al.* 2013), *Telomerase reverse transcriptase* (hTERT) (Palumbo *et al.* 2009), *c-KIT* (Rankin *et al.* 2005), *KRAS* (Cogoi *et al.* 2004; Cogoi & Xodo 2006), *BCL-2* (Dexheimer *et al.* 2006), and *VEGF* (Sun *et al.* 2008). Therefore, the interest in the development of G4-ligands that stabilize G4 structures as an antitumor therapy has arisen (Asamitsu *et al.* 2019; Tian *et al.* 2018). A wide range of G4-ligands have been developed, including ligands that promote G4 structures in the telomere region to block telomerase activity (Mu-Yong Kim *et al.* 2002; Zahler *et al.* 1991) or those targeting G4 structures located in promoters (Siddiqui-Jain *et al.* 2002; Wang *et al.* 2017), and encouragingly some have reached clinical trials (e.g. CX-3543, APTO-253 or CX-5461) (Drygin *et al.* 2009; Khot *et al.* 2019; Local *et al.* 2018). Nevertheless, human genome contains a high number of putative G4s structures, which makes the major obstacle in the development of specific G4-ligands. To overcome this limitation, here we introduce PPRHs as an alternative to specifically target G4-forming sequences. Specifically, we demonstrate their therapeutic potential as a single agent or in combination with 5-FU when targeting selectively a G4 structure located in *TYMS*.

5.3.7. Improving the structure of PPRHs

Seeking to improve the properties of PPRHs in gene silencing, we introduced distinct modifications in their structure. Since we have already validated the antitumor activity of a PPRH directed against the *survivin* gene (HpsPr-C) *in vitro* and *in vivo* (Rodríguez *et al.* 2013), we selected this PPRH to evaluate the effect of these modifications on triplex formation and cell viability assays.

Unmodified oligonucleotides present a rapid clearance from blood, primarily due to excretion in urine and nucleases degradation (Dirin & Winkler 2013). The RNase A family are the predominant nucleases that degrade circulating ribonucleotides, such as siRNAs (Haupenthal *et al.* 2006), whereas DNase I and 3'- exonuclease are the primary enzymes to degrade circulating

deoxyribonucleotides, such as ASOs (Fujihara *et al.* 2012; Putney *et al.* 1981). PPRHs are unmodified DNA molecules, therefore one could speculate that their pharmacokinetics would be similar to that of ASOs (Ciudad *et al.* 2017). To avoid the rapid degradation and enhance the stability, oligonucleotides containing a PS backbone have been developed. PS bonds have the dual effect of conferring nuclease resistance and promoting binding to plasma proteins, especially to albumin. This modification reduces renal clearance and increases the circulation time (Geary *et al.* 2015). Therefore, we introduced PS linkages in the PPRH structure to enhance its stability.

Binding analyses showed that HpsPr-C-PS binds with similar affinity to its target sequence as ssDNA in comparison with HpsPr-C-WT. However, the PS PPRH present lower binding affinity than the WT PPRH when incubated with dsDNA. It has been clearly established that the incorporation of a PS linkage results in the generation of a chiral center and different stereoisomeric forms. These stereoisomers have different functional properties, which can result in a decrease in binding affinity, thus, the minimum number of PS linkages should be used (Eckstein 2014). Interestingly, the PS PPRH induce a higher decrease in cell viability than the WT PPRH, which indicate that the slight loss of binding affinity would be balanced by the higher stability of the PS-PPRH.

To note, even without chemical modifications, PPRHs present higher stability than other oligonucleotides, which is a remarkable advantage (Villalobos *et al.* 2014). Most of the approved oligonucleotides drugs therapies are “naked” and so are dependent on chemical modification to facilitate their tissue delivery (Roberts *et al.* 2020). Our results prove that PS linkages could be considered as a chemical modification to improve the pharmacokinetic and pharmacodynamic, if naked PPRHs were to be administered.

We also tried to deal with the limitation of three purine interruptions in the homopurine track of the PPRHs, thus we evaluated the possibility of establishing other types of triplets, involving inosine nucleosides or T·CG / C·TA triplets (HpsPr-C-I and HpsPr-C-Subs, respectively). On one hand, binding analyses showed that replacing interruptions of one of the arms of the clamp by either Inosines or T·CG / C·TA triplets reduces the triplex formation with its target ssDNA compared with the WT PPRH. On the other hand, and in terms of cell viability, HpsPr-C-I and HpsPr-C-Subs promoted a lower decrease than HpsPr-C-WT. These results indicate that these triplets may decrease stacking interactions within the third strand. Other studies have also showed that

substituting third-strand thymines or cytosines by inosines in triple helix reduces the binding energy of the Hoogsteen third strand (Griffin & Dervan 1989; Mills *et al.* 1996). In addition, it is suggested that T·CG/C·TA triplets generate weaker bounds and that those triplets need to be designed with care, since they may target other sequences (Chandler & Fox 1995, 1996). These results indicate that the use of inosine and T·CG / C·TA triplets as a substitute of the purine interruptions in a PPRH structure is limited.

On the other hand, the structure and stability of a hairpin depends on different variables, such as stem size, loop size, stem and loop composition, base stacking, base pairing, hydrogen bonds on the loop, and closing base pair of the loop (Nayak & Van Orden 2013; Shen *et al.* 2001; Vallone *et al.* 1999). Of these variables, we analyzed the effect on cell viability of different PPRHs differing from the loop size (3, 4 or 5 thymidines). Similar results were obtained with all PPRHs, indicating that the T-loop of a PPRH can range from 3 to 5 residues. Other studies have shown, that in hairpins with identical stem sequences, stability becomes stronger as the loop length decreases since that shorter loop length imparts greater stability to the hairpin structure (Nayak & Van Orden 2013). In general, it is suggested that for DNA the optimal loop consists of 4 or 5 residues, although it has also been shown that hairpins can be formed even with loops <3 (Hilbers *et al.* 1985). Furthermore, we analyzed if stabilising WC bonds in the loop could stabilize the hairpin formation, and thus, promote the triplex formation with its target sequence. To do so, we replace the 5T-loop by TATTA or the TTAA sequence (HpsPr-C-TATTA and HpsPr-C-TTAA, respectively). Our binding results suggest that those loops do not interfere with triplex formation. However, cell viability assays demonstrated that their effect was lower than the WT PPRH. Therefore, other alternatives should be considered to improve hairpin formation, such as the interactions between the closing base pair of the loop (Kuznetsov *et al.* 2008).

Overall, further experiments such as UV-vis Melting Experiments or Fluorescence Melting Experiments should be performed to evaluate the thermodynamic stability of these modifications in the PPRHs. Additionally, survivin mRNA and protein levels should also be analyzed to validate the activity of these PPRHs.

5.4. Delivery

For systemic applications, the main routes of administration for therapeutic nucleic acids are either intravenous or subcutaneous. Once administered, oligonucleotides are rapidly absorbed into the circulation showing a peak in plasma concentration within 3 to 4 h (Geary et al. 2015). If no vehicle is used, namely naked administration, oligonucleotides are distributed to tissues and rapidly eliminated by blood nucleases and renal filtration. Therefore, one of the major objectives in our laboratory is to find vehicles able to protect PPRHs from extracellular and intracellular degradation, to prolong their circulation time, to achieve tissue-specific delivery, and to obtain an efficient release of these molecules at the intracellular and nuclear level so that they can exert their function on their target.

To date, the cationic liposome DOTAP, and the cationic polymer Jet-Polyethylenimine (jetPEI) have been used as vehicles for *in vitro* (Villalobos et al. 2015) and *in vivo* studies (Rodríguez et al. 2013), respectively. However, some issues regarding efficiency, toxicity and specificity encourage us to search for other alternatives for PPRHs delivery, including both non-viral and viral strategies. For both approaches, we used the already validated PPRH directed against *survivin* (HpsPr-C) (Rodríguez et al. 2013).

5.4.5. PPRHs delivery using viral vectors

The use of viruses for therapy has long been studied. Although the earlier viral-based therapies failed, nowadays the understanding of viral biology has enabled the development of several viral vectors that are being marketed around the world (Bulcha et al. 2021). Viral vectors exhibit high transduction efficiencies, capacity of long term expression, and the possibility to achieve targeted gene expression on the desired cells (Thomas et al. 2003), advantages that make these vectors promising candidates for nucleic acids delivery. Therefore, we decided to test the biological response produced by the infection of viral vectors encoding the PPRH against the *survivin* gene.

Since the PPRH sequence would be transcribed from the genome of the vector, we first evaluated the effect of this PPRH made out of a non-modified ribonucleotides, an RNA-PPRH. Reverse Hoogsteen bonds can also be established between RNA sequences, and thus, polypurine sequences can form RNA hairpins (Purshotam et al. 2010). We confirmed that the RNA hairpin directed against *survivin* was also able to specifically bind to ssDNA and dsDNA

forming a triplex structure. Other studies have also corroborated the ability of an RNA sequence to recognize DNA duplexes and form triplexes (McDonald & Maher 1995). Then, we also demonstrated that the RNA-PPRH and a PPRH transcribed from a plasmid were able to decrease cell viability, although higher doses compared with the DNA-PPRH were needed. Moreover, we validated the activity of both the RNA-PPRH and the plasmid based-PPRH in reducing survivin mRNA and protein levels. In a similar way, other groups have described DNA vectors as a system for the expression of siRNAs within mammalian cells (Paddison *et al.* 2002; Sui *et al.* 2002). However, the main limitation of plasmid-based systems is the low efficiency of the transient transfection (Devroe & Silver 2002).

Regarding viral-based systems, we validated the use of an adenoviral vector as a delivery system for PPRHs *in vitro*. We demonstrated the ability of AdV-PPRH to downregulate survivin mRNA and protein levels. Furthermore, we showed that the transduction of AdV-PPRH in HeLa cells provoked a reduction on viability. Several groups have demonstrated that viral vectors have the ability to efficiently deliver therapeutic nucleic acids into mammalian cells, including siRNAs or antisense oligonucleotides (Barton & Medzhitov 2002; Devroe & Silver 2002; Phillips *et al.* 1997; Tomar *et al.* 2003).

In the case of adenovirus vectors, an important obstacle is their immunogenicity, evidenced when the treatment with an adenovirus vector led to the death of an ornithine transcarbamylase deficient patient (Raper *et al.* 2003). Since then, different strategies to overcome safety issues, and to improve the capacity of the transgene size, or the durability of transgene expression have been analyzed. An approach is the removal of different genes of the adenoviral genome to achieve different levels of attenuation (Lee *et al.* 2017). Furthermore, non-human AdV vectors have also been developed (canine, bovine, chimpanzee, ovine, porcine) since humans do not have antibodies against those vectors (Bulcha *et al.* 2021; Ersching *et al.* 2010; Kremer *et al.* 2000; Quinn *et al.* 2013; Xu *et al.* 1997). The great efforts in this field have led to the approval of several AdV vectors, including cancer therapies or Ebola and COVID19 vaccines, which highlight the potential of this technology for nucleic acids delivery (Bulcha *et al.* 2021).

Nevertheless, we have not achieved an efficient delivery of PPRHs using AAVs vectors *in vitro*. It is noteworthy that transduction of AAVs *in vivo* does not tend to reflect what it is observed *in vitro* (Bulcha *et al.* 2021), thus AAVs may

not be discarded for *in vivo* approaches. Their lack of pathogenicity and immunotoxicity and their efficiency make them promising candidates for *in vivo* delivery, which is reflected in the approval of three AAV-based therapies (Glybera™, Luxturna™ and Zolgensma™), although Glybera has been removed from the market due to economic concerns (Keeler & Flotte 2019).

Different viral vectors are currently being tested in many clinical trials, mostly AdV, AAVs and retroviruses (Bulcha *et al.* 2021). Each type of vector is characterized by a set of properties that make it appropriate or inappropriate for some applications. For instance, some viral-based systems can achieve long-period expression, thus viral vectors rise the possibility of reducing the number of administrations of the PPRHs. Furthermore, they also offer the opportunity of achieving transcriptional targeting by placing the PPRH under the control of a cell-type-specific promoter (Adachi *et al.* 2000; Koeneman *et al.* 2000; Yamamoto *et al.* 2001). Moreover, proteins of the capsid can be engineered to increase their tissue selectivity (Douglas *et al.* 1996; Li & Samulski 2020; Reynolds *et al.* 2000, 2001; Thomas *et al.* 2003). Overall, all our results are the proof of principle that viral vector could be considered as a delivery system of PPRHs *in vitro* and in future studies *in vivo*.

5.4.6. PPRHs delivery using non-viral vectors: Synthesis and validation of DOPY

In the present work, we explored the new gemini cationic liposome-based formulation DOPY for PPRH delivery. It is known that cationic lipid-based systems form electrostatic complexes with DNA. This condensation protects DNA from nuclease degradation and confers desirable physicochemical properties in terms of size and charge to facilitate DNA entry into cells (Pichon *et al.* 2010). DOPY is a gemini amphiphilic bis-pyridinium salt connected through a 1,3-xylyl spacer and bearing hydrophobic oleyl moieties on position 4 of the pyridinium rings. As in other chemical vectors, the pyridinium salt confers a positive charge that enables the interaction with DNA (Dubruel *et al.* 2003; Pajuste *et al.* 2013; Petrichenko *et al.* 2015). First, we confirmed that DOPY was able to interact with PPRH by gel retardation assays. Then, we determined that these DOPY/PPRH complexes showed a hydrodynamic diameter of 155 nm, with a dispersion index of 0.25, and a Z-potential of 67.53 ± 1.08 mV, which indicated the excellent stability of the lipoplexes and was in accordance with their cationic nature. Moreover, transmission Electron Microscopy experiment allowed the visualization of the fibrillar structures of the PPRH molecules

covered by DOPY and corroborated the diameter of these lipoplexes (Samimi *et al.* 2018).

At this point, we evaluated the transfection efficiency of DOPY as a vehicle of PPRHs in both gene silencing and repair approaches. In all cases, DOPY demonstrated higher efficiencies of internalization compared to DOTAP or calcium phosphate in SH-SY5Y, PC-3 and DF42 cells. Additionally, we also analyzed the mechanism involved in the internalization of DOPY/PPRH complexes by transfecting PPRHs either in the presence or the absence of different endocytic pathways inhibitors (Lin *et al.* 2018; Macia *et al.* 2006; Vercauteren *et al.* 2010). The decrease in DOPY/PPRH cellular uptake after the treatment with a clathrin-dependent endocytosis inhibitor (Dynasore) or the caveolin-mediated endocytosis inhibitor (Genistein) in both PC-3 and SH-SY5Y cells suggested that these two pathways are involved in the internalization of DOPY/PPRHs complexes, while it was not due to macropinocytosis given that the entry was not affected by the inhibitor 5-(N-ethyl-N-isopropyl) amiloride (EIPA) (Lin *et al.* 2018; Macia *et al.* 2006; Vercauteren *et al.* 2010). Similarly, other studies have observed that transfection in mammalian cells using other lipoplexes also occurs through clathrin-mediated endocytosis and suggested that a caveolae-dependent mechanism should not be excluded (Rejman *et al.* 2005, 2006; Zuhorn *et al.* 2002).

To evaluate the gene silencing efficiency with DOPY, we transfected HpsPr-C PPRH in neuroblastoma cells, since we had previously faced difficulties in transfecting these cells with the commercially available agents. DOPY/PPRH complexes successfully reduced survivin protein levels leading to a decrease on viability in SH-SY5Y cells. Moreover, transfection with the negative control hairpin did not produce any effect on cell viability, thus indicating that the effect on cell survival was produced by the PPRH targeting *survivin*. Other studies with an small-molecule suppressant have also demonstrated an antiproliferative effect when targeting survivin in neuroblastoma cells (Liang *et al.* 2013). In contrast, the transfection of DOTAP/HpsPr-C complexes in SH-SY5Y cells did not reduce survivin protein levels nor cell viability, which corroborates the greater internalization capacity of DOPY. As a positive control, we transfected PC-3 cells using either DOTAP and DOPY, since our previous studies incubating HpsPr-C/DOTAP complexes in this cell line had showed an effective delivery and *survivin* silencing (Rodríguez *et al.* 2013). We showed a great reduction on protein levels and cell viability using both formulations. To note, we used 7.75-fold less amount of DOPY than that of DOTAP, which also indicates that

DOPY/PPRH complexes are more effective in terms of inhibiting *survivin* expression and reducing viability in both SH-SY5Y and PC-3 cells.

One of the goals of this work was to demonstrate the versatility of transfection of DOPY. For that reason, we also tested DOPY as a vehicle for repair-PPRHs. The HpE6rep-L repair-PPRH was designed to correct the c.541 G>T mutation present in the endogenous *locus* of the *dhfr* gene in the DF42 CHO mutant. We demonstrated that HpE6rep-L transfected using DOPY in DF42 mutant cells achieved higher correction frequencies than with DOTAP or calcium phosphate, which are the chemical vehicles routinely used in our laboratory for gene correction strategies (Félix *et al.* 2020a; Solé *et al.* 2016). The HpE6rep-L repair-PPRH was able to specifically correct the mutation in the endogenous *locus* of the *dhfr* gene, restoring its wild-type sequence. In addition, we confirmed that DF42 corrected cells were able to produce a full DHFR protein with restored enzymatic activity, thus proving the effectivity of DOPY as a transfection agent also in gene repair approaches.

Dozens of lipid-based drug delivery systems have been approved by the FDA (Bulbake *et al.* 2017; Savla *et al.* 2017), such as the antifungal agent amphotericin B liposomal (Tollemar *et al.* 2001), the chemotherapy liposomal drugs daunorubicin (FDA 1996), doxorubicin (Franco *et al.* 2018) and cytarabine (Jaeckle *et al.* 2002). The experience with this type of vehicles and the efforts in developing new lipid-based carriers capable of protecting and delivering nucleic acids to target cells resulted in the approval of the first siRNA formulated in a lipid nanoparticle, patisiran (Akinc *et al.* 2019). Recently, the scientific community has proved the versatility and the rapid development of mRNA vaccines based on lipid-nanoparticles delivery for the COVID-19 emergency (European Medicines Agency 2020a, 2021, FDA 2020b, 2020a; Jackson *et al.* 2020; Polack *et al.* 2020). All these milestones encourage to continue with the development of lipid-based systems to improve the delivery of nucleic acids. In this direction, in this work we have developed and tested an alternative cationic liposome-based formulation, DOPY, with the ability to transfect “hard to transfect” cells with oligonucleotides, even at a much lower concentration of liposome compared with DOTAP.

5.5. Concluding remarks

The numerous recent regulatory approvals of therapeutic oligonucleotides highlight the great advances achieved in this field over the last 30 years and the optimistic future for clinical utility. The development of different gene silencing molecules and the advances in improving their delivery, pharmacokinetics and pharmacodynamic have contribute to this landscape. In this field, PPRHs represent an economical alternative with high stability that does not exhibit immunogenicity, hepatotoxicity or nephrotoxicity *in vitro*. During the last decade, we have proved their use as a silencing tool against several targets involved in cancer progression (Noé *et al.* 2020) and we have incorporated this technology to our research on a regular basis (Barros *et al.* 2013; Mencia *et al.* 2011; Oleaga *et al.* 2012). Furthermore, PPRHs have demonstrated their ability to correct point mutations in the DNA (Félix *et al.* 2020b), to cause exon skipping at the genomic level (Noé & Ciudad 2021), and their use as biosensors (Calvo-Lozano *et al.* 2020; Huertas *et al.* 2016, 2018).

In this work we expand the usage of PPRHs as a gene silencing tool against *WEE1*, *CHK1* and *TYMS*, the latter targeting a newly identified G4 structure in the gene sequence. Furthermore, we evaluate different modifications in the PPRHs seeking to improve their pharmacological properties. Finally, we validate an AdV vector and the new cationic liposome formulation DOPY as two novel strategies for PPRHs delivery. We strongly believe that establishing a safe, efficient, and tissue-specific delivery system could broaden the therapeutic chances of PPRHs.

As future perspectives, we are seeking to extend the usage of PPRHs as a detection tool for viruses, including the acute respiratory syndrome coronavirus 2 (SARS-CoV-2), Influenza virus A (H1N1) or Human respiratory syncytial virus (HRSV); and to target new motifs involved in gene expression such as G4FSs, or lncRNAs associated with human diseases or drug resistance. Furthermore, we continue the research of PPRHs delivery, and we are currently evaluating other strategies such as the use of biocompatible and biodegradable Hyaluronic acid/protamine combinations (Alaniz *et al.* 2002; Wang *et al.* 2015), gold nanoparticles functionalized or not with DOPY, or PPRHs conjugated with cell-specific aptamers for targeted therapies (Zhou & Rossi 2017).

6. CONCLUSIONS

1. PPRHs are able to decrease the expression of RSR genes *WEE1* and *CHK1*, leading to a disruption of cell cycle progression, an increase of apoptosis, and a decrease of survival in tumor cells. Moreover, the inhibition of either *WEE1* or *CHK1* using PPRHs can enhance the response to DNA-damaging agents, such as 5-FU or MTX.
2. We identified and validated a new G4 structure in the 5'UTR in the *TYMS* gene that can be targeted by PPRHs and act as regulatory element of *TYMS* expression at the transcriptional and translational level.
3. The PPRH targeting G4-TYMS can promote G4 formation and down-regulate *TYMS* expression. *TYMS* inhibition using this PPRH induces cancer cell death as single agent and shows synergic effect with the classical *TYMS* inhibitor 5-FU.
4. The introduction of PS linkages in the PPRHs backbone produces a slight increase in PPRH activity. The T-loop of a PPRH can range from 3 to 5 residues, without altering the effect of PPRH on cell viability.
5. PPRHs can also work as RNA species, as demonstrated using RNA chemically synthesized, plasmid and viral expression vectors.
6. The AdV based vector encoding the PPRH against *survivin* can downregulate *survivin* mRNA and protein levels, causing a reduction on cell viability. Thus, viral vectors can be considered as delivery system of PPRHs.
7. DOPY can interact with PPRHs forming lipoplexes that can be internalized via clathrin- and caveolae- mediated endocytosis allowing higher efficiencies of cellular uptake and gene silencing than other chemical vehicles. Therefore, DOPY can be considered as a new cationic lipid-based vector suitable for the delivery of therapeutic oligonucleotides.

7. BIBLIOGRAPHY

- Aartsma-Rus, A., Fokkema, I., Verschuuren, J., ... Den Dunnen, J. T. (2009). Theoretic applicability of antisense-mediated exon skipping for Duchenne muscular dystrophy mutations. *Human Mutation*, **30**(3), 293–299.
- Adachi, Y., Reynolds, P. N., Yamamoto, M., ... Curiel, D. T. (2000). Midkine Promoter-based Adenoviral Vector Gene Delivery for Pediatric Solid Tumors. *Cancer Research*, **60**(16).
- Adams, D., Gonzalez-Duarte, A., O’Riordan, W. D., ... Suhr, O. B. (2018). Patisiran, an RNAi therapeutic, for hereditary transthyretin amyloidosis. *New England Journal of Medicine*, **379**(1), 11–21.
- Ahn, J. D., Morishita, R., Kaneda, Y., ... Lee, I. K. (2002, December 29). Novel E2F decoy oligodeoxynucleotides inhibit in vitro vascular smooth muscle cell proliferation and in vivo neointimal hyperplasia. *Gene Therapy*, Nature Publishing Group, pp. 1682–1692.
- Aiuti, A., Roncarolo, M. G., & Naldini, L. (2017). Gene therapy for ADA-SCID, the first marketing approval of an ex vivo gene therapy in Europe: paving the road for the next generation of advanced therapy medicinal products. *EMBO Molecular Medicine*, **9**(6), 737–740.
- Akinc, A., Maier, M. A., Manoharan, M., ... Cullis, P. R. (2019, December 1). The Onpattro story and the clinical translation of nanomedicines containing nucleic acid-based drugs. *Nature Nanotechnology*, Nature Research, pp. 1084–1087.
- Alaniz, L., Cabrera, P. V., Blanco, G., ... Hajos, S. E. (2002). Interaction of CD44 with Different Forms of Hyaluronic Acid. Its Role in Adhesion and Migration of Tumor Cells. *Cell Communication & Adhesion*, **9**(3), 117–130.
- Alberts, B., Johnson, A., Lewis, J., Raff, M., Roberts, K., & Walter, P. (2002). Isolating, Cloning, and Sequencing DNA. Retrieved from <https://www.ncbi.nlm.nih.gov/books/NBK26837/>
- Alea-Reyes, M. E., González, A., Calpena, A. C., Ramos-López, D., de Lapuente, J., & Pérez-García, L. (2017). Gemini pyridinium amphiphiles for the synthesis and stabilization of gold nanoparticles for drug delivery. *Journal of Colloid and Interface Science*, **502**, 172–183.
- Alsaggar, M., & Liu, D. (2015). Physical Methods for Gene Transfer. *Advances in Genetics*, **89**, 1–24.
- Alvarez-Erviti, L., Seow, Y., Yin, H., Betts, C., Lakhal, S., & Wood, M. J. A. (2011). Delivery of siRNA to the mouse brain by systemic injection of targeted exosomes. *Nature Biotechnology*, **29**(4), 341–345.
- Amantana, A., & Iversen, P. L. (2005, October 1). Pharmacokinetics and biodistribution of phosphorodiamidate morpholino antisense oligomers. *Current Opinion in Pharmacology*, Elsevier BV, pp. 550–555.
- Ambrosini, G., Adida, C., & Altieri, D. C. A novel anti-apoptosis gene, survivin, expressed in cancer and lymphoma, 3 *Nature Medicine* 917–921 (1997), Nature Publishing Group, pp. 917–921.
- Ann Liebert, M., & Cho-chung, Y. S. (1998). *CRE-Palindrome Oligonucleotide as a Transcription Factor Decoy and an Inhibitor of Tumor Growth. ANTISENSE & NUCLEIC ACID DRUG DEVELOPMENT*, Vol. 8. Retrieved from www.liebertpub.com

- Anusch, P., & Eugen, U. (1996). Minimally modified oligonucleotides - combination of end-capping and pyrimidine-protection. *Biological Chemistry Hoppe-Seyler*, **377**(1), 67–70.
- Arnold, A. E., Malek-Adamian, E., Le, P. U., ... Shoichet, M. S. (2018). Antibody-Antisense Oligonucleotide Conjugate Downregulates a Key Gene in Glioblastoma Stem Cells. *Molecular Therapy - Nucleic Acids*, **11**, 518–527.
- Asamitsu, S., Obata, S., Yu, Z., Bando, T., & Sugiyama, H. (2019). Recent progress of targeted G-quadruplex-preferred ligands toward cancer therapy. *Molecules*, **24**(3). doi:10.3390/molecules24030429
- Aubets, E., Félix, A. J., Garavís, M., ... Noé, V. (2020a). Detection of a g-quadruplex as a regulatory element in thymidylate synthase for gene silencing using polypurine reverse Hoogsteen hairpins. *International Journal of Molecular Sciences*, **21**(14), 1–22.
- Aubets, E., Noé, V., & Ciudad, C. J. (2020b). Targeting replication stress response using polypurine reverse Hoogsteen hairpins directed against WEE1 and CHK1 genes in human cancer cells. *Biochemical Pharmacology*, 113911.
- Avery, O. T., Macleod, C. M., & McCarty, M. (1944). Studies on the chemical nature of the substance inducing transformation of pneumococcal types: Induction of transformation by a desoxyribonucleic acid fraction isolated from pneumococcus type iii. *Journal of Experimental Medicine*, **79**(2), 137–158.
- Azuhata, T., Scott, D., Takamizawa, S., ... Sandler, A. (2001). The inhibitor of apoptosis protein survivin is associated with high-risk behavior of neuroblastoma. *Journal of Pediatric Surgery*, **36**(12), 1785–1791.
- Bainbridge, J. W. B., Mehat, M. S., Sundaram, V., ... Ali, R. R. (2015). Long-Term Effect of Gene Therapy on Leber's Congenital Amaurosis. *New England Journal of Medicine*, **372**(20), 1887–1897.
- Barros, S., Mencia, N., Rodríguez, L., ... Ciudad, C. J. (2013). The Redox State of Cytochrome C Modulates Resistance to Methotrexate in Human MCF7 Breast Cancer Cells. *PLoS ONE*, **8**(5). doi:10.1371/journal.pone.0063276
- Barton, G. M., & Medzhitov, R. (2002). Retroviral delivery of small interfering RNA into primary cells. *Proceedings of the National Academy of Sciences of the United States of America*, **99**(23), 14943–14945.
- Beck, H., Nähse-Kumpf, V., Larsen, M. S. Y., ... Sørensen, C. S. (2012). Cyclin-dependent kinase suppression by WEE1 kinase protects the genome through control of replication initiation and nucleotide consumption. *Molecular and Cellular Biology*, **32**(20), 4226–36.
- Benada, J., & Macurek, L. (2015). Targeting the Checkpoint to Kill Cancer Cells. *Biomolecules*, **5**(3), 1912.
- Bener, G., Félix, A. J., Sánchez de Diego, C., Pascual Fabregat, I., Ciudad, C. J., & Noé, V. (2016). Silencing of CD47 and SIRP α by Polypurine reverse Hoogsteen hairpins to promote MCF-7 breast cancer cells death by PMA-differentiated THP-1 cells. *BMC Immunology*, **17**(1), 1–12.
- Berg, R. W., Ferguson, P. J., Vincent, M. D., & Koropatnick, D. J. (2003). A "combination oligonucleotide" antisense strategy to downregulate thymidylate synthase and decrease tumor cell growth and drug resistance. *Cancer Gene Therapy*, **10**(4), 278–286.

Bibliography

- Berger, S. H., Jenh, C. H., Johnson, L. F., & Berger, F. G. (1985). Thymidylate synthase overproduction and gene amplification in fluorodeoxyuridine-resistant human cells. *Molecular Pharmacology*, **28**(5).
- Blackford, A. N., & Jackson, S. P. (2017). ATM, ATR, and DNA-PK: The Trinity at the Heart of the DNA Damage Response. *Molecular Cell*, **66**(6), 801–817.
- Brunn, N. D., Dibrov, S. M., Kao, M. B., Ghassemian, M., & Hermann, T. (2014). Analysis of mRNA recognition by human thymidylate synthase. *Bioscience Reports*, **34**(6), 905–913.
- Bulbake, U., Doppalapudi, S., Kommineni, N., & Khan, W. (2017). Liposomal formulations in clinical use: An updated review. *Pharmaceutics*, **9**(2). doi:10.3390/pharmaceutics9020012
- Bulcha, J. T., Wang, Y., Ma, H., Tai, P. W. L., & Gao, G. (2021). Viral vector platforms within the gene therapy landscape. *Signal Transduction and Targeted Therapy*, **6**(1), 1–24.
- Calvo-Lozano, O., Aviñó, A., Friaiza, V., ... Lechuga, L. M. (2020). Fast and accurate pneumocystis pneumonia diagnosis in human samples using a label-free plasmonic biosensor. *Nanomaterials*, **10**(6), 1–18.
- Capecchi, M. R. (1980). High efficiency transformation by direct microinjection of DNA into cultured mammalian cells. *Cell*, **22**(2), 479–488.
- Carreras, C. W., & Santi, D. V. (1995). The Catalytic Mechanism and Structure of Thymidylate Synthase. *Annual Review of Biochemistry*, **64**(1), 721–762.
- Carter, B. Z., Milella, M., Altieri, D. C., & Andreeff, M. (2001). Cytokine-regulated expression of survivin in myeloid leukemia. *Blood*, **97**(9), 2784–2790.
- Casal-Dujat, L., Griffiths, P. C., Rodríguez-Abreu, C., Solans, C., Rogers, S., & Pérez-García, L. (2013). Nanocarriers from dicationic bis-imidazolium amphiphiles and their interaction with anionic drugs. *Journal of Materials Chemistry B*, **1**(38), 4963–4971.
- Casal-Dujat, L., Rodrigues, M., Yagüe, A., ... Peírez-García, L. (2012). Gemini imidazolium amphiphiles for the synthesis, stabilization, and drug delivery from gold nanoparticles. *Langmuir*, **28**(5), 2368–2381.
- Castedo, M., Perfettini, J.-L., Roumier, T., Andreau, K., Medema, R., & Kroemer, G. (2004). Cell death by mitotic catastrophe: a molecular definition. *Oncogene*, **23**(16), 2825–2837.
- Chambers, V. S., Marsico, G., Boutell, J. M., Di Antonio, M., Smith, G. P., & Balasubramanian, S. (2015). High-throughput sequencing of DNA G-quadruplex structures in the human genome. *Nature Biotechnology*, **33**(8), 877–881.
- Chan, P. P., Lin, M., Fawad Faruqi, A., Powell, J., Seidman, M. M., & Glazer, P. M. (1999). Targeted correction of an episomal gene in mammalian cells by a short DNA fragment tethered to a triplex-forming oligonucleotide. *Journal of Biological Chemistry*, **274**(17), 11541–11548.
- Chandler, S. P., & Fox, K. R. (1995). Extension of DNA triple helix formation to a neighbouring (AT)_n site. *FEBS Letters*, **360**(1), 21–25.
- Chandler, S. P., & Fox, K. R. (1996). Specificity of antiparallel DNA triple helix formation. *Biochemistry*, **35**(47), 15038–15048.
- Chen, J., Jia, X., Li, Z., ... Song, P. (2021). Targeting WEE1 by adavosertib inhibits

- the malignant phenotypes of hepatocellular carcinoma. *Biochemical Pharmacology*, **188**, 114494.
- Chen, S., Su, L., Qiu, J., ... Li, D. (2013). Mechanistic studies for the role of cellular nucleic-acid-binding protein (CNBP) in regulation of c-myc transcription. *Biochimica et Biophysica Acta - General Subjects*, **1830**(10), 4769–4777.
- Chu, E. (1996). Identification of in vivo target RNA sequences bound by thymidylate synthase. *Nucleic Acids Research*, **24**(16), 3222–3228.
- Chu, E., Callender, M. A., Farrell, M. P., & Schmitz, J. C. (2003). Thymidylate synthase inhibitors as anticancer agents: From bench to bedside. In *Cancer Chemotherapy and Pharmacology, Supplement*, Vol. 52, Cancer Chemother Pharmacol. doi:10.1007/s00280-003-0625-9
- Chu, E., Copur, S. M., Ju, J., ... Allegra, C. J. (1999). Thymidylate Synthase Protein and p53 mRNA Form an In Vivo Ribonucleoprotein Complex. *Molecular and Cellular Biology*, **19**(2), 1582–1594.
- Chu, E., Koeller, D. M., Casey, J. L., ... Allegra, C. J. (1991). Autoregulation of human thymidylate synthase messenger RNA translation by thymidylate synthase. *Proceedings of the National Academy of Sciences of the United States of America*, **88**(20), 8977–8981.
- Chu, E., Takechi, T., Jones, K. L., ... Allegra, C. J. (1995). Thymidylate synthase binds to c-myc RNA in human colon cancer cells and in vitro. *Molecular and Cellular Biology*, **15**(1), 179–185.
- Chu, E., Voeller, D., Koeller, D. M., ... Allegra, C. J. (1993). Identification of an RNA binding site for human thymidylate synthase. *Proceedings of the National Academy of Sciences of the United States of America*, **90**(2), 517–521.
- Ciudad, C. J., Enriquez, M. M. M., Félix, A. J., Bener, G., & Noé, V. (2019). Silencing PD-1 and PD-L1: The potential of PolyPurine Reverse Hoogsteen hairpins for the elimination of tumor cells. *Immunotherapy*, **11**(5), 369–372.
- Ciudad, C. J., Rodríguez, L., Villalobos, X., Félix, A. J., & Noé, V. (2017). Polypurine Reverse Hoogsteen Hairpins as a Gene Silencing Tool for Cancer. *Current Medicinal Chemistry*, **24**(26), 2809–2826.
- Cogoi, S., Quadrifoglio, F., & Xodo, L. E. (2004). G-rich Oligonucleotide Inhibits the Binding of a Nuclear Protein to the Ki-ras Promoter and Strongly Reduces Cell Growth in Human Carcinoma Pancreatic Cells. *Biochemistry*, **43**(9), 2512–2523.
- Cogoi, S., Shchekotikhin, A. E., & Xodo, L. E. (2014). HRAS is silenced by two neighboring G-quadruplexes and activated by MAZ, a zinc-finger transcription factor with DNA unfolding property. *Nucleic Acids Research*, **42**(13), 8379–8388.
- Cogoi, S., & Xodo, L. E. (2006). G-quadruplex formation within the promoter of the KRAS proto-oncogene and its effect on transcription. *Nucleic Acids Research*, **34**(9), 2536–2549.
- Coma, S., Noé, V., Eritja, R., & Ciudad, C. J. (2005). Strand Displacement of Double-Stranded DNA by Triplex-Forming Antiparallel Purine-Hairpins. *Oligonucleotides*, **15**(4), 269–283.
- Coma, S., Noe, V., Lavarino, C., ... Ciudad, C. J. (2004). Use of siRNAs and antisense oligonucleotides against survivin RNA to inhibit steps leading to

- tumor angiogenesis. *Oligonucleotides*, **14**(2), 100–113.
- Conde, J., Ambrosone, A., Hernandez, Y., ... De La Fuente, J. M. (2015). 15 years on siRNA delivery: Beyond the State-of-the-Art on inorganic nanoparticles for RNAi therapeutics. *Nano Today*, **10**(4), 421–450.
- Cooper, G. M. (2000). The Development and Causes of Cancer. *The Cell, 2nd Edition A Molecular Approach*. Retrieved from <https://www.ncbi.nlm.nih.gov/books/NBK9963/>
- Craig Venter, J., Adams, M. D., Myers, E. W., ... Zhu, X. (2001). The sequence of the human genome. *Science*, **291**(5507), 1304–1351.
- Cressey, D. (2012). Europe nears first approval for gene therapy. *Nature*. doi:10.1038/nature.2012.11048
- Cubero, E., Güimil-García, R., Luque, F. J., Eritja, R., & Orozco, M. (2001). *The effect of amino groups on the stability of DNA duplexes and triplexes based on purines derived from inosine*. *Nucleic Acids Research*, Vol. 29.
- Cuneo, K. C., Morgan, M. A., Sahai, V., ... Lawrence, T. S. (2019). Dose Escalation Trial of the Wee1 Inhibitor Adavosertib (AZD1775) in Combination With Gemcitabine and Radiation for Patients With Locally Advanced Pancreatic Cancer. *Journal of Clinical Oncology*, JCO.19.00730.
- Dana, H., Chalbatani, G. M., Mahmoodzadeh, H., ... Gharagouzlo, E. (2017). Molecular Mechanisms and Biological Functions of siRNA. *International Journal of Biomedical Science : IJBS*, **13**(2), 48–57.
- Dassie, J. P., Liu, X. Y., Thomas, G. S., ... Giangrande, P. H. (2009). Systemic administration of optimized aptamer-siRNA chimeras promotes regression of PSMA-expressing tumors. *Nature Biotechnology*, **27**(9), 839–846.
- de Almagro, M. C., Coma, S., Noé, V., & Ciudad, C. J. (2009). Polypurine hairpins directed against the template strand of DNA knock down the expression of mammalian genes. *Journal of Biological Chemistry*, **284**(17), 11579–89.
- de Almagro, M. C., Mencia, N., Noé, V., & Ciudad, C. J. (2011). Coding polypurine hairpins cause target-induced cell death in breast cancer cells. *Human Gene Therapy*, **22**(4), 451–463.
- De La Faverie, A. R., Guédin, A., Bedrat, A., Yatsunyk, L. A., & Mergny, J. L. (2014). Thioflavin T as a fluorescence light-up probe for G4 formation. *Nucleic Acids Research*, **42**(8), e65.
- Devroe, E., & Silver, P. A. (2002). Retrovirus-delivered siRNA. *BMC Biotechnology*, **2**, 15.
- Dexheimer, T. S., Sun, D., & Hurley, L. H. (2006). Deconvoluting the structural and drug-recognition complexity of the G-quadruplex-forming region upstream of the bcl-2 P1 promoter. *Journal of the American Chemical Society*, **128**(16), 5404–5415.
- Deyle, D. R., & Russell, D. W. (2009, August). Adeno-associated virus vector integration. *Current Opinion in Molecular Therapeutics*, NIH Public Access, pp. 442–447.
- Dirin, M., & Winkler, J. (2013). Influence of diverse chemical modifications on the ADME characteristics and toxicology of antisense oligonucleotides. *Expert Opinion on Biological Therapy*, **13**(6), 875–888.
- Dobbelstein, M., & Sørensen, C. S. (2015). Exploiting replicative stress to treat

- cancer. *Nature Reviews Drug Discovery*, **14**(6), 405–423.
- Doggrell, S. A. (2005). Pegaptanib: The first antiangiogenic agent approved for neovascular macular degeneration. *Expert Opinion on Pharmacotherapy*, **6**(8), 1421–1423.
- Douglas, J. T., Rogers, B. E., Rosenfeld, M. E., Michael, S. I., Feng, M., & Curiel, D. T. (1996). Targeted Gene Delivery by Tropism-Modified Adenoviral Vectors. *Nature Biotechnology*, **14**(11), 1574–1578.
- Drygin, D., Siddiqui-Jain, A., O'Brien, S., ... Rice, W. G. (2009). Anticancer Activity of CX-3543: A Direct Inhibitor of rRNA Biogenesis. *Cancer Research*, **69**(19), 7653–7661.
- Dubruel, P., Christiaens, B., Vanloo, B., ... Schacht, E. (2003). Physicochemical and biological evaluation of cationic polymethacrylates as vectors for gene delivery. *European Journal of Pharmaceutical Sciences*, **18**(3–4), 211–220.
- Duca, M., Vekhoff, P., Oussedik, K., Halby, L., & Arimondo, P. B. (2008). The triple helix: 50 years later, the outcome. *Nucleic Acids Research*, **36**(16), 5123–5138.
- Eckstein, F. (2014, December 1). Phosphorothioates, essential components of therapeutic oligonucleotides. *Nucleic Acid Therapeutics*, Mary Ann Liebert Inc., pp. 374–387.
- EMA. (2020). Novartis receives EU approval for Leqvio®* (inclisiran), a first-in-class siRNA to lower cholesterol with two doses a year** | Novartis. Retrieved April 3, 2021, from <https://www.novartis.com/news/media-releases/novartis-receives-eu-approval-leqvio-inclisiran-first-class-sirna-lower-cholesterol-two-doses-year>
- Enríquez, M. M. M., Félix, A. J., Ciudad, C. J., ... Noé, V. (2018). Cancer immunotherapy using PolyPurine Reverse Hoogsteen hairpins targeting the PD-1/PD-L1 pathway in human tumor cells. *PLoS ONE*, **13**(11), 1–17.
- Ersching, J., Hernandez, M. I. M., Cezarotto, F. S., ... Pinto, A. R. (2010). Neutralizing antibodies to human and simian adenoviruses in humans and New-World monkeys. *Virology*, **407**(1), 1–6.
- European Medicines Agency. (2015). First oncolytic immunotherapy medicine recommended for approval | European Medicines Agency. Retrieved April 2, 2021, from <https://www.ema.europa.eu/en/news/first-oncolytic-immunotherapy-medicine-recommended-approval>
- European Medicines Agency. (2020a). EMA recommends first COVID-19 vaccine for authorisation in the EU | European Medicines Agency. Retrieved January 7, 2021, from <https://www.ema.europa.eu/en/news/ema-recommends-first-covid-19-vaccine-authorisation-eu>
- European Medicines Agency. (2020b). Zalmoxis | European Medicines Agency. Retrieved April 2, 2021, from <https://www.ema.europa.eu/en/medicines/human/EPAR/zalmoxis#authorisation-details-section>
- European Medicines Agency. (2021). EMA recommends COVID-19 Vaccine Moderna for authorisation in the EU | European Medicines Agency. Retrieved January 7, 2021, from <https://www.ema.europa.eu/en/news/ema-recommends-covid-19-vaccine-moderna-authorisation-eu>
- Falleni, M., Pellegrini, C., Marchetti, A., ... Bosari, S. (2003). Survivin gene

Bibliography

- expression in early-stage non-small cell lung cancer. *The Journal of Pathology*, **200**(5), 620–626.
- Faraoni, I., & Graziani, G. (2018, December 1). Role of BRCA mutations in cancer treatment with poly(ADP-ribose) polymerase (PARP) inhibitors. *Cancers*, MDPI AG. doi:10.3390/cancers10120487
- FDA. (1996). FDA approves DaunoXome as first-line therapy for Kaposi's sarcoma. Food and Drug Administration. *Journal of the International Association of Physicians in AIDS Care*, **2**(5), 50–51.
- FDA. (2017). FDA approves CAR-T cell therapy to treat adults with certain types of large B-cell lymphoma | FDA. Retrieved April 2, 2021, from <https://www.fda.gov/news-events/press-announcements/fda-approves-car-t-cell-therapy-treat-adults-certain-types-large-b-cell-lymphoma>
- FDA. (2020a). Moderna COVID-19 Vaccine | FDA. Retrieved January 7, 2021, from <https://www.fda.gov/emergency-preparedness-and-response/coronavirus-disease-2019-covid-19/moderna-covid-19-vaccine>
- FDA. (2020b). Pfizer-BioNTech COVID-19 Vaccine | FDA. Retrieved January 7, 2021, from <https://www.fda.gov/emergency-preparedness-and-response/coronavirus-disease-2019-covid-19/pfizer-biontech-covid-19-vaccine>
- FDA News Release. (2020). FDA Approves First Drug to Treat Rare Metabolic Disorder | FDA. Retrieved December 9, 2020, from <https://www.fda.gov/news-events/press-announcements/fda-approves-first-drug-treat-rare-metabolic-disorder>
- Fedor, M. J., & Williamson, J. R. (2005, May). The catalytic diversity of RNAs. *Nature Reviews Molecular Cell Biology*, Nature Publishing Group, pp. 399–412.
- Félix, A. J., Ciudad, C. J., & Noé, V. (2020a). Correction of the apt Gene Using Repair-Polypurine Reverse Hoogsteen Hairpins in Mammalian Cells. *Molecular Therapy - Nucleic Acids*, **19**(March), 683–695.
- Félix, A. J., Solé, A., Noé, V., & Ciudad, C. J. (2020b). Gene Correction of Point Mutations Using PolyPurine Reverse Hoogsteen Hairpins Technology. *Frontiers in Genome Editing*, **2**, 583577.
- Felsenfeld, G., Davies, D. R., & Rich, A. (1957). Formation of a Three-Stranded Polynucleotide Molecule. *Journal of the American Chemical Society*, American Chemical Society, pp. 2023–2024.
- Ferguson, P. J., Collins, O., Dean, N. M., ... Koropatnick, J. (1999). Antisense down-regulation of thymidylate synthase to suppress growth and enhance cytotoxicity of 5-FUdR, 5-FU and Tomudex in HeLa cells. *British Journal of Pharmacology*, **127**(8), 1777–1786.
- Fire, A., Xu, S., Montgomery, M. K., Kostas, S. A., Driver, S. E., & Mello, C. C. (1998). Potent and specific genetic interference by double-stranded RNA in *Caenorhabditis elegans*. *Nature*, **391**(6669), 806–811.
- Fischer, U., Jänicke, R. U., & Schulze-Osthoff, K. (2003, January 1). Many cuts to ruin: A comprehensive update of caspase substrates. *Cell Death and Differentiation*, Nature Publishing Group, pp. 76–100.
- Forment, J. V., & O'connor, M. J. (2018). Targeting the replication stress response in cancer. *Pharmacology and Therapeutics*, **188**, 155–167.

- Franco, Y. L., Vaidya, T. R., & Ait-Oudhia, S. (2018). Anticancer and cardio-protective effects of liposomal doxorubicin in the treatment of breast cancer. *Breast Cancer: Targets and Therapy*, Dove Medical Press Ltd., pp. 131–141.
- Fujihara, J., Yasuda, T., Ueki, M., Iida, R., & Takeshita, H. (2012, November 1). Comparative biochemical properties of vertebrate deoxyribonuclease I. *Comparative Biochemistry and Physiology - B Biochemistry and Molecular Biology*, Elsevier Inc., pp. 263–273.
- Garber, K. (2006). China Approves World's First Oncolytic Virus Therapy For Cancer Treatment. *JNCI: Journal of the National Cancer Institute*, **98**(5), 298–300.
- Garg, D., Henrich, S., Salo-Ahen, O. M. H., Myllykallio, H., Costi, M. P., & Wade, R. C. (2010). Novel Approaches for Targeting Thymidylate Synthase To Overcome the Resistance and Toxicity of Anticancer Drugs. *Journal of Medicinal Chemistry*, **53**(18), 6539–6549.
- Garraway, L. A., & Lander, E. S. (2013, March 28). Lessons from the cancer genome. *Cell*, Cell Press, pp. 17–37.
- Geary, R. S., Norris, D., Yu, R., & Bennett, C. F. (2015, June 29). Pharmacokinetics, biodistribution and cell uptake of antisense oligonucleotides. *Advanced Drug Delivery Reviews*, Elsevier, pp. 46–51.
- Ghelli Luserna Di Rorà, A., Cerchione, C., Martinelli, G., & Simonetti, G. (2020, September 21). A WEE1 family business: Regulation of mitosis, cancer progression, and therapeutic target. *Journal of Hematology and Oncology*, BioMed Central Ltd. doi:10.1186/s13045-020-00959-2
- Gianani, R., Jarboe, E., Orlicky, D., ... Shroyer, K. R. (2001). Expression of survivin in normal, hyperplastic, and neoplastic colonic mucosa. *Human Pathology*, **32**(1), 119–125.
- Giraldo, S., Alea-Reyes, M. E., Limón, D., ... Pérez-García, L. (2020). π -Donor/ π -Acceptor interactions for the encapsulation of neurotransmitters on functionalized polysilicon-based microparticles. *Pharmaceutics*, **12**(8), 1–19.
- Gmeiner, W. (2012). Novel Chemical Strategies for Thymidylate Synthase Inhibition. *Current Medicinal Chemistry*, **12**(2), 191–202.
- Gold, L. (2015, December 1). SELEX: How It Happened and Where It will Go. *Journal of Molecular Evolution*, Springer New York LLC, pp. 140–143.
- Goñi, J. R., de la Cruz, X., & Orozco, M. (2004). Triplex-forming oligonucleotide target sequences in the human genome. *Nucleic Acids Research*, **32**(1), 354–360.
- Goñi, J. R., Vaquerizas, J. M., Dopazo, J., & Orozco, M. (2006). Exploring the reasons for the large density of triplex-forming oligonucleotide target sequences in the human regulatory regions. *BMC Genomics*, **7**. doi:10.1186/1471-2164-7-63
- Goswami, R., Subramanian, G., Silayeva, L., ... Betapudi, V. (2019, April 24). Gene therapy leaves a vicious cycle. *Frontiers in Oncology*, Frontiers Media S.A., p. 297.
- Gowers, D. M., & Fox, K. R. (1999). *Towards mixed sequence recognition by triple helix formation*. *Nucleic Acids Research*, Vol. 27.
- Gralewska, P., Gajek, A., Marczak, A., & Rogalska, A. (2020). Participation of the ATR/CHK1 pathway in replicative stress targeted therapy of high-grade ovarian

Bibliography

- cancer. *Journal of Hematology & Oncology*, **13**(39). doi:10.1186/s13045-020-00874-6
- Griffin, L. C., & Dervan, P. B. (1989). Recognition of thymine-adenine base pairs by guanine in a pyrimidine triple helix motif. *Science*, **245**(4921), 967–971.
- Gu, X., Lin, H., Shao, J., Zhang, M., & Liang, H. (2005). Analysis of survivin expression in the subtypes of lymphoma. *Chinese-German Journal of Clinical Oncology*, **4**(4), 238–243.
- Hagner, N., & Joerger, M. (2010). Cancer chemotherapy: targeting folic acid synthesis. *Cancer Management and Research*, **2**, 293–301.
- Hair, P., Cameron, F., & McKeage, K. (2013). Mipomersen sodium: First global approval. *Drugs*, **73**(5), 487–493.
- Hanahan, D., & Weinberg, R. A. (2011). Hallmarks of cancer: the next generation. *Cell*, **144**(5), 646–74.
- Hauptenthal, J., Baehr, C., Kiermayer, S., Zeuzem, S., & Piiper, A. (2006). Inhibition of RNase A family enzymes prevents degradation and loss of silencing activity of siRNAs in serum. *Biochemical Pharmacology*, **71**(5), 702–710.
- Havre, P. A., Gunther, E. J., Gasparro, F. P., & Glazer, P. M. (1993). Targeted mutagenesis of DNA using triple helix-forming oligonucleotides linked to psoralen. *Proceedings of the National Academy of Sciences of the United States of America*, **90**(16), 7879–7883.
- Hazan-Halevy, I., Landesman-Milo, D., Rosenblum, D., Mizrahy, S., Ng, B. D., & Peer, D. (2016). Immunomodulation of hematological malignancies using oligonucleotides based-nanomedicines. *Journal of Controlled Release*, **244**, 149–156.
- Heidelberg, C. (1981). On the rational development of a new drug: The example of the fluorinated pyrimidines. *Cancer Treatment Reports*, **65**(Suppl. 3), 3–9.
- Heidelberg, C., Chaudhuri, N. K., Danneberg, P., ... Scheiner, J. (1957). Fluorinated pyrimidines, a new class of tumour-inhibitory compounds. *Nature*, **179**(4561), 663–666.
- Heo, Y. A. (2020, February 1). Golodirsen: First Approval. *Drugs*, Adis, pp. 329–333.
- Hernandez, J. M., Farma, J. M., Coppola, D., ... Shibata, D. (2011). Expression of the antiapoptotic protein survivin in colon cancer. *Clinical Colorectal Cancer*, **10**(3), 188–193.
- Hieronimus, R., & Müller, S. (2019). Engineering of hairpin ribozyme variants for RNA recombination and splicing. *Annals of the New York Academy of Sciences*, **1447**(1), 135–143.
- Hilbers, C. W., Haasnoot, C. A. G., de Bruin, S. H., Joordens, J. J. M., Van Der Marel, G. A., & Van Boom, J. H. (1985). Hairpin formation in synthetic oligonucleotides. *Biochimie*, **67**(7–8), 685–695.
- Hoogsteen, K. (1959). The structure of crystals containing a hydrogen-bonded complex of 1-methylthymine and 9-methyladenine. *Acta Crystallographica*, **12**(10), 822–823.
- Hoogsteen, K. (1963). The crystal and molecular structure of a hydrogen-bonded complex between 1-methylthymine and 9-methyladenine. *Acta Crystallographica*, **16**(9), 907–916.
- Hoy, S. M. (2017). Nusinersen: First Global Approval. *Drugs*, **77**(4), 473–479.

- Huang, R. X., & Zhou, P. K. (2020, December 1). DNA damage response signaling pathways and targets for radiotherapy sensitization in cancer. *Signal Transduction and Targeted Therapy*, Springer Nature, pp. 1–27.
- Huertas, C. S., Aviñó, A., Kurachi, C., ... Lechuga, L. M. (2018). Label-free DNA-methylation detection by direct ds-DNA fragment screening using poly-purine hairpins. *Biosensors and Bioelectronics*, **120**, 47–54.
- Huertas, C. S., Carrascosa, L. G., Bonnal, S., Valcárcel, J., & Lechuga, L. M. (2016). Quantitative evaluation of alternatively spliced mRNA isoforms by label-free real-time plasmonic sensing. *Biosensors and Bioelectronics*, **78**, 118–125.
- Hutcherson, S. L., & Lanz, R. (2002). A randomized controlled clinical trial of intravitreal fomivirsen for treatment of newly diagnosed peripheral cytomegalovirus retinitis in patients with aids. *American Journal of Ophthalmology*, **133**(4), 467–474.
- IARC. (2020). Latest global cancer data : Cancer burden rises to 19.3 million new cases and 10.0 million cancer deaths in 2020, (December), 1–3.
- Ito, R., Asami, S., Motohashi, S., ... Suzuki, T. (2005). Significance of survivin mRNA expression in prognosis of neuroblastoma. *Biological and Pharmaceutical Bulletin*, **28**(4), 565–568.
- Jackson, L. A., Anderson, E. J., Roupheal, N. G., ... Beigel, J. H. (2020). An mRNA Vaccine against SARS-CoV-2 — Preliminary Report. *New England Journal of Medicine*, **383**(20), 1920–1931.
- Jaecle, K. A., Batchelor, T., O’Day, S. J., ... Howell, S. B. (2002). An open label trial of sustained-release cytarabine (DepoCyt[®]) for the intrathecal treatment of solid tumor neoplastic meningitis. *Journal of Neuro-Oncology*, **57**(3), 231–239.
- Johnson & Johnson. (2020). Johnson & Johnson Announces. Retrieved April 1, 2021, from <https://www.jnj.com/johnson-johnson-announces-european-commission-approval-for-janssens-preventive-ebola-vaccine>
- Johnston, P. G., Lenz, H.-J., Leichman, C. G., ... Leichman, L. (1995). Thymidylate Synthase Gene and Protein Expression Correlate and Are Associated with Response to 5-Fluorouracil in Human Colorectal and Gastric Tumors. *Cancer Research*, **55**(7).
- Ju, J., Pedersen-Lane, J., Maley, F., & Chu, E. (1999). Regulation of p53 expression by thymidylate synthase. *Proceedings of the National Academy of Sciences of the United States of America*, **96**(7), 3769–3774.
- Judge, A. D., Sood, V., Shaw, J. R., Fang, D., McClintock, K., & MacLachlan, I. (2005). Sequence-dependent stimulation of the mammalian innate immune response by synthetic siRNA. *Nature Biotechnology*, **23**(4), 457–462.
- Juliano, R. L. (2016, August 19). The delivery of therapeutic oligonucleotides. *Nucleic Acids Research*, Oxford University Press, pp. 6518–6548.
- Kamimura, K., Suda, T., Zhang, G., & Liu, D. (2011). Advances in gene delivery systems. *Pharmaceutical Medicine*, Springer International Publishing, pp. 293–306.
- Kaneda, S., Nalbantoglu, J., Takeishi, K., ... Ayusawa, D. (1990). Structural and functional analysis of the human thymidylate synthase gene. *Journal of Biological Chemistry*, **265**(33), 20277–20284.

Bibliography

- Keam, S. J. (2018). Inotersen: First Global Approval. *Drugs*, **78**(13), 1371–1376.
- Keefe, A. D., Pai, S., & Ellington, A. (2010, July). Aptamers as therapeutics. *Nature Reviews Drug Discovery*, Nature Publishing Group, pp. 537–550.
- Keeler, A. M., & Flotte, T. R. (2019). Recombinant Adeno-Associated Virus Gene Therapy in Light of Luxturna (and Zolgensma and Glybera): Where Are We, and How Did We Get Here? *Annual Review of Virology*, **6**(1), 601–621.
- Kemme, C. A., Nguyen, D., Chattopadhyay, A., & Iwahara, J. (2016, August 7). Regulation of transcription factors via natural decoys in genomic DNA. *Transcription*, Taylor and Francis Inc., pp. 115–120.
- Khot, A., Brajanovski, N., Cameron, D. P., ... Harrison, S. J. (2019). First-in-Human RNA Polymerase I Transcription Inhibitor CX-5461 in Patients with Advanced Hematologic Cancers: Results of a Phase I Dose-Escalation Study. *Cancer Discovery*, **9**(8), 1036–1049.
- Kikin, O., D'Antonio, L., & Bagga, P. S. (2006). QGRS Mapper: A web-based server for predicting G-quadruplexes in nucleotide sequences. *Nucleic Acids Research*, **34**(WEB. SERV. ISS.), W676-82.
- Kim, H. J., Greenleaf, J. F., Kinnick, R. R., Bronk, J. T., & Bolander, M. E. (1996). Ultrasound-mediated transfection of mammalian cells. *Human Gene Therapy*, **7**(11), 1339–1346.
- Kim, N. (2017). The Interplay between G-quadruplex and Transcription. *Current Medicinal Chemistry*, **26**(16), 2898–2917.
- Kim, S., Federman, N., Gordon, E. M., Hall, F. L., & Chawla, S. P. (2017). Rexin-G®, a tumor-targeted retrovector for malignant peripheral nerve sheath tumor: A case report. *Molecular and Clinical Oncology*, **6**(6), 861–865.
- Kim, T. K., & Eberwine, J. H. (2010). Mammalian cell transfection: The present and the future. *Analytical and Bioanalytical Chemistry*, **397**(8), 3173–3178.
- Kiu, K. T., Hwang, T. I. S., Hsieh, H. Y., Shen, C. H., Wang, Y. H., & Juang, G. D. (2014). Expression of survivin in bladder cancer cell lines using quantitative real-time polymerase chain reaction. *Urological Science*, **25**(1), 19–21.
- Klein, T. M., Sanford, J. C., Wolf, E. D., & Wu, R. (1987). High-velocity microprojectiles for delivering nucleic acids into living cells. *Nature*, **327**(6117), 70–73.
- Knauert, M. P., & Glazer, P. M. (2001, October 1). Triplex forming oligonucleotides: Sequence-specific tools for gene targeting. *Human Molecular Genetics*, Oxford University Press, pp. 2243–2251.
- Koeneman, K. S., Kao, C., Ko, S. C., ... Gardner, T. A. (2000). Osteocalcin-directed gene therapy for prostate-cancer bone metastasis. *World Journal of Urology*, **18**(2), 102–110.
- Kogiso, T., Nagahara, H., Hashimoto, E., Ariizumi, S., Yamamoto, M., & Shiratori, K. (2014). Efficient induction of apoptosis by wee1 kinase inhibition in hepatocellular carcinoma cells. *PLoS One*, **9**(6), e100495.
- Kremer, E. J., Boutin, S., Chillon, M., & Danos, O. (2000). Canine Adenovirus Vectors: an Alternative for Adenovirus-Mediated Gene Transfer. *Journal of Virology*, **74**(1), 505–512.
- Krug, L. M., Wozniak, A. J., Kindler, H. L., ... Sharma, S. (2014). Randomized phase II trial of pemetrexed/cisplatin with or without CBP501 in patients with advanced

- malignant pleural mesothelioma. *Lung Cancer (Amsterdam, Netherlands)*, **85**(3), 429–34.
- Kruger, K., Grabowski, P. J., Zaug, A. J., Sands, J., Gottschling, D. E., & Cech, T. R. (1982). Self-splicing RNA: Autoexcision and autocyclization of the ribosomal RNA intervening sequence of tetrahymena. *Cell*, **31**(1), 147–157.
- Kumari, S., Bugaut, A., Huppert, J. L., & Balasubramanian, S. (2007). An RNA G-quadruplex in the 5' UTR of the NRAS proto-oncogene modulates translation. *Nature Chemical Biology*, **3**(4), 218–221.
- Kuznetsov, S. V., Ren, C. C., Woodson, S. A., & Ansari, A. (2008). Loop dependence of the stability and dynamics of nucleic acid hairpins. *Nucleic Acids Research*, **36**(4), 1098–1112.
- Lander, E. S., Linton, L. M., Birren, B., ... Chen, Y. J. (2001). Initial sequencing and analysis of the human genome: International Human Genome Sequencing Consortium (Nature (2001) 409 (860-921)). *Nature*, **412**(6846), 565–566.
- Landmesser, U., Poller, W., Tsimikas, S., Most, P., Paneni, F., & Lü Scher, T. F. (2020). From traditional pharmacological towards nucleic acid-based therapies for cardiovascular diseases. *European Heart Journal*, **41**(40), 3884–3899.
- Laquente, B., Lopez-Martin, J., Richards, D., ... Calvo, E. (2017). A phase II study to evaluate LY2603618 in combination with gemcitabine in pancreatic cancer patients. *BMC Cancer*, **17**(1), 137.
- Lee, C. S., Bishop, E. S., Zhang, R., ... He, T.-C. C. (2017). Adenovirus-mediated gene delivery: Potential applications for gene and cell-based therapies in the new era of personalized medicine. *Genes & Diseases*, **4**(2), 43–63.
- Lee, G. H., Joo, Y. E., Koh, Y. S., ... Kim, S. J. (2006). Expression of survivin in gastric cancer and its relationship with tumor angiogenesis. *European Journal of Gastroenterology and Hepatology*, **18**(9), 957–963.
- Leichman, C. G. (2001). Predictive and prognostic markers in gastrointestinal cancers. *Current Opinion in Oncology*, Curr Opin Oncol, pp. 291–299.
- Leijen, S., Van Geel, R. M. J. M., Pavlick, A. C., ... Shapiro, G. I. (2016). Phase I study evaluating WEE1 inhibitor AZD1775 as monotherapy and in combination with gemcitabine, cisplatin, or carboplatin in patients with advanced solid tumors. *Journal of Clinical Oncology*, **34**(36), 4371–4380.
- Lewis, C. W., Jin, Z., Macdonald, D., ... Chan, G. (2017). Prolonged mitotic arrest induced by Wee1 inhibition sensitizes breast cancer cells to paclitaxel. *Oncotarget*, **8**(43), 73705–73722.
- Li, C., & Samulski, R. J. (2020, April 1). Engineering adeno-associated virus vectors for gene therapy. *Nature Reviews Genetics*, Nature Research, pp. 255–272.
- Li, S., Wang, L., Meng, Y., Chang, Y., Xu, J., & Zhang, Q. (2017). Increased levels of LAPTM4B, VEGF and survivin are correlated with tumor progression and poor prognosis in breast cancer patients. *Oncotarget*, **8**(25), 41282–41293.
- Li, Y., Syed, J., & Sugiyama, H. (2016, November 17). RNA-DNA Triplex Formation by Long Noncoding RNAs. *Cell Chemical Biology*, Elsevier Ltd, pp. 1325–1333.
- Liang, H., Zhang, L., Xu, R., & Ju, X. L. (2013). Silencing of survivin using YM155 induces apoptosis and chemosensitization in neuroblastomas cells. *European Review for Medical and Pharmacological Sciences*, **17**(21), 2909–2915.
- Ligabue, A., Marverti, G., Liebl, U., & Myllykallio, H. (2012). Transcriptional

Bibliography

- Activation and Cell Cycle Block Are the Keys for 5-Fluorouracil Induced Up-Regulation of Human Thymidylate Synthase Expression. *PLoS ONE*, **7**(10). doi:10.1371/journal.pone.0047318
- Lin, H.-P., Singla, B., Ghoshal, P., ... Csányi, G. (2018). Identification of novel macropinocytosis inhibitors using a rational screen of Food and Drug Administration-approved drugs. *British Journal of Pharmacology*, **175**(18), 3640–3655.
- Liu, F., Song, Y. K., & Liu, D. (1999). Hydrodynamics-based transfection in animals by systemic administration of plasmid DNA. *Gene Therapy*, **6**(7), 1258–1266.
- Liu, J., Schmitz, J. C., Lin, X., ... Chu, E. (2002). Thymidylate synthase as a translational regulator of cellular gene expression. *Biochimica et Biophysica Acta - Molecular Basis of Disease*, **1587**(2–3), 174–182.
- Liu, Y., Li, D., Liu, Z., ... Zhang, C. Y. (2015). Targeted exosome-mediated delivery of opioid receptor Mu siRNA for the treatment of morphine relapse. *Scientific Reports*, **5**(1), 17543.
- Local, A., Zhang, H., Benbatoul, K. D., ... Rice, W. G. (2018). APTO-253 Stabilizes G-quadruplex DNA, Inhibits MYC Expression, and Induces DNA Damage in Acute Myeloid Leukemia Cells. *Molecular Cancer Therapeutics*, **17**(6), 1177–1186.
- Longley, D. B., Harkin, D. P., & Johnston, P. G. (2003). 5-Fluorouracil: mechanisms of action and clinical strategies. *Nature Reviews Cancer*, **3**(5), 330–338.
- Lundstrom, K., & Slade, N. (2018). Viral vectors in gene therapy. *Periodicum Biologorum*, **6**(2), 139–143.
- Luo, Y., Rockow-Magnone, S. K., Kroeger, P. E., ... Giranda, V. L. (2001). Blocking Chk1 expression induces apoptosis and abrogates the G2 checkpoint mechanism. *Neoplasia (New York, N.Y.)*, **3**(5), 411–9.
- Luther, D. C., Huang, R., Jeon, T., ... Rotello, V. M. (2020, January 1). Delivery of drugs, proteins, and nucleic acids using inorganic nanoparticles. *Advanced Drug Delivery Reviews*, Elsevier B.V., pp. 188–213.
- Macheret, M., & Halazonetis, T. D. (2015). DNA Replication Stress as a Hallmark of Cancer. *Annual Review of Pathology: Mechanisms of Disease*, **10**(1), 425–448.
- Macia, E., Ehrlich, M., Massol, R., Boucrot, E., Brunner, C., & Kirchhausen, T. (2006). Dynasore, a Cell-Permeable Inhibitor of Dynamin. *Developmental Cell*, **10**(6), 839–850.
- Mak, J. P. Y., Man, W. Y., Ma, H. T., & Poon, R. Y. C. (2014). Pharmacological targeting the ATR-CHK1-WEE1 axis involves balancing cell growth stimulation and apoptosis. *Oncotarget*, **5**(21), 10546–57.
- Makeyev, A. V., Eastmond, D. L., & Lieberhaber, S. A. (2002). *Targeting a KH-domain protein with RNA decoys*.
- Maude, S. L., Laetsch, T. W., Buechner, J., ... Grupp, S. A. (2018). Tisagenlecleucel in Children and Young Adults with B-Cell Lymphoblastic Leukemia. *New England Journal of Medicine*, **378**(5), 439–448.
- Mcdonald, C. D., & Maher, L. J. (1995). Recognition of duplex DNA by RNA polynucleotides. *Nucleic Acids Research*, **23**(3), 500–506.
- Meister, G., & Tuschl, T. (2004, September 16). Mechanisms of gene silencing by

- double-stranded RNA. *Nature*, Nature Publishing Group, pp. 343–349.
- Mencia, N., Selga, E., Noé, V., & Ciudad, C. J. (2011). Underexpression of miR-224 in methotrexate resistant human colon cancer cells. *Biochemical Pharmacology*, **82**(11), 1572–1582.
- Meric-Bernstam, F., & Mills, G. B. (2012, September). Overcoming implementation challenges of personalized cancer therapy. *Nature Reviews Clinical Oncology*, Nature Publishing Group, pp. 542–548.
- Mills, M., Völker, J., & Klump, H. H. (1996). Triple helical structures involving inosine: There is a penalty for promiscuity. *Biochemistry*, **35**(41), 13338–13344.
- Mittal, R., Jaiswal, P., & Goel, A. (2015). Survivin: A molecular biomarker in cancer. *Indian Journal of Medical Research*, **141**(4), 389.
- Mizutani, Y., Wada, H., Yoshida, O., ... Miki, T. (2003). Significance of Thymidylate Synthase Activity in Renal Cell Carcinoma. *Clinical Cancer Research*, **9**(4).
- Mu-Yong Kim, †, Hariprasad Vankayalapati, †, Kazuo Shin-ya, ‡, ... Hurley, L. H. (2002). Telomestatin, a potent telomerase inhibitor that interacts quite specifically with the human telomeric intramolecular G-quadruplex. *Journal of the American Chemical Society*, **124**(10), 2098–2099.
- Müller, S. (2015). Engineering of ribozymes with useful activities in the ancient RNA world. *Annals of the New York Academy of Sciences*, **1341**(1), 54–60.
- Nakagami, H. (2021). Development of COVID-19 vaccines utilizing gene therapy technology. *International Immunology*. doi:10.1093/intimm/dxab013
- Naso, M. F. (2017). Adeno-Associated Virus (AAV) as a Vector for Gene Therapy. *BioDrugs*, **31**(4), 315–332.
- Nasu, S., Yagihashi, A., Izawa, A., ... Watanabe, N. (2002). Survivin mRNA expression in patients with breast cancer. *Anticancer Research*, **22**(3), 1839–1843.
- Nayak, R. K., & Van Orden, A. (2013). Counterion and polythymidine loop-length-dependent folding and thermodynamic stability of DNA hairpins reveal the unusual counterion-dependent stability of tetraloop hairpins. *Journal of Physical Chemistry B*, **117**(45), 13956–13966.
- Nayerossadat, N., Ali, P., & Maedeh, T. (2012). Viral and nonviral delivery systems for gene delivery. *Advanced Biomedical Research*, **1**(1), 27.
- Neumann, E., Schaefer-Ridder, M., Wang, Y., & Hofschneider, P. H. (1982). Gene transfer into mouse lymphoma cells by electroporation in high electric fields. *The EMBO Journal*, **1**(7), 841–845.
- Ni, X., Castanares, M., Mukherjee, A., & Lupold, S. E. (2011). Nucleic Acid Aptamers: Clinical Applications and Promising New Horizons. *Current Medicinal Chemistry*, **18**(27), 4206–4214.
- Nielsen, F. C., Van Overeem Hansen, T., & Sørensen, C. S. (2016, September 1). Hereditary breast and ovarian cancer: New genes in confined pathways. *Nature Reviews Cancer*, Nature Publishing Group, pp. 599–612.
- Nielsen, T. T., & Nielsen, J. E. (2013, September). Antisense gene silencing: Therapy for neurodegenerative disorders? *Genes*, pp. 457–484.
- Noé, V., Aubets, E., Félix, A. J., & Ciudad, C. J. (2020, December 16). Nucleic acids therapeutics using PolyPurine Reverse Hoogsteen hairpins. *Biochemical Pharmacology*, Elsevier Inc., p. 114371.

Bibliography

- Noé, V., & Ciudad, C. J. (2021). Polypurine reverse-hoogsteen hairpins as a tool for exon skipping at the genomic level in mammalian cells. *International Journal of Molecular Sciences*, **22**(7). doi:10.3390/ijms22073784
- Nomura, T., Nakagawa, M., Fujita, Y., Hanada, T., Mimata, H., & Nomura, Y. (2002). Clinical significance of thymidylate synthase expression in bladder cancer. *International Journal of Urology*, **9**(7), 368–376.
- Novartis. (2018). Novartis announces FDA filing acceptance and Priority Review of AVXS-101, a one-time treatment designed to address the genetic root cause of SMA Type 1 | Novartis. Retrieved April 2, 2021, from <https://www.novartis.com/news/media-releases/novartis-announces-fda-filing-acceptance-and-priority-review-avxs-101-one-time-treatment-designed-address-genetic-root-cause-sma-type-1>
- Oleaga, C., Welten, S., Belloc, A., ... Ciudad, C. J. (2012). Identification of novel Sp1 targets involved in proliferation and cancer by functional genomics. *Biochemical Pharmacology*, **84**(12), 1581–1591.
- Pabla, N., Bhatt, K., & Dong, Z. (2012). Checkpoint kinase 1 (Chk1)-short is a splice variant and endogenous inhibitor of Chk1 that regulates cell cycle and DNA damage checkpoints. *Proceedings of the National Academy of Sciences*, **109**(1), 197–202.
- Pack, D. W., Hoffman, A. S., Pun, S., & Stayton, P. S. (2005, July). Design and development of polymers for gene delivery. *Nature Reviews Drug Discovery*, Nature Publishing Group, pp. 581–593.
- Paddison, P. J., Caudy, A. A., Bernstein, E., Hannon, G. J., & Conklin, D. S. (2002). Short hairpin RNAs (shRNAs) induce sequence-specific silencing in mammalian cells. *Genes and Development*, **16**(8), 948–958.
- Pajuste, K., Hyvönen, Z., Petrichenko, O., ... Plotniece, A. (2013). Gene delivery agents possessing antiradical activity: Self-assembling cationic amphiphilic 1,4-dihydropyridine derivatives. *New Journal of Chemistry*, **37**(10), 3062–3075.
- Palumbo, S. M. L., Ebbinghaus, S. W., & Hurley, L. H. (2009). Formation of a unique end-to-end stacked pair of G-quadruplexes in the hTERT core promoter with implications for inhibition of telomerase by G-quadruplex-interactive ligands. *Journal of the American Chemical Society*, **131**(31), 10878–10891.
- Pan, Q., Luo, F., Liu, M., & Zhang, X. L. (2018, August 1). Oligonucleotide aptamers: promising and powerful diagnostic and therapeutic tools for infectious diseases. *Journal of Infection*, W.B. Saunders Ltd, pp. 83–98.
- Panek, R. L., Lu, G. H., Klutchko, S. R., ... Keiser, J. A. (1997). *In Vitro Pharmacological Characterization of PD 166285, a New Nanomolar Potent and Broadly Active Protein Tyrosine Kinase Inhibitor*.
- Parsel, S. M., Grandis, J. R., & Thomas, S. M. (2016, June 23). Nucleic acid targeting: Towards personalized therapy for head and neck cancer. *Oncogene*, Nature Publishing Group, pp. 3217–3226.
- Patil, M., Pabla, N., & Dong, Z. (2014). Checkpoint kinase 1 in DNA damage response and cell cycle regulation. *Cellular and Molecular Life Sciences: CMLS*, **70**(21), 4009–4021.
- Pearson, S., Jia, H., & Kandachi, K. (2004). China approves first gene therapy. *Nature Biotechnology*, **22**(1), 3–4.

- Peery, R. C., Liu, J. Y., & Zhang, J. T. (2017, October 1). Targeting survivin for therapeutic discovery: past, present, and future promises. *Drug Discovery Today*, Elsevier Ltd, pp. 1466–1477.
- Peng, Z. (2005, September). Current status of gendicine in China: Recombinant human Ad-p53 agent for treatment of cancers. *Human Gene Therapy*, Hum Gene Ther, pp. 1016–1027.
- Penon, O., Marín, M. J., Russell, D. A., & Pérez-García, L. (2017). Water soluble, multifunctional antibody-porphyrin gold nanoparticles for targeted photodynamic therapy. *Journal of Colloid and Interface Science*, **496**, 100–110.
- Pestalozzi, B. C., Peterson, H. F., Gelber, R. D., ... Johnston, P. G. (1997). Prognostic importance of thymidylate synthase expression in early breast cancer. *Journal of Clinical Oncology*, **15**(5), 1923–1931.
- Peters, G. J., Backus, H. H. J., Freemantle, S., ... Pinedo, H. M. (2002). Induction of thymidylate synthase as a 5-fluorouracil resistance mechanism. *Biochimica et Biophysica Acta - Molecular Basis of Disease*, **1587**(2–3), 194–205.
- Peters, G. J., Van Triest, B., Backus, H. H. J., Kuiper, C. M., Van Der Wilt, C. L., & Pinedo, H. M. (2000). Molecular downstream events and induction of thymidylate synthase in mutant and wild-type p53 colon cancer cell lines after treatment with 5-fluorouracil and the thymidylate synthase inhibitor raltitrexed. *European Journal of Cancer*, **36**(7), 916–924.
- Petrichenko, O., Rucins, M., Vezane, A., ... Plotniece, A. (2015). Studies of the physicochemical and structural properties of self-assembling cationic pyridine derivatives as gene delivery agents. *Chemistry and Physics of Lipids*, **191**, 25–37.
- Phillips, M. I., Mohuczy-Dominiak, D., Coffey, M., ... Zelles, T. (1997). Prolonged reduction of high blood pressure with an in vivo, nonpathogenic, adeno-associated viral vector delivery of AT1-R mRNA antisense. *Hypertension*, **29**(1), 374–380.
- Phylactou, L. A., Kilpatrick, M. W., & Wood, M. J. A. (1998, September 1). Ribozymes as therapeutic tools for genetic disease. *Human Molecular Genetics*, Oxford Academic, pp. 1649–1653.
- Pichon, C., Billiet, L., & Midoux, P. (2010). Chemical vectors for gene delivery: uptake and intracellular trafficking. *Current Opinion in Biotechnology*, **21**, 640–645.
- Piedra, J., Ontiveros, M., Miravet, S., Penalva, C., Monfar, M., & Chillon, M. (2015). Development of a Rapid, Robust, and Universal PicoGreen-Based Method to Titer Adeno-Associated Vectors. *Human Gene Therapy Methods*, **26**(1), 35–42.
- Pol, J., Kroemer, G., & Galluzzi, L. (2016). First oncolytic virus approved for melanoma immunotherapy. *Oncoimmunology*, **5**(1), e1115641.
- Polack, F. P., Thomas, S. J., Kitchin, N., ... Gruber, W. C. (2020). Safety and Efficacy of the BNT162b2 mRNA Covid-19 Vaccine. *New England Journal of Medicine*, **383**(27), 2603–2615.
- Praseuth, D., Guieysse, A. L., & Hélène, C. (1999, December 10). Triple helix formation and the antigene strategy for sequence-specific control of gene expression. *Biochimica et Biophysica Acta - Gene Structure and Expression*,

Bibliography

- Elsevier, pp. 181–206.
- Pucci, C., Martinelli, C., & Ciofani, G. (2019, September 10). Innovative approaches for cancer treatment: Current perspectives and new challenges. *Ecancermedicalscience*, *ecancer* Global Foundation. doi:10.3332/ecancer.2019.961
- Puig, M., Piedra, J., Miravet, S., Segura, M. M., Chillon, M., & Bosch, A. (2014). *Adenovirus Methods and Protocols, 3rd Edition. Methods in Molecular Biology*, Vol. 1089.
- Purshotam, S., Mohit, C., Sitansh, S., & Abhijit, M. (2010). On the role of Hoogsteen:Hoogsteen interactions in RNA: Ab initio investigations of structures and energies. *RNA*, **16**(5), 942–957.
- Putney, S. D., Benkovic, S. J., & Schimmel, P. R. (1981). A DNA fragment with an α -phosphorothioate nucleotide at one end is asymmetrically blocked from digestion by exonuclease III and can be replicated in vivo. *Proceedings of the National Academy of Sciences of the United States of America*, **78**(12 II), 7350–7354.
- Qin, Y., & Hurley, L. H. (2008, August). Structures, folding patterns, and functions of intramolecular DNA G-quadruplexes found in eukaryotic promoter regions. *Biochimie*, NIH Public Access, pp. 1149–1171.
- Qiu, Z., Oleinick, N. L., & Zhang, J. (2018). ATR/CHK1 inhibitors and cancer therapy. *Radiotherapy and Oncology: Journal of the European Society for Therapeutic Radiology and Oncology*, **126**(3), 450–464.
- Quinn, K. M., Da Costa, A., Yamamoto, A., ... Seder, R. A. (2013). Comparative Analysis of the Magnitude, Quality, Phenotype, and Protective Capacity of Simian Immunodeficiency Virus Gag-Specific CD8 + T Cells following Human-, Simian-, and Chimpanzee-Derived Recombinant Adenoviral Vector Immunization. *The Journal of Immunology*, **190**(6), 2720–2735.
- Rahman, L., Voeller, D., Rahman, M., ... Zajac-Kaye, M. (2004). Thymidylate synthase as an oncogene: A novel role for an essential DNA synthesis enzyme. *Cancer Cell*, **5**(4), 341–351.
- Rankin, S., Reszka, A. P., Huppert, J., ... Neidle, S. (2005). Putative DNA quadruplex formation within the human c-kit oncogene. *Journal of the American Chemical Society*, **127**(30), 10584–10589.
- Raper, S. E., Chirmule, N., Lee, F. S., ... Batshaw, M. L. (2003). Fatal systemic inflammatory response syndrome in a ornithine transcarbamylase deficient patient following adenoviral gene transfer. *Molecular Genetics and Metabolism*, **80**(1–2), 148–158.
- Rejman, J., Bragonzi, A., & Conese, M. (2005). Role of clathrin- and caveolae-mediated endocytosis in gene transfer mediated by lipo- and polyplexes. *Molecular Therapy*, **12**(3), 468–474.
- Rejman, J., Conese, M., & Hoekstra, D. (2006). Gene Transfer by Means of Lipo- and Polyplexes: Role of Clathrin and Caveolae-Mediated Endocytosis. *Journal of Liposome Research*, **16**(3), 237–247.
- Reynolds, P. N., Nicklin, S. A., Kaliberova, L., ... Curiel, D. T. (2001). Combined transductional and transcriptional targeting improves the specificity of transgene expression in vivo. *Nature Biotechnology*, **19**(9), 838–842.

- Reynolds, P. N., Zinn, K. R., Gavrilyuk, V. D., ... Curiel, D. T. (2000). A targetable, injectable adenoviral vector for selective gene delivery to pulmonary endothelium in vivo. *Molecular Therapy*, **2**(6), 562–578.
- Rice, M. C., Czymmek, K., & Kmiec, E. B. (2001). The potential of nucleic acid repair in functional genomics. *Nature Biotechnology*, Nature Publishing Group, pp. 321–326.
- Roberts, T. C., Langer, R., & Wood, M. J. A. (2020, October 1). Advances in oligonucleotide drug delivery. *Nature Reviews Drug Discovery*, Nature Research, pp. 673–694.
- Rodrigues, G. A., Shalaev, E., Karami, T. K., Cunningham, J., Slater, N. K. H., & Rivers, H. M. (2018). Pharmaceutical Development of AAV-Based Gene Therapy Products for the Eye. *Pharmaceutical Research*, **36**(2), 29.
- Rodrigues, M., Calpena, A. C., Amabilino, D. B., Garduño-Ramírez, M. L., & Pérez-García, L. (2014a). Supramolecular gels based on a gemini imidazolium amphiphile as molecular material for drug delivery. *Journal of Materials Chemistry B*, **2**(33), 5419–5429.
- Rodrigues, M., Calpena, A. C., Amabilino, D. B., Ramos-López, D., De Lapuente, J., & Pérez-García, L. (2014b). Water-soluble gold nanoparticles based on imidazolium gemini amphiphiles incorporating piroxicam. *RSC Advances*, **4**(18), 9279–9287.
- Rodríguez, L., Villalobos, X., Dakhel, S., ... Noé, V. (2013). Polypurine reverse Hoogsteen hairpins as a gene therapy tool against survivin in human prostate cancer PC3 cells in vitro and in vivo. *Biochemical Pharmacology*, **86**(11), 1541–1554.
- Rodríguez, L., Villalobos, X., Solé, A., Lliberós, C., Ciudad, C. J., & Noé, V. (2015). Improved design of PPRHs for gene silencing. *Molecular Pharmaceutics*, **12**(3), 867–877.
- Rooney, P. H., Stevenson, D. A., Marsh, S., ... McLeod, H. L. (1998). Comparative genomic hybridization analysis of chromosomal alterations induced by the development of resistance to thymidylate synthase inhibitors. *Cancer Research*, **58**(22), 5042–5.
- Rose, M. G., Farrell, M. P., & Schmitz, J. C. (2002). Thymidylate Synthase: A Critical Target for Cancer Chemotherapy. *Clinical Colorectal Cancer*, **1**(4), 220–229.
- Rundle, S., Bradbury, A., Drew, Y., & Curtin, N. J. (2017). Targeting the ATR-CHK1 axis in cancer therapy. *Cancers*, **9**(5), 1–25.
- Russell, M. R., Levin, K., Rader, J., ... Cole, K. A. (2013). Combination therapy targeting the Chk1 and Wee1 kinases shows therapeutic efficacy in neuroblastoma. *Cancer Research*, **73**(2), 776–784.
- Sahay, G., Querbes, W., Alabi, C., ... Anderson, D. G. (2013). Efficiency of siRNA delivery by lipid nanoparticles is limited by endocytic recycling. *Nature Biotechnology*, **31**(7), 653–658.
- Samaridou, E., Heyes, J., & Lutwyche, P. (2020, January 1). Lipid nanoparticles for nucleic acid delivery: Current perspectives. *Advanced Drug Delivery Reviews*, Elsevier B.V., pp. 37–63.
- Samimi, S., Maghsoudnia, N., Eftekhari, R. B., & Dorkoosh, F. (2018). Lipid-Based Nanoparticles for Drug Delivery Systems. In *Characterization and Biology of*

- Nanomaterials for Drug Delivery: Nanoscience and Nanotechnology in Drug Delivery*, Elsevier, pp. 47–76.
- Samperi, M., Limón, D., Amabilino, D. B., & Pérez-García, L. (2020). Enhancing Singlet Oxygen Generation by Self-Assembly of a Porphyrin Entrapped in Supramolecular Fibers. *Cell Reports Physical Science*, **1**(3), 100030.
- Samperi, M., Pérez-García, L., & Amabilino, D. B. (2019). Quantification of energy of activation to supramolecular nanofibre formation reveals enthalpic and entropic effects and morphological consequence. *Chemical Science*, **10**(44), 10256–10266.
- Samulski, R. J., & Muzyczka, N. (2014). AAV-Mediated Gene Therapy for Research and Therapeutic Purposes. *Annual Review of Virology*, **1**(1), 427–451.
- Sanchez-Vega, F., Mina, M., Armenia, J., ... Schultz, N. (2018). Oncogenic Signaling Pathways in The Cancer Genome Atlas. *Cell*, **173**(2), 321–337.e10.
- Santiago-Ortiz, J. L., & Schaffer, D. V. (2017). Adeno-Associated Virus (AAV) Vectors in Cancer Gene Therapy. *Journal of Controlled Release*, **240**, 287–301.
- Sausville, E., Lorusso, P., Carducci, M., ... Senderowicz, A. (2014). Phase I dose-escalation study of AZD7762, a checkpoint kinase inhibitor, in combination with gemcitabine in US patients with advanced solid tumors. *Cancer Chemotherapy and Pharmacology*, **73**(3), 539–49.
- Savla, R., Browne, J., Plassat, V., Wasan, K. M., & Wasan, E. K. (2017). Review and analysis of FDA approved drugs using lipid-based formulations. *Drug Development and Industrial Pharmacy*, **43**(11), 1743–1758.
- Scagliotti, G., Kang, J. H., Smith, D., ... Pinder-Schenck, M. (2016). PHASE II STUDIES Phase II evaluation of LY2603618, a first-generation CHK1 inhibitor, in combination with pemetrexed in patients with advanced or metastatic non-small cell lung cancer. *Investigational New Drugs*, **34**(5), 625–635.
- Scherer, F., Anton, M., Schillinger, U., ... Plank, C. (2002). Magnetofection: Enhancing and targeting gene delivery by magnetic force in vitro and in vivo. *Gene Therapy*, **9**(2), 102–109.
- Schmitz, J. C., Chen, T. M., & Chu, E. (2004). Small Interfering Double-Stranded RNAs as Therapeutic Molecules to Restore Chemosensitivity to Thymidylate Synthase Inhibitor Compounds. *Cancer Research*, **64**(4), 1431–1435.
- Schmitz, J. C., Liu, J., Lin, X., ... Chu, E. (2001). Translational regulation as a novel mechanism for the development of cellular drug resistance. *Cancer Metastasis Reviews*, **20**(1–2), 33–41.
- Scott, L. J. (2020). Givosiran: First Approval. *Drugs*, pp. 335–339.
- Seto, T., Esaki, T., Hirai, F., ... Shi, X. (2013). Phase I, dose-escalation study of AZD7762 alone and in combination with gemcitabine in Japanese patients with advanced solid tumours. *Cancer Chemotherapy and Pharmacology*, **72**(3), 619–627.
- Shen, Y., Kuznetsov, S. V., & Ansari, A. (2001). Loop dependence of the dynamics of DNA hairpins. *Journal of Physical Chemistry B*, **105**(48), 12202–12211.
- Shintani, Y., Ohta, M., Hirabayashi, H., ... Matsudai, H. (2003). New prognostic indicator for non-small-cell lung cancer, quantitation of thymidylate synthase by real-time reverse transcription polymerase chain reaction. *International Journal*

- of Cancer*, **104**(6), 790–795.
- Shirahata, Y., Ohkohchi, N., Itagak, H., & Satomi, S. (2001). New technique for gene transfection using laser irradiation. *Journal of Investigative Medicine*, **49**(2), 184–190.
- Siddiqui-Jain, A., Grand, C. L., Bearss, D. J., & Hurley, L. H. (2002). Direct evidence for a G-quadruplex in a promoter region and its targeting with a small molecule to repress c-MYC transcription. *Proceedings of the National Academy of Sciences of the United States of America*, **99**(18), 11593–8.
- Solé, A., Ciudad, C. J., Chasin, L. A., & Noé, V. (2016). Correction of point mutations at the endogenous locus of the dihydrofolate reductase gene using repair-PolyPurine Reverse Hoogsteen hairpins in mammalian cells. *Biochemical Pharmacology*, **110–111**, 16–24.
- Solé, A., Delagoutte, E., Ciudad, C. J., Noé, V., & Alberti, P. (2017). Polypurine reverse-Hoogsteen (PPRH) oligonucleotides can form triplexes with their target sequences even under conditions where they fold into G-quadruplexes. *Scientific Reports*, **7**(November 2016), 1–11.
- Solé, A., Villalobos, X., Ciudad, C. J., & Noé, V. (2014). Repair of single-point mutations by polypurine reverse Hoogsteen hairpins. *Human Gene Therapy Methods*, **25**(5), 288–302.
- Song, E., Zhu, P., Lee, S. K., ... Lieberman, J. (2005). Antibody mediated in vivo delivery of small interfering RNAs via cell-surface receptors. *Nature Biotechnology*, **23**(6), 709–717.
- Sørensen, C. S., & Syljuåsen, R. G. (2012). Safeguarding genome integrity: the checkpoint kinases ATR, CHK1 and WEE1 restrain CDK activity during normal DNA replication. *Nucleic Acids Research*, **40**(2), 477–86.
- Sporer, C., Casal, L., Caballero, D., Samitier, J., Errachid, A., & Pérez-García, L. (2009). Novel anionophores for biosensor applications: nano characterisation of SAMS based on amphiphilic imidazolium protophanes and cyclophanes on gold surfaces. *Sensor Letters*, **7**(5), 757–764.
- Springer, A. D., & Dowdy, S. F. (2018, June 1). GalNAc-siRNA Conjugates: Leading the Way for Delivery of RNAi Therapeutics. *Nucleic Acid Therapeutics*, Mary Ann Liebert Inc., pp. 109–118.
- Stein, C. A. (2016, November 1). Eteplirsén approved for Duchenne muscular dystrophy: The FDA faces a difficult choice. *Molecular Therapy*, Nature Publishing Group, pp. 1884–1885.
- Sui, G., Soohoo, C., Affar, E. B., ... Shi, Y. (2002). A DNA vector-based RNAi technology to suppress gene expression in mammalian cells. *Proceedings of the National Academy of Sciences of the United States of America*, **99**(8), 5515–5520.
- Sun, D., Liu, W. J., Guo, K., ... Hurley, L. H. (2008). The proximal promoter region of the human vascular endothelial growth factor gene has a G-quadruplex structure that can be targeted by G-quadruplex-interactive agents. *Molecular Cancer Therapeutics*, **7**(4), 880–889.
- Suzuki, M., Tsukagoshi, S., Saga, Y., Ohwada, M., & Sato, I. (1999). Enhanced expression of thymidylate synthase may be of prognostic importance in advanced cervical cancer. *Oncology*, **57**(1), 50–54.

Bibliography

- Tamm, I., Wang, Y., Sausville, E., ... Reed, J. C. (1998). IAP-Family Protein Survivin Inhibits Caspase Activity and Apoptosis Induced by Fas (CD95), Bax, Caspases, and Anticancer Drugs. *Cancer Research*, **58**(23).
- Tang, J., Erikson, R. L., & Liu, X. (2006). Checkpoint kinase 1 (Chk1) is required for mitotic progression through negative regulation of polo-like kinase 1 (Plk1). *Proceedings of the National Academy of Sciences of the United States of America*, **103**(32), 11964–9.
- Thermo Fisher Scientific - ES. (2003). pSilencer 2.1-U6 neo vector map | Thermo Fisher Scientific - ES. Retrieved April 10, 2021, from <https://www.thermofisher.com/es/es/home/life-science/dna-rna-purification-analysis/napamisc/vector-maps/psilencer-2-1-u6-neo.html>
- Thomas, C. E., Ehrhardt, A., & Kay, M. A. (2003, May 1). Progress and problems with the use of viral vectors for gene therapy. *Nature Reviews Genetics*, Nature Publishing Group, pp. 346–358.
- Tian, T., Chen, Y. Q., Wang, S. R., & Zhou, X. (2018). G-Quadruplex: A Regulator of Gene Expression and Its Chemical Targeting. *Chem*, **4**(6), 1314–1344.
- Tollemar, J., Klingspor, L., & Ringdén, O. (2001). Liposomal amphotericin B (AmBisome) for fungal infections in immunocompromised adults and children. *Clinical Microbiology and Infection*, **7**(SUPPL. 2), 68–79.
- Tomar, R. S., Matta, H., & Chaudhary, P. M. (2003). Use of adeno-associated viral vector for delivery of small interfering RNA. *Oncogene*, **22**(36), 5712–5715.
- Tuerk, C., & Gold, L. (1990). Systematic evolution of ligands by exponential enrichment: RNA ligands to bacteriophage T4 DNA polymerase. *Science*, **249**(4968), 505–510.
- Tüzmen, S., Baskin, Y., Nursal, A. F., ... Hizel, C. (2018). Techniques for nucleic acid engineering: The foundation of gene manipulation. In *Omics Technologies and Bio-engineering: Towards Improving Quality of Life*, Vol. 1, Elsevier Inc., pp. 247–315.
- Vallone, P. M., Paner, T. M., Hilario, J., Lane, M. J., Faldasz, B. D., & Benight, A. S. (1999). Melting studies of short DNA hairpins: Influence of loop sequence and adjoining base pair identity on hairpin thermodynamic stability. *Biopolymers*, **50**(4), 425–442.
- Van den Boorn, J. G., Daßler, J., Coch, C., Schlee, M., & Hartmann, G. (2013, March 1). Exosomes as nucleic acid nanocarriers. *Advanced Drug Delivery Reviews*, Elsevier, pp. 331–335.
- van Harten, A. M., Buijze, M., van der Mast, R., ... Brakenhoff, R. H. (2019). Targeting the cell cycle in head and neck cancer by Chk1 inhibition: a novel concept of bimodal cell death. *Oncogenesis*, **8**(7). doi:10.1038/s41389-019-0147-x
- van Loon, B., Markkanen, E., & Hübscher, U. (2010). Oxygen as a friend and enemy: How to combat the mutational potential of 8-oxo-guanine. *DNA Repair*, **9**(6), 604–616.
- Vasquez, K. M., & Wilson, J. H. (1998). Triplex-directed modification of genes and gene activity. *Trends in Biochemical Sciences*, **23**(1), 4–9.
- Vera, J., Raatz, Y., Wolkenhauer, O., ... Kunz, M. (2015). Chk1 and Wee1 control genotoxic-stress induced G2-M arrest in melanoma cells. *Cellular Signalling*,

- 27(5), 951–960.
- Vercauteren, D., Vandenbroucke, R. E., Jones, A. T., ... Braeckmans, K. (2010). The use of inhibitors to study endocytic pathways of gene carriers: Optimization and pitfalls. *Molecular Therapy*, **18**(3), 561–569.
- Villalobos, X., Rodríguez, L., Prévot, J., Oleaga, C., Ciudad, C. J., & Noé, V. (2014). Stability and Immunogenicity Properties of the Gene-Silencing Polypurine Reverse Hoogsteen Hairpins. *Molecular Pharmaceutics*, **11**(1), 254–264.
- Villalobos, X., Rodríguez, L., Solé, A., ... Noé, V. (2015). Effect of polypurine reverse hoogsteen hairpins on relevant cancer target genes in different human cell lines. *Nucleic Acid Therapeutics*, **25**(4), 198–208.
- Walter, N. G., & Engelke, D. R. (2002, October). Ribozymes: Catalytic RNAs that cut things, make things, and do odd and useful jobs. *Biologist*, Cech, pp. 199–203.
- Wang, F.-Z. Z., Fei, H. R., Cui, Y.-J. J., ... Sun, B.-L. L. (2014). The checkpoint 1 kinase inhibitor LY2603618 induces cell cycle arrest, DNA damage response and autophagy in cancer cells. *Apoptosis*, **19**(9), 1389–1398.
- Wang, S.-K., Wu, Y., Wang, X.-Q., ... Ou, T.-M. (2017). Discovery of Small Molecules for Repressing Cap-Independent Translation of Human Vascular Endothelial Growth Factor (h VEGF) as Novel Antitumor Agents. *Journal of Medicinal Chemistry*, **60**(13), 5306–5319.
- Wang, S., Cao, M., Deng, X., ... Zeng, Y. (2015). Degradable Hyaluronic Acid/Protamine Sulfate Interpolyelectrolyte Complexes as miRNA-Delivery Nanocapsules for Triple-Negative Breast Cancer Therapy. *Advanced Healthcare Materials*, **4**(2), 281–290.
- Wang, T., Tague, N., Whelan, S. A., & Dunlop, M. J. (2021). Programmable gene regulation for metabolic engineering using decoy transcription factor binding sites. *Nucleic Acids Research*, **49**(2), 1163–1172.
- Watson, J. D., & Crick, F. H. C. (1953). Molecular structure of nucleic acids: A structure for deoxyribose nucleic acid. *Nature*, **171**(4356), 737–738.
- WHO. (2021). WHO | World Health Organization. Retrieved February 7, 2021, from <https://www.who.int/>
- Wu, H., Lima, W. F., Zhang, H., Fan, A., Sun, H., & Crooke, S. T. (2004). Determination of the Role of the Human RNase H1 in the Pharmacology of DNA-like Antisense Drugs. *Journal of Biological Chemistry*, **279**(17), 17181–17189.
- Xu, Z. Z., Hyatt, A., Boyle, D. B., & Both, G. W. (1997). Construction of ovine adenovirus recombinants by gene insertion or deletion of related terminal region sequences. *Virology*, **230**(1), 62–71.
- Yamamoto, M., Alemany, R., Adachi, Y., Grizzle, W. E., & Curiel, D. T. (2001). Characterization of the cyclooxygenase-2 promoter in an adenoviral vector and its application for the mitigation of toxicity in suicide gene therapy of gastrointestinal cancers. *Molecular Therapy*, **3**(3), 385–394.
- Yang, D., & Hurley, L. (2006). Structure of the biologically relevant g-quadruplex in the c-MYC promoter. *Nucleosides, Nucleotides and Nucleic Acids*, **25**(8), 951–968.
- Yoon, S., & Rossi, J. J. (2018). Therapeutic Potential of Small Activating RNAs

Bibliography

- (saRNAs) in Human Cancers. *Current Pharmaceutical Biotechnology*, **19**(8), 604–610.
- Zahler, A. M., Williamson, J. R., Cech, T. R., & Prescott, D. M. (1991). Inhibition of telomerase by G-quartet DMA structures. *Nature*, **350**(6320), 718–720.
- Zeman, M. K., & Cimprich, K. A. (2014, January). Causes and consequences of replication stress. *Nature Cell Biology*, NIH Public Access, pp. 2–9.
- Zhang, M., Coen, J. J., Suzuki, Y., ... Chakravarti, A. (2010). Survivin is a potential mediator of prostate cancer metastasis. *International Journal of Radiation Oncology Biology Physics*, **78**(4), 1095–1103.
- Zhang, N., Yin, Y., Xu, S.-J., & Chen, W.-S. (2008). 5-Fluorouracil: mechanisms of resistance and reversal strategies. *Molecules (Basel, Switzerland)*, **13**(8), 1551–69.
- Zhang, Y., Lai, B. S., & Juhas, M. (2019). Recent advances in aptamer discovery and applications. *Molecules*, MDPI AG. doi:10.3390/molecules24050941
- Zhou, J., Li, H., Li, S., Zaia, J., & Rossi, J. J. (2008). Novel dual inhibitory function aptamer-siRNA delivery system for HIV-1 therapy. *Molecular Therapy*, **16**(8), 1481–1489.
- Zhou, J., & Rossi, J. (2017, March 1). Aptamers as targeted therapeutics: Current potential and challenges. *Nature Reviews Drug Discovery*, Nature Publishing Group, pp. 181–202.
- Zhou, Y., Lee, J. H., Jiang, W., Crowe, J. L., Zha, S., & Paull, T. T. (2017). Regulation of the DNA Damage Response by DNA-PKcs Inhibitory Phosphorylation of ATM. *Molecular Cell*, **65**(1), 91–104.
- Zhu, H., Swami, U., Preet, R., & Zhang, J. (2020, September 1). Harnessing dna replication stress for novel cancer therapy. *Genes*, MDPI AG, pp. 1–20.
- Zhu, L., & Mahato, R. I. (2010, October). Lipid and polymeric carrier-mediated nucleic acid delivery. *Expert Opinion on Drug Delivery*, NIH Public Access, pp. 1209–1226.
- Zuhorn, I. S., Kalicharan, R., & Hoekstra, D. (2002). Lipoplex-mediated transfection of mammalian cells occurs through the cholesterol-dependent clathrin-mediated pathway of endocytosis. *Journal of Biological Chemistry*, **277**(20), 18021–18028.
- Zuker, M. (2003). Mfold web server for nucleic acid folding and hybridization prediction. *Nucleic Acids Research*, **31**(13), 3406–3415.

8. APPENDIX

Appendix

In this appendix, the PhD student has collaborated in the writing of a review article about the history of PPRHs, describing their structure and design, the different applications developed during the last decade and their advantages and limitations.

8.3. ARTICLE IV

Nucleic Acids therapeutics using PolyPurine Reverse Hoogsteen hairpins

Véronique Noé, Eva Aubets, Alex J. Félix and Carlos J. Ciudad

Biochemical Pharmacology. 2020:114371. (Impact factor: 4.960).



ELSEVIER

Contents lists available at ScienceDirect

Biochemical Pharmacology

journal homepage: www.elsevier.com/locate/biochempharm

Review

Nucleic acids therapeutics using PolyPurine Reverse Hoogsteen hairpins[☆]Véronique Noé, Eva Aubets, Alex J. Félix, Carlos J. Ciudad^{*}

Department of Biochemistry and Physiology, School of Pharmacy and Food Sciences, & IN2UB, University of Barcelona, 08028 Barcelona, Spain

ARTICLE INFO

Keywords:
PPRH
Cancer therapy
Gene silencing
Gene repair

ABSTRACT

PolyPurine Reverse Hoogsteen hairpins (PPRHs) are DNA hairpins formed by intramolecular reverse Hoogsteen bonds which can bind to polypyrimidine stretches in dsDNA by Watson:Crick bonds, thus forming a triplex and displacing the fourth strand of the DNA complex. PPRHs were first described as a gene silencing tool *in vitro* for *DHFR*, *telomerase* and *survivin* genes. Then, the effect of PPRHs directed against the *survivin* gene was also determined *in vivo* using a xenograft model of prostate cancer cells (PC3). Since then, the ability of PPRHs to inhibit gene expression has been explored in other genes involved in cancer (*BCL-2*, *mTOR*, *topoisomerase*, *C-MYC* and *MDM2*), in immunotherapy (*SIRPa/CD47* and *PD-1/PD-L1* tandem) or in replication stress (*WEE1* and *CHK1*). Furthermore, PPRHs have the ability to target the complementary strand of a G-quadruplex motif as a regulatory element of the *TYMS* gene. PPRHs have also the potential to correct point mutations in the DNA as shown in two collections of CHO cell lines bearing mutations in either the *dhfr* or *aprt* loci. Finally, based on the capability of PPRHs to form triplexes, they have been incorporated as probes in biosensors for the determination of the DNA methylation status of *PAX-5* in cancer and the detection of *mLSU rRNA* for the diagnosis of *Pneumocystis jirovecii*. Of note, PPRHs have high stability and do not present immunogenicity, hepatotoxicity or nephrotoxicity *in vitro*. Overall, PPRHs constitute a new economical biotechnological tool with multiple biomedical applications.

There are a variety of nucleic acids tools dedicated to therapeutics, among them antisense oligonucleotides (ASOs) [1–10], small interfering RNAs (siRNAs) [11–20], microRNAs (mimic and antagomirs) [21–29], aptamers [30–38] and Triplex-Forming Oligonucleotides (TFOs) [39–43]. All of them are relatively short oligonucleotides with the capability of binding to different sequences in the RNA, DNA or even proteins. Therefore, they can inhibit translation, transcription, splicing or protein activity. In the case of ASOs, siRNAs and anti-miRs, the binding or hybridization to their targets are based on Watson:Crick (WC) hydrogen bonds, whereas TFOs rely on Hoogsteen hydrogen bonds. Aptamers bind to their ligands based on the structure they adopt.

Binding via Watson:Crick involves base hybridization of an adenine (A) to a thymine (T) and a guanine (G) to a cytosine (C) [44]. However, there are other type of hydrogen bonds that bind DNA bases in an unconventional way. For example, in the case of purines, one A can bind to another A and one G to another G, in an antiparallel fashion, and these are called Hoogsteen bonds. They were discovered by Karst Hoogsteen, a biochemist born in Groningen in 1923 who emigrated to the United States, and collaborated with Linus Pauling at Caltech, where he

demonstrated the existence of these alternative bonds in 1959 [45,46]. The characteristics of this type of hydrogen bonds make it possible for nucleic acid chains to form triplexes [47–50], and even G-quadruplexes [51–53] (Fig. 1). Karst Hoogsteen left us recently in 2015 (Westfield, NJ.) and this review is dedicated to his memory for the discovery of this type of hydrogen bonds which is the basis of our technology described below.

In our laboratory we developed a new nucleic acid tool termed PolyPurine Reverse Hoogsteen hairpins (PPRHs), whose intramolecular structure is established by Hoogsteen bonds, but hybridization to their targets involve Watson:Crick bonds [54–58].

In this review we will concentrate on the history of PPRHs, describing their structure and design, the different applications developed during the last decade (Fig. 2) and their advantages and limitations.

1. Discovery of PPRHs: design and mechanism

A PPRH molecule consist of a hairpin or clamp formed by

[☆] To the memory of Karst Hoogsteen.

^{*} Corresponding author at: Av. Juan XXIII # 27, 08028 Barcelona, Spain.
E-mail address: cc Ciudad@ub.edu (C.J. Ciudad).

<https://doi.org/10.1016/j.bcp.2020.114371>

Received 28 October 2020; Received in revised form 10 December 2020; Accepted 11 December 2020

Available online 16 December 2020

0006-2952/© 2020 Elsevier Inc. All rights reserved.

Please cite this article as: Véronique Noé, *Biochemical Pharmacology*, <https://doi.org/10.1016/j.bcp.2020.114371>

intramolecular Hoogsteen bonds that can bind to single or double-stranded DNA (dsDNA) by WC bonds. We observed that a hairpin of polypurines with mirror-repeat sequence, joined by 5 thymidines in the center, and bound intramolecularly by Hoogsteen bonds, could bind to a genomic DNA duplex to form a triplex, thus displacing the fourth strand of the complex [59]. In that way, genomic DNA is opened and gene transcription and expression would be inhibited [60].

An advantage of polypurine chains, when making triplexes, is that they can bind to each other by antiparallel Hoogsteen bonds in a pH-independent manner [61]. In contrast, polypyrimidine chains bind in parallel way and in this case, cytosines must be protonated in acidic pH, which is not compatible with therapeutic applications. Nevertheless, different substitutions for generating triplexes in the pyrimidine motif have been used such as 5-methylcytosines [62,63] or cytosine analogs such as N⁶-methyl-8-oxo-2-deoxyadenosines [64], 7,8-dihydro-8-oxoadenines [65] or pseudoisocytosines [66]. In this regard, we demonstrated that PPRHs, using non-modified nucleotides, can bind to polypyrimidine chains at physiological pH [59,67].

We then proceeded to design a PPRH against the gene encoding for dihydrofolate reductase (DHFR), which is a classical target in chemotherapeutic attack [59,68,69], and tested it in mammalian cells following the philosophy as if it were a classical antisense therapy directed against mRNA. The experiment worked and the cells died when the incubation with the PPRH was performed in a selective medium for DHFR lacking glycine, hypoxanthine and thymidine, equivalent as if the cells had been treated with methotrexate (MTX). Then, we realized that as the *dhfr* gene has an inverse orientation in the chromosome, our original design of the PPRH was actually directed against the template DNA strand of the gene and not against its mRNA. In that way, we discovered by "serendipity" that the PPRH had bound to the template DNA strand of the genomic DNA, instead of the mRNA, but yet it was interfering with the expression process [60].

Subsequently, we expanded the design of PPRHs towards different

regions of the *dhfr* gene and directing them to either strand of the dsDNA, finding out that transcription or splicing could be altered [54,60]. Depending on the location of the targeted sequence, we classified PPRHs as Template-PPRHs [60] or Coding-PPRHs [54] if the polypyrimidine stretch was found in the template or coding strand, respectively. The mechanism of action of a Template-PPRH (HpdI3-T) and two Coding-PPRHs (HpsPr-C and HpdI3-C) is depicted in Fig. 3.

Since that moment, we realized that we had in our hands a new agent to inhibit gene expression and, during the last decade, we have expanded its application to other biomedical purposes.

2. Biomedical applications

PPRHs have resulted to be very versatile in their functions and apart from their application as gene silencing molecules, we have shown their ability to correct point mutations in the DNA. Additionally, PPRHs have also been used as biodetectors.

2.1. Gene silencing

After demonstrating that PPRHs were causing *dhfr* gene silencing, we wanted to apply them to a collection of genes representative of anti-cancer targets. We tested PPRHs against genes involved in apoptosis, cancer progression, immunotherapy and replication stress. Additionally, PPRHs have also been directed against G-quadruplex forming sequences (G4FS).

2.1.1. Targeting antiapoptotic genes

The case of *survivin*, as an example of anti-apoptotic gene, deserves special attention given that its targeting leads to effective apoptosis and killing of tumor cells [11,70–74]. Our research group has invested a long-standing effort in studying this gene as a model. *Survivin*, also named *BIRC5*, constitutes a paradigm in cancer therapy since it is

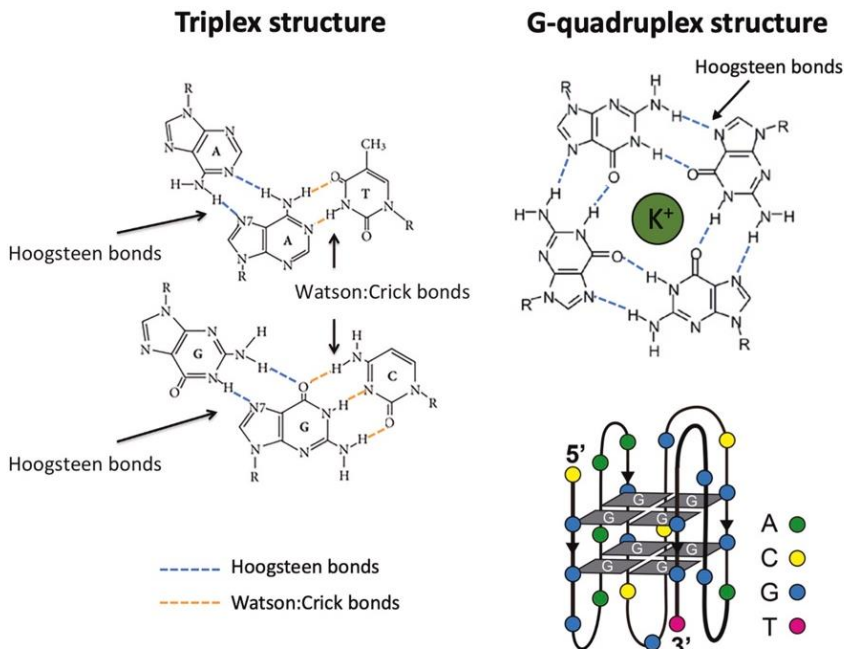


Fig. 1. Chemical representation of Hoogsteen and Watson-Crick base pairing that participate in the formation of triplex (left) or G-quadruplex (right) structures.

overexpressed in many tumors such as bladder [75], breast [3], colon [76], esophagus [77], prostate [78], lung [79], leukemias [80], large-cell non-Hodgkin's lymphoma [81], melanoma [82], neuroblastoma [83], and non-melanoma skin cancers [84], ovary [1], pancreas [85], stomach [86] and uterus [87], whereas is undetectable in most differentiated normal tissues.

We performed a screening of four PPRHs directed against different regions of the *survivin* gene (promoter, intronic or exonic sequences). Cell incubation with these PPRHs led to a decrease in *survivin* mRNA levels and protein, whereas apoptosis was increased, resulting in a reduction of cell viability of more than 90% [55]. The most effective of the tested hairpins was a coding-PPRH directed against the *survivin* promoter (HpsPr-C). EMSA experiments demonstrated that this PPRH was interfering with the binding of transcription factor GATA-3 [55]. Subsequently, *in vivo* experiments were performed with the HpsPr-C coding-PPRH using two different routes of administration, intratumorally or intravenously, in a subcutaneous xenograft tumor model of PC3 prostate cancer. These treatments were effective since they were able to decrease the levels of *survivin* protein and the tumor volume in mice [55], and represented the preclinical proof of principle for PPRHs as gene silencing tools for cancer.

Regarding off-target effects, we started checking the levels of mRNA of 5 non-related genes (*APOA1*, *BCL2*, *DHFR*, *PDK1* and *S100A4*), observing no decrease in the mRNA. Posteriorly, we performed a pharmacogenomic study [88] using the HpsPr-C coding-PPRH against

survivin and its negative control counterpart (Hp-WC) in PC3 prostate cancer cells. This negative control consists of a hairpin bearing in one arm the same sequence that the specific PPRH and, in the opposite arm, the complementary sequence following the WC rules. Therefore, this hairpin is formed by intramolecular WC bonds instead of reverse Hoogsteen bonds, which prevents additional WC bonding to the target DNA. The functional pharmacogenomics analyses of these hairpins revealed that HpsPr-C PPRH led to 244 differentially expressed genes in PC3 cells when applying the $FC > 2$, $p < 0.05$, Benjamini-Hochberg filtering [88]. These differentially expressed genes clustered within the gene sets of Apoptosis and Prostate cancer, Cellular response to stress, and Regulation of cell proliferation [88], according to Gene Set Enrichment Analysis (GSEA) [89]. However, transfection of the negative control hairpin did not result in any differentially expressed genes using the same settings [88].

Additionally, we carried out *in vitro* screenings for hepatotoxicity and nephrotoxicity using HepG2 hepatic and 786-O renal human cell lines, respectively. The unspecific hairpin did not cause any toxicity in HepG2 and 786-O cells. Moreover, the treatment only produced minor changes in gene expression in RT-qPCR arrays containing a selection of genes representative of hepatic and renal toxicity [88].

In addition to *survivin*, we have also explored the action of PPRHs against other antiapoptotic genes [56]. In the particular case of *BCL-2*, we designed 4 different PPRHs, directed against different regions of the gene (promoter, exons and introns). They were tested in 3 different

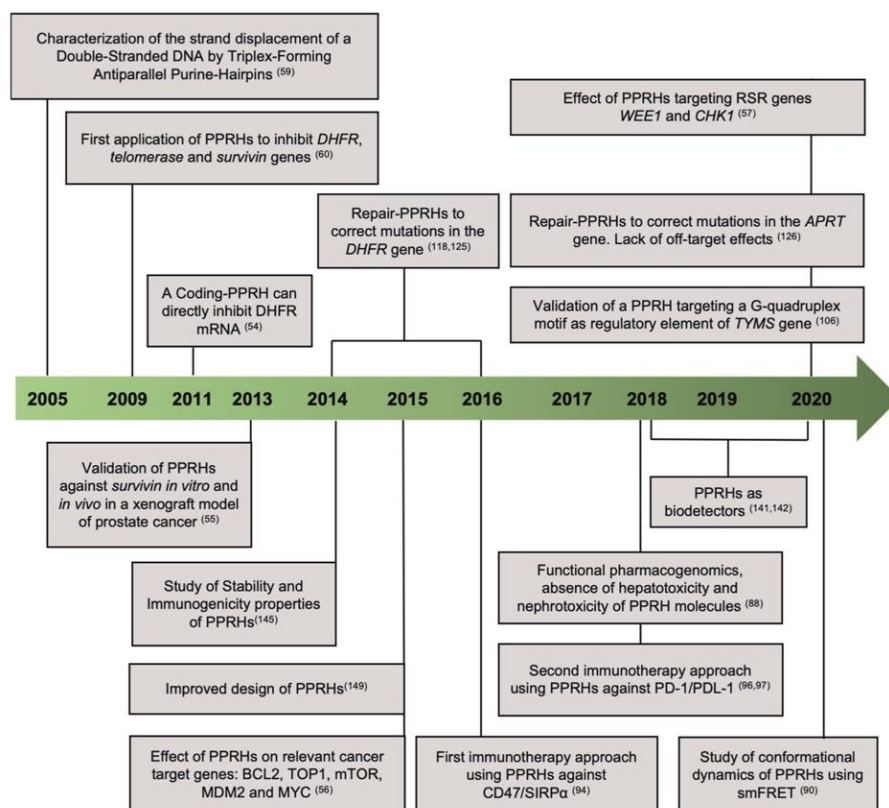


Fig. 2. The timeline of major advances in PPRHs development. Abbreviations used: Replication Stress Response (RSR), Single-molecule Förster Resonance Energy Transfer (smFRET).

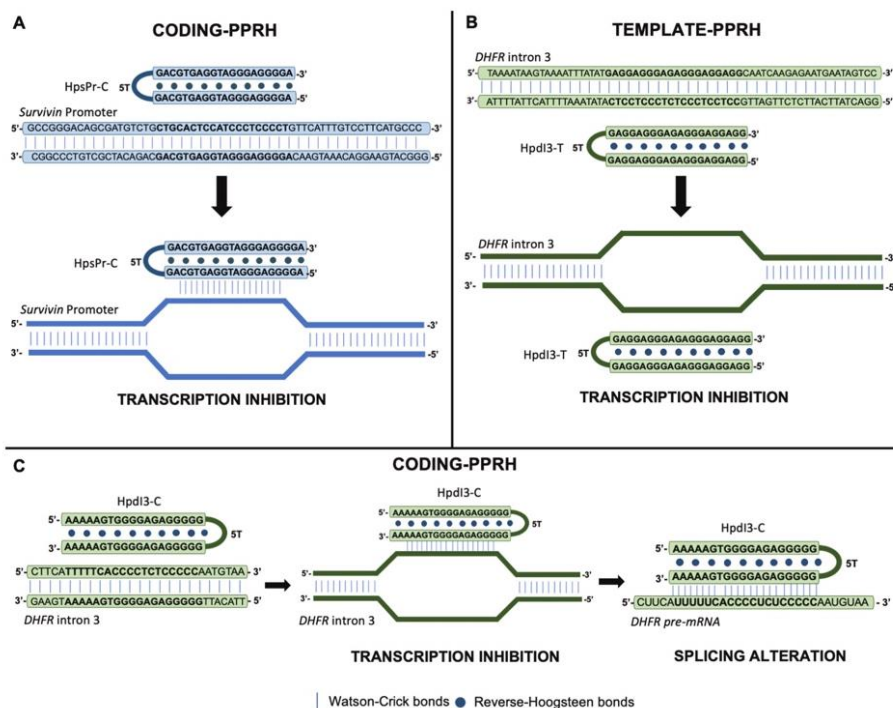


Fig. 3. Mechanism of action PPRHs. Both Coding-PPRHs (A) and Template-PPRHs (B) can form a triplex with its complementary polypyrimidine stretch in the dsDNA by Watson:Crick bonds, resulting in the displacement of the polypurine strand and the specific inhibition of gene transcription. (C) Coding-PPRHs can also bind to the transcribed mRNA, whose sequence and orientation is the same than the coding strand of the DNA, thus altering splicing or translation. The abbreviations used for the nomenclature of the PPRH are: Hp, hairpin; Pr, promoter; s, *survivin*; -C, Coding-PPRH; d, *DHFR*; I, intron; T, Template-PPRH.

human cancer cell lines, pancreatic MIA PaCa cells, prostate PC3 cells, and colon cancer HCF 116 cells. Two PPRHs, against the promoter and Exon 1 were very effective but overall the one showing better results was directed against a polypyrimidine sequence located in the 5'-UTR region of exon 1 (HpBcl2E1-C). The reduction in viability in MIA PaCa cells with this coding PPRH was higher than 95% at a concentration as low as 30 nM. It also produced an eight-fold increase in apoptosis at 100 nM [56]. This specific PPRH has been the subject of a very recent publication studying the multistate conformational dynamics of Polypurine reverse Hoogsteen hairpins when forming a triplex using Single-molecule Förster resonance energy transfer (smFRET) [90]. It was determined that the formation of the hairpin structure by intramolecular Hoogsteen bonds started with a concentration of Mg^{2+} as low as 1 mM [90], manifesting the role of divalent cations in the neutralization of the negative charges to stabilize the hairpin conformation [91]. In addition, the triplex formation upon the binding of HpBcl2E1-C to its dsDNA target started by a very low number of dsDNA molecules after 45 min and took approximately 2 h to obtain the maximum number of triplex molecules [90].

2.1.2. Targeting genes involved in cancer progression

Additionally, we studied the effects of targeting other genes in cancer progression such as *mTOR*, *topoisomerase (TOP1)*, *C-MYC* or *MDM2*. A total of four different PPRHs were designed against *mTOR* and tested in HCT 116 cells. The PPRH directed against the promoter region (HpTorPr-C) was the most effective with more than 90% of cell mortality [56]. Regarding *TOP1* targeting, a template-PPRH directed against intron 2 of the *TOP1* gene (HpTopl2-T) led to a decrease in cell survival

of 95%, 60% and 85% in breast SKBR3, MCF7 and MDA-MB-468 cancer cell lines, respectively [56]. Similarly, the silencing of *C-MYC* using the HpMyc1-T template-PPRH led to a reduction in cell viability of 85%, 80% and 95% in SKBR3, MCF7 and MDA-MB-468 [56]. Finally, a PPRH directed against intron 7 of the *MDM2* gene showed similar results to *C-MYC* inhibition [56].

2.1.3. Targeting genes involved in immunotherapy

In cancer immunotherapy, pharmacological agents are developed to activate or stimulate the host's immune system, thus recognizing and eliminating tumor cells by natural mechanisms [92]. In recent years, PPRHs have been applied for two different immunotherapy approaches. The first one was directed against the *SIRPα/CD47* pathway. It is known that the binding of *SIRPα*, which is mainly expressed on macrophage surface, and *CD47*, overexpressed on tumor cells, disables the phagocytic capacity of macrophages against cancer cells [93]. For that reason, PPRHs designed against *SIRPα* and *CD47* were transfected into macrophages and MCF-7 cancer cells, respectively, with the philosophy to inactivate the "don't eat me" signal. This pretreatment of macrophages and MCF-7 with PPRHs against *SIRPα* and *CD47*, respectively, led to a decrease in the levels of mRNA and protein for both targets and the elimination of tumor cells by macrophages in co-culture experiments [94].

The second immunotherapy approach was focused on the PD-1/PD-L1 tandem. In a similar way, cancer cells overexpress PD-L1 which binds to the PD-1 protein localized on the membrane of T cells, thus avoiding their activation [95]. PPRHs designed against *PD-1* and *PD-L1* were transfected into macrophages and PC3 cells, respectively. The mRNA

and protein levels for both target genes were decreased in the respective cell lines upon incubation with PPRHs [96]. The reduction on PD-1 and PD-L1 expression resulted in the elimination of 90% of the cancer cell population due to the action of macrophages in co-culture experiments. This approach was successful not only in PC3 cells but also in other cancer cell lines such as breast cancer SKBR3, cervix cancer HeLa and melanoma M21 [96].

These studies represented the proof of principle for the usage of PPRHs in immunotherapy strategies [97].

2.1.4. Targeting genes involved in replication stress response

Very recently, we explored targeting genes involved in the replication stress response (RSR) such as *WEE1* and *CHK1*. Cancer cells are dependent of RSR given their high rates of replication and genetic abnormalities [98–100]. Therefore, researchers are investigating inhibitors of this pathway as anticancer treatment [101–105]. We designed three PPRHs against *WEE1* and four against *CHK1*. The most effective PPRH against *WEE1* was directed against the gene promoter and belonged to the template category (HpWEE1Pr-T), and in the case of *CHK1* the best results in terms of decreasing cell viability were obtained with a PPRH directed against intron 1, of the coding category (HpCHK1I1-C) [57]. The effect of both PPRHs were dose- and time-dependent, obtaining a reduction in HeLa cells viability of up to 95% at 100 nM [57]. Furthermore, they were also effective in other human cancer lines such as MCF-7, SKBR3 and HepG2, whereas they showed low activity in non-cancerous cells (HEK-293, ECV304) or non-human Chinese Hamster Ovary (CHO) cells [57]. There was a correlation between the cytotoxicity caused by the PPRHs and the degree of apoptosis observed. In addition, both the levels of mRNA and protein of both targets were decreased [57]. Inhibition of both genes by PPRHs provoked a change in the cell cycle distribution of HeLa cells, producing a decrease in the percentage of cells in G1 and an increase in the population of G2/M [57]. Finally, it was also checked the effect of the combinational therapy of PPRHs against *WEE1* and *CHK1* together with classical chemotherapeutic agents such as 5-Fluorouracil and MTX. In both cases, HpWEE1Pr-T and HpCHK1I1-C showed a synergic effect when incubated with either 5-FU or MTX [57], as calculated by the CompusSyn software [4]. Therefore, in that work we validated the *in vitro* usage of PPRHs against *WEE1* and *CHK1* as a silencing tool of the RSR machinery and as pharmacological agents in cancer therapy.

2.1.5. Targeting G-quadruplex forming sequences

A very interesting and recently discovered application of PPRHs is their capacity to bind to the polypyrimidine complementary strand of a G4FS, thus producing a triplex and the displacement of the G4FS sequence [106]. This finding was detected in the dsDNA region corresponding to the 5'-UTR of the *thymidylate synthase* gene (*TYMS*). The formation of the G4 structure in the polypurine strand upon binding of the PPRH to its complementary polypyrimidine sequence was determined by Thioflavin T staining, which emits fluorescence in the presence of G4 structures [107,108]. The PPRH was binding to the template strand thus inhibiting transcription, whereas the coding strand was adopting the G4 structure [106], which might also interfere with transcription, as stated by others [109,110]. As a result, the levels of *TYMS* mRNA and protein were decreased upon incubation with very low concentrations of the PPRH against *TYMS*, thus producing a high degree of cell death in HeLa and PC3 cancer cells. In addition, the effect of this template-PPRH against *TYMS* was synergic when combined with 5-Fluorouracil. Therefore, PPRHs can constitute a new type of molecule to direct against G-quadruplex regulatory regions containing polypyrimidine stretches.

2.2. Gene repair

In addition to gene silencing approaches, PPRHs have also shown their potential to correct point mutations in the DNA. Gene repair

applications using PPRHs can represent a powerful biomedical application since point mutations are responsible for many human monogenic diseases such as cystic fibrosis [6], Fanconi anemia [111], hemochromatosis [112], hemophilia [113,114], phenylketonuria [115], β -thalassemia [116] or Tay-Sachs disease [117].

The design of repair-PPRHs consists of a polypurine clamp bearing at its 5'-end an extension sequence homologous to the sequence to be repaired but incorporating the desired nucleotide (Fig. 4). The polypurine clamp binds to its polypyrimidine target sequence in the dsDNA near the target mutation, whereas the extension sequence containing the corrected nucleotide serves as a donor to repair the mutation [118,119].

To test the capacity of PPRHs to correct mutations at the endogenous level, we used, as a model, a collection of nonsense mutations in the *dhfr* gene that have mutated a nucleotide (either by substitution, deletion or insertion), and as a result a premature stop codon (TAA, TAG, TGA) appears. Thus, the protein is truncated with loss of its activity [120–124]. Cells were incubated with repair-PPRHs and selection of the repaired clones was performed using deficient -GHT medium (lacking glycine, hypoxanthine and thymidine). DNA sequencing from the surviving colonies revealed the correction of the mutation which restored the DHFR mRNA levels and protein [125]. DHFR enzymatic activity in the repaired clones was also rescued [125].

One can argue that finding a polypyrimidine sequence adjacent to the point mutation can be a limiting factor in some cases. However, the mutation does not necessarily have to be located near the PPRH core. By coupling an additional 5-thymidine connector, repair-PPRHs can be constructed to end up correcting point mutations located 600 nucleotides away from the polypyrimidine target sequence of the PPRH [125,126].

To demonstrate the generality of action of repair-PPRHs, next we attempted to correct point mutations in another gene in mammalian cells, that encoding for *adenine phosphoribosyltransferase* (*aprt*). To this end, a collection of *aprt* mutant CHO cell lines bearing nonsense mutations [7] were subjected to correction with repair-PPRHs [126]. In this instance, after transfection of the repair-PPRHs, a +AAT (including adenine, aminopterin and thymidine) selection medium was applied to select for the *aprt*⁺ cells. A representation of surviving colonies was sequenced demonstrating the correction of the mutation and restoring *APRT* mRNA levels and enzymatic activity [126]. Importantly, the correction of the mutation by the repair-PPRH did not produce any off-target effect in the genome, as revealed by Whole-Genome Sequencing analyses [126]. It is worth noting that repair-PPRHs do not rely on the action of nucleases to stimulate the repair event, in contrast with the current CRISPR/Cas platforms which can generate numerous off-target effects [127–132].

Finally, we got an insight into the molecular mechanism responsible for the repair event. As demonstrated by EMSA, the binding of the repair-PPRH to its polypyrimidine target sequence produced the formation of a D-loop structure [126], which can stimulate DNA repair [133–135].

2.3. PPRHs as detection molecules.

Recently, biosensors based on the capability of the PPRHs to form triplexes have been developed for cancer and microbiological detection (Fig. 5).

In cancer, DNA methylation status is considered an important biomarker for diagnosis and monitoring patients [136,137]. For that purpose, it has been developed an optical biosensor methodology based on PPRH probes capable of capturing in a straightforward manner specific dsDNA fragments by triple helix formation. Then, the methylation state is quantified by using specific antibodies recognizing 5-methylcytosines [138]. Specifically, PPRH probes are attached above a portable custom-made Surface Plasmon Resonance (SPR) biosensor as described in [139]. In that study, the specific dsDNA to be detected by the biosensor corresponded to the promoter region of the *PAX-5* gene, which

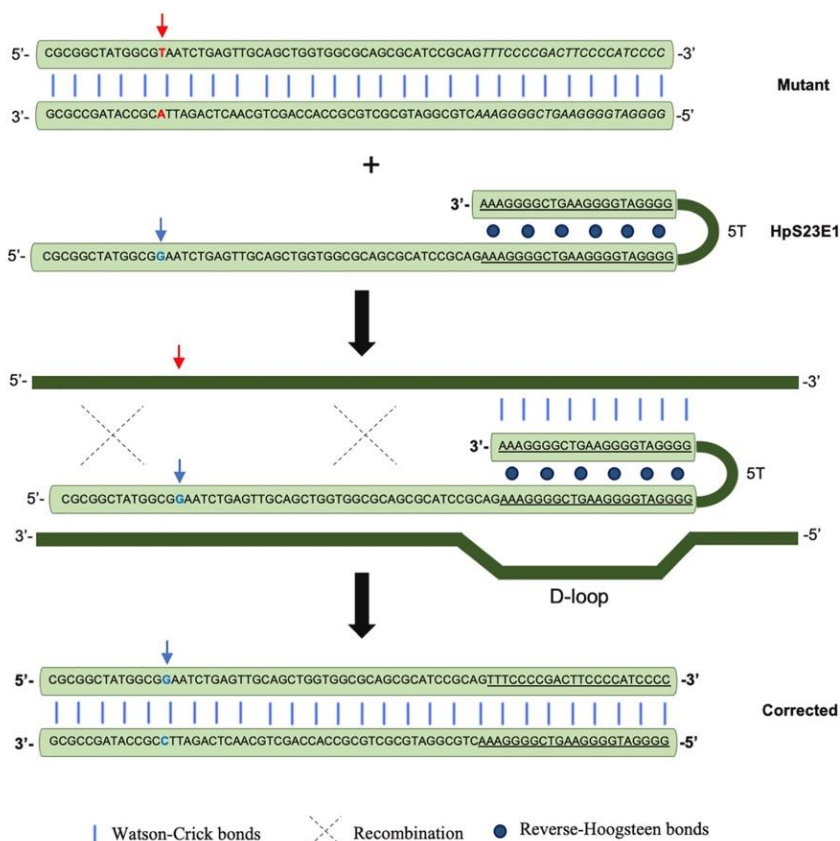


Fig. 4. Scheme depicting the action of a repair-PPRH. A repair-PPRH (HpS23E1) targeting the c.7 G > T single-point substitution (red arrow) in the *aprt* gene of CHO cells is shown. The polypurine hairpin core of the repair-PPRH (underlined) binds to its polypyrimidine target sequence (italics) near the mutation, generating a D-loop structure and stimulating the repair process. The extension sequence in the 5'-end of the repair-PPRH serves as a donor to incorporate the corrected nucleotide (blue arrow) in the mutation site, thus restoring the wild-type sequence.

have been reported to be hypermethylated in some types of cancers [140]. This new detection technology would skip the laborious steps and the sample manipulation needed for other techniques that could lead to erratic analyses [141].

PPRHs have also been used for the fast detection and accurate diagnosis of *Pneumocystis pneumonia* in human samples obtained from bronchoalveolar lavage or nasopharyngeal aspirates [142]. In this case, the PPRH probe detects the *mLSU rRNA* gene from *Pneumocystis jirovecii*. When the PPRH probe hybridizes with the DNA extracted from the sample, it produces a wavelength variation of a reflected light that enables to quantify the analyte bounded to the SPR [142].

3. Advantages of PPRHs

An important property of PPRHs is their stability, given that they are composed of deoxynucleotides instead of ribonucleotides and they adopt a clamp structure. Since DNase I [143] and RNase A families [144] are the predominant nucleases to degrade therapeutic oligonucleotides in blood, we determined the stability of PPRHs in different serum types against their most potent competitor, siRNAs. PPRHs presented a half-life of about 10 h [145] in comparison to siRNAs, which can range from several minutes to 1 h [146–148]. Therefore, PPRHs stability is ten

times longer compared to that of siRNAs. It is worth mentioning that this occurs in the absence of backbone modifications in the PPRH molecule, which makes them more economical to synthesize, approximately ten times less than siRNA molecules, and thus without decreasing their ability to bind to its target sequence. In addition, PPRHs can inhibit gene expression at concentrations ten times lower than those needed for ASOs [60]. If we compare PPRHs with TFOs, which are the other oligonucleotides that bind to genomic DNA, we observed that PPRHs bind to their target DNA at lower concentrations than TFOs, indicating higher affinity. Moreover, in terms of cell viability, PPRHs exert a more potent effect on PC3 and SKBR3 cells than the corresponding TFOs [149].

Another crucial point in gene therapy treatments is to prevent immunogenicity, as it is the case with siRNAs that activate the innate immune response via the Toll-like receptors pathway and increase interleukin-6 levels, tumor necrosis factor alpha and interferon beta [150–152]. However, PPRHs are not immunogenic probably because they are DNA-based molecules of less than 100 nucleotides in length (usually around 50 nt) [145].

Finally, the action of PPRHs is specific, which is conferred by the specificity of the nucleic acid sequence. Although it may seem unusual, polypyrimidine target sequences are indeed found in all genes with a frequency higher than expected, and sometimes even with an extension

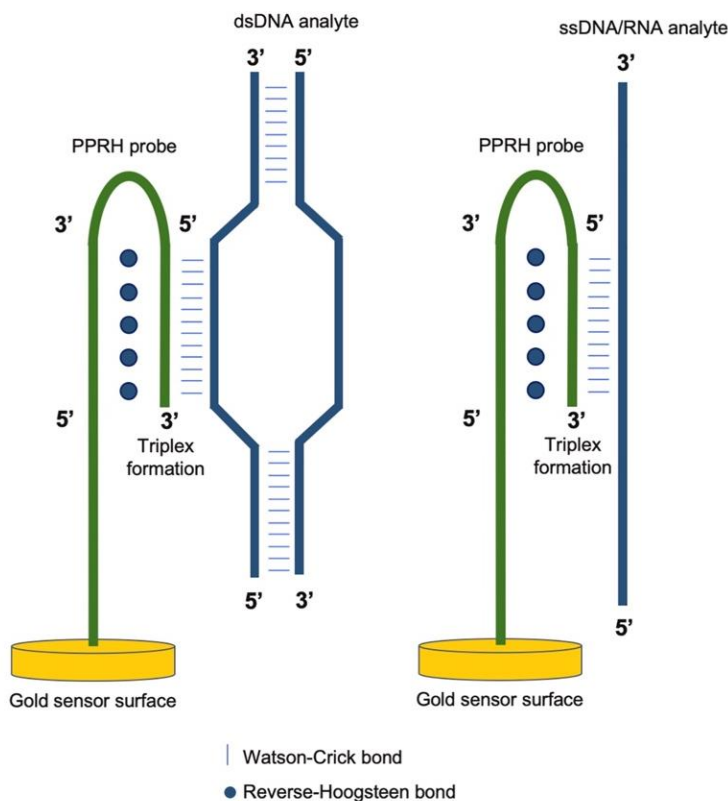


Fig. 5. Schematic representation of biosensors that use PPRHs as probes to detect specific dsDNA fragments (left) or single-stranded nucleic acids (right) by triplex helix formation.

of 50 nucleotides. These polypyrimidine sequences are found mostly in gene regulatory areas such as promoters and intronic regions and to a lesser extent in exons [153,154]. We have tested PPRHs of different lengths at the arm that bind to the dsDNA obtaining very positive effects in the range of 25–30 nt, with a very high specificity [149]. This was verified computationally by BLAST and experimentally by EMSA [55,59,60,149]. As a general procedure, we routinely check the location of the possible targets for PPRHs in a given gene. In the selection of the PPRH target we also consider the possible interference with the binding of transcription or splicing factors. Then, we test PPRHs experimentally to find the one producing the best gene silencing effect.

It should be mentioned that the presence of a perfect polypyrimidine chain in the DNA target is not absolutely necessary, and the existence of up to three purine interruptions in this sequence can be allowed in order to form triplexes with the PPRHs [59]. When this limited number of purines is found, the PPRH contains the complementary pyrimidine to the purine interruptions present within the polypyrimidine target. Therefore, the binding of the PPRH to the dsDNA by WC bonds is completely specific [149]. This opens up the possibilities to design PPRHs against the DNA sequence of any gene in the genome.

4. Limitations of PPRHs

Delivery of oligonucleotides is a crucial point for gene therapy applications. In our experience transfecting PPRHs into cells, we obtained positive results using cationic liposomes which make complexes with the

negative charges present in the phosphodiester bonds of the oligonucleotide [155]. Most of the work *in vitro* has been performed using the N-[1-(2,3-Dioleoyloxy) propyl]-N,N,N trimethylammonium methyl-sulfate (DOTAP) cationic liposome [5,54,60]. Importantly, the concentration ratio PPRH:DOTAP is 1:100 with small variations, and the final concentration of DOTAP is maintained not higher than 10 μ M to avoid the intrinsic cytotoxicity by the liposome on its own. Nevertheless, one of the biggest limitations is the low internalization of PPRHs in hard-to-transfect cells such as lymphoma B cells [156] or neurons [157]. On the other hand, in *in vivo* experiments, PPRHs were complexed to Jet-Polyethylenimine (jetPEI), a cationic polymer that contains repeating amine groups that are protonated to form complexes with DNA [158]. Then, the PPRH/POLYMER complexes were injected intratumorally or intravenously into mice [159]. However, some cationic polymers are cytotoxic due to the presence of amine groups in their structure [160,161]. Therefore, the challenge is to develop optimal vehicles for these types of molecules, ideally a tissue-specific delivery, and achieve an efficient release of the oligonucleotides at the intracellular level so that they can exert their action on the selected therapeutic target. On this direction, different strategies are now being explored: (i) attaching a PPRH to the reported aptamer against nucleolin [162] for a selective internalization, (ii) assembling PPRHs in biodegradable compounds such as hyaluronic acid and protamine sulfate nanocomplexes [163], or (iii) cloning PPRHs in adenoviral vectors to achieve longer expression times in the target cells [164].

Regarding gene correction, up until now, the different approaches

included a selection step to make easier the detection and subsequent characterization of repaired cells [118,125,126]. However, the usage of Next Generation Sequencing (deep-sequencing) would allow the detection of the correction in treated cells without the necessity of a previous selection [165,166]. Another limitation of repair-PPRHs is the low correction frequency obtained after the treatment. This can be improved by synchronization of cells in the S phase of the cell cycle to increase homologous recombination [167-169] or by overexpression of RAD51 [118].

4.1. Final remarks

There is an optimistic future due to the development over the last 30 years of different types of molecules with the ability to silence gene expression: ASOs, siRNAs, aptamers, TFOs and PPRHs, where advances have been made in the specificity, stability, and decrease of the immunogenicity of these molecules.

The possibilities for growth in the biomedical sector are enormous. In fact, the usage of therapeutic oligonucleotides has been considerably increased with the approval by the FDA of the first siRNA for human use (Patisiran) in 2018, specifically developed for the treatment of hereditary transthyretin amyloidosis [170]. In 2019, givosiran was also approved to treat acute hepatic porphyria [171]. In addition, lumasiran has just been approved to treat primary hyperoxaluria [172]. Finally, inclisiran, which is directed against the convertase PCSK9 to reduce LDL cholesterol levels in blood, is currently under regulatory review [173].

Regarding PPRHs, they constitute a new biotechnological tool with multiple biomedical applications: gene silencing, validation of new targets, gene repair and diagnosis. As future perspectives, we are developing more efficient and specific delivery strategies, expanding the usage of PPRHs as detection tools for viruses, including SARS-CoV-2, Influenza and Respiratory Syncytial Virus (RSV), and seeking new targets for PPRHs such as other G4FS involved in gene expression, lncRNAs associated with human diseases or undruggable targets.

Funding

The work was supported by grant RTI2018-093901-B-I00 from Plan Nacional de Investigación Científica (Spain). Our group holds the Quality Mention from Generalitat de Catalunya 2017-SGR-94. EA and AF were awarded with fellowships from Generalitat de Catalunya (FI) and Ministerio de Educación (FPU), respectively.

CRedit authorship contribution statement

Véronique Noé: Writing - review & editing, Supervision, Funding acquisition. **Eva Aubets:** Writing - original draft, Writing - review & editing. **Alex J. Félix:** Writing - original draft, Writing - review & editing. **Carlos J. Ciudad:** Writing - review & editing, Supervision, Conceptualization.

Declaration of Competing Interest

The authors declare that they have no known competing financial interests or personal relationships that could have appeared to influence the work reported in this paper..

References

[1] H. Yoshida, O. Ishiko, T. Sumi, Y. Matsumoto, S. Ogita, Survivin, bcl-2 and matrix metalloproteinase-2 enhance progression of clear cell- and serous-type ovarian carcinomas, *Int. J. Oncol.* 19 (2001) 537-542, <https://doi.org/10.3892/ijo.19.3.537>.
 [2] J.D. Watson, F.H.C. Crick, Molecular structure of nucleic acids: a structure for deoxyribose nucleic acid (reprinted from *Nature*, April 25, 1953), *Nature* 224 (5218) (1969) 470-471, <https://doi.org/10.1038/224470a0>.

[3] K. Tanaka, S. Iwamoto, G. Gon, T. Nohara, M. Iwamoto, N. Tanigawa, Expression of survivin and its relationship to loss of apoptosis in breast carcinomas, *Clin. Cancer Res.* 6 (2000) 127-134.
 [4] T.-C. Chou, Drug combination studies and their synergy quantification using the chou-talalay method, *Cancer Res.* 70 (2) (2010) 440-446, <https://doi.org/10.1158/0008-5472.CAN-09-1947>.
 [5] R. Leventis, J.R. Silvius, Interactions of mammalian cells with lipid dispersions containing novel metabolizable cationic amphiphiles, *Biochim. Biophys. Acta (BBA) - Biomembranes* 1023 (1) (1990) 124-132, [https://doi.org/10.1016/0005-2736\(90\)90017-1](https://doi.org/10.1016/0005-2736(90)90017-1).
 [6] A. Mehdizadeh Hakkak, M. Keramatipour, S. Talebi, A. Brook, J. Tavakoli Afshari, A. Raazi, H.R. Kianifar, Analysis of CFTR gene mutations in children with cystic fibrosis, first report from North-East of Iran, *Iran. J. Basic Med. Sci.* 16 (2013) 917-921 (accessed October 20, 2020).
 [7] G. Phear, W. Armstrong, M. Meuth, Molecular basis of spontaneous mutation at the aprt locus of hamster cells, *J. Mol. Biol.* 209 (4) (1989) 577-582, [https://doi.org/10.1016/0022-2836\(89\)90595-0](https://doi.org/10.1016/0022-2836(89)90595-0).
 [8] J. Scharner, S. Qi, F. Rigo, C.F. Bennett, A.R. Krainer, Delivery of GalNAc-conjugated splice-switching ASOs to non-hepatic cells through ectopic expression of asialoglycoprotein receptor, *Mol. Ther. - Nucleic Acids* 16 (2019) 313-325, <https://doi.org/10.1016/j.omtn.2019.02.024>.
 [9] K. Setoguchi, L. Cui, N. Hachisuka, S. Obchoei, K. Shinkai, F. Hyodo, K. Kato, F. Wada, T. Yamamoto, M. Harada-Shiba, S. Obika, K. Nakano, Antisense oligonucleotides targeting Y-box binding protein-1 inhibit tumor angiogenesis by downregulating Bcl-xL-VEGFR2-tie axes, *Mol. Ther. - Nucleic Acids* 9 (2017) 170-181, <https://doi.org/10.1016/j.omtn.2017.09.004>.
 [10] S. Aguti, V. Bolduc, P. Ala, M. Turmaine, C.G. Bönnemann, F. Muntoni, H. Zhou, Exon-skipping oligonucleotides restore functional collagen VI by correcting a common COL6A1 mutation in ullrich CMD, *Mol. Ther. - Nucleic Acids* 21 (2020) 205-216, <https://doi.org/10.1016/j.omtn.2020.05.029>.
 [11] S. Coma, V. Noe, C. Lavarino, J. Adán, M. Rivas, M. López-Matas, R. Pagan, F. Mitjans, S. Vilaró, J. Piulats, C.J. Ciudad, Use of siRNAs and antisense oligonucleotides against survivin RNA to inhibit steps leading to tumor angiogenesis, *Oligonucleotides* 14 (2) (2004) 100-113, <https://doi.org/10.1089/1545457041526290>.
 [12] D. Kunze, K. Kraemer, K. Erdmann, M. Froehner, M.P. Wirth, S. Fuessel, Simultaneous siRNA-mediated knockdown of antiapoptotic BCL2, Bcl-xL, XIAP and survivin in bladder cancer cells, *Int. J. Oncol.* 41 (2012) 1271-1277, <https://doi.org/10.3892/ijo.2012.1549>.
 [13] J. Shen, R. Samul, R.L. Silva, H. Akiyama, H. Liu, Y. Saishin, S.F. Hackett, S. Zinnen, K. Kossen, K. Fosnaugh, C. Vargeese, A. Gomez, K. Bouhana, R. Aitchison, P. Pavco, P.A. Campochiaro, Suppression of ocular neovascularization with siRNA targeting VEGF receptor 1, *Gene Ther* 13 (3) (2006) 225-234, <https://doi.org/10.1038/sj.gt.3302641>.
 [14] Y. Takei, K. Kadomatsu, Y. Yuzawa, S. Matsuo, T. Muramatsu, A Small interfering RNA targeting vascular endothelial growth factor as cancer therapeutics, *Cancer Res* 64 (10) (2004) 3365-3370, <https://doi.org/10.1158/0008-5472.CAN-03-2682>.
 [15] J.D. Heidel, J.-Y.-C. Liu, Y. Yen, B. Zhou, B.S.E. Heale, J.J. Rossi, D.W. Bartlett, M.E. Davis, Potent siRNA inhibitors of ribonucleotide reductase subunit RRM2 reduce cell proliferation in vitro and in vivo, *Clin. Cancer Res.* 13 (7) (2007) 2207-2215, <https://doi.org/10.1158/1078-0432.CCR-06-2218>.
 [16] D.P. Lane, C.F. Cheok, S. Lain, p53-based cancer therapy, *Cold Spring Harb. Perspect. Biol.* 2 (9) (2010), <https://doi.org/10.1101/cshperspect.a001222>.
 [17] M.G. Stoleriu, V. Steger, M. Mustafa, M. Michaelis, J. Cinatl, W. Schneider, A. Nolte, J. Kurz, H. PeterWendel, C. Schlenk, T. Walker, A new strategy in the treatment of chemoresistant lung adenocarcinoma via specific siRNA transfection of SRF, E2F1, Survivin, HIF and STAT3, *Eur. J. Cardio-Thoracic Surg.* 46 (2014) 877-886, <https://doi.org/10.1093/ejcts/ezu087>.
 [18] T. Yanagi, K. Tachikawa, R. Wilkie-Grantham, A. Hishiki, K.o. Nagai, E. Toyonaga, P. Chivukula, S.-I. Matsuzawa, Lipid nanoparticle-mediated siRNA transfer against PCTAIRE1/PCTK1/Cdk16 inhibits In Vivo cancer growth, *Mol. Ther. - Nucleic Acids* 5 (2016) e327, <https://doi.org/10.1038/mtna.2016.40>.
 [19] D. Schirolli, M.J. Gómara, E. Maurizi, S.D. Atkinson, L. Mairs, K.A. Christie, D. F. Cobice, C.M. McCrudden, M.A. Nesbit, I. Haro, T. Moore, Effective in vivo topical delivery of siRNA and gene silencing in intact corneal epithelium using a modified cell-penetrating peptide, *Mol. Ther. - Nucleic Acids* 17 (2019) 891-906, <https://doi.org/10.1016/j.omtn.2019.07.017>.
 [20] B. Ng, T. Cash-Mason, Y.i. Wang, J. Seitzer, J. Burchard, D. Brown, V. Dudkin, J. Davide, V. Jadhav, L. Sepp-Lorenzino, P.J. Cejas, Intratracheal administration of siRNA triggers mRNA silencing in the lung to modulate T cell immune response and lung inflammation, *Mol. Ther. - Nucl. Acids* 16 (2019) 194-205, <https://doi.org/10.1016/j.omtn.2019.02.013>.
 [21] N. Mencia, E. Selga, V. Noé, C.J. Ciudad, Underexpression of miR-224 in methotrexate resistant human colon cancer cells, *Biochem. Pharmacol.* 82 (11) (2011) 1572-1582, <https://doi.org/10.1016/j.bcp.2011.08.009>.
 [22] L.F.R. Gebert, M.A.E. Rebhan, S.E.M. Crivelli, R. Denzler, M. Stoffel, J. Hall, Miraviren (SPC3649) can inhibit the biogenesis of miR-122, *Nucl. Acids Res.* 42 (2014) 609-621, <https://doi.org/10.1093/nar/gkt852>.
 [23] H. Wang, Y. Bei, P. Huang, Q. Zhou, J. Shi, Q.i. Sun, J. Zhong, X. Li, X. Kong, J. Xiao, Inhibition of miR-155 protects against LPS-induced cardiac dysfunction and apoptosis in mice, *Mol. Ther. - Nucleic Acids* 5 (2016) e374, <https://doi.org/10.1038/mtna.2016.80>.
 [24] C.R. Reschke, L.F.A. Silva, B.A. Norwood, K. Senthilkumar, G. Morris, A. Sanz-Rodriguez, R.M. Conroy, L. Costard, V. Neubert, S. Bauer, M.A. Farrell, D. F. O'Brien, N. Delanty, S. Schorge, R.J. Pasterkamp, F. Rosenow, D.C. Henshall,

- Potent anti-seizure effects of locked nucleic acid antagomirs targeting miR-134 in multiple mouse and rat models of epilepsy. *Mol. Ther. – Nucleic Acids* 6 (2017) 45–56, <https://doi.org/10.1016/j.omtn.2016.11.002>.
- [25] J. Wang, Q. Jiang, O.D. Faletti, C.-M. Tsang, M. Zhao, G. Wu, S.-W. Tsao, M. Fu, Y. Chen, T. Ding, T. Chong, Y. Long, X.u. Yang, Y. Zhang, Y. Cai, H. Li, M. Peng, X. Lyu, X. Li, Exosomal delivery of antagomirs targeting viral and cellular MicroRNAs synergistically inhibits cancer angiogenesis. *Mol. Ther. – Nucleic Acids* 22 (2020) 153–165, <https://doi.org/10.1016/j.omtn.2020.08.017>.
- [26] H. Yan, H. Wang, X. Zhu, J. Huang, Y. Li, K. Zhou, Y. Hua, F. Yan, D.-Z. Wang, Y. Luo, Adeno-associated virus-mediated delivery of anti-miR-199a tough decoys attenuates cardiac hypertrophy by targeting PGC-1 α . *Mol. Ther. – Nucleic Acids* (2020), <https://doi.org/10.1016/j.omtn.2020.11.007>.
- [27] C. Wang, W. Sun, S. Ling, Y.u. Wang, X. Wang, H. Meng, Y. Li, X. Yuan, J. Li, R. Liu, D. Zhao, Q. Lu, A. Wang, Q. Guo, S. Lu, H. Tian, Y. Li, J. Peng, AAV-anti-miR-214 prevents collapse of the femoral head in osteonecrosis by regulating osteoblast and osteoclast activities. *Mol. Ther. – Nucleic Acids* 18 (2019) 841–850, <https://doi.org/10.1016/j.omtn.2019.09.030>.
- [28] A. Gupta, E. Quijano, Y. Liu, R. Bahal, S.E. Scanlon, E. Song, W.-C. Hsieh, D. E. Braddock, D.H. Ly, W.M. Saltzman, P.M. Glazer, Anti-tumor activity of miniPEG-y-modified PNAs to inhibit MicroRNA-210 for cancer therapy. *Mol. Ther. – Nucleic Acids* 9 (2017) 111–119, <https://doi.org/10.1016/j.omtn.2017.09.001>.
- [29] C.J. Cheng, R. Bahal, I.A. Babar, Z. Pincus, F. Barrera, C. Liu, A. Svoronos, D. T. Braddock, P.M. Glazer, D.M. Engelman, W.M. Saltzman, F.J. Slack, MicroRNA silencing for cancer therapy targeted to the tumour microenvironment. *Nature* 518 (7537) (2015) 107–110, <https://doi.org/10.1038/nature13905>.
- [30] C. Tuerk, L. Gold, Systematic evolution of ligands by exponential enrichment: RNA ligands to bacteriophage T4 DNA polymerase. *Science* (80-) 249 (4968) (1990) 505–510, <https://doi.org/10.1126/science.2200121>.
- [31] R. Bavi, Z. Hang, P. Banerjee, M.d. Aquib, M. Jadhav, N. Rane, S. Bavi, R. Bhosale, K. Kodam, B.-H. Jeon, Y. Gu, Dxorubicin-conjugated innovative 16-mer DNA aptamer-based annexin A1 targeted anti-cancer drug delivery. *Mol. Ther. – Nucleic Acids* 21 (2020) 1074–1086, <https://doi.org/10.1016/j.omtn.2020.07.038>.
- [32] X. Ren, Y. Zhao, F. Xue, Y. Zheng, H. Huang, W. Wang, Y. Chang, H. Yang, J. Zhang, Exosomal DNA aptamer targeting α -synuclein aggregates reduced neuropathological deficits in a mouse Parkinson's disease model. *Mol. Ther. – Nucleic Acids* 17 (2019) 726–740, <https://doi.org/10.1016/j.omtn.2019.07.008>.
- [33] A. Affinito, C. Quintavalle, C.L. Esposito, G. Roscigno, C. Giordano, S. Nuzzo, L. Ricci-Vitiani, I. Scognamiglio, Z. Minic, R. Pallini, M.V. Berezovski, V. de Francis, G. Condorelli, Targeting ephrin receptor tyrosine kinase A2 with a selective aptamer for glioblastoma stem cells. *Mol. Ther. – Nucleic Acids* 20 (2020) 176–185, <https://doi.org/10.1016/j.omtn.2020.02.005>.
- [34] K. Tanaka, T. Okuda, Y. Kasahara, S. Ohika, Base-modified aptamers obtained by cell-internalization SELEX facilitate cellular uptake of an antisense oligonucleotide. *Mol. Ther. – Nucleic Acids* (2020), <https://doi.org/10.1016/j.omtn.2020.11.016>.
- [35] H. Li, J. Liu, X. Xiao, S. Sun, H. Zhang, Y. Zhang, W. Zhou, B. Zhang, M. Roy, H. Liu, M. Ye, Z.i. Wang, F. Liu-Smith, J. Liu, A novel aptamer L4A4 specifically targets vemurafenib-resistant melanoma through binding to the CD63 protein. *Mol. Ther. – Nucleic Acids* 18 (2019) 727–738, <https://doi.org/10.1016/j.omtn.2019.10.005>.
- [36] D. Zhao, G.e. Yang, Q. Liu, W. Liu, Y. Weng, Y.i. Zhao, F. Qu, L. Li, Y. Huang, A photo-triggerable controllable siRNA delivery. *Nanoscale* 12 (20) (2020) 10939–10943, <https://doi.org/10.1039/D0NR00301H>.
- [37] H. Rehmani, Y. Li, T. Li, R. Padia, O. Calbay, L. Jin, H. Chen, S. Huang, Addiction to protein kinase C due to PRKCI gene amplification can be exploited for an aptamer-based targeted therapy in ovarian cancer. *Signal Transduct. Target. Ther.* 5 (2020) 1–11, <https://doi.org/10.1038/s41392-020-0197-8>.
- [38] A.D. Ellington, J.W. Szostak, In vitro selection of RNA molecules that bind specific ligands. *Nature* 346 (6287) (1990) 818–822, <https://doi.org/10.1038/346818a0>.
- [39] A.L. Guieysse, D. Praseuth, J.C. Francois, C. Helene, Inhibition of replication initiation by triple helix-forming oligonucleotides. *Biochem. Biophys. Res. Commun.* 217 (1) (1995) 186–194, <https://doi.org/10.1006/bbrc.1995.2762>.
- [40] K.M. Vasquez, J.H. Wilson, Triplex-directed modification of genes and gene activity. *Trends Biochem. Sci.* 23 (1) (1998) 4–9, [https://doi.org/10.1016/S0968-0004\(97\)01158-4](https://doi.org/10.1016/S0968-0004(97)01158-4).
- [41] C.D. Pesce, F. Bolacchi, B. Bongiovanni, F. Cissotta, M. Capozzi, S. Diviacco, F. Quadrioglio, R. Mango, G. Novelli, G. Mossa, C. Esposito, D. Ombres, G. Rocchi, A. Bergamini, Anti-gene peptide nucleic acid targeted to proviral HIV-1 DNA inhibits in vitro HIV-1 replication. *Antiviral Res.* 66 (2005) 13–22, <https://doi.org/10.1016/j.antiviral.2004.12.001>.
- [42] M. Cooney, G. Czernuszewicz, E. Postel, S. Flint, M. Hogan, Site-specific oligonucleotide binding represses transcription of the human c-myc gene in vitro. *Science* (80-) 241 (4864) (1988) 456–459, <https://doi.org/10.1126/science.3293213>.
- [43] G.M. Carbone, E.M. McGuffie, A. Collier, C.V. Catapano, Selective inhibition of transcription of the Ets2 gene in prostate cancer cells by a triplex-forming oligonucleotide. *Nucleic Acids Res.* 31 (2003) 833–843, <https://doi.org/10.1093/nar/gkg198>.
- [44] J.D. Watson, F.H.C. Crick, General implications of the structure of deoxyribonucleic acid. *Nature* 171 (4361) (1953) 964–967, <https://doi.org/10.1038/171964b0>.
- [45] K. Hoogsteen, The structure of crystals containing a hydrogen-bonded complex of 1-methylthymine and 9-methyladenine. *Acta Crystallogr.* 12 (1959) 822–823, <https://doi.org/10.1107/s0365110x59002389>.
- [46] K. Hoogsteen, The crystal and molecular structure of a hydrogen-bonded complex between 1-methylthymine and 9-methyladenine. *Acta Crystallogr.* 16 (1963) 907–916, <https://doi.org/10.1107/s0365110x63002437>.
- [47] S.L. Broitman, D.D. Im, J.R. Fresco, Formation of the triple-stranded polynucleotide helix, poly(A.A.U). *Proc. Nat. Acad. Sci.* 84 (15) (1987) 5120–5124, <https://doi.org/10.1073/pnas.84.15.5120>.
- [48] R.D. Wells, D.A. Collier, J.C. Hanvey, M. Shimizu, F. Wohlrab, The chemistry and biology of unusual DNA structures adopted by oligopurine - oligopyrimidine sequences. *FASEB J.* 2 (14) (1988) 2939–2949, <https://doi.org/10.1096/fasebj.2.14.3053307>.
- [49] A.R. Morgan, R.D. Wells, Specificity of the three-stranded complex formation between double-stranded DNA and single-stranded RNA containing repeating nucleotide sequences. *J. Mol. Biol.* 37 (1) (1968) 63–80, [https://doi.org/10.1016/0022-2836\(68\)90073-9](https://doi.org/10.1016/0022-2836(68)90073-9).
- [50] M.D.F. Kamenetskii, Triplex DNA structures. *Annu. Rev. Biochem.* 64 (1995) 65–95, <https://doi.org/10.1146/annurev.biochem.64.1.65>.
- [51] A.N. Lane, J.B. Chaires, R.D. Gray, J.O. Trent, Stability and kinetics of G-quadruplex structures. *Nucleic Acids Res.* 36 (2008) 5482–5515, <https://doi.org/10.1093/nar/gkn517>.
- [52] M. Gellert, M.N. Lipsett, D.R. Davies, Helix formation by guanylic acid. *Proc. Nat. Acad. Sci.* 48 (12) (1962) 2013–2018, <https://doi.org/10.1073/pnas.48.12.2013>.
- [53] J.T. Davis, G-quartets 40 years later: from 5'-GMP to molecular biology and supramolecular chemistry. *Angew. Chem. Int. Ed.* 43 (6) (2004) 668–698, <https://doi.org/10.1002/anie.200300589>.
- [54] M.C. de Almagro, N. Mencia, V. Noé, C.J. Ciudad, Coding polypurine hairpins cause target-induced cell death in breast cancer cells. *Hum. Gene Ther.* 22 (4) (2011) 451–463, <https://doi.org/10.1089/hum.2010.102>.
- [55] L. Rodríguez, X. Villalobos, S. Dakhel, L. Padilla, R. Hervas, J.L. Hernández, C. J. Ciudad, V. Noé, Polypurine reverse Hoogsteen hairpins as a gene therapy tool against survivin in human prostate cancer PC3 cells in vitro and in vivo. *Biochem. Pharmacol.* 86 (11) (2013) 1541–1554, <https://doi.org/10.1016/j.bcp.2013.09.013>.
- [56] X. Villalobos, L. Rodríguez, A. Solé, C. Lliberós, N. Mencia, C.J. Ciudad, V. Noé, Effect of polypurine reverse Hoogsteen hairpins on relevant cancer target genes in different human cell lines. *Nucleic Acid Ther.* 25 (4) (2015) 198–208, <https://doi.org/10.1089/nat.2015.0531>.
- [57] E. Aubets, V. Noé, C.J. Ciudad, Targeting replication stress response using polypurine reverse Hoogsteen hairpins directed against WEE1 and CHK1 genes in human cancer cells. *Biochem. Pharmacol.* 175 (2020) 113911, <https://doi.org/10.1016/j.bcp.2020.113911>.
- [58] C.J. Ciudad, L. Rodríguez, X. Villalobos, A.J. Félix, V. Noé, Polypurine reverse Hoogsteen hairpins as a gene silencing tool for cancer. *Curr. Med. Chem.* 24 (26) (2017), <https://doi.org/10.2174/0929867324666170301114127>.
- [59] S. Coma, V. Noé, R. Eritja, C.J. Ciudad, Strand displacement of double-stranded DNA by triplex-forming antiparallel purine-hairpins. *Oligonucleotides* 15 (4) (2005) 269–283, <https://doi.org/10.1089/oli.2005.15.269>.
- [60] M.C. de Almagro, S. Coma, V. Noé, C.J. Ciudad, Polypurine hairpins directed against the template strand of DNA knock down the expression of mammalian genes. *J. Biol. Chem.* 284 (17) (2009) 11579–11589, <https://doi.org/10.1074/jbc.M900981200>.
- [61] K.M. Vasquez, P.M. Glazer, Triplex-forming oligonucleotides: principles and applications. *Quart. Rev. Biophys.* 35 (1) (2002) 89–107, <https://doi.org/10.1017/S0033583502003773>.
- [62] J.S. Lee, M.L. Woodsworth, L.J.P. Latimer, A.R. Morgan, Poly(pyrimidine) poly (purine) synthetic DNAs containing 5-methylcytosine form stable triplexes at neutral pH. *Nucl Acids Res* 12 (16) (1984) 6603–6614, <https://doi.org/10.1093/nar/12.16.6603>.
- [63] L. Maher, B. Wold, P. Dervan, Inhibition of DNA binding proteins by oligonucleotide-directed triple helix formation. *Science* (80-) 245 (4919) (1989) 725–730, <https://doi.org/10.1126/science.2549631>.
- [64] S.H. Krawczyk, J.F. Milligan, S. Wadwani, C. Moulds, B.C. Froehler, M. D. Matteucci, Oligonucleotide-mediated triple helix formation using an N3-protonated deoxycytidine analog exhibiting pH-independent binding within the physiological range. *Proc. Nat. Acad. Sci.* 89 (9) (1992) 3761–3764, <https://doi.org/10.1073/pnas.89.9.3761>.
- [65] M.C. Jetter, F.W. Hobbs, 7,8-Dihydro-8-oxoadenine as a replacement for cytosine in the third strand of triple helices. Triplex formation without hypochromicity. *Biochemistry* 32 (13) (1993) 3249–3254, <https://doi.org/10.1021/bi00064a006>.
- [66] M. Egholm, L. Christensen, K.L. Deuholm, O. Buchardt, J. Coull, P.E. Nielsen, Efficient pH-independent sequence-specific DNA binding by pseudoisocytosine-containing bis-PNA. *Nucleic Acids Res.* 23 (2) (1995) 217–222, <https://doi.org/10.1093/nar/23.2.217>.
- [67] A. Aviñó, R. Eritja, C.J. Ciudad, V. Noé, Parallel clamps and polypurine hairpins (PPRH) for gene silencing and triplex-affinity capture: design, synthesis, and use. *Curr. Protoc. Nucleic Acid Chem.* 77 (1) (2019), <https://doi.org/10.1002/epnc.78>.
- [68] S. Penuelas, V. Noé, C.J. Ciudad, Modulation of IMPDH2, survivin, topoisomerase I and vimentin increases sensitivity to methotrexate in HT29 human colon cancer cells. *FEBS J.* 272 (2005) 696–710, <https://doi.org/10.1111/j.1742-4658.2004.04504.x>.
- [69] E. Selga, V. Noé, C.J. Ciudad, Transcriptional regulation of aldo-keto reductase 1C1 in HT29 human colon cancer cells resistant to methotrexate: role in the cell

- cycle and apoptosis, *Biochem. Pharmacol.* 75 (2) (2008) 414–426, <https://doi.org/10.1016/j.bcp.2007.08.034>.
- [70] K. Yamanaka, P. Rocchi, H. Miyake, L. Fazli, B. Vessella, U. Zangemeister-Wittke, M.E. Gleave, A novel antisense oligonucleotide inhibiting several antiapoptotic Bcl-2 family members induces apoptosis and enhances chemosensitivity in androgen-independent human prostate cancer PC3 cells, *Mol. Cancer Ther.* 4 (11) (2005) 1689–1698, <https://doi.org/10.1158/1535-7163.MCT-05-0064>.
- [71] M. Kappler, M. Bache, F. Bartel, M. Kotzsch, M. Panian, P. Würli, K. Blümke, H. Schmidt, A. Meye, H. Taubert, Knockdown of survivin expression by small interfering RNA reduces the clonogenic survival of human sarcoma cell lines independently of p53, *Cancer Gene Ther* 11 (3) (2004) 186–193, <https://doi.org/10.1038/sj.cgt.7700677>.
- [72] R. Blum, J. Jacob-Hirsch, G. Rechavi, Y. Kloog, Suppression of survivin expression in glioblastoma cells by the Ras inhibitor farnesylthiosalicylic acid promotes caspase-dependent apoptosis, *Mol. Cancer Ther.* 5 (2006) 2337–2347, <https://doi.org/10.1158/1535-7163.MCT-06-0193>.
- [73] X. Ling, S. Cao, Q. Cheng, J.T. Keefe, Y.M. Rustum, F. Li, A novel Small Molecule FL118 that selectively inhibits survivin, Mcl-1, XIAP and cIAP2 in a p53-independent manner, shows superior antitumor activity, *PLoS One* 7 (2012), <https://doi.org/10.1371/journal.pone.0045571>.
- [74] A.W. Tolcher, D.I. Quinn, A. Ferrari, F. Ahmann, G. Giaccone, T. Drake, A. Keating, J.S. de Bono, A phase II study of YM155, a novel small-molecule suppressor of survivin, in castration-resistant taxane-pretreated prostate cancer, *Ann. Oncol.* 23 (4) (2012) 968–973, <https://doi.org/10.1093/annonc/mdr353>.
- [75] H.S. Swana, D. Grossman, J.N. Anthony, R.M. Weiss, D.C. Altieri, Tumor content of the antiapoptosis molecule survivin and recurrence of bladder cancer, *N Engl J Med* 341 (6) (1999) 452–453, <https://doi.org/10.1056/NEJM199908053410614>.
- [76] H. Kawasaki, D.C. Altieri, C. De Lu, M. Toyoda, T. Tenjo, N. Tanigawa, Inhibition of apoptosis by survivin predicts shorter survival rates in colorectal cancer, *Cancer Res.* 58 (1998) 5071–5074.
- [77] J. Kato, Y. Kuwabara, M. Mitani, N. Shinoda, A. Sato, T. Toyama, A. Mitsui, T. Nishiwaki, S. Moriyama, J. Kudo, Y. Fujii, Expression of survivin in esophageal cancer: correlation with the prognosis and response to chemotherapy, *Int. J. Cancer.* 95 (2001) 92–95, [https://doi.org/10.1002/1097-0215\(20010320\)95:2<92::AID-IJC1016>3.0.CO;2-9](https://doi.org/10.1002/1097-0215(20010320)95:2<92::AID-IJC1016>3.0.CO;2-9).
- [78] G. Ambrosini, C. Adida, D.C. Altieri, A novel anti-apoptosis gene, survivin, expressed in cancer and lymphoma, *Nat. Med.* 3 (8) (1997) 917–921, <https://doi.org/10.1038/nm0897-917>.
- [79] M. Monzó, R. Rosell, E. Felip, J. Astudillo, J.J. Sánchez, J. Maestre, C. Martín, A. Font, A. Barnadas, A. Abad, A novel anti-apoptosis gene: re-expression of survivin messenger RNA as a Prognosis marker in non-small-cell lung cancers, *J. Clin. Oncol.* 17 (7) (1999) 2100, <https://doi.org/10.1200/JCO.1999.17.7.2100>.
- [80] C. Adida, C. Recher, E. Raffoux, M.-T. Daniel, A.-L. Taksin, P. Rousselot, F. Sigaux, L. Degos, D.C. Altieri, H. Dombret, Expression and prognostic significance of survivin in de novo acute myeloid leukaemia, *Br. J. Haematol.* 111 (1) (2000) 196–203, <https://doi.org/10.1046/j.1365-2141.2000.02328.x>.
- [81] C. Adida, C. Haioun, P. Gaulard, E. Lepage, P. Morel, J. Briere, H. Dombret, F. Reyes, J. Diebold, C. Gisselbrecht, G. Sallès, D.C. Altieri, T.J. Molina, Prognostic significance of survivin expression in diffuse large B-cell lymphomas, *Blood* 96 (2000) 1921–1925, <https://doi.org/10.1182/blood.V96.5.1921.h8001921.1921.1925>.
- [82] D. Grossman, J.M. McNiff, F. Li, D.C. Altieri, Expression and targeting of the apoptosis inhibitor, survivin, in human melanoma, *J. Invest. Dermatol.* 113 (6) (1999) 1076–1081, <https://doi.org/10.1046/j.1523-1747.1999.00776.x>.
- [83] C. Adida, D. Berrebi, M. Peuchmaur, M. Reyes-Mugica, D.C. Altieri, Anti-apoptosis gene, survivin, and prognosis of neuroblastoma, *The Lancet* 351 (9106) (1998) 882–883, [https://doi.org/10.1016/S0140-6736\(05\)70294-4](https://doi.org/10.1016/S0140-6736(05)70294-4).
- [84] D. Grossman, J.M. McNiff, F. Li, D.C. Altieri, Expression of the apoptosis inhibitor, survivin, in nonmelanoma skin cancer and gene targeting in a keratinocyte cell line, *Lab. Invest.* 79 (1999) 1121–1126.
- [85] K. Satoh, K. Kaneko, M. Hirota, A. Masamune, A. Satoh, T. Shimosegawa, Expression of survivin is correlated with cancer cell apoptosis and is involved in the development of human pancreatic duct cell tumors, *Cancer* 92 (2001) 271–278, [https://doi.org/10.1002/1097-0142\(20010715\)92:2<271::AID-CNCR1319>3.0.CO;2-0](https://doi.org/10.1002/1097-0142(20010715)92:2<271::AID-CNCR1319>3.0.CO;2-0).
- [86] C. De Lu, D.C. Altieri, N. Tanigawa, Expression of a novel antiapoptosis gene, survivin, correlated with tumor cell apoptosis and p53 accumulation in gastric carcinomas, *Cancer Res.* 58 (1998) 1808–1812.
- [87] Y. Saitoh, Analysis of Bcl-2, Bax and Survivin genes in uterine cancer, *Int. J. Oncol.* 15 (1999) 137–141, <https://doi.org/10.3892/ij.15.1.137>.
- [88] A.J. Félix, C.J. Ciudad, V. Noé, Functional pharmacogenomics and toxicity of PolyPurine Reverse Hoogsteen hairpins directed against survivin in human cells, *Biochem. Pharmacol.* 155 (2018) 8–20, <https://doi.org/10.1016/j.bcp.2018.06.020>.
- [89] A. Subramanian, P. Tamayo, V.K. Mootha, S. Mukherjee, B.L. Ebert, M.A. Gillette, A. Paulovich, S.L. Pomeroy, T.R. Golub, E.S. Lander, J.P. Mesirov, Gene set enrichment analysis: a knowledge-based approach for interpreting genome-wide expression profiles, *Proc. Natl. Acad. Sci.* 102 (43) (2005) 15545–15550, <https://doi.org/10.1073/pnas.0506580102>.
- [90] D. Bandyopadhyay, P.P. Mishra, Real-time monitoring of the multistate conformational dynamics of polypurine reverse hoogsteen hairpin to capture their triplex-affinity for gene silencing by smFRET microscopy, *J. Phys. Chem. B* 124 (38) (2020) 8230–8239, <https://doi.org/10.1021/acs.jpcc.0c05493.s001>.
- [91] J.R. Morgan, D.V.X. Nguyen, A.R. Frohman, S.R. Rybka, J.A. Zehala, Reversible metal-dependent destabilization and stabilization of a stem-chelate-loop probe binding to an unmodified DNA target, *Bioconjugate Chem.* 23 (10) (2012) 2020–2024, <https://doi.org/10.1021/bc3003293>.
- [92] B. Seliger, Strategies of Tumor immune evasion, *BioDrugs* 19 (6) (2005) 347–354, <https://doi.org/10.2165/00063030-200519060-00002>.
- [93] H.L. Matlung, K. Szilagyi, N.A. Barclay, T.K. van den Berg, The CD47-SIRPα signaling axis as an innate immune checkpoint in cancer, *Immunol. Rev.* 276 (1) (2017) 145–164, <https://doi.org/10.1111/immr.12527>.
- [94] G. Bener, A.J. Félix, C. Sánchez de Diego, I. Pascual Fabregat, C.J. Ciudad, V. Noé, Silencing of CD47 and SIRPα by PolyPurine reverse Hoogsteen hairpins to promote MCF-7 breast cancer cells death by PMA-differentiated THP-1 cells, *BMC Immunol.* 17 (1) (2016), <https://doi.org/10.1186/s12865-016-0170-z>.
- [95] H.O. Alsab, S. Sau, R. Alzhrani, K. Tatiparti, K. Bhishe, S.K. Kashaw, A.K. Iyer, PD-1 and PD-L1 checkpoint signaling inhibition for cancer immunotherapy: mechanism, combinations, and clinical outcome, *Front. Pharmacol.* 8 (2017) 1–15, <https://doi.org/10.3389/fphar.2017.00561>.
- [96] M.M.M. Enriquez, A.J. Félix, C.J. Ciudad, V. Noé, Cancer immunotherapy using PolyPurine Reverse Hoogsteen hairpins targeting the PD-1/PD-L1 pathway in human tumor cells, *PLoS One* 13 (2018), <https://doi.org/10.1371/journal.pone.0206818>.
- [97] C.J. Ciudad, M.M. Medina Enriquez, A.J. Félix, G. Bener, V. Noé, Silencing PD-1 and PD-L1: the potential of PolyPurine Reverse Hoogsteen hairpins for the elimination of tumor cells, *Immunotherapy* 11 (5) (2019) 369–372, <https://doi.org/10.1021/imt-2018-0215>.
- [98] C.S. Sorensen, R.G. Syljuasen, Safeguarding genome integrity: the checkpoint kinases ATR, CHK1 and WEE1 restrain CDK activity during normal DNA replication, *Nucleic Acids Res.* 40 (2) (2012) 477–486, <https://doi.org/10.1093/nar/gkr697>.
- [99] M. Dobbstein, C.S. Sorensen, Exploiting replicative stress to treat cancer, *Nat. Rev. Drug Discov.* 14 (6) (2015) 405–423, <https://doi.org/10.1038/nrd4553>.
- [100] S. Rundle, A. Bradbury, Y. Drew, N.J. Curtin, Targeting the ATR-CHK1 axis in cancer therapy, *Cancers (Basel)*. 9 (2017) 1–25, <https://doi.org/10.3390/cancers9050041>.
- [101] K.C. Cuneo, M.A. Morgan, V. Sahai, M.J. Schipper, L.A. Parsels, J.D. Parsels, T. Devasia, M. Al-Hawari, C.S. Cho, H. Nathan, J. Maybaum, M.M. Zalupski, T. S. Lawrence, Dose escalation trial of the Wee1 inhibitor adavosertinib (AZD1775) in combination with gemcitabine and radiation for patients with locally advanced pancreatic cancer, *J. Clin. Oncol.* 37 (29) (2019) 2643–2650, <https://doi.org/10.1200/JCO.19.00730>.
- [102] S. Leijen, R.M.J.M. van Geel, A.C. Pavlick, R. Tibes, L. Rosen, A.R.A. Razak, R. Lam, T. Demuth, S. Rose, M.A. Lee, T. Freshwater, S. Shumway, L.W. Liang, A. M. Oza, J.H.M. Schellens, G.I. Shapiro, Phase I Study Evaluating WEE1 inhibitor AZD1775 as monotherapy and in combination with gemcitabine, cisplatin, or carboplatin in patients with advanced solid tumors, *J. Clin. Oncol.* 34 (36) (2016) 4371–4380, <https://doi.org/10.1200/JCO.2016.67.5991>.
- [103] C.L. Heidler, E.K. Roth, M. Thiemann, C. Blattmann, R.L. Perez, P.E. Huber, M. Kovac, B. Anthor, G. Neu-Yilik, A.E. Kulozik, Prexasertib (LY2066368) reduces clonogenic survival by inducing apoptosis in primary patient-derived osteosarcoma cells and synergizes with cisplatin and talazoparib, *Int. J. Cancer* 147 (4) (2020) 1059–1070, <https://doi.org/10.1002/ijc.32814>.
- [104] M. Suzuki, T. Yamamori, T. Bo, Y. Sakai, O. Inanami, MK-8776, a novel Chk1 inhibitor, exhibits an improved radiosensitizing effect compared to UCN-01 by exacerbating radiation-induced aberrant mitosis, *Transl. Oncol.* 10 (4) (2017) 491–500, <https://doi.org/10.1016/j.tranon.2017.04.002>.
- [105] G. Scagliotti, J.H. Kang, D. Smith, R. Rosenber, K. Park, S.-W. Kim, W.-C. Su, T. E. Boyd, D.A. Richards, S. Novello, S.M. Hynes, S.P. Myrand, J.i. Lin, E.N. Smyth, S. Wijayawardana, A.B. Lin, M. Pinder-Schenck, Phase II evaluation of LY2063618, a first-generation CHK1 inhibitor, in combination with pemetrexed in patients with advanced or metastatic non-small cell lung cancer, *Invest. New Drugs* 34 (5) (2016) 625–635, <https://doi.org/10.1007/s10637-016-0368-1>.
- [106] E. Aubets, A.J. Félix, M. Garavís, L. Reyes, A. Avinó, R. Ertija, C.J. Ciudad, V. Noé, Detection of a g-quadruplex as a regulatory element in thymidylate synthase for gene silencing using polypurine reverse hoogsteen hairpins, *Int. J. Mol. Sci.* 21 (2020) 1–22, <https://doi.org/10.3390/ijms21145028>.
- [107] A. Renaud de la Faverie, A. Guédin, A. Bedrat, L.A. Yatsunyk, J.-L. Mergny, Thioflavin T as a fluorescence light-up probe for G4 formation, *Nucleic Acids Res.* 42 (2014), <https://doi.org/10.1093/nar/gku111>.
- [108] J. Mohanty, N. Barooah, V. Dhamodharan, S. Harikrishna, P.I. Pradeepkumar, A. C. Bhasikuttan, Thioflavin T as an efficient inducer and selective fluorescent sensor for the human telomeric G-quadruplex DNA, *J. Am. Chem. Soc.* 135 (1) (2013) 367–376, <https://doi.org/10.1021/ja309588h>.
- [109] S. Coghi, A.E. Shechetkin, L.E. Xodo, HRAS is silenced by two neighboring G-quadruplexes and activated by MAZ, a zinc-finger transcription factor with DNA unfolding property, *Nucleic Acids Res.* 42 (13) (2014) 8379–8388, <https://doi.org/10.1093/nar/gku574>.
- [110] T. Tian, Y.-Q. Chen, S.-R. Wang, X. Zhou, G-quadruplex: a regulator of gene expression and its chemical targeting, *Chem* 4 (6) (2018) 1314–1344, <https://doi.org/10.1016/j.chempr.2018.02.014>.
- [111] M. Castella, R. Pujol, E. Callén, J.P. Trujillo, J.A. Casado, H. Gille, F.P. Lach, A. D. Auerbach, D. Schindler, J. Benítez, B. Porto, T. Ferro, M. Arturo, J. Sevilla, L. Madero, E. Cela, C. Beléndez, C.D. De Heredia, T. Olivé, J.S. De Toledo, I. Badell, M. Torrent, J. Estella, Á. Dasí, A. Rodríguez-Villa, P. Gómez, J. Barbot, M. Tapia, A. Molinés, Á. Figuera, J.A. Buen, J. Surrallés, Origin, functional role, and clinical impact of fanconi anemia fca mutations, *Blood* 117 (2011) 3759–3769, <https://doi.org/10.1182/blood-2010-08-299917>.

- [112] P.C.J.L. Santos, R.D. Caçado, A.C. Pereira, I.T. Schetter, R.A.G. Soares, R. A. Pagliusi, R.D.C. Hirata, M.H. Hirata, A.C. Teixeira, M.S. Figueiredo, C. S. Chlatonne, J.E. Krieger, E.M. Guerra-Shinohara, Hereditary hemochromatosis: mutations in genes involved in iron homeostasis in Brazilian patients, *Blood Cells, Mol., Dis.* 46 (4) (2011) 302–307, <https://doi.org/10.1016/j.bcmd.2011.02.008>.
- [113] A.A.G. Tantawy, Molecular genetics of hemophilia A: Clinical perspectives, *Egypt. J. Med. Hum. Genet.* 11 (2) (2010) 105–114, <https://doi.org/10.1016/j.ejmhg.2010.10.005>.
- [114] A.C. Goodeve, Hemophilia B: molecular pathogenesis and mutation analysis, *J. Thromb. Haemost.* 13 (2015) 1184–1195, <https://doi.org/10.1111/jth.12958>.
- [115] Y.-W. Lee, D.H. Lee, N.-D. Kim, S.-T. Lee, J.Y. Ahn, T.-Y. Choi, Y.K. Lee, S.-H. Kim, J.-W. Kim, C.-S. Ki, Mutation analysis of PAH gene and characterization of a recurrent deletion mutation in Korean patients with phenylketonuria, *Exp. Mol. Med.* 40 (5) (2008) 533, <https://doi.org/10.3858/emmm.2008.40.5.533>.
- [116] B. Boonyawat, C. Monsereus, C. Traivaree, The Application of Clinical Genetics Dovespress Molecular analysis of beta-globin gene mutations among Thai beta-thalassemia children: results from a single center study, *Appl. Clin. Genet.* (2014) 7–253, <https://doi.org/10.2147/TACG.S73058>.
- [117] R. Myerowitz, Tay-Sachs disease-causing mutations and neutral polymorphisms in the Hex A gene, *Hum. Mutat.* 9 (1997) 195–208, [https://doi.org/10.1002/\(SICI\)1098-1004\(1997\)9:3<195::AID-HUMU1>3.0.CO;2-7](https://doi.org/10.1002/(SICI)1098-1004(1997)9:3<195::AID-HUMU1>3.0.CO;2-7).
- [118] A. Solé, X. Villalobos, C.J. Ciudad, V. Noé, Repair of single-point mutations by polypurine reverse hoogsteen hairpins, *Hum. Gene Ther. Methods* 25 (5) (2014) 288–302, <https://doi.org/10.1089/hgtb.2014.049>.
- [119] A.J. Félix, A. Solé, V. Noé, C.J. Ciudad, Gene correction of point mutations using polypurine reverse hoogsteen hairpins technology, *Front. Genom. Ed.* 2 (2020), 583577, <https://doi.org/10.3389/fgeed.2020.583577>.
- [120] A.M. Carothers, G. Urlaub, R.W. Steigerwalt, L.A. Chasin, D. Grunberger, Characterization of mutations induced by 2-(N-acetoxy-N-acetyl)aminofluorene in the dihydrofolate reductase gene of cultured hamster cells, *Proc. Nat. Acad. Sci.* 83 (17) (1986) 6519–6523, <https://doi.org/10.1073/pnas.83.17.6519>.
- [121] G. Urlaub, P.J. Mitchell, C.J. Ciudad, L.A. Chasin, Nonsense mutations in the dihydrofolate reductase gene affect RNA processing, *Mol. Cell. Biol.* 9 (7) (1989) 2868–2880, <https://doi.org/10.1128/MCB.9.7.2868>.
- [122] L.A. Chasin, G. Urlaub, P. Mitchell, C. Ciudad, J. Barth, A.M. Carothers, R. Steigerwalt, D. Grunberger, RNA processing mutants at the dihydrofolate reductase locus in Chinese hamster ovary cells, *Prog. Clin. Biol. Res.* 340A (1990) 295–304, <http://www.ncbi.nlm.nih.gov/pubmed/2388917>.
- [123] A.M. Carothers, G. Urlaub, D. Grunberger, L.A. Chasin, Splicing mutants and their second-site suppressors at the dihydrofolate reductase locus in Chinese hamster ovary cells, *Mol. Cell. Biol.* 13 (8) (1993) 5085–5098, <https://doi.org/10.1128/MCB.13.8.5085>.
- [124] A.M. Carothers, G. Urlaub, J. Mucha, W. Yuan, L.A. Chasin, D. Grunberger, A mutational hot spot induced by N-hydroxy-aminofluorene in dihydrofolate reductase mutants of Chinese hamster ovary cells, *Carcinogenesis* 14 (10) (1993) 2181–2184, <https://doi.org/10.1093/carcin/14.10.2181>.
- [125] A. Solé, C.J. Ciudad, L.A. Chasin, V. Noé, Correction of point mutations at the endogenous locus of the dihydrofolate reductase gene using repair-Polypurine Reverse Hoogsteen hairpins in mammalian cells, *Biochem. Pharmacol.* 110–111 (2016) 16–24, <https://doi.org/10.1016/j.bcp.2016.04.002>.
- [126] A.J. Félix, C.J. Ciudad, V. Noé, Correction of the aptt gene using repair-polypurine reverse hoogsteen hairpins in mammalian cells, *Mol. Ther. – Nucleic Acids* 19 (2020) 663–695, <https://doi.org/10.1016/j.omtn.2019.12.015>.
- [127] T.J. Cradick, E.J. Fine, C.J. Antico, G. Bao, CRISPR/Cas9 systems targeting β -globin and CCR5 genes have substantial off-target activity, *Nucleic Acids Res.* 41 (2013) 9584–9592, <https://doi.org/10.1093/nar/gkt714>.
- [128] F. Allen, L. Crepaldi, C. Ainslet, A.J. Strong, V. Kleshchevnikov, P. De Angeli, P. Paleniková, A. Khodak, V. Kiselev, M. Kosicki, A.R. Bassett, H. Harding, Y. Galanty, F. Muñoz-Martínez, E. Metzakovian, S.P. Jackson, L. Parts, Predicting the mutations generated by repair of Cas9-induced double-strand breaks, *Nat. Biotechnol.* 37 (1) (2019) 64–72, <https://doi.org/10.1038/nbt.4317>.
- [129] K.R. Anderson, M. Haussler, C. Watanabe, V. Janakiraman, J. Lund, Z. Modrusan, J. Stinson, Q. Bei, A. Buechler, C. Yu, S.R. Thammannala, L. Tam, M.-A. Sowick, T. Alcantar, N. O’Neil, J. Li, L. Ta, L. Lima, M. Roose-Girma, X. Rairdan, S. Durinck, S. Warming, CRISPR off-target analysis in genetically engineered rats and mice, *Nat. Methods* 15 (7) (2018) 512–514, <https://doi.org/10.1038/s41592-018-0011-5>.
- [130] Y. Lin, T.J. Cradick, M.T. Brown, H. Deshmukh, P. Ranjan, N. Sarode, B.M. Wile, P.M. Vertino, F.J. Stewart, G. Bao, CRISPR/Cas9 systems have off-target activity with insertions or deletions between target DNA and guide RNA sequences, *Nucleic Acids Res.* 42 (11) (2014) 7473–7485, <https://doi.org/10.1093/nar/gku402>.
- [131] K.A. Schaefer, W.-H. Wu, D.F. Colgan, S.H. Tsang, A.G. Bassuk, V.B. Mahajan, Unexpected mutations after CRISPR–Cas9 editing in vivo, *Nat. Methods* 14 (6) (2017) 547–548, <https://doi.org/10.1038/nmeth.4293>.
- [132] G. Cullot, J. Boutin, J. Toutain, F. Prat, P. Pennamen, C. Rooryck, M. Teichmann, E. Rousseau, I. Lamrissi-Garcia, V. Guyonnet-Duperat, A. Bibeyran, M. Lalanne, V. Prouzet-Mauléon, B. Turc, C. Ged, J.M. Blouin, E. Richard, S. Dabernat, F. Moreau-Gaudry, A. Bedel, CRISPR–Cas9 genome editing induces megabase-scale chromosomal truncations, *Nat. Commun.* 10 (2019) 1–14, <https://doi.org/10.1038/s41467-019-09006-2>.
- [133] H. Parekh-Olmedo, M. Drury, E.B. Kmiec, Targeted nucleotide exchange in saccharomyces cerevisiae directed by short oligonucleotides containing locked nucleic acids, *Chem. Biol.* 9 (10) (2002) 1073–1084, [https://doi.org/10.1016/S1074-5521\(02\)00236-3](https://doi.org/10.1016/S1074-5521(02)00236-3).
- [134] M.D. Drury, E.B. Kmiec, DNA pairing is an important step in the process of targeted nucleotide exchange, *Nucleic Acids Res.* 31 (2003) 899–910, <https://doi.org/10.1093/nar/gkg171>.
- [135] M.D. Drury, E.B. Kmiec, Double displacement loops (double d-loops) are templates for oligonucleotide-directed mutagenesis and gene repair, *Oligonucleotides* 14 (4) (2004) 274–286, <https://doi.org/10.1089/oli.2004.14.274>.
- [136] A.P. Feinberg, B. Vogelstein, Hypomethylation distinguishes genes of some human cancers from their normal counterparts, *Nature* 301 (5895) (1983) 89–92, <https://doi.org/10.1038/301089a0>.
- [137] C.J. Marsit, E.A. Houseman, B.C. Christensen, K. Eddy, R. Bueno, D.J. Sugarbaker, H.H. Nelson, M.R. Karagas, K.T. Kelsey, Examination of a CpG island methylator phenotype and implications of methylation profiles in solid tumors, *Cancer Res.* 66 (21) (2006) 10621–10629, <https://doi.org/10.1158/0008-5472.CAN-06-1687>.
- [138] V. Ladopoulos, H. Hofemeister, M. Hoogenkamp, A.D. Riggs, A.F. Stewart, C. Bonifer, The Histone methyltransferase KMT2B is required for RNA polymerase II association and protection from DNA methylation at the MagohB CpG island promoter, *Mol. Cell. Biol.* 33 (7) (2013) 1383–1393, <https://doi.org/10.1128/MCB.01721-12>.
- [139] C.S. Huertas, L.G. Carrascosa, S. Bonnal, J. Valcárcel, L.M. Lechuga, Quantitative evaluation of alternatively spliced mRNA isoforms by label-free real-time plasmic sensing, *Biosens. Bioelectron.* 78 (2016) 118–125, <https://doi.org/10.1016/j.bios.2015.11.023>.
- [140] C.B. Moelans, A.H.J. Verschuur-Maes, P.J. van Diest, Frequent promoter hypermethylation of BRCA2, CDH13, MSH6, PAX5, PAX6 and WT1 in ductal carcinoma in situ and invasive breast cancer, *J. Pathol.* 225 (2) (2011) 222–231, <https://doi.org/10.1002/path.2930>.
- [141] C.S. Huertas, A. Aviño, C. Kurachi, A. Piqué, J. Sandoval, R. Eritja, M. Esteller, L.M. Lechuga, Label-free DNA-methylation detection by direct ds-DNA fragment screening using poly-purine hairpins, *Biosens. Bioelectron.* 120 (2018) 47–54, <https://doi.org/10.1016/j.bios.2018.08.027>.
- [142] O. Calvo-Lozano, A. Aviño, V. Friaiza, A. Medina-Escuela, C.S. Huertas, E. J. Calderón, R. Eritja, L.M. Lechuga, Fast and accurate pneumocystis pneumonia diagnosis in human samples using a label-free plasmic biosensor, *Nanomaterials* 10 (2020) 1–18, <https://doi.org/10.3390/NANO10061246>.
- [143] C.Q. Pan, J.S. Uumer, A. Herzka, R.A. Lazarus, Mutational analysis of human DNase I at the DNA binding interface: implications for DNA recognition, catalysis, and metal ion dependence: mutational analysis of human DNase, *Protein Sci.* 7 (3) (1998) 628–636, <https://doi.org/10.1002/pro.5560070312>.
- [144] J. Hauptenthal, C. Baehr, S. Kiermayer, S. Zeuzem, A. Pipper, Inhibition of RNase A family enzymes prevents degradation and loss of silencing activity of siRNAs in serum, *Biochem. Pharmacol.* 71 (5) (2006) 702–710, <https://doi.org/10.1016/j.bcp.2005.11.015>.
- [145] X. Villalobos, L. Rodríguez, J. Prévot, C. Oleaga, C.J. Ciudad, V. Noé, Stability and immunogenicity properties of the gene-silencing polypurine reverse hoogsteen hairpins, *Mol. Pharm.* 11 (1) (2014) 254–264, <https://doi.org/10.1021/mp400431f>.
- [146] D.M. Dykxhoorn, D. Palliser, J. Lieberman, The silent treatment: siRNAs as small molecule drugs, *Gene Ther.* 13 (6) (2006) 541–552, <https://doi.org/10.1038/sj.gt.3302703>.
- [147] D.W. Bartlett, M.E. Davis, Effect of siRNA nuclease stability on the in vitro and in vivo kinetics of siRNA-mediated gene silencing, *Biotechnol. Bioeng.* 97 (4) (2007) 909–921, <https://doi.org/10.1002/bit.21285>.
- [148] J.M. Layzer, A.P. McCaffrey, A.K. Tanner, Z. Huang, M.A. Kay, B.A. Sullenger, In vivo activity of nuclease-resistant siRNAs, *RNA* 10 (2004) 766–771, <https://doi.org/10.1261/ra.5239604>.
- [149] L. Rodríguez, X. Villalobos, A. Solé, C. Lliberós, C.J. Ciudad, V. Noé, Improved design of PPRHs for gene silencing, *Mol. Pharm.* 12 (3) (2015) 867–877, <https://doi.org/10.1021/mp5007008>.
- [150] M. Sioud, Induction of inflammatory cytokines and interferon responses by double-stranded and single-stranded siRNAs is sequence-dependent and requires endosomal localization, *J. Mol. Biol.* 348 (5) (2005) 1079–1090, <https://doi.org/10.1016/j.jmb.2005.03.013>.
- [151] A.D. Judge, V. Sood, J.R. Shaw, D. Fang, K. McClintock, I. MacLachlan, Sequence-dependent stimulation of the mammalian innate immune response by synthetic siRNA, *Nat. Biotechnol.* 23 (4) (2005) 457–462, <https://doi.org/10.1038/nbt1081>.
- [152] V. Hornung, M. Guenther-Biller, C. Bourquin, A. Ablasser, M. Schlee, S. Uematsu, A. Noronha, M. Manoharan, S. Akira, A. de Fougerolles, S. Endres, G. Hartmann, Sequence-specific potent induction of IFN- α by short interfering RNA in plasmacytoid dendritic cells through TLR7, *Nat. Med.* 11 (3) (2005) 263–270, <https://doi.org/10.1038/nm1191>.
- [153] J.R. Goñi, X. de la Cruz, M. Orozco, Triplex-forming oligonucleotide target sequences in the human genome, *Nucleic Acids Res.* 32 (2004) 354–360, <https://doi.org/10.1093/nar/gkh188>.
- [154] J.R. Goñi, J.M. Vaquerizas, J. Dopazo, M. Orozco, Exploring the reasons for the large density of triplex-forming oligonucleotide target sequences in the human regulatory regions, *BMC Genomics* 7 (1) (2006), <https://doi.org/10.1186/1471-2164-7-63>.
- [155] D.A. Balazs, W.T. Godbey, Liposomes for use in gene delivery, *J. Drug Delivery* 2011 (2011) 1–12, <https://doi.org/10.1155/2011/326497>.
- [156] N. Zhao, J. Qi, Z. Zeng, P. Parekh, C.-C. Chang, C.-H. Tung, Y. Zu, Transfecting the hard-to-transfect lymphoma/leukemia cells using a simple cationic polymer nanocomplex, *J. Control. Rel.* 159 (1) (2012) 104–110, <https://doi.org/10.1016/j.jconrel.2012.01.007>.

- [157] A.A. Alabdullah, B. Al-Abdulaziz, H. Alsalem, A. Magrashi, S.M. Pulicat, A. A. Almzroua, F. Almohanna, A.M. Assiri, N.A. Al Tassan, B.R. Al-Mubarak, Estimating transfection efficiency in differentiated and undifferentiated neural cells, *BMC Res. Notes* 12 (1) (2019), <https://doi.org/10.1186/s13104-019-4249-5>.
- [158] O. Boussif, F. Lezoualc'h, M.A. Zanta, M.D. Mergny, D. Scherman, B. Demeneix, J. P. Behr, A versatile vector for gene and oligonucleotide transfer into cells in culture and in vivo: polyethylenimine. *Proc. Nat. Acad. Sci.* 92 (16) (1995) 7297–7301, <https://doi.org/10.1073/pnas.92.16.7297>.
- [159] W.T. Godbey, K.K. Wu, A.G. Mikos, Poly(ethyleneimine) and its role in gene delivery, *J. Control. Rel.* 60 (2-3) (1999) 149–160, [https://doi.org/10.1016/S0168-3659\(99\)00090-5](https://doi.org/10.1016/S0168-3659(99)00090-5).
- [160] P. Xu, S.-Y. Li, Q. Li, J. Ren, E.A. Van Kirk, W.J. Murdoch, M. Radosz, Y. Shen, Biodegradable cationic polyester as an efficient carrier for gene delivery to neonatal cardiomyocytes, *Biotechnol. Bioeng.* 95 (5) (2006) 893–903, <https://doi.org/10.1002/bit.21036>.
- [161] B.I. Florea, C. Meaney, H.E. Junginger, G. Borchard, Transfection efficiency and toxicity of polyethylenimine in differentiated Calu-3 and nondifferentiated COS-1 cell cultures, *AAAPS J.* 4 (3) (2002) 1–11, <https://doi.org/10.1208/ps040312>.
- [162] R. Yazdian-Robati, P. Bayat, F. Oroojalian, M. Zargari, M. Ramezani, S. M. Taghdisi, K. Abnous, Therapeutic applications of AS1411 aptamer, an update review, *Int. J. Biol. Macromol.* 155 (2020) 1420–1431, <https://doi.org/10.1016/j.jbiomac.2019.11.118>.
- [163] S. Wang, M. Cao, X. Deng, X. Xiao, Z. Yin, Q. Hu, Z. Zhou, F. Zhang, R. Zhang, Y. Wu, W. Sheng, Y.i. Zeng, Degradable hyaluronic acid/protamine sulfate interpolyelectrolyte complexes as miRNA-delivery nanocapsules for triple-negative breast cancer therapy, *Adv. Healthcare Mater.* 4 (2) (2015) 281–290, <https://doi.org/10.1002/adhm.201400222>.
- [164] C.S. Lee, E.S. Bishop, R. Zhang, X. Yu, E.M. Farina, S. Yan, C. Zhao, Z. Zeng, Y. I. Shu, X. Wu, J. Lei, Y. Li, W. Zhang, C. Yang, K.e. Wu, Y. Wu, S. Ho, A. Athiviraham, M.J. Lee, J.M. Wolf, R.R. Reid, T.-C. He, Adenovirus-mediated gene delivery: potential applications for gene and cell-based therapies in the new era of personalized medicine, *Genes Dis.* 4 (2) (2017) 43–63, <https://doi.org/10.1016/j.gendis.2017.04.001>.
- [165] F.J. Román-Rodríguez, L. Ugalde, L. Álvarez, B. Díez, M.J. Ramírez, C. Risueno, M. Cortón, M. Bogliolo, S. Bernal, F. March, C. Ayuso, H. Hanenberg, J. Sevilla, S. Rodríguez-Perales, R. Torres-Ruiz, J. Surrallés, J.A. Bueren, P. Río, NHEJ-mediated repair of CRISPR-Cas9-induced DNA breaks efficiently corrects mutations in HSPCs from patients with fanconi anemia, *Cell Stem Cell* 25 (5) (2019) 607–621.e7, <https://doi.org/10.1016/j.stem.2019.08.016>.
- [166] J.J. Salk, M.W. Schmitt, L.A. Loeb, Enhancing the accuracy of next-generation sequencing for detecting rare and subclonal mutations, *Nat. Rev. Genet.* 19 (5) (2018) 269–285, <https://doi.org/10.1038/nrg.2017.117>.
- [167] E.E. Brachman, E.B. Kmiec, Gene repair in mammalian cells is stimulated by the elongation of S phase and transient stalling of replication forks, *DNA Repair* 4 (4) (2005) 445–457, <https://doi.org/10.1016/j.dnarep.2004.11.007>.
- [168] A. Majumdar, N. Puri, B. Cuenoud, F. Natt, P. Martin, A. Khorlin, N. Dyatkina, A. J. George, P.S. Miller, M.M. Seidman, Cell cycle modulation of gene targeting by a triple helix-forming oligonucleotide, *J. Biol. Chem.* 278 (13) (2003) 11072–11077, <https://doi.org/10.1074/jbc.M211837200>.
- [169] P. Olsen, M. Randol, S. Krauss, Implications of cell cycle progression on functional sequence correction by short single-stranded DNA oligonucleotides, *Gene Ther.* 12 (2005) 546–551, <https://doi.org/10.1038/sj.gt.3302437>.
- [170] D. Adams, A. Gonzalez-Duarte, W.D. O'Riordan, C.-C. Yang, M. Ueda, A. V. Kristen, I. Tourmev, H.H. Schmidt, T. Coelho, J.L. Berk, K.-P. Lin, G. Vita, S. Attarian, V. Planté-Bordeneuve, M.M. Mezei, J.M. Campistol, J. Buades, T. H. Brannagan III, B.J. Kim, J. Oh, Y. Parman, Y. Sekijima, P.N. Hawkins, S. D. Solomon, M. Polydefkis, P.J. Dyck, P.J. Gandhi, S. Goyal, J. Chen, A.L. Strahs, S.V. Nochor, M.T. Sweetser, P.P. Garg, A.K. Vaishnav, J.A. Gollob, O.B. Suhr, Patisiran, an RNAi therapeutic, for hereditary transthyretin amyloidosis, *N. Engl. J. Med.* 379 (1) (2018) 11–21, <https://doi.org/10.1056/NEJMoa1716153>.
- [171] L.J. Scott, Givosiran: First Approval, *Drugs* 80 (3) (2020) 335–339, <https://doi.org/10.1007/s40265-020-01269-0>.
- [172] FDA Approves First Drug to Treat Rare Metabolic Disorder | FDA, (n.d.). <<https://www.fda.gov/news-events/press-announcements/fda-approves-first-drug-treat-rare-metabolic-disorder>> (accessed December 9, 2020).
- [173] K.K. Ray, R.S. Wright, D. Kallend, W. Koenig, L.A. Leiter, F.J. Raal, J.A. Bisch, T. Richardson, M. Jaros, P.L.J. Wijngaard, J.J.P. Kastelein, Two phase 3 trials of inclisiran in patients with elevated LDL cholesterol, *N. Engl. J. Med.* 382 (16) (2020) 1507–1519, <https://doi.org/10.1056/NEJMoa1912387>.

